HETEROLOGOUS EXPRESSION OF THE GAUT1:GAUT7 COMPLEX AND MECHANISMS OF HOMOGALACTURONAN BIOSYNTHESIS

by

ROBERT ALEXANDER AMOS

(Under the Direction of Debra Mohnen)

ABSTRACT

Homogalacturonan (HG) is a pectic glycan in the plant cell wall that contributes to plant growth and development, cell wall structure and function, and interacts with other glycans and proteoglycans in the wall. HG is synthesized by the galacturonosyltransferase (GAUT) gene family. Two members of this family, GAUT1 and GAUT7, form a heteromeric enzyme complex in Arabidopsis thaliana. Progress in studying plant cell wall glycosyltransferases (GTs) has been limited by the difficulty of purifying these low abundance enzymes from native plant tissues and slow progress in developing viable heterologous expression systems. Here, we established a heterologous GAUT expression system in HEK293 cells and showed that co-expression of recombinant GAUT1 with GAUT7 results in the production of a soluble GAUT1:GAUT7 complex that catalyzes elongation of HG products in vitro. The reaction rates, progress curves, and product distributions exhibited major differences dependent upon small changes in the degree of polymerization (DP) of the oligosaccharide acceptor. GAUT1:GAUT7 displayed > 45fold increased catalytic efficiency with DP11 acceptors relative to DP7 acceptors. Although GAUT1:GAUT7 synthesized high molecular weight polymeric HG (> 100 kDa) in a substrate concentration-dependent manner typical of distributive (non-processive) glycosyltransferases

with DP11 acceptors, reactions primed with short-chain acceptors resulted in a bimodal product distribution of glycan products that has previously been reported as evidence for a processive model of GT elongation. As an alternative to the processive glycosyltransfer model, a two-phase distributive elongation model is proposed in which a slow phase, which includes the *de novo* initiation of HG and elongation of short-chain acceptors, is distinguished from a phase of rapid elongation of intermediate and long-chain acceptors. Upon reaching a critical chain length of DP11, GAUT1:GAUT7 elongates HG to high molecular weight products. Two-phase elongation is potentially a common feature of polysaccharide synthesis and may explain why many GTs yield product distributions that deviate from the results predicted for strictly processive or distributive mechanisms of synthesis. The high yield of GAUT1:GAUT7 expressed in HEK293 cells and the thorough biochemical and kinetic characterization described here provides a standard for future studies of polysaccharide biosynthesis from plant cell walls and other organisms.

INDEX WORDS: plant cell wall, glycosyltransferase, protein complex, enzyme mechanism, processivity, homogalacturonan, pectin, pectic glycan, galacturonosyltransferase, polygalacturonide transferase

HETEROLOGOUS EXPRESSION OF THE GAUT1:GAUT7 COMPLEX AND MECHANISMS OF HOMOGALACTURONAN BIOSYNTHESIS

by

ROBERT ALEXANDER AMOS

B.S., University of Georgia, 2009

A Dissertation Submitted to the Graduate Faculty of The University of Georgia in Partial Fulfillment of the Requirements for the Degree

DOCTOR OF PHILOSOPHY

ATHENS, GEORGIA

2019

© 2019

Robert Alexander Amos

All Rights Reserved

HETEROLOGOUS EXPRESSION OF THE GAUT1:GAUT7 COMPLEX AND MECHANISMS OF HOMOGALACTURONAN BIOSYNTHESIS

by

ROBERT ALEXANDER AMOS

Major Professor: Committee: Debra Mohnen Maor Bar-Peled David Garfinkel Ron Orlando Zachary Wood

Electronic Version Approved:

Suzanne Barbour Dean of the Graduate School The University of Georgia May 2019

DEDICATION

To Mom and Dad for endless love and support.

ACKNOWLEDGEMENTS

I would like to extend a special show of gratitude to my mentor, Dr. Debra Mohnen, for providing me with this opportunity and for persisting with me during the difficult trials of this project. Completion of this project was only possible with the assistance of many of my colleagues at the Complex Carbohydrate Research Center and the Department of Biochemistry and Molecular Biology. I would like to thank the members of my research committee: Dr. Zac Wood, Dr. David Garfinkel, Dr. Ron Orlando, and Dr. Maor Bar-Peled for the guidance necessary to direct this project to a successful conclusion, as well as Dr. Melani Atmodjo, Dr. Ajaya Biswal, Dr. Li Tan, and all members of the Mohnen lab. I also thank our collaborators Dr. Kelley Moremen, Dr. Jeong-Yeh Yang, Dr. Breeanna Urbanowicz, Dr. Sivakumar Pattathil, and everyone else who took time to provide me with your knowledge and good ideas, especially Dr. Malcolm O'Neill, Dr. Alan Darvill, Dr. Carl Bergmann, Dr. Michael Hahn, Dr. David Blum, Dr. Michael Adams, Dr. Lance Wells, Dr. Dusty Brown, Dustin Middleton, and DJ Bernsteel.

TABLE OF CONTENTS

Pag
ACKNOWLEDGEMENTS
LIST OF TABLESi:
LIST OF FIGURESx
INTRODUCTION
CHAPTER
1 LITERATURE REVIEW: GLYCOSYLTRANSFERASE ACTIVITIES OF
HETEROLOGOUSLY-EXPRESSED PLANT CELL WALL MATRIX
POLYSACCHARIDE BIOSYNTHETIC GENES AND THEIR SIGNIFICANCE
FOR WALL POLYMER FUNCTION
Abstract
Introduction: Plant cell walls as quality factors in fruit and other plant-derived
commercial products
Models of crosslinked plant cell wall polysaccharide networks10
Strategies for identifying cell wall glycosyltransferase (CWGT) activities1
Heterologous expression systems for plant cell wall GTs
The biosynthesis of extended-chain backbone polymers30
Enzymatic rates and kinetic analyses
Heterologous expression of complexes4
Conclusion4

	TABLES	49
2	A TWO-PHASE MODEL FOR THE NON-PROCESSIVE BIOSYNTHESIS OF	7
	HOMOGALACTURONAN POLYSACCHARIDES BY THE GAUT1:GAUT7	
	COMPLEX	65
	Abstract	66
	Introduction	67
	Results	70
	Discussion	103
	Experimental procedure	110
	Supplementary table	118
CONCLU	SIONS	119
REFEREN	NCES	132
APPEND	ICES	
A	ACTIVITY VARIATION OF GAUT1:GAUT7 PRODUCED IN HEK293	
	CELL CULTURES	155
В	ACTIVITY OF GAUT1:GAUT7 ACTIVE-SITE DXD MUTANTS	167
C	PURIFICATION OF ACTIVE ENZYMES BY SIZE EXCLUSION	
	CHROMATOGRAPHY TO REMOVE PROTEIN AGGREGATES	186
D	STABILITY OF GAUT1:GAUT7 AND GAUT1 ENZYMES FOLLOWING	
	NICKEL-AFFINITY PURIFICATION	194
Е	EFFORTS TO DETERMINE THE SPECIFIC ACTIVITY OF GAUT1 RELATI	VE
	TO GAUT1:GAUT7	201
F	STOICHIOMETRY OF THE GAUT1:GAUT7 COMPLEX	207

G	ELISA-BASED HG:GALAT ACTIVITY ASSAY	216
Н	COMPARISON OF METHODS FOR ASSAYING HG:GALAT ACTIVITY	.224

LIST OF TABLES

Page
Table 1.1: Plant cell wall GTs of known function determined by heterologous expression49
Table 1.2: Chain length of plant cell wall polysaccharides synthesized in vivo and in vitro58
Table 1.3: Enzymatic rates and reaction kinetics of plant cell wall polysaccharides
synthesized in vitro61
Table 1.4: Data from references used to calculate enzymatic rates in Table 1.364
Table 2.1: Results of Michaelis-Menten kinetics assays experiments of the
Arabidopsis heterologously-expressed GAUT1:GAUT7 complex
Table A.1: Protein expression levels from 12 total co-expressions of GAUT1:GAUT7 in
HEK293 cultures
Table A.2: HG:GalAT activity measurements of GAUT1:GAUT7 purified from 12 different co-
expression trials in HEK293 cells
Table A.3: Recommended modifications to standard assay conditions for comparison
of specific activity of different GTs166
Table B.1: Putative DXD motif locations in GAUT1 and GAUT7169
Table B.2: Primer sequences used to create DXD mutations
Table B.3: Concentrations of purified constructs measured by UV-Vis and fluorescence174
Table D.1: Percentage of HG:GalAT activity recovered during GAUT1:GAUT7 and
GAUT1 stability assays at 4°C198

Table D.2: Relative activity of GAUT1 compared to GAUT1:GAUT7 following	
storage at 4°C	199
Table F.1: Molecular weight of GAUT1 and GAUT7 monomers and complexes	208
Table F.2: Molecular weight of GAUT1:GAUT7 measurements by SEC-MALS	214
Table H.1: Methods for assaying HG:GalAT activity	224

LIST OF FIGURES

Page	•
Figure I.1: Structure of homogalacturonan)
Figure 1.1: Methods for identifying CWGTs for <i>in vitro</i> activity verification15	5
Figure 1.2: Polysaccharide chain elongation patterns for processive, distributive, and two-phase	
distributive glycosyltransfer39)
Figure 2.1: Heterologous expression of the GAUT1:GAUT7 complex)
Figure 2.2: Biochemical characterization of HG:GalAT activity of the	
GAUT1:GAUT7 complex74	ŀ
Figure 2.3: Effect of divalent and monovalent metal ions on the acceptor-dependent	
HG:GalAT activity of the GAUT1:GAUT7 complex76	í
Figure 2.4: Elongation of medium-chain length HG acceptors (DP11-15) by GAUT1:GAUT779)
Figure 2.5: GAUT1:GAUT7 elongates DP11 acceptors in a manner dependent on the	
available donor:acceptor ratio81	l
Figure 2.6: Comparison of acceptor elongation activity using HG acceptors of	
different degrees of polymerization84	ļ
Figure 2.7: Elongation of short-chain HG acceptors and de novo initiation of	
high molecular weight HG polysaccharides88	3
Figure 2.8: Elongation of DP3 and DP7 acceptors detected by MALDI-TOF MS90)
Figure 2.9: Elongation of DP7 acceptors results in a bimodal product distribution under	
a donor:acceptor ratio ranging from 10 to 20091	

Figure 2.10: Digestion by endopolygalacturonase (EPG) of HG synthesized by
acceptor-dependent elongation of <i>de novo</i> synthesis92
Figure 2.11: Non-processive elongation of HG acceptors
Figure 2.12: Boiled enzyme controls, T0 starting acceptors for Fig. 2.1195
Figure 2.13: SEC separation with fluorescence detection of DP7-2AB acceptor and
high molecular weight products
Figure 2.14: Addition of NaCl or incubation of GAUT1 alone prevents
high MW HG biosynthesis102
Figure 2.15: A proposed model for HG synthesis by GAUT1:GAUT7106
Figure A.1: Expression and activity comparison for 12 GAUT1:GAUT7
co-expression cultures
Figure B.1: Location of putative DXD mutants in GAUT1 and GAUT7 full-length sequences 168
Figure B.2: Fluorescence in culture medium of each mutant expressed in 20 mL cell cultures .174
Figure B.3: Standard curve for WT used to determine fluorescence mg/mL175
Figure B.4: SDS-PAGE of equal loading of enzymes based on UV-Vis and fluorescence
measurements
Figure B.5: Initial assay of purified DXD mutant enzymes under standard conditions177
Figure B.6: Linearity assay for low activity WT conditions (Culture #1)178
Figure B.7: Assay of WT and DXD mutant enzymes under low activity conditions (#1)178
Figure B.8: Linearity assay for low activity WT conditions (Culture #2)179
Figure B.9: Assay of WT and DXD mutant enzymes under low activity conditions (#2)180
Figure B.10: Summary of mutant activities relative to WT
Figure B 11: Activity of GAUT7 double mutant compared to WT

Figure C.1: Size exclusion chromatography of GAUT1 and GAUT1:GAUT7 protein	188
Figure C.2: Purification of GAUT1:GAUT7 main and aggregate peaks	190
Figure C.3: HG:GalAT activity assay of GAUT1:GAUT7 main and aggregate protein peaks	
following SEC	191
Figure C.4: SDS-PAGE of main protein peaks following SEC purification	192
Figure D.1: GAUT1:GAUT7 versus GAUT1 stability assays	196
Figure D.2: Percentage of HG:GalAT activity recovered during GAUT1:GAUT7 and GAUT1	-
stability assays	197
Figure E.1: Preliminary assay of GAUT1 and GAUT1:GAUT7 activity purified from	
100 mL cultures	203
Figure E.2: Relative initial rate activity of GAUT1	204
Figure E.3: Relative activity of GAUT1 after main peak purification	205
Figure F.1: In-gel GFP fluorescence quantitation of GAUT1 and GAUT7 monomers vs.	
non-reduced complex	210
Figure F.2: Linear dilution of in-gel GFP fluorescence signal	212
Figure F.3: SEC-MALS of GFP-tagged and fully processed GAUT1:GAUT7 complex	213
Figure G.1: CCRC-M38 reactivity toward HG acceptor mix	218
Figure G.2: Sensitivity of CCRC-M38 antibody to HG acceptors enriched for homogenous	
degrees of polymerization	219
Figure G.3: Acceptor-dependent activity detected by ELISA	220
Figure G.4: GAUT1 <i>de novo</i> synthesis activity detected by FLISA	221

INTRODUCTION

The plant cell wall is a polysaccharide and glycoprotein-rich multi-functional extracellular matrix. Biosynthesis and deposition of cell wall polysaccharides begins early during the division of new plant cells. The controlled deposition and loosening of the cell wall is essential for proper development and adhesion of growing plant cells, and the presence of the cell wall provides mature cells with mechanical strength and defense against environmental stresses and pathogenic attack. Several of the plant cell wall polysaccharides are unique to plants, but the study of plant glycobiology has universal relevance because the biosynthetic machinery of polysaccharides shares structures and mechanisms that are homologous throughout all kingdoms of life.

One plant-specific plant polysaccharide is homogalacturonan (HG), a linear polymer of α-1,4-linked galacturonic acid (GalA) residues that is the simplest and most abundant polysaccharide in the family known as pectins. Because plant cell walls are deposited in temporally-organized layers, HG is particularly enriched in the middle lamella, an adhesive layer between cells, and in the primary cell wall (Atmodjo et al., 2013). Although the mass of mature cell walls tends to be dominated by cellulose in the secondary cell wall (Albersheim et al., 2010), the early deposition of HG and abundance in these outer layers means that it is especially important for the dynamic nature of the growing plant cell.

With a GalA carboxylic acid group pK_a near 3, HG is an anionic polysaccharide at physiological conditions (Ridley et al., 2001). The anionic character of HG can be modified by

methylesterification of the carboxylic acid group at O-6 *in vivo*. Methylesterification of up to 80% in some species and tissues has been identified (Atmodjo et al., 2013). The structure of HG is shown in Fig. I.1. The activity describing the synthesis of HG is HG:α-1,4-D-galacturonosyltransferase, abbreviated HG:GalAT. In addition to *Arabidopsis thaliana*, HG:GalAT activity from at least 8 different plant species has been previously characterized (Ridley et al., 2001).

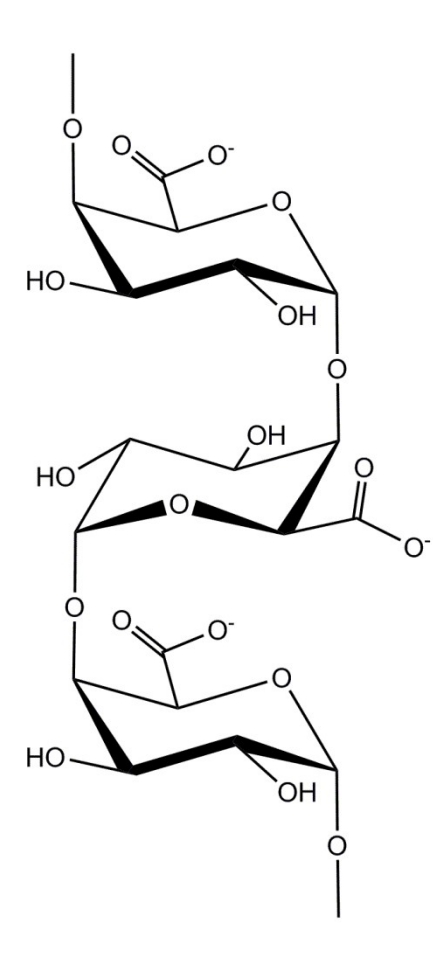


Figure I.1. Structure of homogalacturonan. Homogalacturonan (HG) is a linear homopolysaccharide of α -1,4-linked galacturonic acid (GalA). HG is shown here in the non-esterified, anionic form, as synthesized *in vitro* by HG:GalAT.

HG is synthesized by a family of glycosyltransferases (GTs) annotated as galacturonosyltransferase (GAUT). After partial purification of *Arabidopsis thaliana* membranes enriched for HG:GalAT activity, two putative GTs were identified by tandem mass spectrometry of trypsin-digested solubilized membrane fractions. The HG:GalAT activity of one of these proteins, identified as GAUT1, was demonstrated by both by transient expression of the transmembrane-truncated protein construct in HEK293 cell media and by immunoabsorbtion of HG:GalAT activity by polyclonal antibodies directed against the amino acid sequence for GAUT1 (Sterling et al., 2006).

A multi-gene family containing 15 putative GAUT genes and 10 additional genes named GalAT-like (GATL) was identified. The other protein found in the HG:GalAT membrane fraction identified by mass spectrometry did not yield HG:GalAT activity when expressed in HEK293 cells (Sterling et al., 2006). This protein, identified as GAUT7, was later found to exist in a disulfide-linked complex with GAUT1 when immunoprecipitated from Arabidopsis membranes. Anchoring of GAUT1 within the Golgi membrane was shown to require GAUT7, but it remained unknown whether GAUT7 had any catalytic role in HG biosynthesis (Atmodjo et al., 2011).

The first major goal of the project presented in this dissertation was to establish a heterologous protein expression system that could yield high level expression of the GAUT1:GAUT7 complex. Expression of putative plant cell wall GTs in heterologous systems is an essential part of the process of identifying and confirming biosynthetic activities. The Golgilocalized GTs that synthesize plant cell wall polysaccharide linkages are notoriously low abundance and difficult to study using native plant sources. Measurement of cell wall polysaccharide biosynthetic activity by heterologous expression of GTs is a scientific endeavor

that has a history spanning 20 years since the first successful results were published (Edwards et al., 1999; Perrin et al., 1999).

Chapter 1 presents a review of the literature, focusing on the biochemistry of plant cell wall matrix polysaccharide biosynthetic GTs. Nearly a decade ago, a research article briefly summarized the progress in expression of plant cell wall GTs with proven biosynthetic activity. That article described 10 unique activities, including the HG:GalAT activity of GAUT1 (Petersen et al., 2009). In the total 20-year history of such heterologous expression projects, at least 26 unique activities have now been published. As far as we are aware, this chapter is the only up-to-date review of all currently known plant cell wall matrix polysaccharide biosynthetic activities that have been demonstrated using heterologously expressed enzymes. The changing nature of cell wall models and the strategies used to identify cell wall GTs are summarized. This review is a comprehensive attempt to analyze what is known about the biosynthetic activities, including the reaction kinetics, the polymer chain lengths synthesized, and the enzymatic mechanisms. From this review, we are able to discern the limits of the current data and propose unanswered questions related to cell wall biosynthesis.

Chapter 2 focuses on the expression and activity of the GAUT1:GAUT7 complex. This work expands on previous studies of the GAUT gene family by demonstrating heterologous co-expression and high-yield purification of the disulfide-linked complex. A new activity, the *de novo* initiation of HG synthesis by GAUT1:GAUT7 is presented. Reaction kinetics and polysaccharide chain length analysis are used to propose a complete model of the mechanism of HG biosynthesis by the GAUT1:GAUT7 complex. Because the two standard models for polysaccharide synthesis, known as the processive and distributive mechanisms, were insufficient to describe HG synthesis, we proposed an alternative mechanism, the "two-phase

distributive mechanism." As a result of the work presented here, GAUT1:GAUT7 may be considered the most thoroughly studied cell wall polysaccharide biosynthetic enzyme.

The groundwork publications in which HG:GalAT activity was discovered are revisited in the conclusion section, in light of the discovery of the two-phase distributive mechanism. Future directions in HG synthesis are proposed. The appendices include a summary of additional results related to the study of GAUT proteins expressed in HEK293 cells and preliminary data that address future directions made possible from the results of this project.

CHAPTER 1

LITERATURE REVIEW

GLYCOSYLTRANSFERASE ACTIVITIES OF HETEROLOGOUSLY-EXPRESSED PLANT CELL WALL MATRIX POLYSACCHARIDE BIOSYNTHETIC GENES AND THEIR SIGNIFICANCE FOR WALL POLYMER FUNCTION

ABSTRACT

The life cycle and development of plants requires the biosynthesis, deposition, and degradation of cell wall matrix polysaccharides. The structures of the diverse cell wall matrix polysaccharides influence commercially important properties of plant cells, including growth, biomass recalcitrance, organ abscission, and the shelf life of fruits. This review is a comprehensive summary of the matrix polysaccharide glycosyltransferase (GT) activities that have been verified using in vitro assays following heterologous GT protein expression. Plant cell wall biosynthetic GTs are primarily integral transmembrane proteins localized to the endoplasmic reticulum and Golgi of the plant secretory system. The low abundance of these enzymes in plant tissues makes them particularly difficult to purify from native plant membranes in quantities sufficient for enzymatic characterization, which is essential to study the functions of the different GTs. Numerous activities in the synthesis of the major cell wall matrix glycans, including pectins, xylans, xyloglucan, mannans, mixed-linkage glucans, and arabinogalactan components of AGP proteoglycans have been mapped to specific genes and multi-gene families. Cell wall GTs include those that synthesize the polymer backbones, those that elongate side branches with extended glycosyl chains, and those that add single monosaccharide linkages onto polysaccharide backbones and/or side branches. Three main strategies have been used to identify genes encoding GTs that synthesize cell wall linkages: analysis of membrane fractions enriched for cell wall biosynthetic activities, mutational genetics approaches investigating cell wall compositional phenotypes, and omics-directed identification of putative GTs from sequenced plant genomes. Here we compare the heterologous expression systems used to produce, purify, and study the enzyme activities of plant cell wall GTs, with an emphasis on the eukaryotic systems Nicotiana benthamiana, Pichia pastoris, and human embryonic kidney (HEK293) cells.

We discuss the enzymatic properties of GTs including kinetic rates, the chain lengths of polysaccharide products, acceptor oligosaccharide preferences, elongation mechanisms for the synthesis of long-chain polymers, and the formation of GT complexes. Future directions in the study of matrix polysaccharide biosynthesis are proposed.

Introduction: Plant cell walls as quality factors in fruit and other plant-derived commercial products

Plants synthesize diverse cell wall polymers whose chemical structures contribute to the value of many plant-derived commercial products including wood, fiber and fabric quality, thickening agent properties, drug efficacy, and fruit texture and shelf life. Plant cells are distinguished from other types of biomass by the presence of the plant cell wall (PCW), an extracellular matrix of polysaccharides and glycoproteins. The composition of plant cell walls varies among species and tissues. Cellulose and hemicellulosic polysaccharides can account for > 60% of the dry mass of wood (Hoch, 2007). The fresh weight of tissues with high water content, such as apples, can consist of < 10% cell wall material, the majority of which is pectic polysaccharides (Ng et al., 2013). The study of PCW polysaccharides is central to understanding the physical, chemical and textural properties that give value to plant products.

The deposition, crosslinking, remodeling, loosening, and degradation of matrix polysaccharides occurs in a dynamic manner that influences the progression of plant development (Drakakaki, 2015; Cosgrove, 2016a). The cell wall must have a structure strong enough to maintain cell integrity in response to internal turgor pressure but malleable enough to allow limited and directed cellular expansion (Cosgrove, 2016a). During the fruit ripening process, the cell wall loses structure due to degradation of matrix polysaccharides (pectin and

hemicellulose) and loss of adhesion between polymers in the middle lamella (Seymour et al., 2013; Paniagua et al., 2014). A controlled depolymerization of cell wall structure leads to loosening of cellular adhesion and the associated loss of fruit firmness and the leakage of internal juices that occurs during the ripening process (Toivonen and Brummell, 2008; Paniagua et al., 2014; Dheilly et al., 2016).

Enzymes categorized as glycosyl hydrolases (GHs), lyases, and glycosidases catalyze the degradation of polysaccharide linkages. These families of degradative enzymes are secreted by plants and have been attractive candidates for mutational genetic studies to delay and control fruit softening. The down-regulation of two pectin-degrading genes, *polygalacturonasel* in strawberries and *pectate lyase* in tomatoes, both resulted in extended firmness, a phenotype that may be exploited to increase shelf life (Quesada et al., 2009; Kumar et al., 2014; Uluisik et al., 2016; Wang et al., 2018). The relationship between polygalacturonasel secretion and apple softening was consistent with detection of the gene in 'Royal Gala' apples, a cultivar that softens relatively rapidly, but not in 'Scifresh' apples, whose flesh maintains increased tensile strength during ripening (Ng et al., 2013).

This review highlights progress made in the identification of the biosynthetic glycosyltransferases (GTs) that catalyze the formation of cell wall matrix polysaccharide linkages. The full network of genes associated with cell wall biosynthesis include cellulose and non-cellulosic GTs, lignin pathway biosynthetic enzymes, transcription factors, methyltransferases, acetyltransferases, wall structural proteins, extensins, expansins, and GHs involved in cell wall remodeling. Discovery of the functions of cell wall biosynthetic genes expands the possible targets for mutational genetic studies directed at breeding plants with favorable commercial properties. This review on genes encoding confirmed non-cellulosic

glycosyltransferases exemplifies how the depolymerization of the crosslinked cell wall matrix polysaccharide network observed during organ abscission, senescence, and fruit ripening are made possible by the temporally directed process of cell wall biosynthesis.

Models of crosslinked plant cell wall polysaccharide networks

During cellular division and formation of new plant cells, deposition of cell wall polysaccharides begins concurrent with the delivery of secretory lipids to form a cell plate (Drakakaki, 2015). Plant cells use different growth mechanisms, primarily diffuse growth observed in leaves (Cosgrove, 2018), linear diffuse growth observed in roots, and tip-growth frequently represented by pollen tubes (Palin and Geitmann, 2012). These mechanisms share the coupling of cellular expansion with the secretion of matrix polysaccharides by the plant secretory system (Drakakaki, 2015; van de Meene et al., 2017). Continued secretion of polysaccharides results in three PCW layers, in order of deposition: the middle lamella, the primary wall, and the secondary wall (Cosgrove, 2016b).

Visualization of the precise events of polysaccharide deposition at the moment of cytokinesis is limited due to the available fluorescence microscopy techniques, however, it has been shown that pectic polysaccharides are particularly enriched during cell plate formation (Daher and Braybrook, 2015; Drakakaki, 2015). As new layers of polysaccharides are secreted, internal pressure pushes the early layers outward, resulting in a pectin-rich middle lamella that forms an intercellular space where water and solutes can freely diffuse. A standard view proposes that crosslinking of homogalacturonan (HG) within the middle lamella is a major factor in controlling cellular adhesion, and that loss of this crosslinking is a necessary step in organ abscission and fruit ripening (Daher and Braybrook, 2015).

Cellulose and hemicelluloses are also deposited early during cell plate formation (Drakakaki, 2015). Cellulose is present in the middle lamella and primary walls, but crystalline cellulose microfibrils are more prominently associated with the secondary wall deposited after the cell has stopped expanding (Cosgrove, 2014). A major polysaccharide associated with early cellular development, the β-1,3-glucan callose, is degraded and is not synthesized by mature cells (Drakakaki, 2015).

The layered, heterogeneous nature of plant cell walls has caused frequent debate and revisions to cell wall models in the literature. The cell wall controls cellular expansion by resisting internal turgor pressure, which is often referred to as the "load-bearing" function of cell walls that maintains cellular morphology (Cosgrove, 2016b). Based on the changing understanding of which matrix polysaccharides directly contact cellulose, various polysaccharide components have been assigned the role of "load-bearing" in different cell wall models. An influential early model proposed that the cellulose microfibrils are embedded within, but not contacting, a separate non-cellulosic polysaccharide matrix (Keegstra et al., 1973; Cosgrove, 2016a). Later models recognized the existence of direct contacts between cellulose and xyloglucan (XG), formulating cellulose-XG as the load-bearing network, and pectin as a separate gel-like network (Carpita and Gibeaut, 1993; Cosgrove, 2016a). A complete model of how the cell wall creates a load-bearing network must account for all of the cross-linking interactions, a broad category of covalent and non-covalent contacts that provide strength to the cell wall.

Physical crosslinking of cellulose microfibrils is observable using high-resolution microscopy (Mccann et al., 1990). Cellulose-XG interactions may create adhesion zones that are resistant to depolymerization even though XG may only contact cellulose at limited surfaces (Dick-Perez et al., 2011; Park and Cosgrove, 2015; Cosgrove, 2016a). Xylan binds to the

surface of microfibrils through hydrogen-bonding interactions (Busse-Wicher et al., 2014; Busse-Wicher et al., 2016; Grantham et al., 2017), and antiparallel xylan chains may dimerize through GlcA-sidechain-mediated Ca²⁺ bridges (Pereira et al., 2017). The collection of crosslinking interactions also consists of direct covalent and glycosidic linkages between matrix polysaccharide domains and ferulic acid on lignin, a non-polysaccharide component of PCWs (Tan et al., 2013; de Oliveira et al., 2015).

Pectic polysaccharides also participate in PCW crosslinking interactions. Calcium ions mediate the formation of gel-like complexes between the carboxylic acid groups of GalA in antiparallel HG chains (Grant et al., 1973; Morris et al., 1982; Cabrera et al., 2008). HG crosslinks can be blocked by methylation of the anionic group, reduction of Ca²⁺ concentration, or the presence of chelators. Another pectic polysaccharide, RG-II, forms borate-mediated dimers through an apiose side chain diester, with possible contributions from other side chain monosaccharides such as L-Gal (Ridley et al., 2001; Sechet et al., 2018). Pectic polysaccharides appear to be spatially close to cellulose microfibrils (Wang et al., 2012; Wang and Hong, 2016; Broxterman and Schols, 2018) and possibly also XG (Park and Cosgrove, 2015). The chemical structures mediating pectin interactions with cellulose and XG have not been modeled, but the unexpected observation by solid-state NMR of potential cellulose-pectin contacts at a higher frequency than cellulose-XG contacts has been central to a growing interest in pectic polysaccharides as part of a single load-bearing network involving all cell wall polysaccharides, departing from earlier models (Wang et al., 2012; Cosgrove, 2016a; Wang and Hong, 2016).

The control of HG-Ca²⁺ crosslinks by regulating pectin methylesterification provides a model by which release of tight pectin crosslinks leads to sliding of adjacent wall fibers, allowing internal cell pressure to promote cell expansion. As previously-deposited HG chains

closely associated with cellulose microfibrils become load-bearing polymers in a stretched state, deposition of new HG may remove Ca²⁺ ions from older HG-Ca²⁺ structures, loosening interfibril interactions and priming the cell wall for turgor pressure-mediated expansion (Peaucelle et al., 2012). Uncertainty remains regarding the *in vivo* existence of calcium-linked pectin structures, particularly in the outer layers of cell walls within the apoplast (Hocq et al., 2017; Voiniciuc et al., 2018b). Deposition of de-esterified pectin occurs in root hair tips, which is inconsistent with the model presented by pollen tube tips, in which HG is deposited in a non-crosslinked methyl-esterified form (Mravec et al., 2017). However, chelation of calcium causes cellular separation (Daher and Braybrook, 2015), and downregulation of the pectin biosynthetic gene GAUT4 in transgenic switchgrass causes a reduction in total cell wall calcium (Biswal et al., 2018a). These observations support HG-Ca²⁺ as important for growth and cellular adhesion, as proposed in standard models.

Part of the challenge of building a model of the plant cell wall includes identifying the complete set of genes responsible for cell wall polysaccharide biosynthesis.

Strategies for identifying cell wall glycosyltransferase (CWGT) activities

Plant cell wall matrix polysaccharides are synthesized intracellularly and exported by post-Golgi vesicular transport in the secretory pathway (Kim and Brandizzi, 2014). GTs localized to the Golgi apparatus produce a distinct punctate pattern and co-localize with Golgi markers when transiently expressed as fusion proteins with green fluorescent protein (Boevink et al., 1998; Atmodjo et al., 2011). The correlation of this fluorescent punctate pattern with Golgi localization has been confirmed with higher resolution images obtained using immunogold

labeling, which visualizes individual Golgi stacks (Zhang and Staehelin, 1992; Boevink et al., 1998).

Prior to the identification of individual GTs, biosynthetic activities were measured using microsomal membrane fractions enriched for Golgi-localized enzymes. ER-and-Golgi-enriched microsomal membrane fractions retain integral membrane proteins following centrifugation (Fujiki et al., 1982). These techniques have been used to measure the biosynthesis of PCW matrix polysaccharides since at least the 1960s, with the measurement of Golgi membrane-linked synthesis of the α -1,4-galacturonic acid backbone of HG (Villemez et al., 1965) and the β -1,4-glucan backbone of XG (Ray et al., 1969).

The first enzymes synthesizing specific PCW linkages were identified in 1999, the XG side-chain fucosyltransferase FUT1 (Perrin et al., 1999) and a galactomannan-specific galactosyltransferase (Edwards et al., 1999). Here, we summarize various strategies that have been developed for the identification of putative CWGTs for expression as recombinant proteins. These strategies fall into three broad categories: activity purification, mutational genetics, and omics-directed GT selection. A complementary gain-of-function assay method has also been used as an *in vivo* system to detect synthesis of polysaccharides not normally found in Arabidopsis. The general outline of using these strategies to identify CWGTs) is depicted in Fig. 1.1.

Several factors contributed to the acceleration of GT identification after 1999. The Arabidopsis genome sequence was published and made available in 2000 (Arabidopsis Genome Initiative, 2000) and the Arabidopsis Information Resource has been continually maintained as a database of all annotated Arabidopsis genes since then (Berardini et al., 2015). Lacking complete genomes, some of the early studies mapped gene sequences to expressed sequence tag libraries

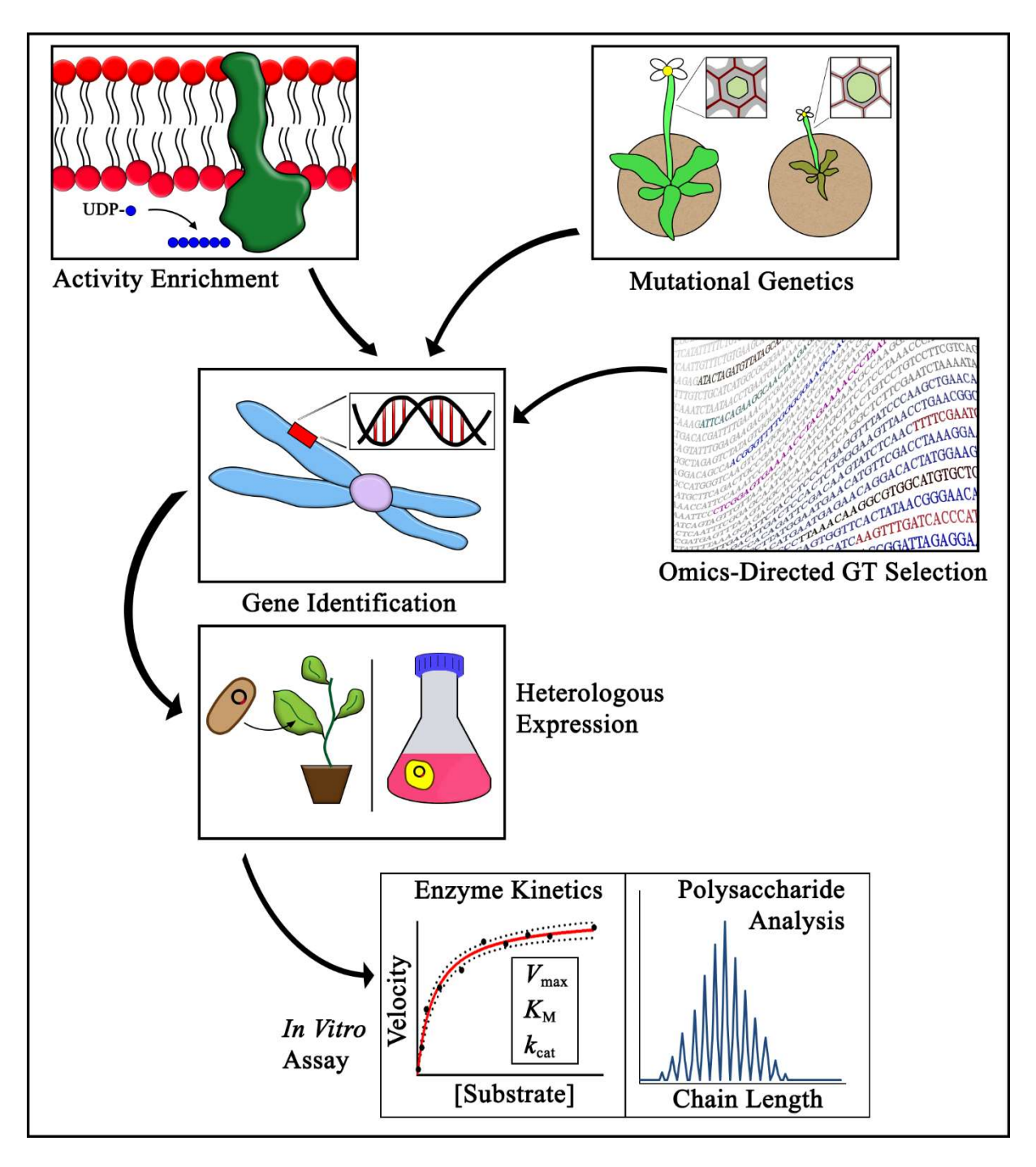


Figure 1.1. Methods for identifying CWGTs for *in vitro* activity verification. The activities of plant cell wall glycosyltransferases have been identified using three main strategies outlined in this review: activity enrichment, mutational genetics, and omics-directed GT selection. Heterologous expression and *in vitro* assays are critical steps in the process of verifying the

synthesis of specific cell wall linkages associated with different families of CWGTs. Purification of enzymes following heterologous expressional enables advanced studies of GT mechanism, including enzyme kinetics and polysaccharide chain length analyses.

(Perrin et al., 1999; Dhugga et al., 2004) or to protein sequence data (Edwards et al., 1999). The Carbohydrate Active Enzymes database (CAZy) was also developed which serves as an essential resource for studies of carbohydrate-acting enzymes. The CAZy database groups characterized and putative GTs and other carbohydrate-active enzymes into families with shared catalytic, mechanistic, and structural characteristics (Lombard et al., 2014).

The families of plant cell wall glycosyltransferases (CWGTs) of known activity, identified following heterologous expression, are summarized in Table 1. Many more genes exist for which mutational genetics and other methods have provided data in support of proposed putative activities, but only enzymes which have been heterologously expressed are considered in this review to have verified activities.

Activity Enrichment

A long-discussed problem in glycobiology is the difficulty of identifying Golgi-localized GTs due to their low abundance (Fukuda et al., 1996; Sandhu et al., 2009). The first plant CWGT mapped to an activity, FUT1, was estimated to be less than 0.01% of total cellular protein (Faik et al., 2000). Activity enrichment requires an activity assay that can detect transfer of a sugar in a specific anomeric configuration and glycosyl linkage using proteins present in microsomal membrane preparations. Incubation of a microsomal enzyme source with nucleotide sugar donors, which are often radiolabeled to enhance detection sensitivity, can lead to incorporation of products into either exogenously added oligosaccharide acceptors or onto endogenous acceptors within the microsomes.

Because the composition of cell wall polysaccharides is different across species, tissues, and developmental stages, techniques have taken advantage of tissues enriched for a specific

CWGT activity. The mannan synthase that synthesizes the β -1,4-mannose backbone of galactomannan (GM) (CSLA9 in Arabidopsis) and the galactosyltransferase (GalT) that adds α -1,6-galactose side chains to the mannan backbone were identified using guar and fenugreek seed endosperms, respectively. Because legume seed endosperms produce large amounts of GM as a storage polysaccharide in early development, GM biosynthetic activities and transcription for these two genes is highly upregulated. N-terminal sequencing of peptides within the activity-enriched fraction identified the putative GT (Edwards et al., 1999; Dhugga et al., 2004). A similar technique was used to identify the glucan synthase that synthesizes the β -1,4-linked backbone of XG (CSLC4 in Arabidopsis) because nasturtium seeds deposit large amounts of XG as a storage polysaccharide (Cocuron et al., 2007).

Synthesis of the homogalacturonan backbone, α-1,4-linked GalA, has been detected using microsomal preparations from varied plant sources, including pea (Villemez et al., 1965), tobacco (Doong et al., 1995a), Azuki bean (Yasui, 2009), and *petunia axillaris* (Akita et al., 2002). Sequential purification led to a semi-purified Arabidopsis membrane fraction enriched for proteins with the predicted GT sequences for GAUT1 and GAUT7. Activity was traced over multiple purification steps using an assay in which GalA is transferred from UDP-GalA onto oligogalacturonide acceptors (Sterling et al., 2006). Recently, development of an assay to measure the transfer of rhamnose from UDP-Rha onto acceptors with the [-4-GalA-α-1-2-Rha-α-1-] disaccharide backbone-repeat of rhamnogalacturonan-I (RG-I) enabled the detection of RG-I biosynthetic activity in Azuki bean epicotyls (Uehara et al., 2017). Because RG-I is upregulated in Arabidopdis seed coat mucilage, RRT1 was identified by the predicted GT sequence downregulated following knockdown of two mucilage-related transcription factors (Takenaka et al., 2018).

Mutational Genetics

A second strategy identifies CWGTs from cell wall-specific phenotypes caused by mutations in unique GT sequences. Because the monosaccharide linkages of cell wall polysaccharides are known, deficiency in a particular monosaccharide linkage in a mutant is generally hypothesized to be due to a mutation in an enzyme associated with synthesis of that linkage.

In a landmark study, 11 genes were identified in a screen of 5200 mutagenized plants by screening for losses or changes in cell wall monosaccharide composition and were annotated MUR1-MUR11 (Reiter et al., 1997). Two of the genes identified in that study, MUR2 (FUT1) and MUR3 have been mapped to XG backbone biosynthetic functions. The *mur2* mutant was strongly deficient in cell wall fucose, specifically XG fucosylation (Reiter et al., 1997; Vanzin et al., 2002). FUT1 was independently identified by an activity enrichment method using solubilized pea epicotyls (Perrin et al., 1999), and these activity results were consistent with the fucosyl transferase defect caused by the mutant (Vanzin et al., 2002). MUR3 was found to encode the galactosyltransferase that adds the galactose L side chain of XG. The *mur3* mutant was also defective in XG fucosylation because the galactose transferred by MUR3 serves as the acceptor for fucose during the synthesis of the F side chain by FUT1 (Madson et al., 2003).

Another series of mutants, the *irregular xylem* or *irx* mutants, have proposed functions in cell wall synthesis. The irregular xylem phenotype was originally described in three mutants, annotated *irx1-irx3*, based on a collapsed xylem phenotype visible in cross-sections of stem vascular tissues. This phenotype was predicted to be relevant to the loss of secondary cell wall polysaccharides necessary to maintain cell wall integrity during water transport and transpiration (Turner and Somerville, 1997). Additional mutations yielding the irregular xylem phenotype

have been visualized (Brown et al., 2005), leading to the identification of IRX10-L and IRX10 GTs that synthesize the β -1,4-linked xylose backbone of xylan (Jensen et al., 2014; Urbanowicz et al., 2014). Four related proteins with a similar mutant phenotype, IRX9, IRX9-L, IRX14, and IRX14-L, are putative xylan biosynthetic GTs, but their activities have not been confirmed *in vitro* (Smith et al., 2017).

At least two other CWGTs have been identified based on their mutational genetic phenotypes. XAX1, a XylT that adds xylose side chains to grass arabinoxylans, was identified in a reverse genetics screen focused on GT61 enzymes due to a cell wall xylan deficiency (Chiniquy et al., 2012). XGD1, which adds xylose to the HG backbone, was identified from mutants that were 25% deficient in xylose composition (Jensen et al., 2008).

Omics-Directed GT Selection

The omics-directed GT selection approach bypasses the step of first measuring activities within native plant microsomal enzyme sources or identifying a putative GT from mutant phenotypes. Rather, omics data are analyzed using bioinformatics to predict GTs from genomic sequences prior to recombinant expression and assaying of an enzyme's GT activity. GTs have common features that are conserved across species which may include the presence of transmembrane (TM) domains, conserved motifs, and three-dimensional structural folds (Lairson et al., 2008). Structural features most commonly exploited in bioinformatics approaches have been the type II TM structure and the presence of Asp-X-Asp (DXD) motifs that participate in nucleotide sugar substrate binding in GT A fold type glycosyltransferases (Sarria et al., 2001; Egelund et al., 2004; Lairson et al., 2008; Qu et al., 2008).

The CAZy database groups putative GTs annotated in genomic databases into families that are predicted to share structural folds and sequence similarities based on their primary amino acid sequences. (Lombard et al., 2014). A GT clone collection consisting of over 400 Arabidopsis GT sequences, representing 88% of the putative CWGTs listed in CAZy, has been created to simplify the process of heterologous expression (Lao et al., 2014). Given the limited number of nucleotide sugar donors needed to synthesize all PCW glycosyl linkages, GTs can be screened for activity even without a predicted donor substrate. For example, XGD1 expressed in *N. benthamiana* was incubated with five different radiolabeled UDP-sugars, but only UDP-xylose led to significant levels of radiolabel detected in polymeric products (Jensen et al., 2008). The technique of nucleotide sugar suite screening is effective due to the tendency of GTs to hydrolyze specific nucleotide sugar substrates *in vitro*, transferring the glycosyl residue to water in the absence of an exogenously-added acceptor. Therefore, many GT activities can be detected without knowledge of the proper acceptor substrate (Sheikh et al., 2017).

A prominent example of a CWGT discovered through prediction from sequence homology is the β -1,4-GalT activity of GALS1. The GT92 family was proposed following the phylogenetic analysis of a β -1,4-galactosyltransferase from *C. elegans* (Titz et al., 2009). In studying the Arabidopsis GT92 proteins of unknown function, a combination of mutational genetics in which plants had a deficiency in β -1,4-galactan in the cell wall and omics-directed GT selection revealed that the protein later annotated as GALS1 incorporated galactose into β -1,4-galactan acceptors using UDP-Gal as a sugar donor (Liwanag et al., 2012a). This enzyme was later found to have a secondary activity, in which GALS1 can terminate chain elongation by transfer of an Ara_p residue onto the same acceptors (Laursen et al., 2018a).

The reasoning leading to the discovery of the GalT activity of GALS1 is unlikely to apply to all GT families. The GalT activity of GALS1 was predicted because GT92-family proteins contain β-1,4-galactan synthases in other organisms (Liwanag et al., 2012a). In contrast, a GT family is not necessarily limited to a single nucleotide sugar donor. For example, the GT8 family, which contains GAUT family enzymes that transfer GalA from UDP-GalA (Sterling et al., 2006), also contains enzymes that use UDP-Glc (Gibbons et al., 2002b), UDP-Gal (Persson et al., 2001), UDP-Xyl (Inamori et al., 2012; Yu et al., 2015), and UDP-GlcNAc sugar donors (Yoko-o et al., 2003; Chen et al., 2016). Within this single GT family, activities also vary between single-addition linkages, polysaccharide chain polymerization activities, and protein Olinked glycan synthesis. Classification within a CAZy family may only be expected to predict the three-dimensional structural fold and the stereospecificity of the linkage (retention vs. inversion of the anomeric configuration relative to the nucleotide sugar donor) (Lombard et al., 2014).

The cellulose synthase-like (CSL) superfamily contains several sub-clades with predicted β-linked polysaccharide synthesis activities (Little et al., 2018). Four monosaccharides (D-Glc, D-Gal, D-Man, and D-Xyl) can form β-linked polysaccharide backbones in plant cell walls. Using a combination of all of the approaches described above, each β-linked hemicellulose (xyloglucan, mixed-linkage glucan, xylan, mannan, galactomannan) has been assigned to one or more of the CSL families. Monosaccharide composition was not able to directly implicate *csld* mutants in the biosynthesis of a particular hemicellulosic polysaccharide, but incubation of microsomal membranes prepared from *N. benthamiana* leaves transfected with CSLD genes with the four possible UDP-sugars was instrumental to identifying the CSLD family as mannan synthases. Enhanced activity from microsomes expressing CSLD5 or co-expressed CSLD2:CSLD3 was only detected with UDP-Man (Verhertbruggen et al., 2011; Yin et al.,

2011). Uncertainties remain regarding gene redundancy within the CSLD family, the size of mannan polysaccharides synthesized, and mechanistic details of mannan synthesis. The activity of CSLD is considered not to have been definitively identified (Little et al., 2018). However, current activity assays suggest that the CSLA and CSLD families both encode mannan synthases.

With the mapping of most or all PCW backbone synthesizing enzymes to one or more GT families (conclusive identification of the RG-I backbone polymerizing activity remains to be confirmed), the identity of the GTs that catalyze the synthesis of the more challenging and numerous side-chain linkages remains to be completed. Omics-directed GT selection has provided powerful approaches to identify GTs that synthesize side-chain linkages among the hundreds of putative GTs in plant genomes. XXT1, one of the XylT enzymes that synthesize the X side chain of XG, was identified by prediction due to its grouping in GT34, the same family as the previously-identified fenugreek mannan GalT. The XylT activity was first detected in pea microsomes, and then the XXT enzyme was identified as the only one of 7 expressed GT34 enzymes with XylT activity (Faik et al., 2002). The GT77 family containing the RGXT family of four enzymes with XylT activity involved in RG-II side chain A synthesis was identified using a bioinformatics approach aimed at searching for cell wall GTs of previously-unidentified function (Egelund et al., 2004; Egelund et al., 2006). Coexpression servers were used to predict the activity of the xylan-active GUX family which adds GlcA onto the xylan backbone. This GT coexpresses with other xylan biosynthetic enzymes (Mortimer et al., 2010; Rennie et al., 2012).

Omics-based bioinformatic approaches have been particularly fruitful for identifying enzymes related to arabinogalactan protein (AGP) glycosylation. The GT31 family in Arabidopsis contains the GALT and HPGT families that initiate Gal synthesis on hydroxyproline residues, At1g77810 which elongates β -1,3-Gal backbones, and the GalT31 family that elongates

β-1,6-Gal side branches (Qu et al., 2008; Basu et al., 2013; Geshi et al., 2013; Ogawa-Ohnishi and Matsubayashi, 2015; Showalter and Basu, 2016). The Arabidopsis FUT family, GT37, is unique in that this family contains enzymes that function in the synthesis of different types of PCW polysaccharides and glycoconjugates including xyloglucan and AGPs. Mutational genetics revealed that fucosylation is important for root expansion, and the high expression of FUT4 and FUT6 in roots led to their identification as having AGP-specific FucT activities (Sarria et al., 2001; Tryfona et al., 2014).

Recent advances in the production of suitable acceptor substrates with PCW-relevant glycan linkages hold promise for increasing the rate of identifying CWGTs. The purification of heterogeneous acceptor mixes of complex glycans such as AGPs has enhanced detection of GT activity from the putative genes identified by omics-directed selection (Xu et al., 2005; Geshi, 2014). The availability of a heterogeneous mixture of AGP oligosaccharide acceptors makes it possible to identify enzyme activity by incubating the expressed enzyme with an acceptor mixture and a wide range of radiolabeled nucleotide sugar donors, followed by the use of structure-specific hydrolases to map the location of radiolabel incorporation. AGP-specific gene families GALT31A, GALT29A, and GlcAT14 were identified using this approach (Geshi et al., 2013; Dilokpimol and Geshi, 2014; Dilokpimol et al., 2014). Some uncertainties remain over the functional redundancy of the large number of β-Gal transferase activities that synthesize 1,4; 1,3; and 1,6 AGP linkages (Showalter and Basu, 2016). More precise acceptors will be necessary to understand the length control or regiospecificity of enzymes within this family.

Some acceptors, especially complex polysaccharides such as RG-II with many highly specific side-chain linkages, cannot easily be purified. New bacterial hydrolases capable of catalyzing the cleavage of almost all of the specific linkages within the RG-II side chains have

been identified and biochemically characterized (Ndeh et al., 2017). The availability of hydrolytic enzymes allows for the production of acceptor substrates for activity assays, and the specific hydrolysis of enzymatically-formed glycan linkages is a common method to verify the activity of a recombinant enzyme. Additionally, large libraries of glycan epitopes have been synthetically produced that will be useful to define the acceptor substrate specificity of individual GTs (Bartetzko and Pfrengle, 2018). The structural complexity of PCW glycans will require a combination of the above techniques to resolve outstanding questions in cell wall biosynthesis.

Gain-of-Function Assays

The gain-of-function assay method does not involve heterologous expression of an identified putative GT to confirm enzyme activity. Instead, gain-of-function assays take advantage of the ability of the intracellular machinery of transgenic cell cultures to synthesize polysaccharides not normally detected in the native organism. Mixed-linkage glucans (MLGs) are unbranched, unsubstituted β-glucan chains that contain both 1,3 and 1,4 linkages arranged in a nonrepeating but nonrandom fashion. MLGs are a class of cell wall polysaccharide upregulated in grasses, but are not synthesized by Arabidopsis (Doblin et al., 2009). The synthesis of MLG has now been mapped to three different families, CSLF, CSLH, and CSLJ, by overexpression of representative enzymes in either Arabidopsis or tobacco cells (Burton et al., 2006; Doblin et al., 2009; Dimitroff et al., 2016; Little et al., 2018). Similarly, xylan structures are different across species, and Arabidopsis has a limited ability to synthesize arabinose-containing side chains (arabinoxylan). Two GT61 enzymes that synthesize arabinoxylan side-chains, XAT and XAX, were discovered by gain-of-function assays that led to the detection of arabinoxylan in

Arabidopsis cell walls (Anders et al., 2012; Chiniquy et al., 2012). Similar techniques have recently been developed to study mannan synthesis in *Pichia pastoris* (Voiniciuc et al., 2019).

Heterologous expression systems for plant cell wall GTs

Membrane-based eukaryotic expression: Nicotiana benthamiana and Pichia pastoris

N. benthamiana and P. pastoris are the two eukaryotic systems most commonly used to express CWGTs. Microsomal membranes enriched for the protein of interest are prepared following transient expression of gene constructs in N. benthamiana leaves or P. pastoris cells. Activity can be measured directly in the membrane fraction or the protein of interest can be purified by affinity chromatography following solubilization of membranes. Radiolabeled nucleotide sugar donors are frequently used to distinguish polysaccharide products synthesized in vitro from previously-synthesized polysaccharides within the membrane preparation. The main advantage of these systems is the expression of full-length, membrane-bound proteins, which is especially beneficial for the multi-TM-domain containing GT2-family enzymes of the CSL superfamily (Liepman et al., 2005; Cocuron et al., 2007; Yin et al., 2011)

When microsomal membrane preparations are used, the expressed proteins exist in unknown concentrations relative to the entire membrane protein population, which is a heterogeneous mixture of proteins derived from the ER and Golgi of the host organism. Typically, activity assays are completed using an equivalent amount of microsomal membrane protein compared to background controls to account for native biosynthetic activities (Liwanag et al., 2012a; Rennie et al., 2012; Basu et al., 2013). Proteins have been purified from these sources that have been able to yield activity, but protein concentration was generally too small to

be measured (Liwanag et al., 2012a; Rennie et al., 2012), making these systems unsuitable for precise kinetics or x-ray crystallography studies.

Soluble eukaryotic expression: HEK293 cells

Most Golgi-localized GTs are predicted to have a type II membrane protein structure, with a single TM domain and a catalytic domain that faces the Golgi lumen (Kellokumpu et al., 2016). For GTs with this type II membrane structure, systems have been established allowing soluble protein expression. Truncation of the TM domain and coupling with a recombinant N-terminal secretion signal allows eukaryotic hosts to process soluble GTs using the secretory pathway. The human embryonic kidney cell system (HEK293 cells) and a vector library of all known human GTs has been established, resulting in high-yield soluble expression (Moremen et al., 2018). Recent efforts have begun to adapt this system for the expression of plant cell wall biosynthetic GTs.

The highest yield of a heterologously expressed CWGT that has been reported was for FUT1 from two HEK293 cell lines, HEK293F and HEK293S, ranging from ~100-120 mg/L cell culture volume (Urbanowicz et al., 2017). The enhanced yields from HEK293 cells have made possible the solutions of the first two crystal structures of CWGTs, FUT1 and XXT1 (Urbanowicz et al., 2017; Culbertson et al., 2018). Xys1 from Arabidopsis and a green algal species (*Klebsormidium flaccidum*), XXT2, and the GAUT1:GAUT7 complex have also been expressed in HEK293F cells in sufficient quantities for detailed enzymatic characterization and kinetics studies (Urbanowicz et al., 2014; Amos et al., 2018; Jensen et al., 2018; Ruprecht et al., 2018).

Secretory pathway proteins undergo folding and post-translational modification within the endoplasmic reticulum. Two post-translational modifications important for protein folding are *N*-glycosylation and disulfide bond formation. Protein glycosylation is a major part of the quality control system by which eukaryotic cells prevent misfolded proteins from exiting the ER and entering the later compartments of the secretory system (Xu and Ng, 2015). The ability of eukaryotic expression systems to carry out these posttranslational modifications may be necessary for successful protein expression and GT recovery.

Soluble bacterial expression: Escherichia coli

E. coli is frequently the preferred system for heterologous expression of enzymes due to the relatively inexpensive growth media and minimal training required to express proteins (Kaur et al., 2018). However, E. coli has been largely ineffective for the expression of CWGTs, likely due to insufficient protein translational folding and N-glycosylation (Welner et al., 2017; Kaur et al., 2018). Some bacteria, notably C. jejuni, do have N-glycosylation pathways. Efforts have been made to engineer E. coli cells with the N-glycosylation locus of C. jejuni and to use periplasmic-directed expression vectors to assist in the folding of heterologously-expressed eukaryotic proteins (Fisher et al., 2011; Valderrama-Rincon et al., 2012). In general, however, the protein glycosylation pathways in E. coli are not comparable to those of eukaryotic systems (Nothaft and Szymanski, 2013). The oxidative environment of the periplasm performs protein folding and disulfide bond formation in E. coli, but the system of chaperones and oxidizing enzymes are not capable of properly folding many complex eukaryotic enzymes (Groff et al., 2014; Hatahet et al., 2014).

A high-throughput study has recently been published in which expression in *E. coli* was attempted for 46 CWGTs. Soluble versions of CWGTs that have been successfully expressed in eukaryotic sources, including IRX10L (Xys1), MUR3, GALS1, and GAUT1, were either not expressed or expressed at very low yields, and none them were purified or assayed for activity (Welner et al., 2017). Large-scale cultures *E. coli* may only expect to yield, at most, low microgram quantities of soluble protein. Reversibly glycosylated peptide-1 (RGP1), which is a cytosolic mutase, not a Golgi-localized CWGT, was expressed with a yield of ~1 mg from a 2L culture (Welner et al., 2017). The lack of success of purifying soluble CWGTs in this wideranging study is consistent with the known theoretical limitations associated with the recombinant expression of complex eukaryotic proteins in bacterial systems.

The xyloglucan xylosyltransferase (XXT)-family enzymes and the AGP enzyme GalT31A are the only examples of CWGTs from which *E. coli* expressed proteins have yielded activity (Chou et al., 2012; Vuttipongchaikij et al., 2012a). In one study, 3-7 µg of XXT enzyme was recovered from a 75 mL culture by purifying enzymes directly from supernatants using glutathione beads (Vuttipongchaikij et al., 2012a). GalT31A was purified by a similar method, also yielding low microgram amounts (Geshi et al., 2013). Another study purified sufficient amounts of protein to compare the kinetic rates of three family members, XXT1, XXT2, and XXT5 (Culbertson et al., 2016), but it remains unlikely that optimized expression in *E. coli* will yield the milligram quantities of enzyme needed for structural studies that have been obtained using HEK293 cells.

The biosynthesis of extended-chain backbone polymers

Plant cell walls contain polysaccharides that have been measured as long-chain polymers consisting of hundreds to thousands of monosaccharide units. Estimation of polysaccharide size requires careful consideration of the source of the cell wall material, structural information potentially lost during the chemical and enzymatic extraction of polysaccharides from heterogeneous plant tissues, and differences in measurement techniques. Size exclusion chromatography (SEC), multiangle light scattering (MALS), nuclear magnetic resonance (NMR), atomic force microscopy (AFM), and mass spectrometry (MS) have been the primary methods by which chain length has been measured. Table 2 summarizes estimated chain lengths of major matrix polysaccharides made by plants, and compares these sizes to the products synthesized *in vitro* by recombinant enzymes.

Estimates of cell wall polymer chain length

As indicated in Table 2, there are major discrepancies between the sizes of polymers synthesized *in vivo* with the sizes of polymers synthesized *in vitro* that have been measured. Reactions using recombinant enzymes could provide a promising tool to make more accurate measurements of PCW polysaccharide length by making possible precise control of the reaction components and isolation of a single polysaccharide product. In most cases, size information from *in vitro* reactions has not been measured or is inconsistent with the expected polysaccharide sizes based on products extracted from plant cells.

Current estimates suggest that the longest PCW polymers are XG, mannan, and MLG. All three of these polysaccharides are synthesized by CSL-family GT2 enzymes (Table 1), indicating a possible connection between chain length and GT domain structure. Size exclusion

chromatography has resulted in estimates of XG chain lengths spanning two orders of magnitude (9-900 kDa). Measurements from AFM (90 kDa) are consistent with this backbone polysaccharide being synthesized to high degrees of polymerization *in vivo* (Park and Cosgrove, 2015). However, no current estimate exists for the size of XG or MLG synthesized *in vitro*. Both short-chain and high molecular weight (MW) mannan structures have been isolated (Ebringerová et al., 2005). Whereas pure mannan synthesized *in vitro* by CSLA9 was confined to very large molecular weights, glucomannan eluted with much broader retention volumes (Liepman et al., 2005; Voiniciuc et al., 2019).

Measurements of HG extracted from plants have suggested a more constrained polymer size. Size exclusion chromatography has suggested a range of 14-20 kDa (degree of polymerization; DP 81-117) for the HG backbone, and HG was measured by AFM as ~60 kDa (DP 320). Short HG glycans less than 10 residues are also embedded within RG-I domains, both as complex heteropectins and as part of larger AGP-linked proteoglycans (Nakamura et al., 2002; Tan et al., 2013). HG polysaccharides have been synthesized *in vitro* with chain lengths longer than these expected sizes. GAUT1:GAUT7 appears to be able to synthesize long-chain HG polymers of an indefinite size (> 100 kDa; DP > 500) *in vitro* (Amos et al., 2018). These results suggest that length control, at least for HG, may not be an intrinsic property of CWGTs, and may require more complex mechanisms *in vivo*.

Estimates from *in vivo* synthesized polysaccharides may be high if the extent of branching and size chains are not considered. The RG-I polysaccharide was originally measured as a long chain of 100-1000 kDa based on size exclusion chromatography of the full polysaccharide (McNeil et al., 1980; Albersheim et al., 2010). SEC-MALS estimates have measured the debranched GalA-Rha disaccharide backbone of citrus RG-I as 15 kDa, accounting

for only 26% of the mass of a full 56 kDa polymer (Yapo et al., 2007). The differences in size reported for RG-I could be explained by the different source materials (sycamore vs. citrus) or the variation in branching patterns. AG side branches associated with RG-I are themselves branched, and the longer estimates (up to DP 200) likely do not represent a single core polysaccharide (Yapo, 2011). AGs associated with AGP proteins are also highly branched with estimates of 5-25 kDa accounting for the entire polymer (Ellis et al., 2010).

Limitations of chain length estimation by size exclusion chromatography

Although size exclusion chromatography is a common method used for measuring polysaccharide size, it may result in over-estimation of chain length. Polysaccharides are generally compared to commercially available dextran standards. Differences in polysaccharide stiffness relative to dextrans and the non-globular conformation of polysaccharides may cause these methods to report inaccurate molecular weights (Harding, 1991). Size exclusion may also misrepresent polysaccharide length due to the potential for aggregation of polymers or changes to the particle conformations resulting from substitution and decoration. (Mort et al., 1991; Park and Cosgrove, 2015).

Glucuronoxylan was estimated as having an average chain length of DP 93 using NMR spectroscopy based on the ratio of reducing end to internal signals, corresponding to a molecular weight of ~12 kDa. The same polysaccharide elutes at a position larger than a 70 kDa based on dextran standards (Pena et al., 2007). This polysaccharide provides an example in which size exclusion may over-estimate the size of a polymer by at least 5-fold. Additional size exclusion chromatography-based molecular weight measurements of glucuronoxylan ranged from 5-130 kDa (Ebringerová et al., 2005).

Depending on the standards used in a given experiment, pectic polysaccharides synthesized *in vitro* have been observed to elute at retention volumes larger than 100 kDa and even 500 kDa based on dextran standards (Doong et al., 1995a; Sterling et al., 2001; Amos et al., 2018). Most standard columns may have limited resolving power at these high MW, resulting in dextran standards > 100 kDa tending to elute with overlapping chromatographic patterns and peaks near the column excluded volume. Under donor substrate-limiting conditions, in which GAUT1:GAUT7 synthesizes HG polymers of approximately DP 30-50 (~5-9 kDa) as indicated by individual bands on polyacrylamide gels, the same donor-limited polysaccharides elute at intermediate sizes between 12 kDa and 50 kDa based on dextran standards (Amos et al., 2018), again indicating that these cell wall polymers appear larger by size exclusion analysis than when measured by other approaches.

Mechanisms of high molecular weight polysaccharide elongation

The elongation of long-chain polysaccharides can occur by an enzymatic mechanism in which a single acceptor molecule binds to the active site and undergoes multiple rounds of elongation before release from the enzyme. This mechanism of synthesis is referred to as enzyme processivity. Because the polysaccharide grows progressively longer during processive synthesis, it must slide along the enzyme without becoming fully detached following each monosaccharide transfer (Breyer and Matthews, 2001). Processive mechanisms can be distinguished from distributive (also called non-processive) mechanisms, in which the enzyme releases the polysaccharide chain following each individual monosaccharide transfer.

Processive enzymes tend to have structural elements that enclose the elongating substrate (Breyer and Matthews, 2001). Several mechanisms exist by which a substrate can be physically

constrained within an enzyme active site, preventing diffusion of the product into the surrounding environment. Some glycosyl hydrolases retain their polysaccharide substrates within a tunnel abundant in aromatic amino acyl residues that interact with the sliding carbohydrate chain (Beckham et al., 2014). DNA polymerases form multi-enzyme complexes with sliding clamp enzymes that maintain the DNA-enzyme interaction (Breyer and Matthews, 2001).

The crystal structure of the bacterial cellulose synthase BcsA demonstrates one of the clearest examples of a mechanism for a processive GT. The cellulose synthases, which are CAZy GT2-family enzymes, have multiple TM domains that form a pore through which the growing polysaccharide chain translocates. BscA accommodates a cellulose chain 10 glucose residues in length, spanning from the cytosolic GT domain to the periplasmic pore exit (Morgan et al., 2013). This structural motif, common to GT2-family enzymes, shares homology with other enzymes that synthesize secreted or extracellular matrix polysaccharides, including chitin and hyaluronic acid (Bi et al., 2015).

Notably, all of the CSL-family proteins, implicated in the synthesis of PCW β-1,4-glucans (XG, heteromannan, and MLG), are GT2-family enzymes and are predicted to share this multi-TM domain structure (Davis et al., 2010). In contrast, many other GTs have type II membrane domain structures containing only a single TM domain and do not have a similar translocation pore/tunnel. Xys1 is a rare example that has no predicted TM domain (Smith et al., 2017). Xys1 and the type II membrane complex GAUT1:GAUT7 synthesize xylan and HG using distributive (non-processive) mechanisms (Urbanowicz et al., 2014; Amos et al., 2018). Xylan and HG are both long-chain polysaccharides (Table 2), suggesting that processivity is not a requirement for the synthesis of extended polymeric glycans. On the basis of the membrane

structure of the biosynthetic CWGTs, RG-I and AGP may also be predicted to be elongated by non-processive mechanisms.

Solubility limitations of long-chain polysaccharides

The ability to detect high MW products *in vitro* can be hindered by issues with the solubility of longer-chain oligosaccharides. The β -1,4-glucan backbone of XG has minimal solubility above DP 6 and the β -1,4-mannan backbone of mannan is insoluble above DP 8. These insoluble polymers are synthesized by GT2-family CSL enzymes. However, XG extracted from plant cells is soluble due to the presence of side-chain decorations that reduces the amount of intermolecular hydrogen bonding, distinguishing XG from the glucan chains of cellulose microfibrils (Yuguchi et al., 2005). We propose that a likely purpose of the multi-TM domain structure that confers processivity on these transferases is to protect these polysaccharides against aggregation during elongation before other enzymes in the pathway can add side chain decorations (or in the case of cellulose, to enable controlled fiber formation).

The structures of glycosyl hydrolases suggest a connection between processivity and insoluble crystalline polysaccharides, represented by cellulose and chitin (Vaaje-Kolstad et al., 2013). The bacteria Serratia marcescens has three GH18 chitinases, ChiA, ChiB, and ChiC. Both ChiA and ChiB have deep clefts for binding to a chitin chain and display higher levels of processivity in activity assays, which is consistent with the hypothesis that processive enzymes enclose their substrates within tunnels. The non-processive chitinase ChiC does not have a similar deep cleft lined with aromatic residues to facilitate processive sliding. Accordingly, ChiC hydrolyzes the soluble form of chitin, chitosan, at higher rates. The structural and activity differences within this family of chitinases suggest that GH enzymes evolved processivity to

enhance activity on chains detached from insoluble crystalline polysaccharides while sacrificing enzymatic efficiency (Horn et al., 2006; Vaaje-Kolstad et al., 2013).

Preference for long-chain acceptors – the two-phase mechanism

It has been frequently observed that CWGTs assayed *in vitro* either require acceptors above a certain minimum chain length or show large activity increases toward longer acceptors. These rate increases are often observed with oligosaccharides of a size of DP of 5 to 10 (Table 1). Due to limited availability and the insolubility of oligosaccharide acceptors described above, most CWGTs have not been studied using acceptors of varying DPs.

Increased activity with longer-chain acceptors, and the relevance of this to enzyme mechanism, has been most thoroughly studied in HG elongation by GAUT1:GAUT7. Relative to a DP 7 acceptor, DP 11 acceptors are elongated at a \sim 6-fold higher rate. DP 11 acceptors also have a \sim 7-fold higher affinity, as estimated by the K_M value measured in Michaelis-Menten kinetics assays. Enzyme kinetics analyses support a comparison of enzymes by combining information on the rate of synthesis (k_{cat}) with the affinity of the enzyme for a substrate (K_M) to yield a value known as the specificity constant (k_{cat}/K_M), which is a measure of the catalytic efficiency of a reaction (Copeland, 2002). For GAUT1:GAUT7, the catalytic efficiency of a DP 11 HG acceptor is > 45-fold higher than for that of a DP 7 HG acceptor. The presence of a lag phase during elongation of DP 7 HG acceptors means that the initial-rate preference for DP 11 acceptors is possibly much higher than this value (Amos et al., 2018).

Earlier measures of HG synthesis using solubilized tobacco microsomes were unable to detect elongation of acceptors with a DP < 10 (Doong and Mohnen, 1998). Similarly, solubilized *P. axillaris* microsomes detected some elongation of acceptors DP 5-10, but large rate increases

were observed with DP \geq 12 acceptors (Akita et al., 2002). The elongation of short-chain acceptors and the *de novo* initiation of new HG chains were able to be detected *in vitro* using purified GAUT1:GAUT7 enzyme, but with low initial rates of synthesis (Amos et al., 2018). Microsomal sources did not detect these activities, which was likely due to the relatively low enzyme purity and activity measurements achievable using the semi-purified membranes.

There are several other examples in which CWGTs have a minimum acceptor size. XXT1 transfers Xyl to XG backbone acceptors of DP > 4. Activity is increased \sim 6-fold using DP 6 acceptors relative to DP 5 acceptors (Faik et al., 2002; Cavalier and Keegstra, 2006). The fenugreek GalT that transfers side chain Gal monosaccharides onto mannan backbones has a similar \sim 5-fold increase in activity with DP 6 acceptors compared to DP 5 acceptors, and no activity for DP 1-4 oligosaccharides (Edwards et al., 1999). GUX1 transfers GlcA to xylan backbone acceptors with a preference for DP 6 oligosaccharides, which is a \sim 10-fold increase over DP 2 acceptors (Rennie et al., 2012). GalS1 likewise prefers to elongate galactan acceptors with a DP \geq 5, and the same galactosyltransferase activity from mung bean microsomes was shown to be \sim 3-fold greater for DP 7 acceptors than DP 5 acceptors (Ishii et al., 2004; Liwanag et al., 2012a).

These observations are consistent with a proposed two-phase kinetic mechanism which may be common to CWGTs, in which longer-chain acceptors are elongated at significantly increased rates compared to acceptors below a certain critical DP (Amos et al., 2018). The consequence of two-phase elongation is that elongation of short-chain acceptors may not be detected in some assays because the transfer requires longer incubation times or occurs below the detection limit. Although all of the above-mentioned cell wall-related GTs with preference for longer acceptors appear to be distributive, two-phase elongation is also a feature of bacterial GT2

enzymes, which are known to be processive (Forsee et al., 2006; Levengood et al., 2011). The expected polysaccharide elongation patterns for the three mechanisms of chain elongation: processive, distributive, and two-phase distributive glycosyltransfer are depicted in Fig. 1.2. Chain elongation analysis is integral to determining the mechanisms used by CWGTs to synthesize the full-length polysaccharides deposited into mature cell walls. Without structural data, elongation analysis is the only method to distinguish between these three forms of GT mechanism.

Initiation, elongation, and length control during polysaccharide biosynthesis

The existence of multi-enzyme families presents the possibility that some CWGTs are limited to the initiation of new polysaccharide chains, whereas other genes in the same family extend polymers during an elongation phase. The low catalytic efficiency of short-chain acceptors also contributes to difficulties in measuring chain initiation. Synthesis of XG, mannan, and MLG backbones has been measured using microsomal enzyme sources without the addition of exogenous acceptors (Table 1). In each case, it is unclear whether the heterologously expressed enzymes elongated endogenous acceptors previously synthesized by the plant cells, or if the CSL-family enzymes responsible for these activities are able to initiate chain synthesis *de novo*. If many families of GTs have some mechanism for two-phase elongation, then chain initiation may be a relatively inefficient, difficult-to-measure process and potentially a mechanism by which plant cells balance initiation and elongation activities *in vivo*.

A possible function of CWGT families with apparently redundant functions is that each enzyme within a family synthesizes different chain lengths of polysaccharide products. The study of these multi-enzyme families is still in its infancy, and the mechanisms of polysaccharide

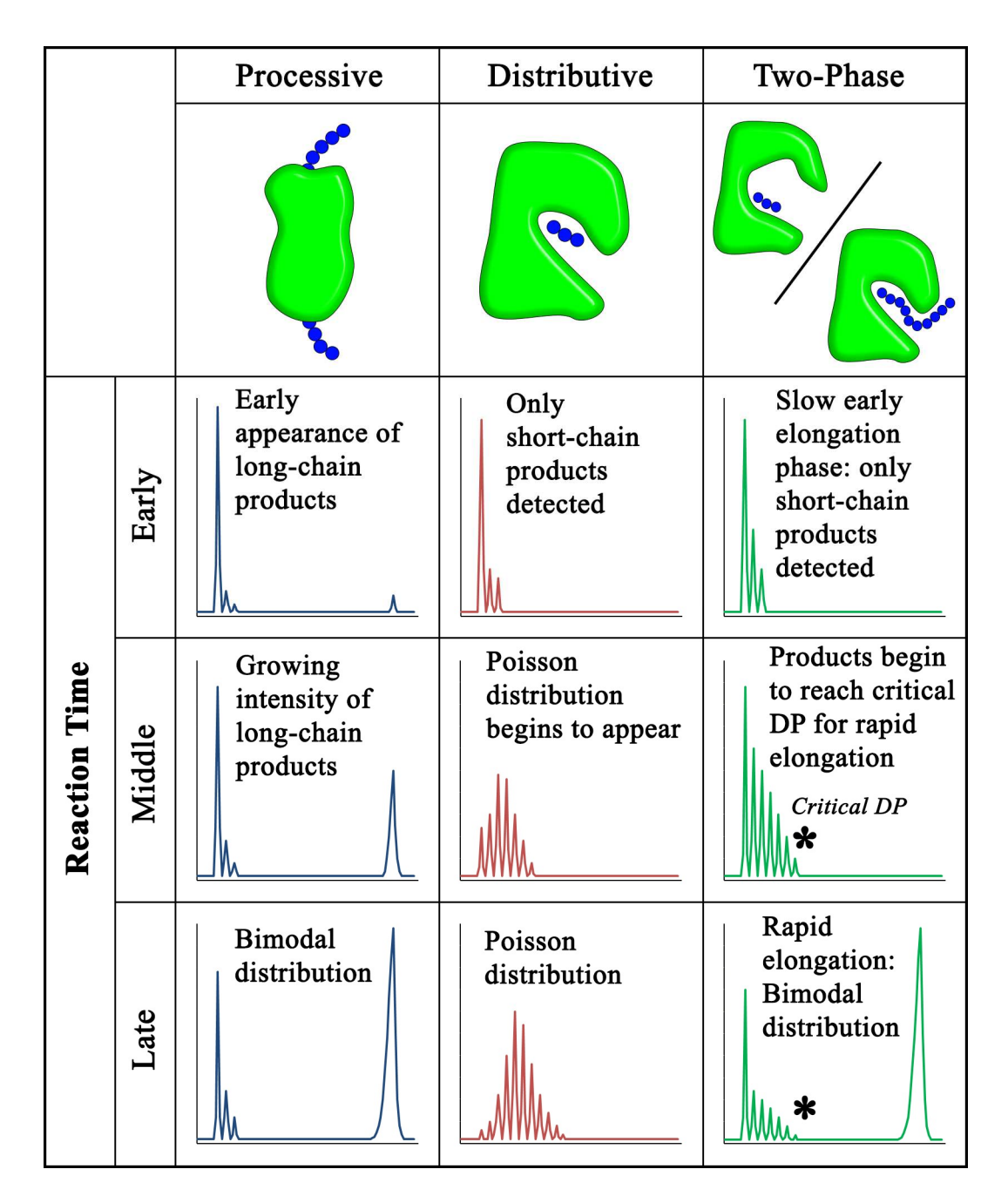


Figure 1.2. Polysaccharide chain elongation patterns for processive, distributive, and two- phase distributive glycosyltransfer. Glycosyltransferases synthesize polysaccharides by different mechanisms that result in characteristic product profiles over the progress of an elongation reaction. The hypothetical product profiles shown correspond to the elongation of a short-chain acceptor (left) into longer-chain products (right). Three panels are shown for each

proposed mechanism corresponding to the early, middle, and late stages of reaction progress. Product profiles are representative of several methods that are used to obtain chain length information, including HPLC, MALDI-MS, and polyacrylamide gel electrophoresis. In processive elongation, formation of an enzyme-substrate catalytic complex that is maintained through many rounds of monosaccharide transfer leads to a bimodal distribution of low and high MW products (Levengood et al., 2011; Raga-Carbajal et al., 2016). In distributive elongation, dissociation of the acceptor substrate following each round of addition and the lack of acceptor length bias leads to a Poisson distribution of products over time (Keys et al., 2014; Urbanowicz et al., 2014). A two-phase distributive mechanism accumulates short-chain products during the early phase of the reaction followed by rapid elongation of high MW polysaccharides resulting from large increases in catalytic efficiency for acceptors with chain lengths longer than a "Critical DP" (Vionnet and Vann, 2007; Amos et al., 2018). The product distribution of a twophase distributive mechanism can resemble the bimodal distribution observed by processive glycosyltransferases. Chain length analysis may be suggestive of a particular elongation mechanism, but processivity cannot necessarily be inferred without direct evidence, such as the multi-TM translocation pore found in crystal structures of the BcsA:BscB cellulose synthase complex and proposed for other GT2-family structures (Morgan et al., 2013; Bi et al., 2015).

length control during biosynthesis remain poorly understood. Fine control of polysaccharide length may make novel targets for mutational genetics control of plant cell phenotypes and also may be of value during production of biomaterials such as glycoconjugate vaccines (Fiebig et al., 2018). Chain length analysis experiments using heterologously expressed CWGTs enables the possibility of determining if length control is an intrinsic property of GTs or if plants require more complicated mechanisms to regulate polysaccharide chain length.

Enzymatic rates and kinetic analyses

Recombinant expression of soluble CWGTs allows for the measurement of reaction rates, which is effectively impossible to accurately measure in microsomal membrane fractions where the enzyme of interest is an unknown fraction of the total protein. Measurement of reaction rates will advance the understanding of how these low-abundance enzymes are able to promote the development of tissues containing large masses of polysaccharides. Additional questions related to the rates of GT activity include how plant cells balance biosynthesis with degradation and remodeling activities, how well different GTs compete for a limited supply of nucleotide sugar donors within a biosynthetic compartment, and how the rates of backbone synthesis compare to side-chain decoration. The CWGTs with measured reaction rates are summarized in Table 3.

Although published kinetic rates are limited to a small number of CWGTs, a consistent observation is that the turnover rates are slow relative to other classes of enzymes. Popular textbooks depict turnover numbers for enzymes ranging from 0.5 – 600,000 s⁻¹, with most enzymes catalyzing 100 or more events per second (Berg et al., 2002). CWGTs, however, typically function at a relatively low rate near or less than 1 s⁻¹ (Table 3). Analysis of published kinetic rates from several thousand enzymes led to the conclusion that most enzymes function at

moderate rates, with the median less than 10 s⁻¹ (Bar-Even et al., 2011). Unless the minimalistic conditions used in assays of CWGT activity do not sufficiently replicate proper conditions to measure full enzyme activities, current data suggests that CWGTs are likely to fall into this category of "moderately efficient" enzymes with low enzymatic rates.

Many CWGTs exist in multi-gene families. To the limited extent where the enzyme activities of different members of the same gene family have been tested, enzymes catalyze the same apparent activity at different rates. XXT5 was found to have 8-10-fold lower catalytic rates than other XXT family members (Culbertson et al., 2016), which could be a common trend among multi-gene families (Table 2). The reason for these different activities from members of the same gene family is not presently understood. However, the possibilities include expression in cellular subcompartments that have different substrate concentrations or the production of glycans of different abundance and chain length.

The apparently slow rates of CWGTs may result in false-negative recovery of activity due to expression below the detection limit. In two separate studies of XXT-family enzymes, both using *E. coli* as an expression host, activity for XXT5 was only detected in the study which used a 26-fold higher enzyme concentration (Chou et al., 2012; Culbertson et al., 2016). In those cases where heterologous expression is in a plant system, background activity can make it difficult to conclude whether the expressed enzymes are active. Inconsistent results have been reported in GUX family enzymes, where activity for GUX3 was detected after overexpression in tobacco BY2 cells but not in *N. benthamiana* microsomes (Lee et al., 2012a; Rennie et al., 2012). It remains uncertain whether GUX3 is an active xylan glucuronosyltransferase or rather a noncatalytic complex member, as has been proposed (Rennie et al., 2012).

Kinetic analysis was central to modeling the proposed two-phase mechanism by which GAUT1:GAUT7 initiates polysaccharide synthesis at a slower rate than the rate of elongation of longer-chain polymers (Amos et al., 2018). This result explained why in earlier measurements of HG synthesis from tobacco microsomes, only HG acceptors of $DP \ge 10$ were found to enhance activity above basal levels in 2-min reactions (Doong and Mohnen, 1998). Elongation of differently-sized acceptors may not necessarily be assumed to be detectable on the same time scales and are likely to require extended kinetic studies accounting for the possibility of reaction phases that have non-linear initial rates. For some polymers, studying the full reaction cycle of polysaccharide synthesis may be limited given the insolubility of longer synthesis products, primarily the unbranched homopolymers with β -1,4 linkages as discussed above.

Slower rates may also be indicative of the necessity of a GT to function with complex partners for full activity. Because Xys1 is likely to function in a complex, the reported rate is likely to under-estimate xylan backbone synthesis rate given that the full catalytic tertiary structure may not be present when the single enzyme is expressed. In asparagus, co-expression of IRX10 (homolog of Arabidopsis Xys1) with homologous proteins IRX9 and IRX14 led to higher activity and longer chain length products, suggesting the potential for enhanced activity as a full xylan synthase complex (Zeng et al., 2016). GAUT1 was also found to elongate products to a smaller chain length without GAUT7 (Amos et al., 2018). More detailed studies of individually expressed and co-expressed CWGTs may present a relationship between enzymatic rates and the chain length of products synthesized *in vitro*.

The kinetic measurement of GALS1 provides an example of a bifunctional enzyme that may have roles in both chain elongation and termination (Laursen et al., 2018a). The potential for a single CWGT to transfer monosaccharides from two different nucleotide sugar substrates

underscores the usefulness of screening GT activity with all possible nucleotide sugar substrates because a particular GT may not be limited to a single donor substrate. GALS1 has a 7.4-fold lower K_M for UDP-Xyl than for UDP-Ara_p (Laursen et al., 2018a), suggesting a preference for galactan chain elongation over chain termination that may be a mechanism of controlling chain length directly through the differences in enzyme affinity for these two substrates. K_M is not a direct measure of the equilibrium dissociation constant of an enzyme for its substrate, but K_M values can be interpreted as a relative measure of substrate affinity (Copeland, 2002).

Preliminary evidence attributes rates to cellulose synthesis that are similar to the synthesis of matrix polysaccharides such as HG. CesA8 from hybrid aspen was expressed in *P. pastoris* cells and synthesized β-1,4-Glc cellulose backbone polymers, however, kinetic assays were reported in units of relative activity (Purushotham et al., 2016). A bacterial cellulose synthase was reported to have a turnover number of 2.9 s⁻¹ (Du et al., 2016). Cellulose synthase proteins, like many matrix GTs, function in heteromeric complexes *in vivo*, and the enhancement of activity resulting from complex formation remains to be studied.

Heterologous expression of complexes

Eukaryotic GTs commonly form homo- and heterocomplexes. At least 25 heteromeric GT complexes have been identified from plants, mammals, and yeasts (Kellokumpu et al., 2016). GT complex formation may serve many functions, and several of the most relevant functions are enumerated below (adapted from (Kellokumpu et al., 2016)):

1. Enhanced activity: Quantitative activity measurements detect a fold-change difference when two or more GTs are co-expressed, or activities cannot be detected without co-expression of an interacting partner.

- 2. Substrate channeling: Glycosylation is a non-template driven process, and organization of GTs into complexes can protect a glycan from the action of competing enzymes.
- 3. Golgi localization: Some Golgi-localized GTs do not have TM domains and require interaction partners that serve as membrane anchors for targeting and retention in the proper Golgi sub-compartment.

Complex formation among CWGTs was reviewed previously, and seven proven and putative CWGT hetercomplexes were identified including GAUT1:GAUT7, ARAD1:ARAD2, RGP1:RGP2 and RGP5, the wheat xylan synthase complex, CSLC4:XXT, IRX9:IRX14, and CSLD2:CSLD3 (Oikawa et al., 2013). Several new discoveries have contributed to the effort to define the functional roles of these complexes. Previously, the XG biosynthetic enzyme CSLC4 was discovered to interact with XXT-family enzymes (Chou et al., 2012). Recent studies have demonstrated that all of the enzymes that synthesize the four major monosaccharide linkages in XG (CSLC4, XXT, MUR3, XLT2, and FUT1) interact in close proximity, possibly organizing into a multi-enzyme XG biosynthetic heterocomplex organized around CSLC4 (Chou et al., 2015).

Xylan synthase complexes have now been identified in two species, wheat and asparagus. The previously-purified wheat xylan synthase complex, with XylT, GlcAT, and AraT activities, was mapped to six individual genes, including enzymes from the GT43 (homolog to IRX14), GT47 (homolog to IRX10), and GT75 (homolog to RGP1, the UDP-arabinopyranose mutase) families (Zeng et al., 2010; Jiang et al., 2016). The asparagus xylan synthase complex is homologous to the three families of proposed Arabidopsis xylan synthase enzymes, IRX9, IRX10, and IRX14. Two of the enzymes that elongate galactan backbone and side branches in AGPs (GalT29A and GalT31A) may also interact as a heterocomplex (Dilokpimol et al., 2014).

Functional roles of plant cell wall GT complexes

Following the above numbering scheme for three proposed roles of GT complexes, contributions of CWGT studies to the functions of GT complexes are presented below:

- 1. Enhanced activity: Co-expression of GAUT1 with GAUT7 leads to the synthesis of high MW HG polysaccharides. GAUT1 expressed alone has a minimal ability to elongate HG acceptors (Amos et al., 2018). Expression of IRX10 leads to minimal elongation of xylan acceptors. Both the highest activity and the longest products were obtained when all three complex members (IRX9, IRX10, and IRX14A) were co-expressed (Zeng et al., 2016). In each case, it is not yet known whether the shorter elongation ability is due to a general decrease in activity or if complex formation creates a domain structure that enhances the ability of GAUT1:GAUT7 or IRX9:IRX10:IRX14 to elongate longer-chain polymers.
- 2. Substrate channeling: Each enzyme in the XG biosynthesis pathway has a sequential activity (Table 1). The solublility of the glucan backbone is strongly impaired above DP 6, but branching of XG by decoration with Xyl, Gal, and Fut side-chain residues enhances solubility (Scheller and Ulvskov, 2010). CSLC4 is a multi-TM pore-forming enzyme that extrudes a growing glucan chain into the Golgi lumen (Davis et al., 2010), and complex formation may allow each enzyme to remain in close proximity so that side-chain residues are quickly added before the glucan backbone reaches a chain length at which it becomes insoluble.
- 3. Golgi localization: Co-expression of complex members in both the wheat and asparagus xylan synthase complexes was required for full Golgi localization and export from the ER (Jiang et al., 2016; Zeng et al., 2016). Complex assembly in the ER may be a step in the eukaryotic quality control pathway that prevents misfolded proteins, or in this case, unassembled

complexes, from progressing further in the secretory pathway. In the xylan synthase complex, IRX10 lacks a TM domain, and requires interaction with IRX9 and IRX14 for Golgi retention (Zeng et al., 2016). In the HG biosynthetic complex, GAUT1 loses its TM domain *in vivo* after truncation and requires GAUT7 for Golgi retention (Atmodjo et al., 2011). Expression of GAUT1 without GAUT7 results in a large amount of truncation products, high MW aggregates, and GAUT1 homocomplexes, which also supports the notion that co-expression is a necessary part of the folding and quality control process (Amos et al., 2018).

CONCLUSION

Molecular descriptions of plant cell wall biosynthesis have advanced over the past 20 years due to the successful development of heterologous expression systems allowing the purification and *in vitro* assay of biosynthetic genes. At least 26 independent glycosyltransferase activities have been identified corresponding to the synthesis of cell wall polysaccharide backbone and side-chain linkages. Many of these activities are associated with multi-gene families, leading to the potential for understanding the functions of hundreds of biosynthetic genes. Recent successes with expression in HEK293 cell cultures have provided the first examples of large-scale purification of CWGTs for biochemical characterization and crystallographic studies. For the first time, questions related to the mechanisms of biosynthesis and length control of polysaccharides can be investigated, and homogenous cell wall polysaccharides can be synthesized and isolated for the study of their structural properties. Matrix polysaccharides contribute to the complex changes in cellular size, shape, mechanical strength, and adhesion that occur during plant development. The potential for the control of cell

wall biosynthesis makes the cell wall biosynthetic GTs promising targets for genetic manipulation to enhance commercially desirable traits of fruits and other plant-derived products.

TABLES

Table 1.1. Plant cell wall GTs of known function determined by heterologous expression. All CWGTs are organized by polysaccharide synthesized. Abbreviated gene annotations are used (e.g. CSLC4 rather than "Cellulose synthase-like4"). Additional annotations found in the literature are listed below the gene name in parentheses. Standard abbreviations for monosaccharides are used. All acceptors are standardized to degree of polymerization (DP) for chain length formatting (e.g. xylohexaose (Xyl₆) is listed as "Xylan backbone oligosaccharides, DP6"). Listed references are original research publications in which the enzyme (or enzyme family) was heterologously expressed or reviews that contain additional information listed in the table.

Enzyme or Family	Mono- sacch. Trans- ferred	Activity: Product Synthesized	CAZy GT	Acceptor	Activity Notes	Homology / Redundancy (Arabidopsis)	Reference					
	Xyloglucan (XG)											
CSLC	D-Glc	β-1,4-Glc XG Backbone	2	Unknown: endogenous acceptors or <i>de novo</i> synthesis in <i>P. Pastoris</i> .	Unknown elongation size: limited solubility of β-glucan oligosaccharides with chain lengths larger than DP6. High MW polymerization unknown.	Five-member family. Activity for CSLC4 only.	(Cocuron et al., 2007) (Davis et al., 2010)					
XXT	D-Xyl	α-1,6-Xyl side chain initiation on XG backbone X Side chain	34	XG backbone oligosaccharides, DP 4-6. Limited solubility of β-glucan oligosaccharides with chain lengths larger than DP 6. DP 3 acceptor tested, no activity detected.	Single addition to GGGGGG synthesizes GGXGGG. Less efficient second product, GGXXGG. DP ≥ 4 acceptor required for activity. DP 6 acceptor preferred to DP 5.	Five-member family. Activity for XXT1, 2, 4, and 5.	(Faik et al., 2002) (Cavalier and Keegstra, 2006) (Vuttipongchai kij et al., 2012a) (Culbertson et al., 2016) (Ruprecht et al., 2018) (Culbertson et al., 2018)					
MUR3	D-Gal	β-1,2-Gal addition to X sidechain (Xyl residue transferred by XXT) L Side chain	47	XG oligosaccharides extracted from <i>mur3</i> -deficient plants with acceptor sites for Gal transfer, unknown size/DP.	Single addition to XXXG synthesizes XXLG.	One homolog: XLT2. Activity predicted from mutant phenotype.	(Madson et al., 2003)					

Enzyme or Family	Mono- sacch. Trans- ferred	Activity: Product Synthesized	CAZy GT	Acceptor	Activity Notes	Homology / Redundancy (Arabidopsis)	Reference
FUT1 (MUR2)	L-Fuc	α-1,2-Fuc addition to L sidechain (Gal residue transferred by MUR3) F side chain	37	XG oligosaccharides with acceptor sites for Fuc transfer, DP4: XXLG or XLLG.	Single addition to XXLG synthesizes XXFG. Single addition to XLLG synthesizes XLFG.	10-member FUT family. XG-related activity for FUT1 only. FUT4 and FUT6 transfer Fuc to AGP side chains.	(Perrin et al., 1999) (Faik et al., 2000) (Vanzin et al., 2002) (Ciceron et al., 2016) (Rocha et al., 2016) (Urbanowicz et al., 2017)
		1		Xyl	an		, ,
Xys1 (IRX10- L)	D-Xyl	β-1,4-Xyl Xylan Backbone	47	Xylan backbone oligosaccharides, DP 2-6. Xyl monosaccharide tested, no activity detected.	Elongation of DP 6 acceptor up to DP ~21 detected by MALDI. High MW polymerization unknown.	One homolog, IRX10 with similar activity. Two related GT43 enzymes (IRX14 and IRX14-L) are putative xylan backbone transferases. Activity not confirmed.	(Urbanowicz et al., 2014) (Jensen et al., 2014) (Jensen et al., 2018) (Zeng et al., 2010) (Lee et al., 2012b) (Jiang et al., 2016) (Zeng et al., 2016)

Enzyme or Family	Mono- sacch. Trans- ferred	Activity: Product Synthesized	CAZy GT	Acceptor	Activity Notes	Homology / Redundancy (Arabidopsis)	Reference
GUX	D- GlcA	α-1,2-GlcA side chain initiation on xylan backbone	8	Xylan backbone acceptors, DP 2-6. Xyl monosaccharide tested, no activity detected.	Single addition to DP 6 acceptor. Fifth Xylose from nonreducing end preferred (XXXXGX). Some product contains single addition on third Xylose from nonreducing end (XXGXGX). Strong preference for longer acceptors (DP ≥ 6).	Five-member family. Activity for GUX1, 2 and 4. GUX3 activity inconsistent from two independent publications: GUX3 and GUX5 may be noncatalytic.	(Rennie et al., 2012) (Lee et al., 2012a)
XAT1	L-Ara	α-1,3-Ara side chain initiation on xylan backbone	61	Unknown: endogenous xylan acceptors in Arabidopsis. Gain-of-function evidence only.	Single addition to xylan acceptors of unknown size. Digested products reveal a pattern of DP 5 products containing an Ara side chain on the second Xyl from the nonreducing end (XAXX).	Arabinoxylans are low-abundance in Arabidopsis. Two putative GT61 homologs.	(Anders et al., 2012)
XAX1	D-Xyl	β-1,2-Xyl addition to α-1,3- linked Ara side chain (residues transferred by XAT1) on grass xylan	61	Unknown: endogenous xylan acceptors in <i>N. benthamiana</i> . Gain-of-function evidence only.	Unknown product size/structure: Most likely product detected by NMR is a xylan backbone oligosaccharide, DP 4, containing a Xyl-Ara side chain on the second Xyl from the nonreducing end (XAXX).	Arabinoxylans are low-abundance in Arabidopsis. No identified homologs.	(Chiniquy et al., 2012)
		1	1	Mannan / Gluco			
CSLA	D- Man	β-1,4-Man and β- 1,4-Glc linkages Glucomannan (GM) backbone	2	Unknown: endogenous acceptors or <i>de novo</i> synthesis in Drosophila S2 cells and in <i>P. Pastoris</i> .	Synthesizes β-1,4-linked polymers containing Glc, Man, or GlcMan depending on substrate availability. High MW products (> 100 kDa) detected by size exclusion.	Nine-member family. Activity for CSLA2, 7, and 9. Mutational evidence for CSLA3 activity.	(Dhugga et al., 2004) (Liepman et al., 2005) (Goubet et al., 2009) (Voiniciuc et al., 2019)

Enzyme or Family	Mono- sacch. Trans- ferred	Activity: Product Synthesized	CAZy GT	Acceptor	Activity Notes	Homology / Redundancy (Arabidopsis)	Reference
CSLD	D- Man	β-1,4-Man Mannan backbone	2	Unknown: endogenous acceptors or <i>de novo</i> synthesis in <i>N. benthamiana</i> .	Unknown elongation size. High MW polymerization unknown.	Six-member family. Activity for CSLD5 and co-expressed CSLD2:CSLD3, but not CSLD2 or CSLD3 individually.	(Yin et al., 2011) (Verhertbrugg en et al., 2011)
GalT	D-Gal	α-1,6-Gal side chain initiation on mannan backbone	34	 β-1,4-Man mannan backbone oligosaccharides DP 5-10. Limited solubility of β-mannan oligosaccharides with chain lengths larger than DP 8. DP 1-4 acceptors tested, no 	Single addition to mannan backbone. Unknown regiospecificity of addition. Addition to glucomannan backbone not confirmed <i>in vitro</i> .	Fenugreek enzyme. Putative Arabidopsis homolog MUCI10.	(Edwards et al., 1999) (Voiniciuc et al., 2015)
				activity detected.	CI AH C)		
COLE	G1	(1.2.1.1) 0.01		Mixed-Linkage		lago et est	(D) 1
CSLF	D-Glc	(1,3;1,4)-β-Glc MLG backbone	2	Unknown: endogenous acceptors or <i>de novo</i> synthesis in Arabidopsis, <i>N. benthamiana</i> , and <i>P. Pastoris</i> .	Unknown length of MLG backbone products. Varying DP3:DP4 ratios from barley (~1.6:1) and sorghum (1.0:1) CSLF6 orthologs.	MLG not detected in Arabidopsis. 10-member family in <i>Poaceae</i> . Activity for CSLF6, Gain-of-function evidence for CSLF2 and 4.	(Burton et al., 2006) (Kim et al., 2015) (Dimitroff et al., 2016) (Little et al., 2018)
CSLH	D-Glc	(1,3;1,4)-β-Glc MLG backbone	2	Unknown: endogenous acceptors or <i>de novo</i> synthesis in Arabidopsis. Gain-of-function evidence only.	Unknown length of MLG backbone products. DP3:DP4 ratio ~3.6 from barley enzyme.	MLG not detected in Arabidopsis. Barley enzyme.	(Doblin et al., 2009) (Little et al., 2018)

Enzyme or Family	Mono- sacch. Trans- ferred	Activity: Product Synthesized	CAZy GT	Acceptor	Activity Notes	Homology / Redundancy (Arabidopsis)	Reference
CSLJ	D-Glc	(1,3;1,4)-β-Glc MLG backbone	2	Unknown: endogenous acceptors or <i>de novo</i> synthesis in N. benthamiana.	Unknown length of MLG backbone products. DP3:DP4 ratio ~1.3 from barley enzyme.	MLG not detected in Arabidopsis. Barley enzyme.	(Little et al., 2018)
		1		Homogalactu	ironan (HG)		
GAUT XGD1	D-GalA D-Xyl	α-1,4-GalA HG backbone β-1,3-Xyl side chain initiation on	8	HG backbone oligosaccharides, DP 3-15. De novo synthesis from UDP-GalA. HG backbone oligosaccharide acceptor	Elongation to HMW polymers >100 kDa. Large rate increase with acceptors DP≥11. Single addition to HG backbone.	15-member family. Activity for GAUT1:GAUT7 complex, GAUT1, 4, and 11. High MW polymerization detected with GAUT1:GAUT7 complex only. Activity only for XGD1. Six additional	(Sterling et al., 2006) (Atmodjo et al., 2011) (Amos et al., 2018) (Biswal et al., 2018a) (Voiniciuc et al., 2018a) (Jensen et al., 2008)
		HG backbone Xylogalacturonan (XGA)		mix, DP 12-14.	Unknown pattern of transfer or regiospecificity.	homologs in GT47 subgroup C, no functions assigned.	2008)
DDT1	- D1	1 4 D1 1' 1	106	Rhamnogalactu		E 1 C 1	(TT 1 . 1
RRT1	L-Rha	α-1,4-Rha linkage within RG-I backbone disaccharide: [-2)-α-Rha-(1,4)-α-GalA-(1-]	106	RG-1 repeating disaccharide acceptors of DP 5-14 containing GalA on the non-reducing end. DP 3-4 acceptors tested, no activity detected.	Single addition. GalAT activity needed for disaccharide elongation. Highest relative activity with DP 10 acceptor.	Four-member family. Activity for RRT1, RR2, RRT3, RRT4 detected.	(Uehara et al., 2017) (Takenaka et al., 2018)

Enzyme or Family	Mono- sacch. Trans- ferred	Activity: Product Synthesized	CAZy GT	Acceptor	Activity Notes	Homology / Redundancy (Arabidopsis)	Reference
GALS	D-Gal and L- Ara _p	β-1,4-Gal side branch elongation of AG side branch linked to RG-I backbone RG-I/AG side branch Secondary activity: Arap termination of β-1,4-Gal side branch, unknown linkage.	92	AG oligosaccharides (β-1,4-Gal), DP 4-7. DP 1-3 acceptors tested, minimal or no activity detected. Rhamnogalactur	Elongation of DP 5 acceptor to DP ~11 detected by carbohydrate gel electrophoresis. High MW polymerization unknown. Acceptors of DP ≥ 5 preferred. Single addition of Ara _p prevents further elongation of chain. ~10-fold higher affinity for UDP-Gal over UDP-Arap.	Three-member family. GalT activity for GALS1, 2, and 3. Lower activity / less transfers for GALS2 and 3. ArapT activity for GALS1 only.	(Liwanag et al., 2012a) (Laursen et al., 2018a) (Ebert et al., 2018)
RGXT	D-Xyl	α-1,3-Xyl addition to Fuc in RG-II side chain A	77	L-Fuc monosaccharide. Full oligosaccharide acceptor containing RG-II backbone and side chain A residues not tested.	Single addition to synthesize Xyl-Fuc disaccharide.	Four-member family. Activity for all RGXT1, 2, 3, and 4.	(Egelund et al., 2006) (Egelund et al., 2008) (Petersen et al., 2009) (Liu et al., 2011)
	T	1		Arabinogalactan		T	
GALT	D-Gal	β-1,4-Gal backbone initiation on AGP hydroxyproline residue AGP backbone (initition only)	31	Synthetic peptide acceptor consisting of 7 or 14 Ala-Hyp [AO] dipeptide repeats . Deglycosylated protein acceptor containing 51 [AO] repeats.	Single addition to initiate AG chain on AGP. Relatively higher activity with synthetic peptides than with deglycosylated protein acceptor. Unknown pattern of transfer or regiospecificity.	Five-member family. Activity for GALT2- 6. GALT1 is non-cell wall related.	(Basu et al., 2013) (Basu et al., 2015b) (Basu et al., 2015a) (Showalter and Basu, 2016)

Enzyme or Family	Mono- sacch. Trans- ferred	Activity: Product Synthesized	CAZy GT	Acceptor	Activity Notes	Homology / Redundancy (Arabidopsis)	Reference
HPGT	D-Gal	β-1,4-Gal backbone initiation on AGP Hydroxyproline residue	31	Synthetic peptide acceptor consisting of repeats containing non-contiguous Hyp residues.	Single addition to initiate AG chain on AGP. Relatively higher activity with peptides containing more repeats.	Three-member family. Activity for HPGT1, 2, and 3.	(Ogawa- Ohnishi and Matsubayashi, 2015)
		AGP backbone (initiation only)					
Atlg	D-Gal	β-1,3-Gal	31	β-1,3-Gal disaccharide	Single addition to disaccharide	No identified	(Qu et al.,
77810		AG backbone		acceptor.	synthesizes DP3 products. Continued elongation of AGP backbone unknown.	homologs.	2008)
GALT2 9A	D-Gal	β-1,6-Gal side branch elongation and initiation on β-1,3-Gal backbone AG side branch	29	Heterogeneous AGP acceptor mix on a synthetic peptide expressed and glycosylated in <i>N. benthamiana</i> , providing acceptor sites for β-1,6-Gal and β-1,3-Gal addition. β1-3-Gal acceptor of MW	Elongation of β -1,3 (backbone) and β -1,6- (side branch) acceptors. Unknown length of elongation or specific acceptor preferences.	No identified homologs.	(Dilokpimol et al., 2014)
GALT3	D-Gal	β-1,6-Gal side	31	25 kDa (~DP150). Heterogeneous AGP	Elongation of β-1,6- (side chain)	No identified	(Geshi et al.,
1A	D Gui	branch elongation AG side branch	31	acceptor mix on a synthetic peptide expressed and glycosylated in N . benthamiana, providing acceptor sites for β -1,6-Gal and β -1,3-Gal addition.	acceptors. Elongation of DP 3, but not DP 2, acceptors. Unknown length of elongation.	homologs.	2013)
				β-1,6-Gal trisaccharide acceptor.			

Enzyme or Family	Mono- sacch. Trans- ferred	Activity: Product Synthesized	CAZy GT	Acceptor	Activity Notes	Homology / Redundancy (Arabidopsis)	Reference
GlcAT 14	D- GlcA	β-1,6-GlcA side chain addition to β-1,3-Gal AGP backbone β-1,6-Gal AGP side branches	14	Heterogeneous AGP acceptor mix on a synthetic peptide expressed and glycosylated in <i>N. benthamiana</i> . AGP side chain oligosaccharides (β-1,6-Gal) DP 3-11 and backbone oligosaccharides (β-1,3-Gal) DP 5 and 7.	Single addition to both β-1,6 (side chain) and β-1,3 (backbone) linkages within AGP polysaccharides. Unknown pattern of elongation. No activity detected with β-1,3-Gal oligosaccharides DP < 5.	Three member family. Activity for GlcAT14A, B, and C.	(Knoch et al., 2013a) (Dilokpimol and Geshi, 2014)
FUT4 / FUT6	L-Fuc	α-1,2-Fuc addition to various α-1,3-Ara linked to the β-1,6-Gal AGP side branches	37	Non-fucosylated AGP polysaccharide extracted by Yariv reagent from tobacco BY2 cells.	Single addition to L-Ara side chain residues in both β-1,6 (side chain) linkages within AGP polysaccharides. Unknown pattern of elongation.	10-member FUT family. FUT4 and FUT6 are AGP-specific, redundancy unknown. Two known Fuc acceptor sites in AGP.	(Wu et al., 2010a)

Table 1.2. Chain length of plant cell wall polysaccharides synthesized *in vivo* and *in vitro*. Chain length values (kDa and DP) are either stated directly in references, inferred from reported data, or are a range of figures compiled within reviews. If only the kDa or DP value was reported, the other value was estimated from the molecular weight of component monosaccharides. In some cases, the chain length in DP cannot be estimated due to large amounts of heterogeneity and side-chain branching, indicated by N/A. Use of a tilde (~) indicates estimated values and use of a greater-than sign (>) indicates that high molecular weight polymers that elute near the void volume of a size exclusion column are unable to be precisely measured and the reported size is compared to a dextran standard. Abbreviations: SEC, size exclusion chromatography. AFM, atomic force microscopy. MALS, multiangle light scattering. MS, mass spectrometry. MALDI-Matrix-assisted laser desorption/ionization. TLC, thin-layer chromatography. PACE, polysaccharide analysis using carbohydrate gel electrophoresis.

Polysaccharide	Extracted from sar	nples synthesized in	vivo	Synthesized in vitro					
	Chain Length (kDa)	Chain Length (degree of polymerization)	Method	Ref	Chain Length (kDa)	Chain Length (degree of polymerization)	Method	Ref	
Xyloglucan (XG)	9-900 Storage XG: >1000 kDa	28-2800	SEC	(Park and Cosgrove, 2015)	due to high r	ssumed to be long ratio of 4-linked rminal-glucose.	Linkage analysis	(Cocuron et al., 2007)	
	90 kDa	280	AFM	(Park and Cosgrove, 2015)					
Xylan	Glucuronoxylan: ~12	93	NMR	(Pena et al., 2007)	~3-5	~21-34	MALDI-MS	(Urbanowic z et al., 2014) (Jensen et al., 2018)	
	Glucuronoxylan: 5-130 Arabinoxylan and complex heteroxylan: 64-380	N/A	SEC	(Ebringerová et al., 2005)					
Mannan / Glucomannan (GM)	Woody: 1-64 GalMan: 960-1260	~10-400 ~6000-7800	SEC	(Ebringerová et al., 2005)	Pure mannan: >2000 >6000 GM: 64-560, peak 130 ~800		SEC	(Liepman et al., 2005)	
	Konjac GM: 1020 250 ~1-4	~6000 ~1500 11-20	SEC- MALS MALDI- MS	(Makabe et al., 2009) (Xu et al., 2013) (Lundqvist et al., 2002)					
Mixed-Linkage Glucan (MLG)	>250	>1500	SEC	(Carpita and McCann, 2010)	Unknown: products analyzed after lichenase digestion. Long-chain products not measured.		N/A	(Dimitroff et al., 2016)	

Polysaccharide	Extracted from sa	amples synthesized in	vivo	Synthesized in vitro				
	Chain Length (kDa)	Chain Length (degree of polymerization)	Method	Ref	Chain Length (kDa)	Chain Length (degree of polymerization)	Method	Ref
Homogalacturonan (HG)	~14-20	81-117	SEC	(Yapo et al., 2007)	>100	>500	SEC	(Amos et al., 2018)
	~60	~320	AFM	(Round et al., 2010)				
	Embedded within RG-I domains: ~1-2	4-10	MS, NMR	(Nakamura et al., 2002) (Tan et al., 2013)				
Rhamnogalacturona n-I (RG-I)	6 (12% of 50 kDa branched polymer) Full polymer:	~20	SEC	(Shi et al., 2017)	Unknown: due to disaccharide backbone, only single addition to acceptor can be detected.		Anion exchange chromatogra phy and tandem MS	(Takenaka et al., 2018)
	23-900 Debranched: 15 Full polymer: 56	N/A ~40 N/A	SEC- MALS	(Yapo, 2011) (Yapo et al., 2007)				
Arabinogalactan from RG-I (AG)	Galactans: ~1-8 Arabinans: ~1-27	2-50	SEC	(Yapo, 2011)	Galactans: ~1-2	11	TLC and PACE	(Laursen et al., 2018a)
Arabinogalactan Protein (AGP)	5-25 kDa	30-120	SEC	(Ellis et al., 2010)	Unknown: product size not analyzed.		N/A	(Dilokpimo l et al., 2014) (Geshi et al., 2013)

Table 1.3. Enzymatic rates and reaction kinetics of plant cell wall polysaccharides synthesized *in vitro*. All units listed in this table are standardized from reported data. ${}^{a}K_{M}$ values are converted to μM if reported in mM. ${}^{b}R$ at are converted to pmol/min c from reported data. ${}^{c}k_{cat}$ values are converted to c from reported data. ${}^{d}E$ nzyme amounts are converted into pmol if reported in ng using the predicted molecular weights of full-length or truncated proteins. Microsomal protein cannot be used to calculate kcat values due to an unknown concentration of target protein within microsomes. Calculations used to standardize reported values are explained with the original values from each reference in Table 1.4.

Enzyme	Variable Substrate	Saturating Subsatrate	Donor Conc.	Acceptor Conc.	K _M ^a Variable Substrate (μΜ)	Rate ^b (pmol/min)	kcat ^c : Turnover number (s ⁻¹)	Enzyme amount ^d	Reaction time (min)	Ref	
	Backbone (polymerizing) transferases										
Xys1	Xylohexaos e Acceptor	UDP-Xyl Donor	800	0-4000	1.17	0.39	0.0004 s ⁻¹	15.8 pmol	120	(Urbanowicz et al., 2014)	
GAUT1: GAUT7	UDP-GalA Donor	HG mix DP7- 23 Acceptor	5-2000	100	151 ± 10.6	165.4 ± 3.4	0.92 ± 0.02	3 pmol	5	(Amos et al., 2018)	
	HG DP7-23 mix Acceptor	UDP-GalA Donor	1000	0.01-50	0.8 ± 0.1	359.0 ± 10.2	1.99 ± 0.06	3 pmol	5		
	HG DP11 Acceptor	UDP-GalA Donor	1000	0.01-100	1.4 ± 0.2	705.0 ± 53.9	3.92 ± 0.3	3 pmol	5		
	HG DP7 Acceptor	UDP-GalA Donor	1000	0.01-100	10.0 ± 1.4	109.8 ± 3.7	0.61 ± 0.02	3 pmol	30		
GalS1	UDP-Xyl Donor	Galacto- pentaose Acceptor	0-500	50	142 ± 12	656 ± 42	N/A	25 μg microsomal protein	15	(Laursen et al., 2018a)	
	UDP-Ara <i>p</i> Donor	Galacto- pentaose Acceptor	0-3000	50	1057 ± 222	454 ± 51	N/A	25 μg microsomal protein	60		

Enzyme	Variable Substrate	Saturating Subsatrate	Donor Conc.	Acceptor Conc.	K _M ^a Variable Substrate (μM)	Rate ^b (pmol/min)	kcat ^c : Turnover number (s ⁻¹)	Enzyme amount ^d	Reaction time (min)	Reference
	Side-chain transferases									
XXT1	UDP-Xyl Donor	Cellohexaose Acceptor	0-4000	1000	490 ± 40	509.25 ± 14.25	0.11 ± 0.003	75 pmol	30	(Culbertson et al., 2016)
XXT2	UDP-Xyl Donor	Cellohexaose Acceptor	0-4000	1000	640 ± 90	373.5 ± 17.25	0.083 ± 0.004	75 pmol	30	(Culbertson et al., 2016)
XXT5	UDP-Xyl Donor	Cellohexaose Acceptor	0-4000	1000	4800 ± 330	166.5 ± 74.75	0.01 ± 0.004	287.5 pmol	60	(Culbertson et al., 2016)
FUT1	GDP-Fuc Donor	XXLG Oligo- saccharide Acceptor	0-400	750	25.32 ± 4.2	14.1 ± 0.2	$0.063 \pm 0.0008 \text{ s}^{-1}$	3.7 pmol	20	(Urbanowicz et al., 2017)
	XXLG Oligo- saccharide Acceptor	GDP-Fuc	200	0-800	201 ± 12.0	N/A	N/A	3.7 pmol	20	
GUX1	UDP-GlcA Donor	Xylohexaose Acceptor	10-3000	400	165 ± 25	N/A (arbitrary units)	N/A	100 μg microsomal protein	60	(Rennie et al., 2012)

Enz	zyme	Notes	Reference
Xys	rs1	Activity is reported as $V_{\text{max}} = 0.39 \text{ pmol UDP min}^{-1}$. Reactions contain 15.8 pmol enzyme. Calculated turnover number = 0.0004 s^{-1} .	(Urbanowicz et al., 2014)
	AUT1: AUT7	Reactions contain 100 nM enzyme in 30 μL volume. Calculated enzyme amount = 3 pmol per reaction.	(Amos et al., 2018)
Gal	lS1	Reactions contain 1 μg μL ⁻¹ total microsomal protein in 25 μL volume.	(Laursen et al., 2018a)
XX	T1	Reactions contain various UDP-Xyl concentrations. The range of values tested is not reported and are assumed to be 0-4000 μ M from Figure 3 in (XXT5 2016). Turnover number (k_{cat}) is reported as $6.79 \pm 0.19 \text{ min}^{-1}$. Calculated $k_{cat} = 0.11 \pm 0.003 \text{ s}^{-1}$. Reactions contain 3 μ M XXT1 in 25 μ L volume. Calculated enzyme amount = 75 pmol. Calculated activity in pmol/min = 509.25 ± 14.25 .	(Culbertson et al., 2016)
XX	KT2	Reactions contain various UDP-Xyl concentrations. The range of values tested is not reported and are assumed to be 0-4000 μ M from Figure 3 in (XXT5 2016). Turnover number (k_{cat}) is reported as 4.98 ± 0.23 min ⁻¹ . Calculated $k_{cat} = 0.083 \pm 0.004$ s ⁻¹ . Reactions contain 3 μ M XXT1 in 25 μ L volume. Calculated enzyme amount = 75 pmol. Calculated activity in pmol/min = 373.5 ± 17.25.	(Culbertson et al., 2016)
XX	XT5	Reactions contain various UDP-Xyl concentrations. The range of values tested is not reported and are assumed to be 0-4000 μ M from Figure 3 in (XXT5 2016). Activity (k_{cat}) is reported as 0.58 ± 0.26 min ⁻¹ . Calculated $k_{cat} = 0.01 \pm 0.004$ s ⁻¹ . Reactions contain 11.5 μ M XXT1 in 25 μ L volume. Calculated enzyme amount = 287.5 pmol. Calculated activity in pmol/min = 166.5 ± 74.75 .	(Culbertson et al., 2016)
FU'	T1	Turnover number (k_{cat}) is reported as 3.8 ± 0.05 min ⁻¹ . Calculated $k_{cat} = 0.063 \pm 0.0008$ s ⁻¹ . Reactions contain 200 ng enzyme in 5-10 μ L volume. Calculated enzyme molecular weight = 54.4 kDa based on FUT1 sequence, residues 81-558. Calculated enzyme amount = 3.7 pmol. Calculated activity in pmol/min = 14.1 \pm 0.2.	(Urbanowicz et al., 2017)
GU	JX1	Purified GUX1 protein of an unknown concentration corresponding to 100 µg of microsomal protein was assayed.	(Rennie et al., 2012)

CHAPTER 2

A TWO-PHASE MODEL FOR THE NON-PROCESSIVE BIOSYNTHESIS OF HOMOGALACTURONAN POLYSACCHARIDES BY THE GAUT1:GAUT7 COMPLEX

Robert A. Amos, Sivakumar Pattathil, Jeong-Yeh Yang, Melani A. Atmodjo, Breeanna R. Urbanowicz, Kelley W. Moremen, Debra Mohnen. J Biol Chem. 2018 Dec 7;293(49):19047-19063. Reprinted here with permission of publisher.

ABSTRACT

Homogalacturonan (HG) is a pectic glycan in the plant cell wall that contributes to plant growth and development, cell wall structure and function, and interacts with other glycans and proteoglycans in the wall. HG is synthesized by the galacturonosyltransferase (GAUT) gene family. Two members of this family, GAUT1 and GAUT7, form a heteromeric enzyme complex in Arabidopsis thaliana. Here, we established a heterologous GAUT expression system in HEK293 cells and show that co-expression of recombinant GAUT1 with GAUT7 results in the production of a soluble GAUT1:GAUT7 complex that catalyzes elongation of HG products in vitro. The reaction rates, progress curves, and product distributions exhibited major differences dependent upon small changes in the degree of polymerization (DP) of the oligosaccharide acceptor. GAUT1:GAUT7 displayed > 45-fold increased catalytic efficiency with DP11 acceptors relative to DP7 acceptors. Although GAUT1:GAUT7 synthesized high-molecularweight polymeric HG (> 100 kDa) in a substrate concentration-dependent manner typical of distributive (non-processive) glycosyltransferases with DP11 acceptors, reactions primed with short-chain acceptors resulted in a bimodal product distribution of glycan products that has previously been reported as evidence for a processive model of GT elongation. As an alternative to the processive glycosyltransfer model, a two-phase distributive elongation model is proposed in which a slow phase, which includes the *de novo* initiation of HG and elongation of short-chain acceptors, is distinguished from a phase of rapid elongation of intermediate and long-chain acceptors. Upon reaching a critical chain length of DP11, GAUT1:GAUT7 elongates HG to high molecular weight products.

INTRODUCTION

Homogalacturonan (HG) is a plant cell wall polysaccharide and glycan component of more complex polysaccharides and proteoglycans that contributes to the structure and mechanical strength of the wall and has roles in plant growth, development, morphology, and response to biotic and abiotic stress (Atmodjo et al., 2013; Tan et al., 2013; Cosgrove, 2016a; Voxeur and Hofte, 2016). HG is a linear homopolymer of 1,4-linked α-D-galactopyranosyluronic acid (GalA) that may be partially methylesterified at *O*-6 and acetylated at *O*-2 and *O*-3. It is the simplest and most abundant glycan in the family of cell wall polysaccharides known as pectins, which include HG, rhamnogalacturonan I (RG-I) and rhamnogalacturonan II (RG-II) (Atmodjo et al., 2013).

The pectic polysaccharides make contacts with each other (Atmodjo et al., 2013), cellulose (Dick-Perez et al., 2011; Wang et al., 2012; Wang and Hong, 2016), hemicelluloses (Dick-Perez et al., 2011; Atmodjo et al., 2013), and proteoglycans (Tan et al., 2013) within the wall through covalent and noncovalent interactions. The presence of pectin provides a barrier to the deconstruction of cellulosic biomass and partially obstructs degradative enzymes from accessing cellulose and hemicelluloses during the processing and saccharification of plant biomass (Lionetti et al., 2010; Atmodjo et al., 2013; Chung et al., 2014; Biswal et al., 2018b). Reducing the content of pectin in woody and grass biofuel feedstocks has been shown to enhance biofuel production by increasing both biomass yield and the recovery of sugar (Biswal et al., 2015; Biswal et al., 2018a; Biswal et al., 2018b). Our current understanding of pectin synthesis and structure, however, is insufficient to explain its diverse functions in the plant or how reductions to pectin synthesis correlate with phenotypes such as increased plant growth and reduced recalcitrance to deconstruction.

The identified encoding HG biosynthetic gene an enzyme was Galacturonosyltransferasel (GAUTI), a CAZy (Lombard et al., 2014) Family 8 of glycosyltransferase (GT). The in vitro synthesis HG. or homogalacturonan:galacturonosyltransferase (HG:GalAT) activity was mapped to GAUT1 following mass spectrometry (MS) sequencing of Arabidopsis thaliana solubilized membrane proteins (Sterling et al., 2006; Atmodjo et al., 2013). Subsequent co-immunoprecipitation, MS sequencing, and bimolecular fluorescence complementation revealed that GAUT1 functions as a disulfide-linked heterocomplex with the homologous protein, GAUT7 (Atmodjo et al., 2011). In vivo, GAUT1 is truncated at its N-terminus by 167 residues and requires GAUT7 for localization in the Golgi (Atmodjo et al., 2011). Based on these results, GAUT7 was proposed to be a noncatalytic membrane anchor for GAUT1 (Sterling et al., 2006; Atmodjo et al., 2011). A more detailed study of the function of the GAUT1:GAUT7 complex and the mechanism of HG synthesis required the establishment of a recombinant protein expression system that could coexpress GAUT1 and GAUT7 and properly post-translationally fold and process the active GT complex.

Progress in studying plant cell wall biosynthesis has been hampered by difficulties associated with expressing and biochemically characterizing the relevant glycosyltransferases (Petersen et al., 2009; Culbertson, 2015). Because plant cell wall biosynthetic GTs are typically large *N*-glycosylated proteins that contain hydrophobic transmembrane regions and may exist as multi-enzyme complexes, most successful purifications of such recombinant GTs have been achieved using eukaryotic expression systems, namely *Nicotiana benthamiana* (Wu et al., 2010b; Chiniquy et al., 2012; Liwanag et al., 2012b; Geshi et al., 2013), *Pichia pastoris* (Petersen et al., 2009; Basu et al., 2013; Knoch et al., 2013b), and HEK293 cells (Sterling et al., 2006;

Urbanowicz et al., 2014; Urbanowicz et al., 2017), with the latter being a particularly successful host for recombinant expression and enzymatic characterization of soluble forms of eukaryotic GTs (Meng et al., 2013; Praissman et al., 2014; Subedi et al., 2015; Praissman et al., 2016; Halmo et al., 2017; Sheikh et al., 2017; Moremen et al., 2018). Here, we show that the HEK293 cell system can be used to express the heteromeric, disulfide-linked GAUT1:GAUT7 complex from *A. thaliana* in sufficient quantities to enable a comprehensive characterization of its enzymatic properties.

Heteromeric and homomeric GT complexes have been identified in glycan biosynthetic pathways shared by model eukaryotic organisms, including *Homo sapiens*, *Saccharomyces cerevisiae*, and *A. thaliana* (Kellokumpu et al., 2016). GT complexes have diverse biological functions and appear in *N*- and *O*-linked glycan, proteoglycan, and glycolipid synthesis pathways (Kellokumpu et al., 2016). In addition to the GAUT1:GAUT7 complex, at least six examples of proven and putative GT complexes involved in the synthesis of plant cell wall glycans are known (Oikawa et al., 2013; Jiang et al., 2016; Zeng et al., 2016). Various hypotheses for the biological significance of GT complexes have been proposed, including enhancement of enzymatic activity, substrate channeling, and Golgi localization (Oikawa et al., 2013; Kellokumpu et al., 2016).

Here we demonstrate that the GAUT1:GAUT7 complex can synthesize high molecular weight (MW) HG polysaccharides *in vitro* and we expand upon the original model of the GAUT1:GAUT7 complex (Atmodjo et al., 2011). We propose a two-phase model of polysaccharide elongation in which short-chain acceptors are elongated slowly, followed by a rapid elongation phase once the glycans reach an intermediate, critical degree of polymerization. This model reconciles data showing that HG extracted from plant cell walls consists of long polymers containing > 100 GalA units (Yasui, 2009) with reports that *in vitro* HG elongation

occurs through a non-processive mechanism (Doong and Mohnen, 1998; Akita et al., 2002; Ishii, 2002; Yasui, 2009). The activity reported also provides a basis for the initiation of HG polysaccharides by the GAUT1:GAUT7 complex and proposes that GAUT7 has a previously-unrecognized role in contributing to the synthesis of high MW polysaccharides.

RESULTS

GAUT1 and GAUT7 form a complex when co-expressed in HEK293F cells.

The co-immunoprecipitation of GAUT1 with GAUT7 from *A. thaliana* solubilized membranes revealed that GAUT1 and GAUT7 function as a GAUT1:GAUT7 heterocomplex covalently linked by disulfide bonds (Atmodjo et al., 2011). In an effort to obtain sufficient amounts of purified, soluble GAUT1:GAUT7 complex, recombinant *GAUT1* and *GAUT7* constructs were heterologously co-expressed in HEK293F suspension culture cells and the GAUT1:GAUT7 complex was characterized following purification.

Individual *GAUT1* and *GAUT7* constructs lacking their *N*-terminal transmembrane domains (*GAUT1*Δ167 and *GAUT7*Δ43) were generated as secreted fusion proteins harboring chimeric *N*-terminal fusion tags. GAUT1 purified from *A. thaliana* membranes is *N*-terminally truncated by 167 residues *in vivo* (Atmodjo et al., 2011). The fusion tags were composed of a signal sequence, His tag, AviTag, superfolder GFP, and TEV protease recognition site followed by the respective GAUT domains using a strategy previously employed for the expression of a large library of mammalian glycosylation enzyme expression constructs (Moremen et al., 2018). The constructs were transfected into HEK293F cells and the secreted fusion proteins were purified from the medium by Ni²⁺-Sepharose affinity chromatography.

Co-expression of *GAUT1*Δ167 and *GAUT7*Δ43 (hereafter referred to as GAUT1 and GAUT7) resulted in the production of secreted GAUT1:GAUT7 complex (Fig. 2.1A, Lane 7), which required reducing conditions (+DTT) to separate GAUT1 and GAUT7 into monomers (Fig. 2.1A, Lane 2). Treatment of the complex with Peptide-*N*-Glycosidase F (PNGase F) led to a reduction in the molecular weight of both GAUT1 and GAUT7, indicating that both proteins are *N*-glycosylated (Fig. 2.1A, Lanes 3 and 5). From a 1L culture, a total of 47.5 mg of the enzyme complex was purified.

Expression of GAUT1 alone resulted in the secretion of a GAUT1 homocomplex that could be purified and identified by SDS-PAGE under non-reducing conditions (Fig. 2.1B, Lane 5). However, heterologous expression of GAUT1 in the absence of GAUT7 also resulted in the formation of large amounts of truncation products and high molecular weight aggregates (Fig. 2.1B, Lanes 3 and 5). Expression of GAUT7 alone led to no detectable secretion of the GAUT7 fusion protein into the culture medium. These results suggest that co-expression of GAUT1 and GAUT7 and the formation of a disulfide-bonded heterocomplex is required for proper folding and secretion of the active GAUT1:GAUT7 complex.

Recombinant GAUT1:GAUT7 catalyzes the transfer of GalA residues from UDP-GalA onto homogalacturonan acceptors.

The GAUT1:GAUT7 complex isolated from *A. thaliana* membranes has previously been shown to transfer GalA from UDP-GalA onto HG acceptors (HG:GalAT activity) (Atmodjo et al., 2011). Here, we employed similar HG:GalAT acceptor-dependent activity assays to examine HG extension by the recombinant GAUT1:GAUT7 complex produced in HEK293F cells. The

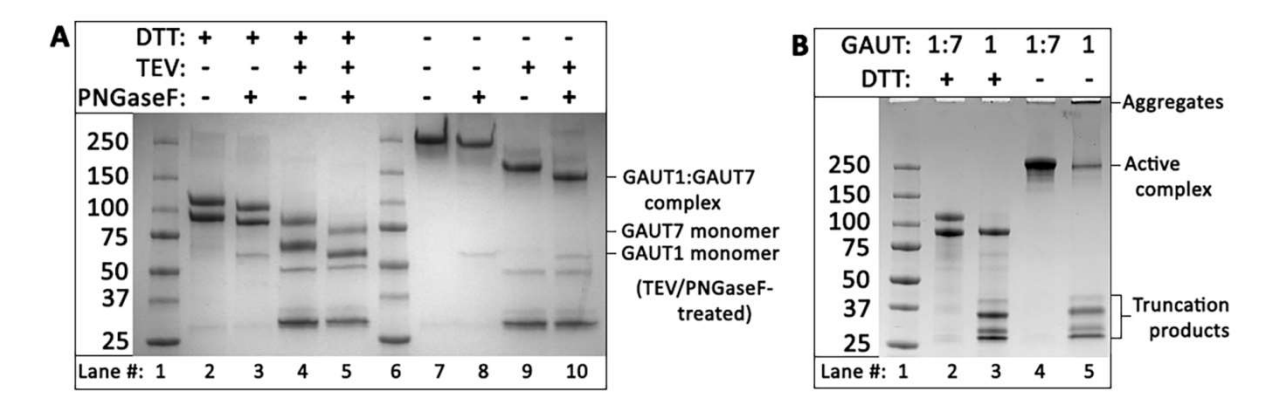


Figure 2.1. Heterologous expression of the GAUT1:GAUT7 complex. A, Coomassie blue-stained SDS-PAGE gel of purified GAUT1Δ167 co-expressed with GAUT7Δ43 detected under reducing (+DTT, Lanes 2-5) and non-reducing (-DTT, Lanes 7-10) conditions. Incubation with TEV protease (+TEV, Lanes 4-5 and 9-10) removes *N*-terminal GFP/His₆ tags, which electrophorese as ~30 kDa bands post-cleavage. Incubation with PNGase F (+PNGase F, Lanes 3, 5, 8, and 10) removes *N*-glycosylation. After six days of incubation, medium from transfected HEK293F cells was purified by Ni-affinity chromatography, protein concentration was quantified by UV-Vis spectroscopy, and 4 μg of purified protein was separated by SDS-PAGE after overnight incubation with or without TEV and PNGase F. The locations of the GAUT1:GAUT7 complex after TEV and PNGaseF treatment under non-reducing conditions and the GAUT1 and GAUT7 monomers under reducing conditions are designated on the right side of the figure. B, Coomassie blue-stained SDS-PAGE gel of purified GAUT1 (Lanes 3 and 5) compared to the GAUT1:GAUT7 complex (Lanes 2 and 4). Proteins are detected under reducing (+DTT, Lanes 2-3) and non-reducing (-DTT, Lanes 4-5) conditions.

co-expressed complex, containing intact N-terminal tags and N-glycosylation was used in all assays.

The activity of the purified enzyme was determined by radioactive incorporation of ¹⁴C-labeled GalA from UDP-[¹⁴C]GalA onto the non-reducing ends of an HG acceptor mix enriched for HG oligosaccharides with a degree of polymerization (DP) of DP7-23 (Doong and Mohnen, 1998; Scheller et al., 1999; Atmodjo et al., 2011). To assess the stability of the enzyme, GAUT1:GAUT7 activity was assayed immediately after Ni²⁺-Sepharose affinity purification and also after three days of storage at -80°C. GAUT1:GAUT7 retained 100% activity after storage at -80°C (Fig. 2.2A). Single-thawed aliquots retained ~40% activity after storage for 15 months. The enzyme complex has a pH optimum of 7.2 (Fig. 2.2B) and shows maximal activity in the presence of 0.1-1.0 mM MnCl₂ (Fig. 2.2C). A lower level of activity was obtained when GAUT1:GAUT7 was assayed with CoCl₂ (Fig. 2.2C). Manganese ion cofactors have been visualized in X-ray crystal structures of related GT8 enzymes, LgtC (Persson et al., 2001) and glycogenin (Gibbons et al., 2002a), and make active-site contacts with UDP-sugar substrates. All of the other divalent and monovalent metal cations tested (NiSO₄, FeCl₂, CuSO₄, CaCl₂, ZnSO₄, MgCl₂, NaCl, and KCl) yielded less than 5% of the activity observed with MnCl₂ (Fig. 2.3).

Based on the assays outlined above, a standard reaction condition was defined: 5 min reactions containing 100 nM GAUT1:GAUT7, 1 mM UDP-GalA, 10 μ M HG acceptor, and 0.25 mM MnCl₂ in a pH 7.2 HEPES buffer containing 0.05% BSA. Using the standard conditions outlined, Michaelis-Menten kinetics were measured for the donor, UDP-GalA, and for the HG acceptor mixture with the non-variable substrate held at saturating conditions. The GAUT1:GAUT7 complex shows a standard hyperbolic Michaelis-Menten curve for UDP-GalA with a $K_{\rm M}$ of 151 μ M (Fig. 2.2D). Substrate inhibition was observed at HG acceptor

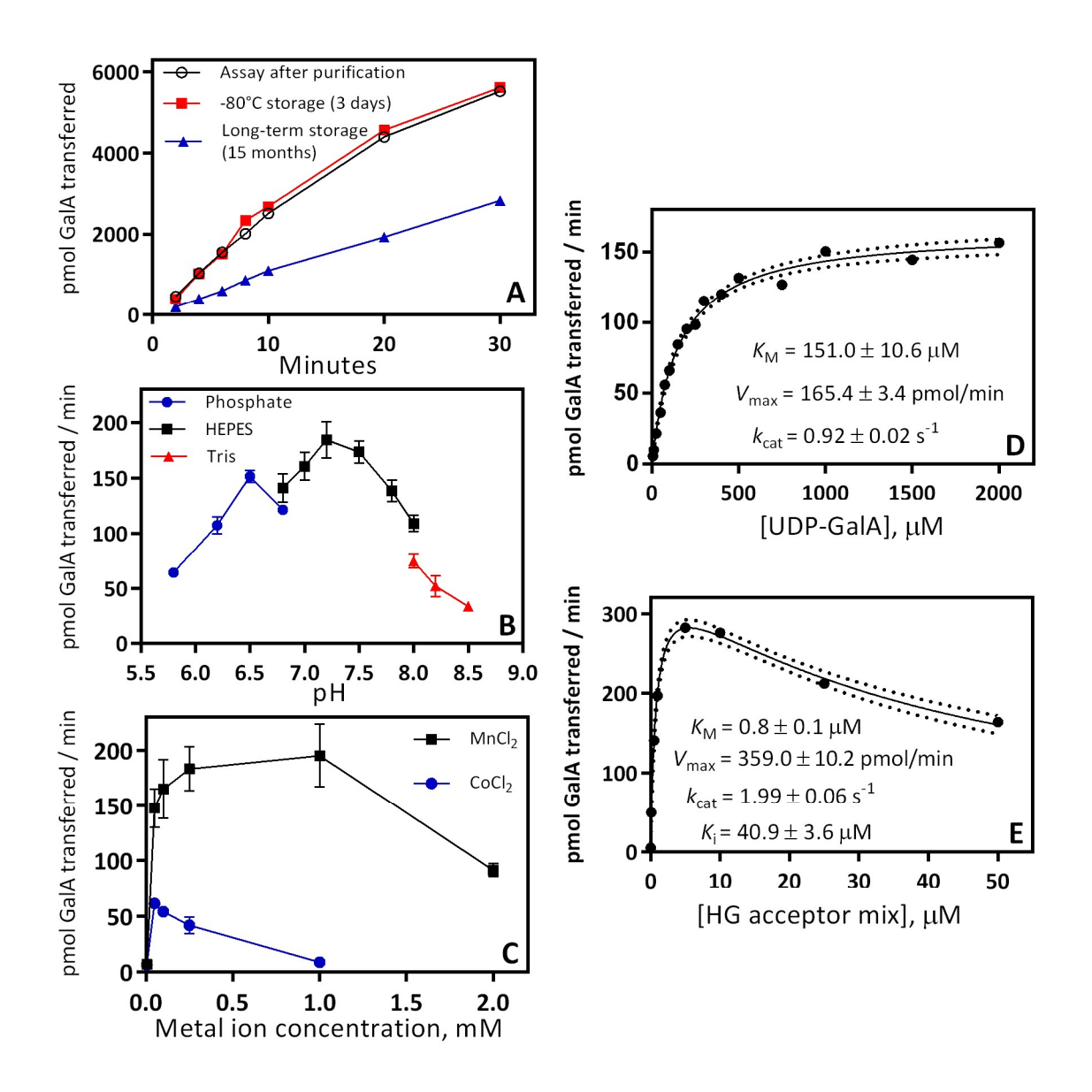


Figure 2.2. Biochemical characterization of HG:GalAT activity of the GAUT1:GAUT7 complex. A, Reaction progress from 2-30 min. GAUT1:GAUT7 enzyme was assayed for HG:GalAT activity immediately after Ni-affinity purification (open circles) to identify starting activity, after storage at -80°C for three days (boxes) to test effects of freeze-thawing, and after storage at -80°C for 15 months (triangles) to test effects of long-term storage at -80°C. Activity was measured in 30 μL reactions containing 100 nM GAUT1:GAUT7, 5 μM UDP-[¹⁴C]GalA, 1 mM total UDP-GalA, 10 μM HG acceptor mix, HEPES buffer pH 7.2, 0.25 mM MnCl₂, and 0.05% BSA. **B**, Effect of pH on enzyme activity. **C**, Effect of divalent cations on enzyme

activity. **D**, Michaelis-Menten kinetics for the UDP-GalA donor. UDP-GalA concentration from 5-2000 μM was tested with an HG acceptor mix concentration of 100 μM. Kinetic constants were calculated by nonlinear regression using Graphpad Prism 7. Dotted lines represent a 95% confidence interval. **E**, Michaelis-Menten kinetics for the HG acceptor mix (DP7-23). HG acceptor concentration from 0.01-50 μM was tested in reactions with 1 mM UDP-GalA. In **B-E**, all specific activity measurements were assayed in 5 min reactions. In **B** and **C**, error bars represent the standard deviation from at least three independent experiments. In **A**, **D**, and **E**, data points represent results from individual experiments. Replicate data from kinetics experiments are displayed in Table 2.1.

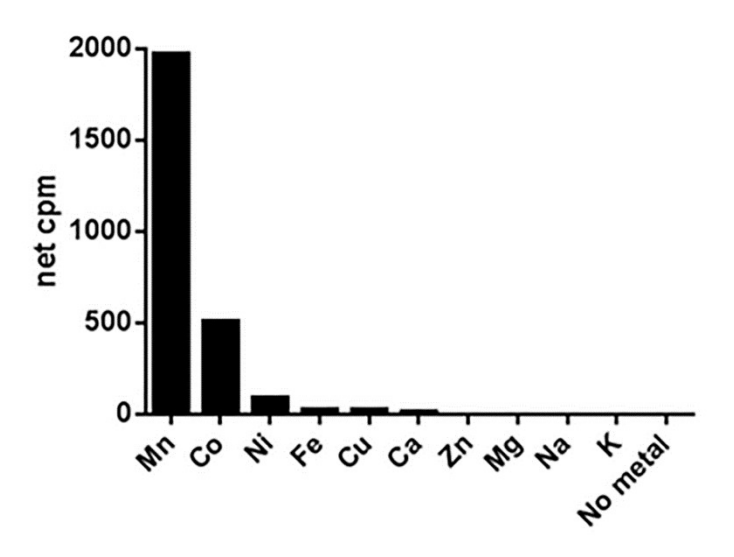


Figure 2.3. Effect of divalent and monovalent metal ions on the acceptor-dependent HG:GalAT activity of the GAUT1:GAUT7 complex . Metal-depleted GAUT1:GAUT7 was generated by overnight dialysis against HEPES, pH 7.2 buffer containing Chelex-100. After addition of the indicated metals at 0.25 mM in the reaction buffer, GAUT1:GAUT7 was assayed for activity in 5 min reactions containing 100 nM GAUT1:GAUT7, 5 μ M UDP-[14 C]GalA, 1 mM total UDP-GalA, HEPES buffer pH 7.2, and 0.05% BSA. The activity of all metals other than Mn $^{2+}$ and Co $^{2+}$ yielded less than 5% of the Mn $^{2+}$ activity. Data represent a single experiment. Replicate experiments for Mn $^{2+}$ and Co $^{2+}$ are displayed in Fig. 2C.

concentrations > 5 μ M (Fig. 2.2E). Substrate inhibition at high concentrations of HG acceptor is expected if GAUT1:GAUT7 functions through an ordered kinetic mechanism in which the UDP-GalA donor binds to the active site prior to the HG acceptor (Piszkiewicz, 1977; Cornish-Bowden, 2012). This ordered substrate binding scheme has also been shown in crystal structures and inhibition assays for homologous GT8-family enzymes (Persson et al., 2001; Gibbons et al., 2002a; Ly et al., 2002; Chaikuad et al., 2011). k_{cat} values for the elongation of HG acceptors ranged from 0.92-1.99 s⁻¹. Results from six independent assays are summarized in Table 2.1.

GAUT1:GAUT7 synthesizes high molecular weight polysaccharides in vitro by elongation of medium-chain HG acceptors ($DP \ge 11$) using a distributive mechanism.

The mechanism of HG backbone synthesis has not been clearly defined due to conflicting results from prior studies of this activity. HG:GalAT activity from detergent-solubilized microsomal membranes and from GAUT1:GAUT7 partially purified by immunoprecipitation has previously been shown to add between 1 to approximately 30 GalA residues onto DP13-DP15 acceptors (Doong and Mohnen, 1998; Akita et al., 2002; Sterling et al., 2006; Yasui, 2009), without detection of high MW polymeric HG. These results suggested that GAUT1:GAUT7 uses a distributive mechanism, in which single GalA units are added during each catalytic event followed by the release of the HG acceptor, and also that GAUT1:GAUT7 does not synthesize high MW HG polymers *in vitro*. In contrast, intact *Nicotiana tabacum* microsomal membranes produce an HG-containing product of approximately 105 kDa (Doong et al., 1995b; Doong and Mohnen, 1998). However, in those experiments, it was not shown whether the high MW product was free HG polysaccharide or a more complex glycan or proteoglycan

containing HG. The synthesis of high MW HG polysaccharides has not yet been described from *in vivo* or *in vitro* experiments.

We used recombinant GAUT1:GAUT7 and HG acceptors enriched for homogeneous degrees of polymerization to measure the size of products synthesized by HG:GalATs. We reasoned that if the GAUT1:GAUT7 complex elongates HG acceptors by a distributive mechanism, the chain length of the products synthesized should be dependent on the ratio of donor to acceptor substrates (Levengood et al., 2011; Keys et al., 2014).

The degree of HG acceptor elongation by GAUT1:GAUT7 in vitro was determined by size exclusion chromatography, high-percentage PAGE, and MALDI-TOF. Using 1 mM UDP-GalA and varying amounts of DP11 HG acceptor, reactions were performed under two conditions: 10 µM HG acceptor (100:1 molar excess of UDP-GalA donor) (Fig. 2.4A and 2.4B), and 100 µM HG acceptor (10:1 molar excess of UDP-GalA donor) (Fig. 2.4C and 2.4D). DP11 acceptors were rapidly elongated under both assay conditions. The products synthesized were larger at all time points when a 100:1 molar excess of UDP-GalA over HG acceptor was used (Fig. 2.4A and 2.4B). The high MW products are measured to be > 100 kDa, but pectin MW may be overestimated relative to dextran standards due to the potential for aggregation or anomalous behavior in size exclusion columns (Mort, 1991). As observed in high-percentage polyacrylamide gels in which individual bands corresponding to HG products up to DP30 could be distinguished, the DP11 acceptor was elongated to an estimated DP of 30-50 (< 10 kDa) when incubated at a 10:1 donor:acceptor ratio (Fig. 2.4D). Comparison of these two reaction conditions showed that in vitro HG synthesis by GAUT1:GAUT7 matches the results expected for a distributive GT mechanism in which the narrow product distribution has a DP dependent on the available donor:acceptor ratio, as discussed for polysialyltransferases (Keys et al., 2014).

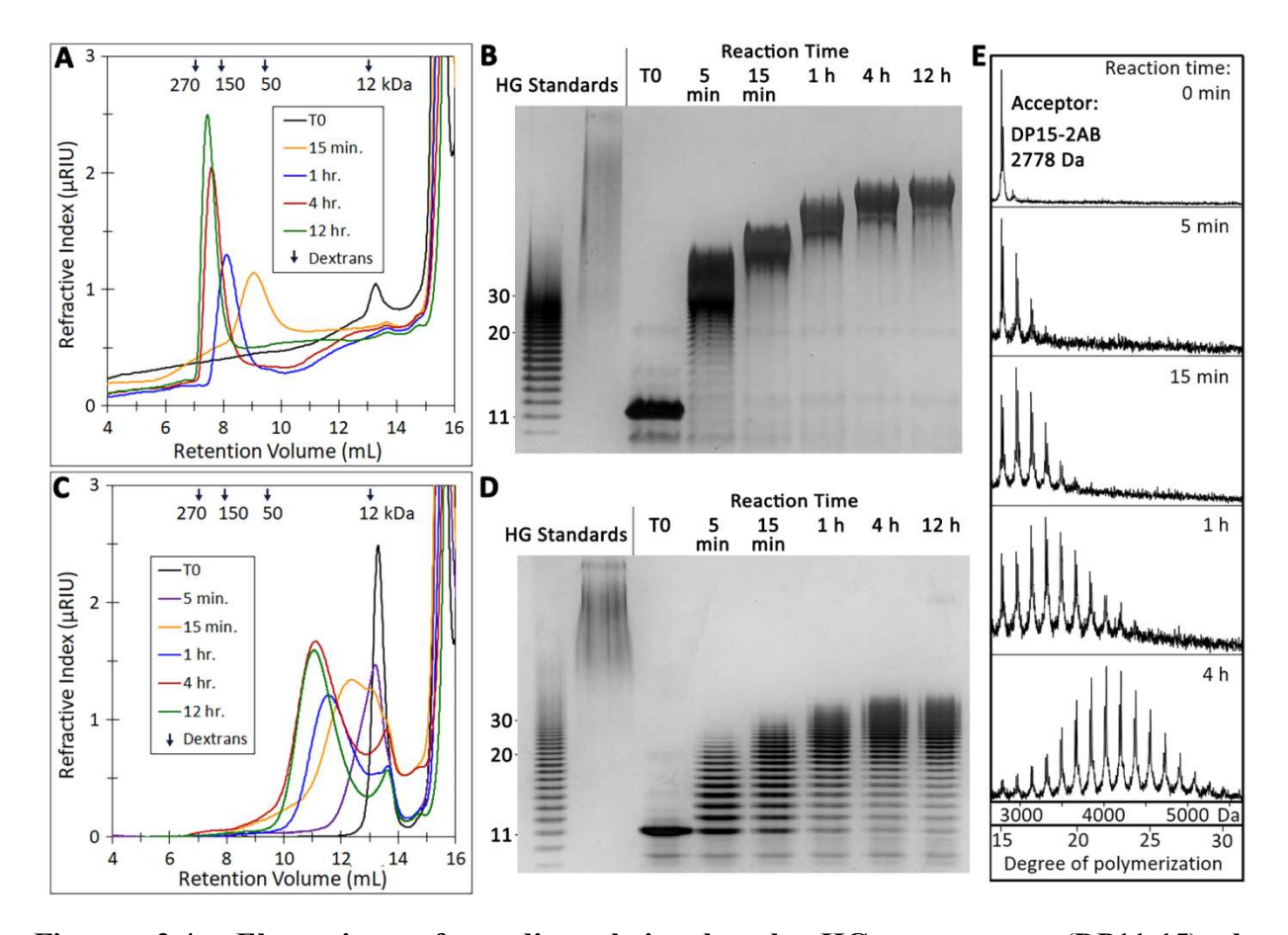


Figure 2.4. Elongation of medium-chain length HG acceptors (DP11-15) by GAUT1:GAUT7. A, Size exclusion chromatography of the products synthesized in a reaction containing 100 nM GAUT1:GAUT7, 1 mM UDP-GalA, and 10 μM DP11 acceptor. Reactions were incubated for indicated times and injected into a Superose 12 column. Selected peaks are indicated. Arrows represent the peak retention volume of dextran standards (270, 150, 50, and 12 kDa avg. MW). B, High-percentage polyacrylamide gel stained with a combination of alcian blue/silver. Reactions containing 10 μM of a DP11 acceptor were incubated, and aliquots representing 200 ng of acceptor oligosaccharide were separated on a 30% PAGE gel. HG standards include the HG oligosaccharide acceptor mix (Lane 1) and high MW commercial polygalacturonic acid (PGA) (Lane 2). Individual bands of discrete DP that can be counted in the HG standard are indicated on the left side of the gel. C, Size exclusion chromatography of

products synthesized in a reaction containing 100 μ M DP11 acceptor. **D**, High-percentage PAGE of a reaction containing 100 μ M DP11 acceptor. **E**, MALDI-TOF MS analysis of products produced by GAUT1:GAUT7 in reactions containing 100 μ M DP15 HG acceptor and 1 mM UDP-GalA. Reaction products were reducing-end labeled with 2-AB after the indicated reaction times. The series of ions (m/z) with a mass separation of 176 Da is consistent with sequential addition of GalA to the DP15 acceptor.

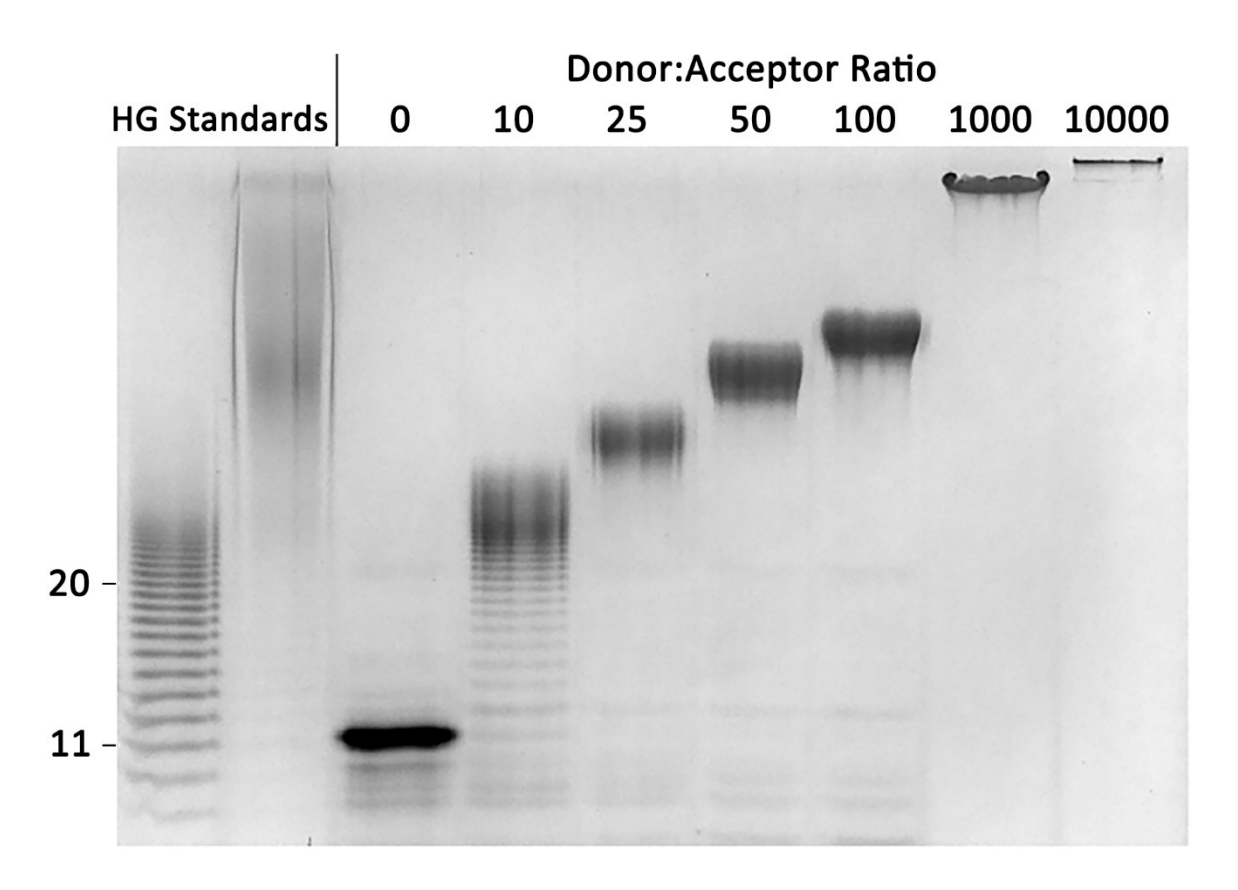


Figure 2.5. GAUT1:GAUT7 elongates DP11 acceptors in a manner dependent on the available donor:acceptor ratio. Following incubation of GAUT1:GAUT7 with the indicated ratios of UDP-GalA donor to DP11 acceptor for 12 h, samples were loaded into high-percentage PAGE gels stained with alcian blue/silver. Larger products were detected with increasing donor:acceptor ratio. For ratios of 0-100, 25 μ M acceptor was incubated with varying amounts of UDP-GalA. For ratios of 1000 and 10000, 1 mM UDP-GalA was incubated with 1 μ M and 0.1 μ M acceptor, respectively. HG oligosaccharide standards (lane 1) and PGA (lane 2) are described in Fig. 3B.

Overnight incubation of GAUT1:GAUT7 with donor:acceptor ratios ranging from 10 to 10,000 further demonstrated that GAUT1:GAUT7 synthesizes high MW products given available UDP-GalA (Fig. 2.5).

Labeling of the reducing ends of HG acceptors with the fluorescent tag 2-aminobenzamide (2-AB) has been used to detect HG elongation using high-performance anion-exchange chromatography (Ishii, 2002). Fluorescent labeling of oligosaccharides has also been shown to enhance detection of oligosaccharides by MALDI-TOF (Urbanowicz et al., 2014). We therefore used MALDI-TOF to test the pattern of elongation of a DP15 fluorescently-labeled HG acceptor in reactions incubated from 5 min up to 4 h. Over time, products up to DP30 were detected (Fig. 2.4E). The apparent Poisson distribution of HG products formed over time is also typical of a distributive mechanism of synthesis (Urbanowicz et al., 2014). However, it should be noted that as observed in PAGE gels, (Fig. 2.4D), products larger than DP30 were also synthesized under these reaction conditions, indicating that the apparent Poisson distribution observed by MALDI-TOF was partially due to the loss of higher MW signals. Longer-chain oligosaccharides may be poorly ionized or may have precipitated when exposed to acidic conditions during the labeling procedure.

Elongation of short-chain HG acceptors ($DP \le 7$) occurs with low efficiency relative to longer-chain acceptors ($DP \ge 11$).

Prior assays of HG:GalAT activity from N. tabacum- and P. axillaris-solubilized membranes demonstrated a preference of the enzyme for exogenous HG acceptors of DP \geq 10-12, but also indicated that acceptors as short as DP5 can be elongated (Doong and Mohnen, 1998; Akita et al., 2002). To more clearly define the acceptor specificity of GAUT1:GAUT7, we

compared the rates of elongation of homogenous HG acceptors enriched for DPs of 3, 7, 11, and 15.

GAUT1:GAUT7 elongates HG acceptors at least as small as DP3 (Fig. 2.6A). GalA transfer is most rapid using longer-chain acceptors (DP ≥ 11). The rate of transfer to DP11 and DP15 acceptors was approximately equal from 5-60 min. Activity was detected using shorter acceptors (DP7 and DP3), but the initial rates of synthesis were low relative to the longer DP acceptors. The highest rates of synthesis for longer-chain acceptors were detected in the initial linear phase of the reaction, as expected for a standard steady-state reaction progress curve. A lag phase was observed during the elongation of DP7 and DP3 acceptors, and longer incubation periods were required to detect above-background levels of activity.

Reaction kinetics were measured using increasing amounts of DP11 (Fig. 2.6B) and DP7 (Fig. 2.6C) HG acceptors. The reaction kinetics using the DP11 HG acceptor appear similar to the results observed using the HG acceptor mix (Fig. 2.2E), with inhibition observed at concentrations above 5 μ M. Because activity with the DP7 acceptor was near-background level when measured at 5 min, a 30 min incubation time was used. Standard hyperbolic Michaelis-Menten kinetics were observed under these conditions. The catalytic efficiency, defined as k_{cat}/K_M , of a DP11 acceptor was 45-fold higher than a DP7 acceptor, representing a strong preference for longer-chain acceptors. This measurement may underestimate the difference in catalytic efficiency between DP7 and DP11 acceptors because the low initial rates and the lag phase observed only with short-chain acceptors makes it difficult to calculate true initial rates of synthesis.

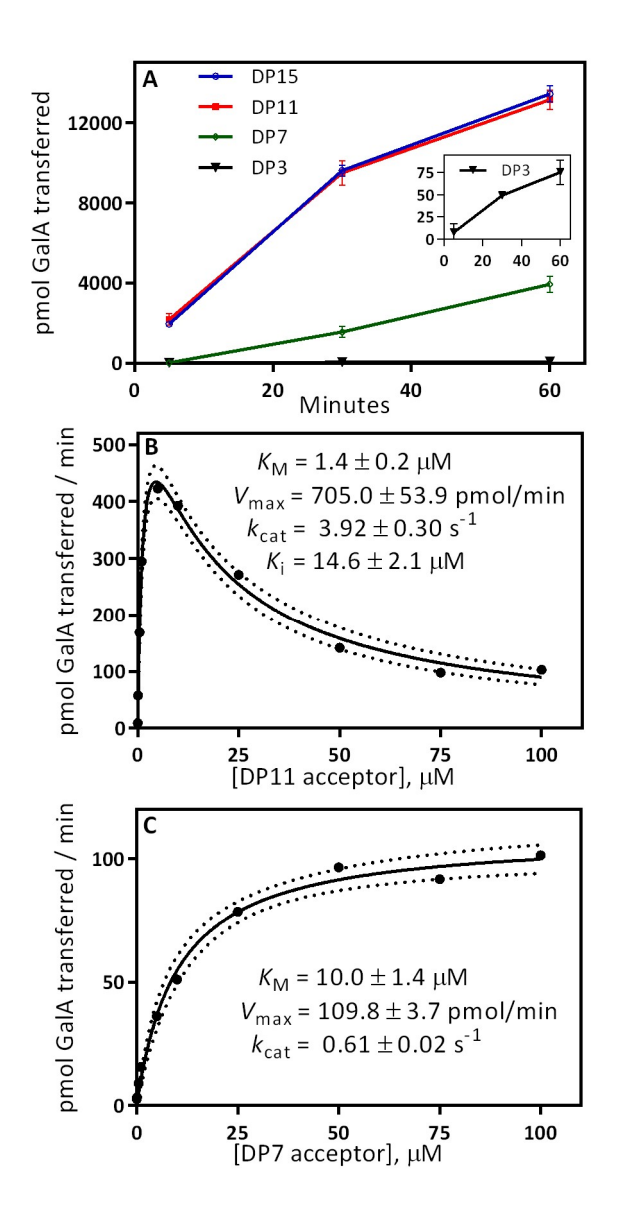


Figure 2.6. Comparison of acceptor elongation activity using HG acceptors of different degrees of polymerization. A, GAUT1:GAUT7 elongation activity from 5-60 min. Activity was measured in 30 μL reactions containing 100 nM GAUT1:GAUT7, 5 μM UDP-[14C]GalA, 1 mM total UDP-GalA, and 10 μM of purified, homogenous DP acceptor, as indicated. Error bars represent the standard deviation from three independent experiments. The inset shows activity using a DP3 acceptor. B, Michaelis-Menten kinetics for the DP11 acceptor. HG acceptor concentration from 0.01-100 μM was tested in reactions with 1 mM UDP-GalA. Kinetic constants were calculated by nonlinear regression with substrate inhibition using Graphpad

Prism 7. Dotted lines represent a 95% confidence interval. **C**, Michaelis-Menten kinetics for the DP7 acceptor. HG acceptor concentration from 0.01-100 µM was tested in reactions with 1 mM UDP-GalA. Kinetic constants were calculated by nonlinear regression using the standard Michaelis-Menten equation. In **B** and **C**, data points represent results from individual experiments. Results from replicate kinetics experiments are displayed in Table 2.1.

Elongation of short-chain HG acceptors and de novo synthesis in the absence of exogenous oligosaccharide acceptors leads to a bimodal product distribution with minimal observable intermediates.

As shown in Fig. 2.6, initial rates of synthesis using short-chain HG acceptors (DP \leq 7) are low relative to longer-chain acceptors. To test whether the DP7 acceptor is elongated by a different reaction mechanism distinct from longer-chain acceptors, the degree of DP7 acceptor elongation was measured by size exclusion chromatography, high-percentage PAGE, and MALDI-TOF. Reactions were carried out using 100 μ M acceptor (10:1 molar excess of UDP-GalA donor) (Fig. 2.7A and 2.7B).

Unlike the results observed using a DP11 HG acceptor (Fig. 2), a bimodal distribution of high MW and short-chain products was synthesized during the elongation of a DP7 acceptor, even under conditions of a low molar ratio of UDP-GalA to acceptor. Polysaccharides of intermediate molecular weights were not observed. When detecting low MW products, addition of only 1-2 GalA residues was observed at all time points (Fig. 2.7B and Fig. 2.8B). Unlike DP11 elongation, a Poisson distribution of HG oligomers was not observed. Instead, the intensity of high MW products increased with reaction time from 1-12 h. A similar bimodal product distribution was observed with donor:acceptor ratios ranging from 10 to 200 (Fig. 2.9).

Having identified that GAUT1:GAUT7 can elongate short-chain acceptors as small as DP3, the complex was tested for the ability to initiate HG synthesis *de novo* in the absence of exogenously added acceptors. Prior attempts to identify *de novo* initiation of HG using detergent-solubilized membrane fractions yielded no measurable activity, leading to the conclusion that the enzyme only functions in the elongation step of HG biosynthesis (Atmodjo et al., 2013).

Three monoclonal antibodies previously shown to react with HG (CCRC-M38, CCRC-M131, and JIM5) (Pattathil et al., 2010) were used in ELISA assays to determine if GAUT1:GAUT7 could synthesize HG *de novo*. Following incubation with 1 mM UDP-GalA, all three anti-HG antibodies reacted with GAUT1:GAUT7-synthesized product in a time and concentration-dependent manner (Fig. 2.7C). Control ELISA assays confirmed that the anti-HG antibodies detected HG acceptor controls but had no reactivity toward GAUT1:GAUT7 itself or toward UDP-GalA (Fig. 2.7D). To the best of our knowledge, this is the first evidence that GAUT1:GAUT7 can synthesize HG *de novo*.

The *de novo* synthesis product synthesized in overnight reactions was of high MW, similar to the products of overnight reactions with DP7 and DP3 acceptors (Fig. 2.7E). The *de novo* synthesis product is a more uniform MW than the relatively polydisperse product formed following elongation of DP7 acceptors. The polysaccharides synthesized *de novo* were sensitive to digestion by the HG-specific enzyme, endopolygalacturonase (Fig. 2.10). These results demonstrate that in addition to elongation of acceptors of all degrees of polymerization, GAUT1:GAUT7 can initiate the synthesis of high MW HG *de novo*.

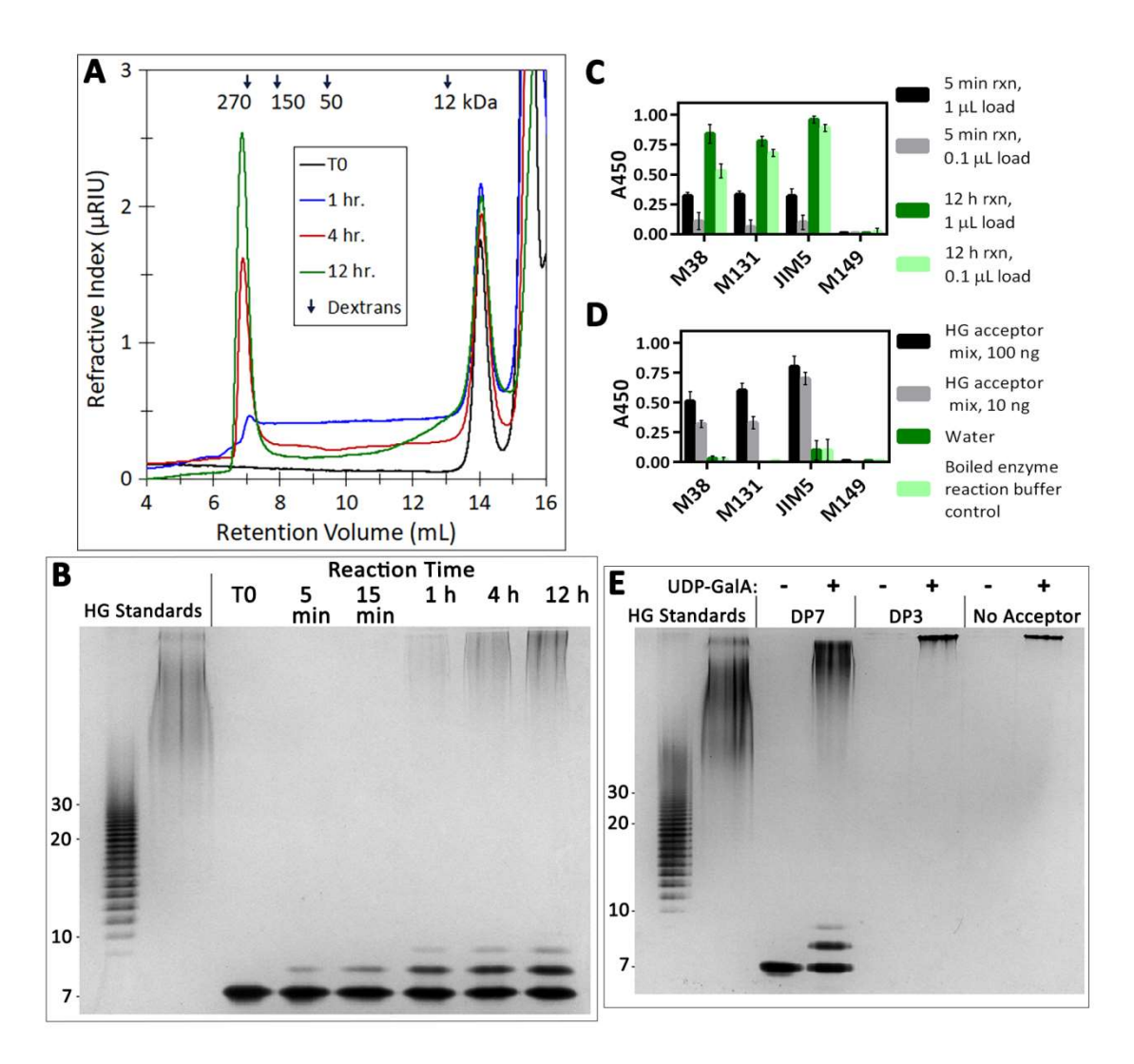


Figure 2.7. Elongation of short-chain HG acceptors and *de novo* initiation of high molecular weight HG polysaccharides. A, Size exclusion chromatography of the products synthesized in a reaction containing 100 nM GAUT1:GAUT7, 1 mM UDP-GalA, and 100 μM DP7 HG acceptor. Reactions were incubated for the indicated times and injected into a Superose 12 column. Selected peaks are indicated. Arrows represent the peak retention time of dextran standards. B, High-percentage polyacrylamide gel stained with a combination of alcian blue/silver. Reactions containing 100 μM DP7 acceptor were incubated for the indicated times, and an aliquot representing 200 ng acceptor oligosaccharide was removed and separated on a 30% PAGE gel. HG oligosaccharide standards (lane 1) and PGA (lane 2) are described in Fig.

3B. C, Detection of HG polysaccharides synthesized *de novo* by ELISA. Reactions (30 μL total volume) containing 100 nM GAUT1:GAUT7 and 1 mM UDP-GalA were incubated for 5 min or 12 h. At the indicated time points, aliquots containing 1 μL or 0.1 μL reaction volume (1/30 or 1/300 of the total reaction volume) were boiled and spotted onto a 96-well plate. Reaction products were detected by anti-HG antibodies CCRC-M38, CCRC-M131, and JIM5, but showed no reactivity toward anti-xylan antibody CCRC-M149. **D**, Anti-HG antibody ELISA controls. In **C** and **D**, error bars represent the standard deviation from a total of four replicate measurements from two independent experiments. **E**, High-percentage polyacrylamide gel of products synthesized *de novo* by GAUT1:GAUT7, or in the presence of DP3 or DP7 acceptors, stained with a combination of alcian blue/silver. Reactions (30 μL total volume) containing 100 μM DP7, DP3, or no acceptor (*de novo* synthesis) were incubated 24 h, then 5 μL was removed for separation on a 30% polyacrylamide gel.

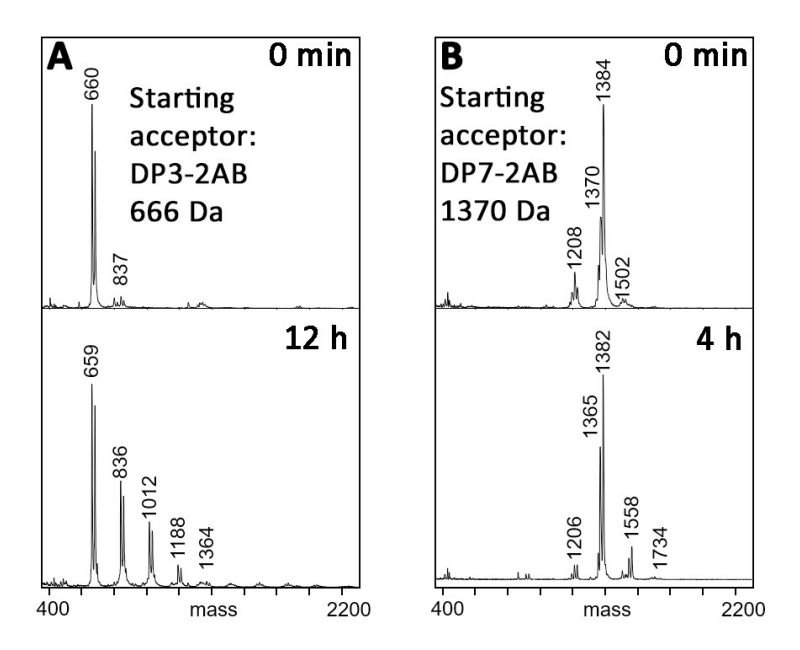


Figure 2.8. Elongation of DP3 and DP7 acceptors detected by MALDI-TOF MS. After incubation of GAUT1:GAUT7 with 1 mM UDP-GalA and A, DP3 acceptor (1 mM) for 12 h or B, DP7 acceptor (100 μM) for 4 h, addition of only 1-4 GalA units can be detected by MALDI-TOF MS analysis of 2-AB-labeled HG elongation products. Using either acceptor, longer-chain HG products were not detected after longer reaction incubation times (up to 48 h, data not shown). The series of ions (m/z) with a mass separation of 176 Da is consistent with sequential addition of GalA.

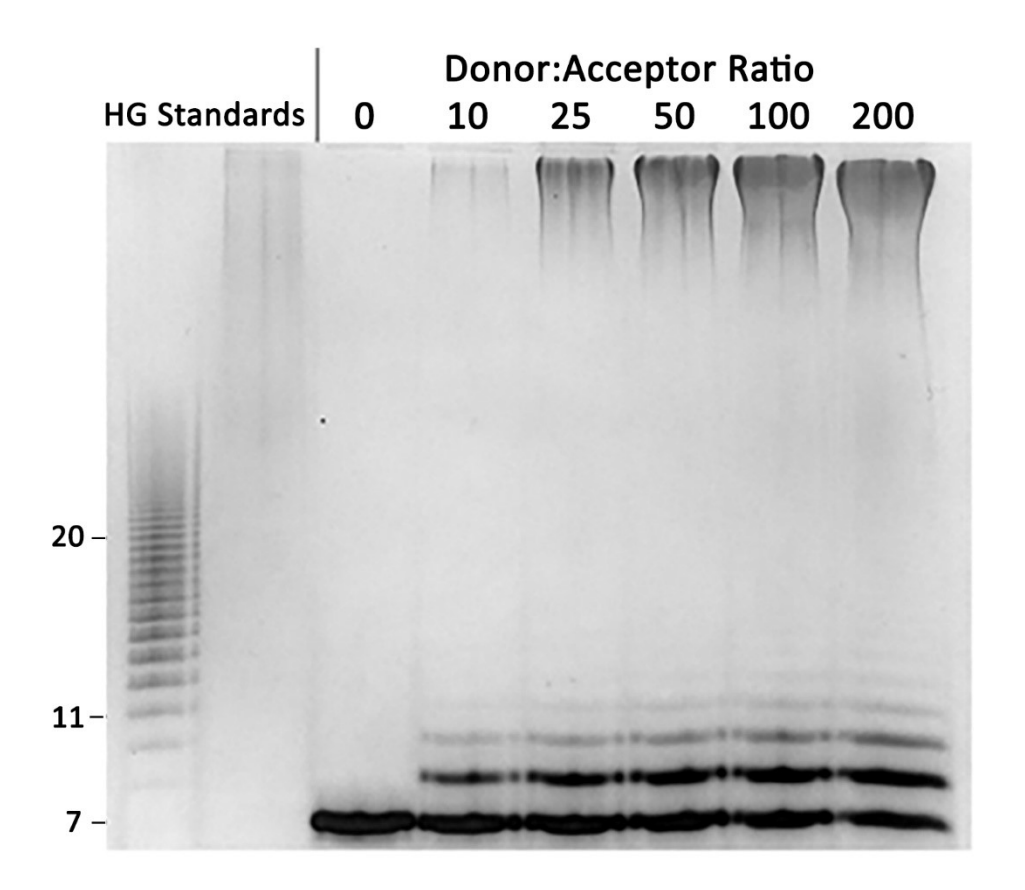


Figure 2.9. Elongation of DP7 acceptors results in a bimodal product distribution under a donor:acceptor ratio ranging from 10 to 200. Following incubation of GAUT1:GAUT7 with the indicated ratios of UDP-GalA donor to DP11 acceptor for 12 h, samples were loaded into high-percentage PAGE gels stained with alcian blue/silver. High MW products were detected under all donor:acceptor ratios tested. For all reactions, 25 μM DP7 acceptor was incubating with increasing amounts of UDP-GalA. HG oligosaccharide standards (lane 1) and PGA (lane 2) are described in Fig. 3B.

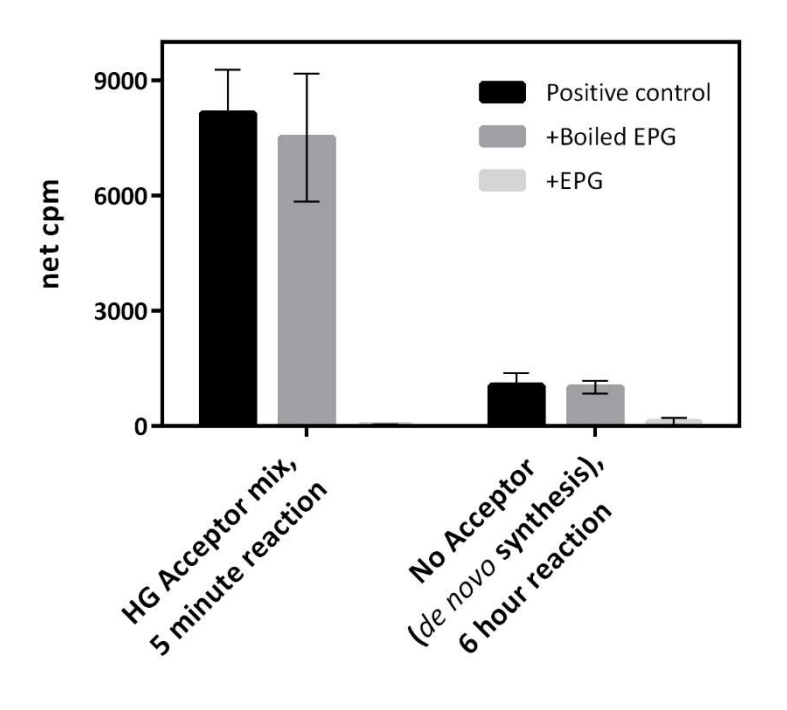


Figure 2.10. Digestion by endopolygalacturonase (EPG) of HG synthesized by acceptor-dependent elongation and *de novo* synthesis. Acceptor-dependent activity was measured in 5 minute reactions containing 100 nM GAUT1:GAUT7, 5 μM UDP-[¹⁴C]GalA and 10 μM HG mix. *De novo* synthesis activity was measured in 6-hour reactions containing 500 nM GAUT1:GAUT7 and 5 μM UDP-[¹⁴C]GalA. Following addition of sodium acetate buffer, pH 4.2, samples were incubated for 18 h with H₂O (positive control), 20 mU of endopolygalacturonase, or EPG deactivated by boiling. Error bars represent the standard deviation from three independent experiments.

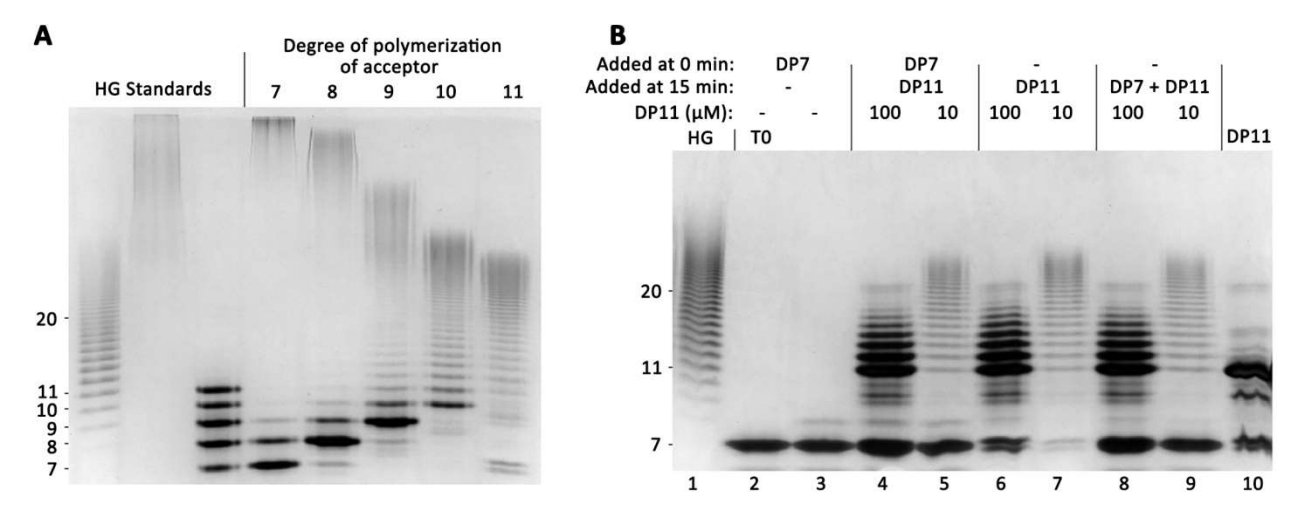


Figure 2.11. Non-processive elongation of HG acceptors. A, High-percentage polyacrylamide gel separation of products synthesized by GAUT1:GAUT7 stained with a combination of alcian blue/silver. Reactions containing 100 nM GAUT1:GAUT7, 1 mM UDP-GalA, and 100 µM acceptor of DP 7-11 were incubated for 12 h. An aliquot representing 200 ng acceptor oligosaccharide was removed and separated on a 30% PAGE gel. To reactions containing preboiled enzyme are displayed in Fig. 2.12. HG standards are described in Fig. 3B. Lane 3 is a mixture of HG DP 7-11 standards, 50 ng each. B, Competition assay to test for a processive elongation mechanism. UDP-GalA (1 mM) and either no acceptor or HG DP7 acceptor (100 μM) were added during a pre-incubation phase (0-15 min.) to allow formation of enzymeacceptor processive elongation complexes. Additional acceptors were added during the reaction phase (15-20 min), as indicated. Samples were boiled after 20 min. In the T0 sample (Lane 2), reaction was boiled immediately upon addition of DP7 acceptor. In the DP7 control reaction (Lane 3), no additional acceptor was added at 15 min. Competition assay samples (Lanes 4-5): reactions containing 100 nM GAUT1:GAUT7 were pre-incubated (0 min.) with 1 mM UDP-GalA and 100 μ M DP7 acceptor. After 15 min, DP11 acceptor was added (100 μ M = 10:1 donor:acceptor ratio, 10 µM = 100:1 donor:acceptor ratio). DP11 standard reaction controls

(Lanes 6-7): no acceptor was added during the pre-incubation phase. DP11 acceptor was added after 15 min. Simultaneous incubation reaction controls (Lanes 8-9): no acceptor was added during the pre-incubation phase. A mix of $100 \mu M$ DP7 and indicated DP11 acceptor was added after 15 min. DP11 standard (Lane 10) shows the DP11 acceptor and the presence of background bands due to minor impurities.

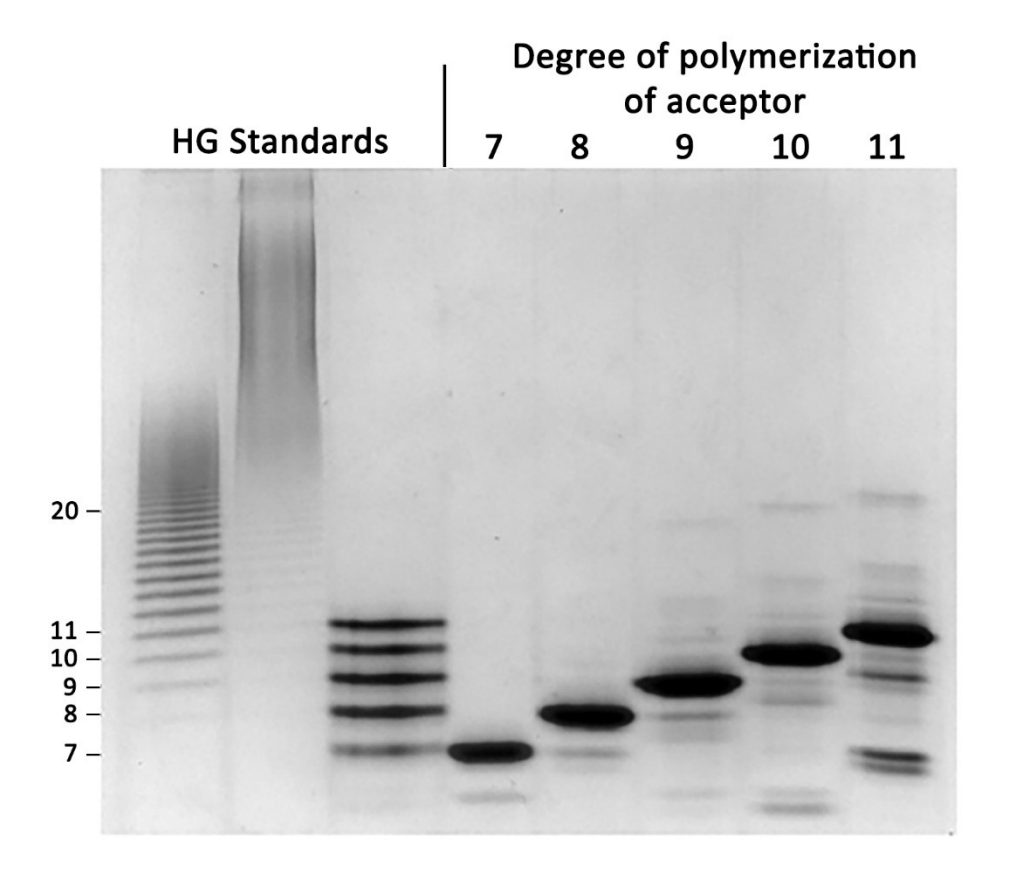


Figure 2.12. Boiled enzyme controls, T0 starting acceptors for Fig.6A. As in Fig. 6A, reactions containing 100 nM GAUT1:GAUT7, 1 mM UDP-GalA, and 100 μM acceptor of DP 7-11 were incubated for 12 h. Enzyme was inactivated by pre-boiling prior to the reaction. HG oligosaccharide standards (lane 1) and PGA (lane 2) are described in Fig. 3B. Lane 3 is a mixture of HG DP 7-11 standards, 50 ng each.

A two-phase model of distributive elongation is favored over a processive model for HG synthesis.

During *in vitro* HG polymerization by GAUT1:GAUT7, small differences in the chain length of HG acceptors appeared to affect the mechanism of elongation. We investigated whether short- and long-chain acceptors are elongated using distinct mechanisms by further defining the role of acceptor DP on product size distribution. GAUT1:GAUT7 was incubated for 12 h in the presence of a low donor:acceptor ratio (10:1) of intermediately-sized HG acceptors ranging from DP7-DP11 (Fig. 2.11A). As previously observed, elongation of the DP11 acceptor resulted in products ranging in size from DP11 to a DP of \sim 30-50. The majority of the starting acceptor was incorporated into larger sized HG products. In contrast, all acceptors of DP \leq 10 were elongated relatively poorly, as indicated by the appreciable amount of acceptors remaining unelongated even following a 12 h incubation. Quantitation using fluorescently tagged acceptors indicated that < 3% of the original DP7 acceptor was elongated to high MW products in overnight reactions (Fig. 2.13)

Product size was inversely related to the size of the HG acceptor, with high MW polymeric HG observed following incubation with smaller acceptors. Contrary to the DP10 and DP11 acceptors, elongation of DP7 and DP8 acceptors resulted in a bimodal product distribution, with an intermediate distribution for DP9. (Fig. 2.11A).

Three observations appeared to support the hypothesis that GAUT1:GAUT7 uses distinct processive and distributive mechanisms depending on the chain length of the acceptor, and that short-chain acceptors were elongated by a processive mechanism. First, a bimodal product distribution formed over time (Fig. 2.7B and E). The archetypal processive model for GT activity proposes that a single acceptor molecule remains tightly bound without dissociating from the

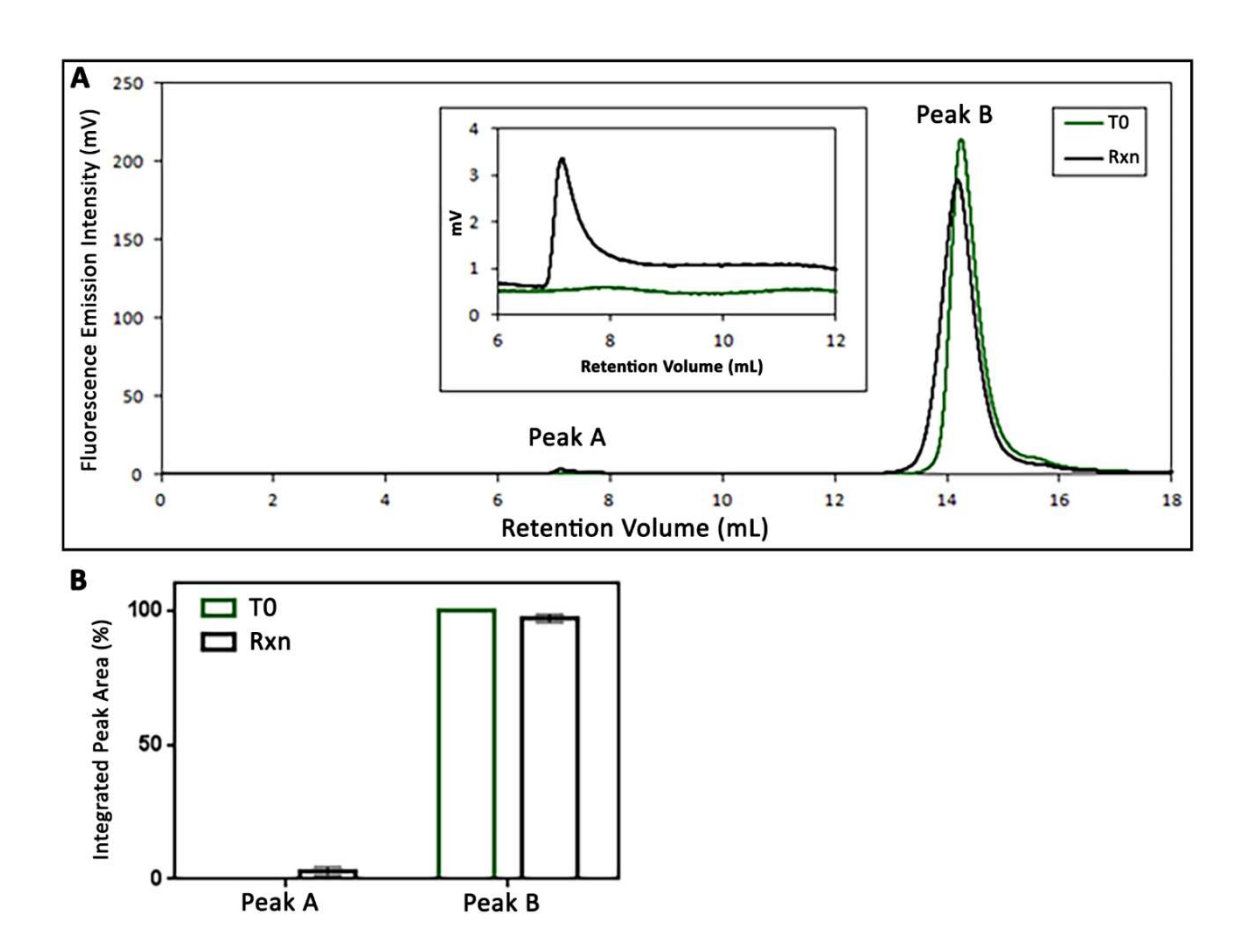


Figure 2.13. SEC separation with fluorescence detection of DP7-2AB acceptor and high molecular weight products. A, Following a 24 h incubation of GAUT1:GAUT7 with 100 μM DP7-2AB, high molecular weight polysaccharides (Peak A) were measured by size exclusion chromatography with fluorescence detection. The non-symmetrical Peak B contains the unreacted DP7-2AB acceptor and DP8-9 elongation products, as demonstrated in Fig. 5B and Fig. S2. The inset is a magnification of Peak A. GAUT1:GAUT7 was pre-boiled in T0 control samples, representing the unreacted DP7-2AB acceptor (dark green). B, Quantitation was performed by integration of peak area using Chromeleon software. Total area in Peak A and Peak B was normalized to 100%. From three replicate experiments, the percentage of integrated peak area in Peak A, representing the proportion of the starting acceptor that was elongated to high MW products, was 2.9%.

enzyme until after many rounds of elongation, leading to the formation of high MW products with minimal observable intermediates (Bloom and Goodman, 2001; Levengood et al., 2011; Keys et al., 2014). Second, a lag phase was observed during early points in the progress curve (Fig. 2.6A). The lag phase has been proposed to be a feature common to processive enzymes due to the low affinity of short-chain acceptors which are not capable of filling a requisite number of "acceptor subsites" within an extended active-site domain (Levengood et al., 2011; Fiebig et al., 2018). Third, the amount of acceptors within the starting pool used during the reaction was low, measured at < 3% (Fig. 2.13). In traditional measures of processivity, if < 10% of the total starting acceptor pool is elongated, then it has been assumed that each acceptor has only associated with the enzyme in a single priming event (Bambara et al., 1995; Bloom and Goodman, 2001). All three of these observations were suggestive of the processive model, but did not directly demonstrate the existence of tight enzyme-acceptor binding complexes demanded by that model. Because these results were inconsistent with the rapid elongation of DP ≥ 11 acceptors in a non-processive manner, we considered that the processive model may not accurately describe the elongation of HG by GAUT1:GAUT7.

To directly test for evidence of a processive elongation mechanism in the presence of low DP acceptors, a competition assay was designed. GAUT1:GAUT7 was pre-incubated with UDP-GalA and a DP7 acceptor for 15 min at a 1000-fold excess of acceptor over enzyme. We reasoned that 15 min was a sufficient pre-incubation time to allow all enzyme molecules to bind to the acceptor and to begin processive synthesis. Following pre-incubation, a DP11 acceptor was added, and incubation was continued for another 5 min (Fig. 2.11B, Lane 4-5). If the DP7 HG served as an acceptor for processive catalysis, the DP11 acceptor would not have been able to compete for binding to GAUT1:GAUT7 or to serve as an acceptor. The results show,

however, that the DP11 HG acceptor was able to compete for enzyme binding and was elongated during the 5 min reaction period.

The DP11 acceptor was elongated to the same chain lengths as two control reactions: a standard 5 min reaction with no competing DP7 acceptor added during the pre-incubation period (Fig. 2.11B Lane 6-7) and a 5 min reaction in which DP7 and DP11 acceptors were added at the same time (Lane 8-9). These results argue against the hypothesis that short-chain acceptors are synthesized by a processive mechanism, in which the growing acceptor should have formed tight binding complexes with the enzyme, making it unavailable for binding to DP11 acceptors. Furthermore, there was no effect on the size distribution of the products synthesized by elongation of DP11 acceptors in the presence of DP7. This result is consistent with the enzyme having a strong preference for binding to longer-chain acceptors and releasing the acceptor following each round of GalA transfer.

The competition assay argues against the hypothetical processive elongation model because the results suggest that GAUT1:GAUT7 and HG acceptors do not form tight enzyme-acceptor binding complexes. An alternative, two-phase model proposes that acceptors of all sizes are elongated by a distributive mechanism and the bimodal product distribution results from large differences in catalytic efficiency between shorter and longer-chain acceptors. Small acceptors are inefficiently elongated by the enzyme, as evidenced by the > 45-fold difference in catalytic efficiency between DP7 and DP11 acceptors. Acceptors are only rapidly elongated after reaching a critical DP, estimated to be DP11 (Fig. 2.11A). The relative inefficiency of short-chain acceptors results in a slow rate of synthesis during the early phase of chain elongation. In reactions containing only DP7 acceptors, high MW products are observed because there is an

effective increase in the donor:acceptor ratio for the small number of acceptors that reach the critical DP, causing them to become rapidly elongated.

Synthesis of high MW HG is dependent upon GAUT1:GAUT7 complex formation and electrostatic interactions.

HG is a negatively charged polymer. It has been shown for other charged polymers, including polysialic acid (Keys et al., 2014) and DNA (Nardone et al., 1986), that electrostatic substrate-enzyme interactions affect product size distribution and the mechanism by which enzymes maintain contact with their charged substrates. We hypothesized that electrostatic HG-enzyme interactions may be involved in acceptor binding and elongation by GAUT1:GAUT7. Prior evaluation of a homology model of the GAUT1 GT8 domain using LgtC from *N. meningitidis* as a template identified a patch of positively-charged residues near the active site of GAUT1 that could create an extended acceptor binding groove (Yin et al., 2010). We predicted that incubation with NaCl would disrupt these interactions and limit the ability of GAUT1:GAUT7 to maintain the contacts with the HG acceptor needed for efficient transfer. We tested whether addition of NaCl affected product formation by GAUT1:GAUT7.

The presence of 100 mM NaCl in reactions containing a 1000:1 ratio of UDP-GalA to DP11 HG acceptor inhibited the synthesis of high MW HG products, even under long reaction times (Fig. 2.14A). In reactions containing a 10:1 donor:acceptor ratio and 0, 50, and 100 mM NaCl, elongation of a DP7 acceptor was likewise inhibited with increasing salt concentration (Fig. 2.14B). Individual bands of intermediate-sized products (DP > 20) were detectable following reactions containing NaCl, leading to the loss of the bimodal product distribution. This result also argues against DP7 being elongated processively. Short-chain elongation products

were visible in both reactions, but addition of NaCl to the reaction appears to prevent high MW product formation.

Synthesis of intermediate-sized HG upon elongation of a 10:1 donor:acceptor ratio of DP11 acceptor was only weakly affected by the presence of NaCl (Fig. 2.14B). For both DP7 and DP11 acceptors, product size was limited to approximately DP30-50 when GAUT1:GAUT7 was assayed with 100 mM NaCl. We propose that the electrostatic interactions guide the rapid elongation phase by orienting longer-chain acceptors within the active site for GalA transfer to the non-reducing end. The NaCl concentrations used here are within the physiological range and may not otherwise be expected to have such a strong inhibitory effect, as many glycosyltransferases are regularly purified, stored, and assayed under similar NaCl concentrations (Culbertson et al., 2016; Moremen et al., 2018).

The possibility that previously-unidentified structural domains are required for the synthesis of high MW HG opens the possibility that GAUT7 also contributes to the function of the complex. The activity of GAUT1 expressed and purified in the absence of GAUT7 was tested. Upon incubation of GAUT1 with DP11 and DP7 acceptors (Fig. 2.14C), high MW product was not observed. The size of the products synthesized by GAUT1 was limited to ~DP30-50, even in reactions containing a large excess of donor (10 μM acceptor, 100:1 donor:acceptor ratio). The consistency of this result with the reduced product sizes observed following incubation of GAUT1:GAUT7 with NaCl suggests that GAUT7 also contributes to an acceptor-binding domain/pocket required for high MW polymerization. Due to poor expression of GAUT1 and GAUT7 as individual enzymes, the nature of the contribution of GAUT7 to HG synthesis remains to be more thoroughly investigated.

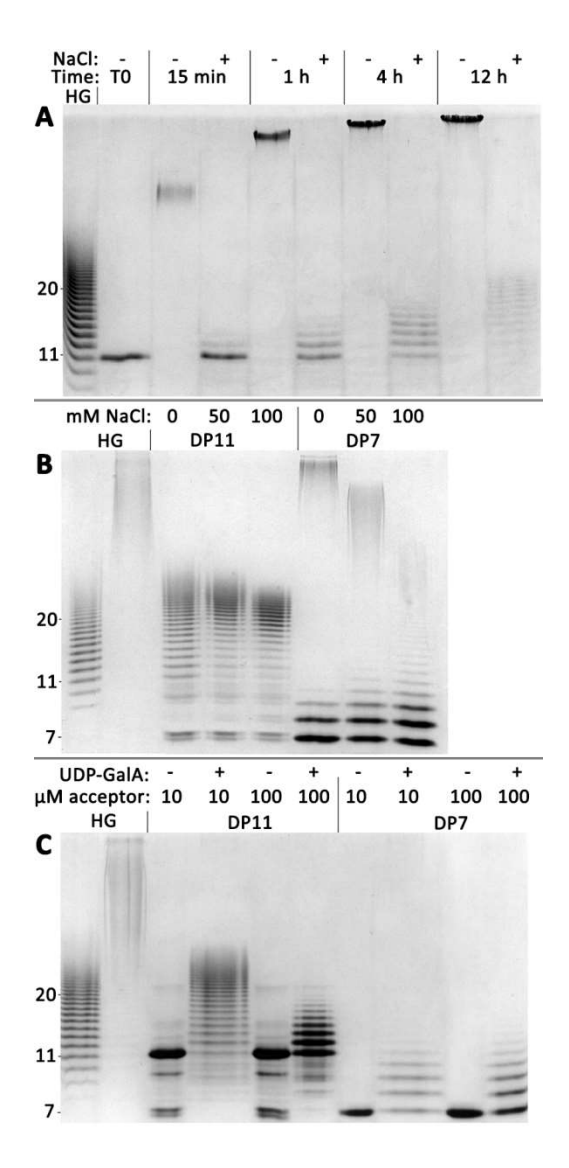


Figure 2.14. Addition of NaCl or incubation of GAUT1 alone prevents high MW HG synthesis. A, Reactions containing 100 nM GAUT1:GAUT7, 1 mM UDP-GalA, and 1 μM DP11 acceptor (1000:1 donor:acceptor ratio) were incubated for indicated times with or without the addition of 100 mM NaCl. B, Reactions containing 100 nM GAUT1:GAUT7, 1 mM UDP-GalA, and 100 μM DP11 or DP7 acceptor (10:1 donor:acceptor ratio) were incubated with 0, 50, or 100 mM NaCl for 12 h. C, Reactions containing 100 nM GAUT1, 1 mM UDP-GalA, and 10 μM or 100 μM DP11 or DP7 acceptor (100:1 or 10:1 donor:acceptor ratio, respectively) were incubated for 12 h.

DISCUSSION

Soluble expression of plant cell wall glycosyltransferases using the HEK293F cell system

Plant cell wall matrix polysaccharides are synthesized in the secretory pathway by the coordinated efforts of an estimated 200 glycosyltransferases that generate the backbone and sidechain linkages of pectins and hemicelluloses, including xylans and xyloglucan. A study published in 2009 identified a total of nine plant cell wall GTs that had in vitro activities verified by expression in a heterologous system (Petersen et al., 2009). In the years since that publication, numerous additional plant cell wall GT in vitro activities have been demonstrated and mapped to individual genes or multi-gene families (Wu et al., 2010b; Chiniquy et al., 2012; Lee et al., 2012a; Liwanag et al., 2012b; Rennie et al., 2012; Vuttipongchaikij et al., 2012b; Basu et al., 2013; Geshi et al., 2013; Knoch et al., 2013b; Dilokpimol et al., 2014; Urbanowicz et al., 2014; Basu et al., 2015a; Ogawa-Ohnishi and Matsubayashi, 2015; Culbertson et al., 2016; Laursen et al., 2018b). Similar to activities assayed from native plant membranes, the use of recombinant enzymes produced in microsomal membranes from sources such as P. pastoris or N. benthamiana may suffer from difficulties including low protein yields and unknown concentrations of the protein of interest (Rennie et al., 2012). Here, the HEK293F cell expression system was used for robust co-expression of a disulfide-linked enzymatically active GT complex in a soluble secreted form. In addition to the expression of the GAUT1:GAUT7 heterocomplex, the HEK293F cell system has been used to express the plant cell wall GTs Xylan Synthase-1 (Xys1) and Fucosyltransferase1 (Fut1) (Urbanowicz et al., 2014; Urbanowicz et al., 2017).

The results described here expand upon previous reports of HG synthesis by demonstrating that the GAUT1:GAUT7 complex can synthesize high MW polysaccharides *in vitro* using a distributive mechanism. Previously, intact and partially solubilized *Nicotiana tabacum* membranes were shown to incorporate [14C]GalA into high MW polysaccharides with an apparent mass > 100 kDa (Doong et al., 1995b; Doong and Mohnen, 1998). It was uncertain if the large size of the polysaccharide products detected in cellular membrane preparations was due to the initiation of polymeric HG or due to incorporation of [14C]GalA into large endogenous acceptors of an unknown size. We demonstrate here that as long as a sufficient concentration of UDP-GalA is available, recombinant GAUT1:GAUT7 is capable of producing high MW polysaccharides *in vitro*.

A hypothetical model of distributive HG elongation is depicted in Fig. 2.15 as a series of five steps. Binding of UDP-GalA (1) is followed by HG acceptor binding (2). The binding of longer-chain acceptors is enhanced by structural features of the GAUT1:GAUT7 complex, including charged interactions within an extended acceptor-binding groove that also appears to require the presence of GAUT7. GalA is transferred to the non-reducing end of the HG acceptor (3). The HG acceptor, elongated by a single GalA residue departs from the active site (4) followed by departure of UDP (5). The conformational state of the enzyme is then reset for the next round of glycosyl transfer. Numbered GalA units in the acceptor molecule (center images) represent subsites within the proposed extended acceptor binding domain.

The two-phase model is more complete than traditional descriptions of distributive glycosyltransfer mechanisms because it accommodates the observation of distinct, acceptor size-dependent slow and rapid elongation phases. This phenomenon may be common to GTs, but

would not be observed unless the reaction progress is independently assayed with a wide range of oligosaccharide acceptors. Elongation of short-chain acceptors exhibits several characteristics that have previously been proposed to be common to processive GTs, including a bimodal product distribution, the lack of intermediate-sized products, a lag phase during the early time points of the reaction progress, and large proportions of the starting acceptors remaining unelongated (Bambara et al., 1995; Bloom and Goodman, 2001; Levengood et al., 2011; Keys et al., 2014; Raga-Carbajal et al., 2016). However, here we show that HG acceptors of $DP \ge 11$ are elongated *in vitro* by a distributive mechanism with greater catalytic efficiency than smaller HG acceptors.

For several polymerases which favor longer acceptors, a model has been proposed in which oligosaccharides must be elongated to a certain minimum length before the transferase exhibits maximum activity. Longer acceptors can fill acceptor-binding subsites within the active site groove (Forsee et al., 2006; Levengood et al., 2011; Fiebig et al., 2018). This "acceptor subsites" model is compatible with the slower rates of synthesis that have been observed with $DP \leq 7$ HG acceptors. Only acceptors longer than the critical DP can efficiently bind to the active site and be rapidly elongated. The nearly-identical rates of transfer to DP11 or DP15 HG acceptors support an HG acceptor size of DP11 as being sufficient for maximum activity. The model that we present expands upon the hypothesis presented during the analysis of the processive bacterial galactan polymerase GlfT2 (Levengood et al., 2011) because we argue that acceptor subsites and kinetic lag phases are features that are not necessarily limited to processive polymerases.

Processive polymerization mechanisms may require enzymes that physically constrain and enclose the growing acceptor chain, such as cellulose synthase (Morgan et al., 2013), DNA-binding enzymes (Nardone et al., 1986; Breyer and Matthews, 2001), or putatively,

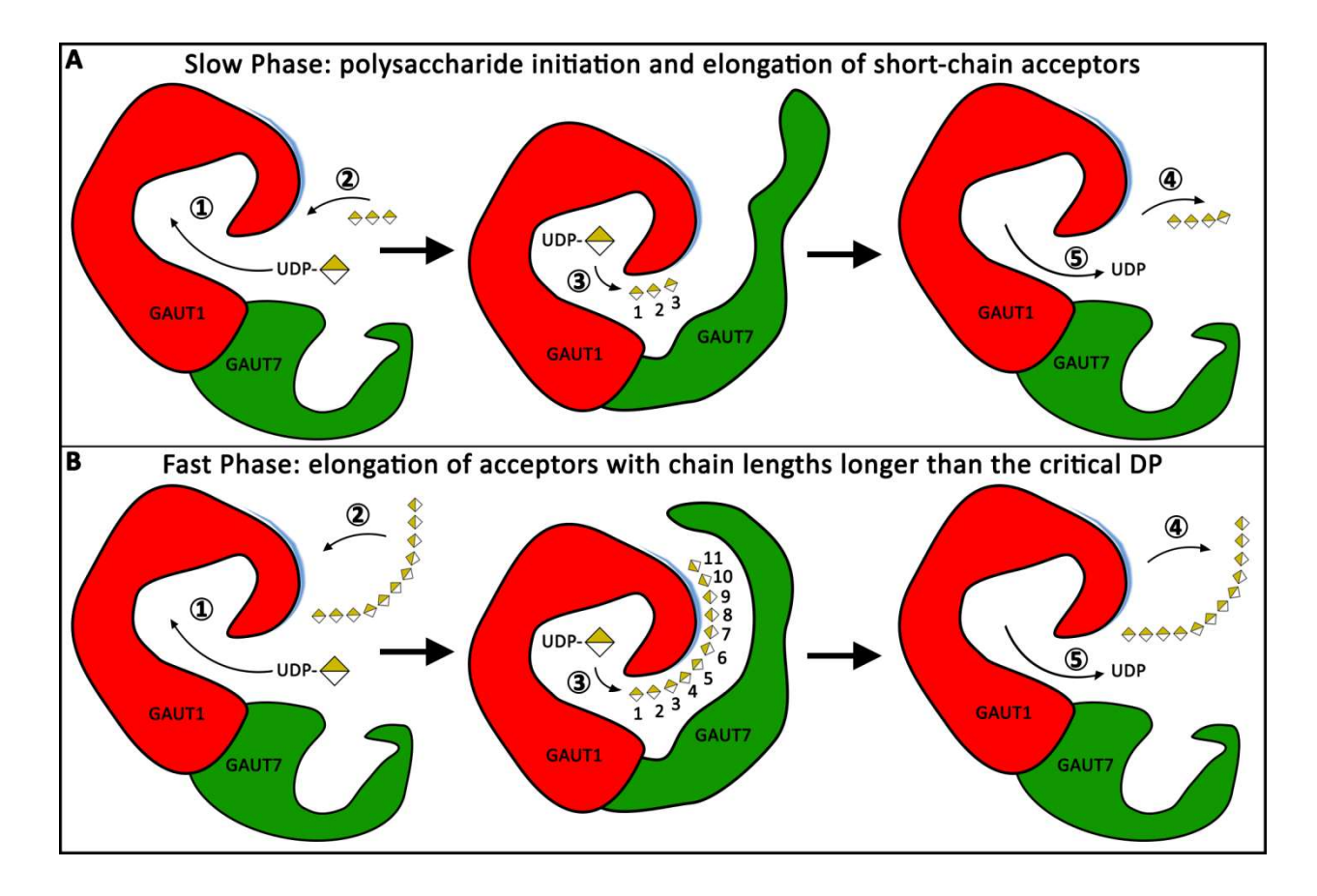


Figure 2.15. A proposed model for HG synthesis by GAUT1:GAUT7. Distributive elongation of a DP11 acceptor by the GAUT1:GAUT7 complex is shown as a series of five steps, with GAUT1 in red and GAUT7 in green. A patch of positively charged residues proposed to be necessary for the binding and orientation of growing acceptor chains is indicated in blue. In the center images, individual GalA units are numbered 1-11 to visualize binding of the acceptor along an extended acceptor-binding groove. Numbered steps (circled) are outlined in the discussion. A, Slow phase of HG synthesis, representing the initiation of new polysaccharide chains and the elongation of short-chain acceptors. Short-chain acceptors are inefficiently elongated and cannot fill subsites along the extended acceptor-binding groove. B, Fast phase of HG synthesis, representing the elongation of HG acceptors with chain lengths longer than the critical DP, estimated to be DP11.

multi-TM channel-forming GTs such as the xyloglucan backbone synthase CSLC4 (Davis et al., 2010; Pauly and Keegstra, 2016). Many Type II GTs have a single GT domain, and have no obvious structural basis for confining the growing glycan chain within a processive tunnel. Rather than inferring a processive model by induction from end-point product distribution data, the competition assay that we present (Fig. 2.11) is part of a recent push to find direct assays to test for the formation of enzyme:acceptor complexes that would serve as positive evidence for the archetypal processive model (Levengood et al., 2011). The competition assay showed that longer, more efficient acceptors can compete for binding to the enzyme following a preincubation period sufficient for formation of processive enzyme:acceptor complexes. The results of this assay show that GAUT1:GAUT7, at least *in vitro*, does not remain tightly bound to the HG polymer during elongation, a key feature that distinguishes distributive from processive polymerases.

A two-phase model with distinct differences in elongation rates between short-chain and longer-chain acceptors has been previously described for the non-processive *in vitro* activity of K92 polysialyltransferase from *Escherichia coli*, which has a similar critical acceptor chain length, approximately DP10-12 (Vionnet and Vann, 2007). Heparosan synthase from *Pasteurella multocida* provides a similar example of a non-processive transferase in which a slow initiation phase is observed (Chavaroche et al., 2010). Two-phase elongation provides an alternative hypothesis for the interpretation of bimodal or polydisperse product distributions that may be observed in studies of GT activity. As an example, levansucrase from *Bacillus subtilis* was determined to have a processive activity on the basis of a bimodal product distribution, which was lost upon addition of DP16 acceptors (Raga-Carbajal et al., 2016). If levansucrase functions similarly to GAUT1:GAUT7, then longer-chain acceptors are more efficiently elongated. The

bimodal product distribution would result from large differences in catalytic efficiency and acceptor preference based on chain length. The buildup of inefficient short-chain acceptors and rapid elongation as soon as the acceptor reaches a critical DP can explain non-Poissonian product distributions for GTs that have not been directly shown to be processive.

In vitro polymer initiation and extension in the absence of a glycan primer has been demonstrated for at least four bacterial capsular polysaccharides (DeAngelis and White, 2002; Fiebig et al., 2014a; Fiebig et al., 2014b; Litschko et al., 2015), including two negatively charged polysaccharides: Neisseria meningitidis serogroup X and serogroup A. The de novo synthesis products are both synthesized as high MW polysaccharides with relatively homogenous product dispersity compared to acceptor-primed reactions (Fiebig et al., 2014a; Fiebig et al., 2014b). For the de novo initiation of HG polysaccharides, a proposed candidate for the primer is a molecule of UDP-GalA, similar to elongation of β-1,4-linked GlcNAc oligomers synthesized by hyaluronan synthase that retain UDP at the reducing end (Weigel et al., 2015; Weigel et al., 2017). Alternatively, the primer could be monomeric GalA formed following hydrolysis of UDP-GalA. The large size of the products synthesized de novo, containing several hundred GalA units per reducing end, have prevented the primer for de novo synthesis from being identified in the current study.

Anionic polymers such as HG may have electrostatic enzyme-acceptor interactions which aid polymerization by promoting the proper binding and orientation of growing acceptor chains. The proposed positively-charged acceptor-binding groove was identified using a homology model of the GT8 domain of GAUT1 (Yin et al., 2010). Future structural and acceptor binding studies will be necessary to confirm the existence of this extended binding groove. Basic residues located in the acceptor-binding pocket influence processivity and product dispersity in a

polysialyltransferase from *N. meningitidis* (Keys et al., 2014). Incubation with NaCl disrupts polymer sliding in enzymes that bind to DNA, such as the endonuclease BamHI (Nardone et al., 1986). In the case of the non-processive activity of GAUT1:GAUT7, strong inhibition of activity by NaCl may be due to disruption of electrostatic interactions that contribute to the ability of acceptors to bind to the charged acceptor-binding groove.

The model described in this report provides a basis for the synthesis of high MW HG polysaccharides. GAUT1:GAUT7 uses a distributive mechanism in which rapid elongation requires that the acceptor reach an intermediate chain length, approximately DP11. The significance of this acceptor size, including comparisons to other GTs that function using multiphase elongation mechanisms, will require further investigation. The relative inefficiency of elongation of short-chain acceptors may provide a mechanism by which HG polymer size and chain initiation are regulated in vivo. This model is consistent with previous reports that HG:GalAT activity is non-processive (Doong and Mohnen, 1998; Akita et al., 2002; Ishii, 2002; Yasui, 2009). While the precise role of GAUT7 remains uncertain, GAUT1 appears to be unable to synthesize high MW products in the absence of GAUT7. Proper folding and secretion of the complex requires co-expression of GAUT1 with GAUT7, but GAUT7 also appears to have a functional role in contributing to HG polymer synthesis. The results reported here provide a comprehensive characterization of the *in vitro* distributive activity of a heterologously expressed plant cell wall polysaccharide biosynthetic GT complex, with implications for investigations of kinetic mechanisms and processivity of GT heterocomplexes.

EXPERIMENTAL PROCEDURES

Cloning, expression, and purification of GAUT1 and GAUT7 in HEK293F cells. Gateway expression vectors for transient expression in HEK293F cells, and cloning and expression methods, were adapted from other publications (Moremen et al., 2018). Constructs to generate truncated forms of A. thaliana GAUT1 (UniProt Q9LE59, residues 168-673) and GAUT7 (UniProt Q9ZVI7, residues 44-619) were amplified from previously-cloned vector templates containing A. thaliana GAUT1 and GAUT7 sequences (Sterling et al., 2006) using Phusion High Fidelity Polymerase (Thermo Scientific). Two rounds of PCR, using gene-specific and Gateway attB-site containing universal primers, were performed. PCR products were introduced into Gateway pDONR221 entry vectors using BP Clonase (Invitrogen). Coding sequences were recombined into a Gateway-adapted version of the mammalian destination vector pGEn2 using LR Clonase (Invitrogen) to generate final chimeric fusion protein sequences containing an Nterminal signal sequence, 8xHis tag, AviTag, "superfolder" GFP, and a TEV protease recognition site, followed by the truncated GAUT coding regions. Primers used for entry vector cloning are listed below, with universal attB-site sequences in lowercase and gene-specific sequences in uppercase:

GAUT1Δ167F, (5'-aacttgtactttcaaggcCGGGCAAATGAGTTAGTTCAGC-3');

GAUT1R, (5'-acaagaaagctgggtcctaTTCATGAAGGTTGCAACGACG-3');

GAUT7Δ43F, (5'-aacttgtactttcaaggcCACAATGGCTTTCACTCTCTG-3');

GAUT7R, (5'-acaagaaagctgggtcctaAGGATTCACGTTACAGTCAC-3');

Universal PrimerF, (5'-ggggacaagtttgtacaaaaaagcaggctctgaaacttgtactttcaaggc-3');

Universal PrimerR, (5'- ggggaccactttgtacaagaaaagctgggtc-3')

Sequences were verified following cloning into entry and expression vectors. Expression plasmids were purified using Purelink HiPure Plasmid Gigaprep Kits (Invitrogen). HEK293F suspension culture cells grown to a cell density of 2.5*10⁶ in Freestyle 293 Expression Medium (Thermo Fisher Scientific) were used for transfection. Transfection of DNA, either *GAUT1*Δ167 or *GAUT1*Δ167 co-transfected with *GAUT7*Δ43, was done at a total concentration of 3 μg/mL total culture volume with polyethylenimine (9 μg/mL). Cells were incubated in a humidified shaking 37°C CO₂ incubator at 150 rpm for 24 h before 1:1 dilution in Freestyle 293 medium supplemented to a final concentration of 2.2 mM valproic acid (Sigma). Medium containing secreted protein was collected after 6 days total incubation time.

Secreted proteins were purified from suspension culture medium by Ni-affinity purification using HisTrap HP (GE Healthcare) columns connected to an ÄKTA FPLC system (GE Healthcare). Vacuum-filtered culture medium was injected into HisTrap HP columns at 1 mL/min, washed with column buffer, and eluted using a gradient from 20-300 mM imidazole (20 column volumes). Fractions containing protein were exchanged into a storage buffer containing 50 mM HEPES, pH 7.2, 0.25 mM MnCl₂, and 20% glycerol using a PD-10 desalting column (GE Healthcare) and concentrated using a 30 kDa MW cutoff Amicon Ultra Centrifugal Filter Unit (Millipore).

The concentration of Ni-affinity purified proteins was determined by UV-Vis spectroscopy (Nanodrop) using a 10 cm path-length cuvette and purification was confirmed by SDS-PAGE on a 4-15% gradient gel (Bio-Rad).

Metal-depleted GAUT1:GAUT7 was generated by overnight dialysis against HEPES, pH 7.2 buffer containing Chelex-100. Activity was measured under standard conditions with the

addition of 0.25 mM of the following metals: MnCl₂, CoCl₂, NiSO₄, FeCl₂, CuSO₄, CaCl₂, ZnSO₄, MgCl₂, NaCl, KCl, or no metal.

Synthesis of UDP-[¹⁴C]GalA and HG oligosaccharide acceptors. UDP-D-[¹⁴C] galactopyranosyluronic acid was synthesized enzymatically from UDP-D-[¹⁴C]glucopyranosyluronic acid (PerkinElmer) as described (Liljebjelke et al., 1995; Atmodjo et al., 2011). The batch specific activity value of 249 mCi / mmol was used to convert cpm readings from scintillation counting to reported pmol values in activity assay figures.

Non-radiolabeled UDP-D- galactopyranosyluronic acid was purchased from CarboSource Services (http://www.ccrc.uga.edu).

The HG acceptor mix, enriched for HG oligosaccharides of DP7-23, was generated by partial digestion of polygalacturonic acid with endopolygalacturonase and the purity was confirmed by HPAEC-PAD as described (Doong and Mohnen, 1998). HG acceptors enriched for homogenous degrees of polymerization of 7-15 were purified by HPAEC-PAD as described (Doong and Mohnen, 1998). Trigalacturonic acid (DP3) was purchased from Sigma.

Deglycosylation, fusion tag removal, and protein gel electrophoresis. Recombinant tobacco etch virus (TEV) protease and Peptide-N-Glycosidase F (PNGaseF) were expressed as N-terminal His/GFP fusion proteins in *Escherichia coli* and purified by Ni-affinity chromatography as described (Meng et al., 2013). Recombinant proteins were incubated at a 1:10 ratio of TEV and PNGase F relative to the GAUT1:GAUT7 complex overnight at room temperature to cleave the fusion tags and N-glycan structures.

Protein samples (4 µg) were mixed with Laemmli sample buffer (Laemmli, 1970) containing 25 mM DTT to reduce the samples. DTT was omitted in non-reduced samples. Samples were boiled for 10 min and resolved by 4-15% gradient Tris-glycine SDS-PAGE gel.

Electrophoresis was performed in a running buffer containing 25 mM Tris, 192 mM glycine, and 0.1% (wt/vol) SDS using 150 mV constant voltage.

HG:GalAT activity radiolabeled filter assays. Unless otherwise noted, HG:GalAT activity was measured under the standard condition in 30 μL reactions containing 100 nM GAUT1:GAUT7, 5 μM UDP-[14C]GalA, 1 mM total UDP-GalA, 10 μM HG acceptor, HEPES buffer pH 7.2, 0.25 mM MnCl₂, and 0.05% BSA. Reactions were incubated at 30°C, and 5 min was used as a standard time for linear range specific activity comparisons. As indicated in the text, reactions were modified from the standard condition to include acceptors enriched for a homogenous degree of polymerization, higher concentrations of acceptors to modify the donor:acceptor ratio, or in the absence of exogenous acceptors for samples labeled "de novo" synthesis.

HG:GalAT activity was measured using a filter assay as described (Sterling et al., 2005), with modifications. Reactions were terminated by addition of 400 mM NaOH (5 μL). Reactions were spotted onto 2x2 cm squares of Whatman 3MM chromatography paper coated with cetylpyridinium chloride (CPC). Filters were air dried for 5 min prior to three 15 min rounds of washing in a 4L bath containing 150 mM NaCl, for a total washing period of 45 min. Filters were air dried for at least 2 h prior to scintillation counting. Scintillation counting was performed using a PerkinElmer Tri-Carb 2910 TR liquid scintillation counter, ¹⁴C program, 1-min count time per sample. Background cpm was measured in each assay using T0 samples, in which NaOH was added to the reaction mixture prior to the addition of enzyme. Background cpm was subtracted from net cpm readings for all reaction samples, and cpm was converted to total pmol transferred.

Alcian blue-stained polyacrylamide gel electrophoresis. Reactions were incubated under standard conditions described above, except UDP-[¹⁴C]GalA was omitted from the reaction buffer. Reactions were terminated by boiling. Aliquots containing an estimated 200-500 ng total polysaccharide were analyzed.

Polyacrylamide gel electrophoresis and visualization by a combination of alcian blue and silver nitrate staining was performed as described, with modifications (Sterling et al., 2006). Samples were mixed with a loading buffer (final concentration 0.1 M Tris, pH 6.8, 0.01% phenol red and 10% glycerol), loaded onto a stacking gel (5% acrylamide (Bio-Rad), 0.64 M Tris, pH 6.8), and separated over a 30% acrylamide resolving gel (0.38 M Tris, pH 8.8, 30% acrylamide) at 17.5 mA for 60 min. The gel was stained for 20 min with 0.1% alcian blue in 40% ethanol and washed with at least three changes of water until background staining was eliminated. Silver staining and developer was performed using a silver staining kit (Bio-Rad). Staining was terminated by addition of 5% acetic acid.

Size exclusion chromatography of HG:GalAT products. Scaled up reactions with a total volume of 400 μL were incubated, using concentrations of reagents consistent with small-scale, nonradioactive, standard condition HG:GalAT assays. At each indicated time point, a 50 μL aliquot was removed and the reaction was stopped by boiling. Denatured enzyme was removed from the sample by centrifugation at 12,000 rpm for 5 min, and the polysaccharide sample was frozen at -20°C until analysis. For T0 samples, an equivalent aliquot was removed prior to addition of UDP-GalA to the reaction.

Size exclusion chromatography (SEC) was performed using a Superose 12 10/300GL column connected to a Dionex system at a flow rate of 0.5 mL/min in 50 mM ammonium formate buffer. The refractive index of polysaccharide products was measured. Dextran

standards (270, 150, 50, and 12 kDa) (Sigma) were used as molecular weight standards. The peak retention volume of each dextran standard is indicated by an arrow at the top of each SEC figure. The molecular weight estimations of pectins may be overestimations due to anomalous behavior of pectins compared to dextrans during SEC (Mort, 1991).

For 2AB-labeled polysaccharides measured by fluorescence detection, reactions were incubated for 12 h, polysaccharide reducing ends were chemically labeled with 2-AB (described below), and reaction products were injected onto the SEC column under the same conditions as above. An RF 2000 fluorescence detector, under high sensitivity (x16) settings, was used for detection. Quantitation of high MW polysaccharide was performed by fluorescence signal integration of product and acceptor peaks in Chromeleon 6.80 software (Dionex).

MALDI of 2AB-labeled HG oligosaccharide products. Following incubation under indicated reaction conditions and times, HG products were incubated with 0.2 M 2-aminobenzamide (2AB) and 1 M sodium cyanoborohydride in 10% acetic acid to chemically label the reducing ends of HG oligosaccharides, as described (Ishii, 2002; Urbanowicz et al., 2014). Samples were dialyzed four times against water in a 3500 MW cutoff tubing (VWR Scientific) and recovered by lyophilization. Retention of HG oligosaccharides during dialysis has been described (Mort, 1991).

Nafion 117 solution (Sigma) was applied to a Bruker MSP 96 ground steel target and air dried, as described (Jacobs and Dahlman, 2001; Praissman et al., 2014). Following 2-AB labeling, reaction samples were mixed 1:1 with a 20 mg/mL 2,5-dihydroxybenzoic acid matrix solution in 50% methanol. Positive or negative ion matrix-assisted laser desorption ionization with time-of-flight detection (MALDI-TOF) mass spectrometry spectra were acquired using an LT Bruker LT Microflex spectrometer.

Enzyme-linked immunosorbent assay (ELISA) of HG:GalAT activity using anti-HG monoclonal antibodies. Monoclonal antibodies directed against plant cell wall polysaccharides were previously characterized (Pattathil et al., 2010). Antibodies directed against HG (CCRC-M38, CCRC-M131, and JIM5) and xylan (CCRC-M149) were used in this study. Antibody immunoreactivity, and supplier information is available WallMabDB (http://www.wallmabdb.net). Following incubation under standard reaction conditions unless otherwise noted, aliquots containing either 1 µL (1/30 of reaction) or 0.1 µL (1/300 of reaction) were diluted to a final volume of 50 µL and reactions were terminated by boiling. ELISAs were performed as previously described (Pattathil et al., 2012). The 50 µL diluted reaction sample was incubated in a 96-well plate (Costar 3598) and evaporated to dryness overnight. Nonspecific spots on the plate were blocked by incubation for 1 h in 0.1 M Tris-buffered saline (TBS) containing 1% Nonfat Dry Milk (Publix) (200 µL). Primary antibodies (50 µL), diluted 10-fold from the hybridoma supernatant, were dispensed into each well and incubated for 1 h. All wells were washed with 300 µL wash buffer (0.1 M TBS containing 0.1% Nonfat Dry Milk) for a total of three washes. Secondary antibodies were diluted to 1:5000 in wash buffer. For CCRC series antibodies, anti-mouse (Sigma A4416), and for JIM series antibodies, anti-rat (Sigma A9037) secondary antibodies conjugated with horseradish peroxidase (50 µL) were incubated for 1 h. Plates were washed with wash buffer for a total of 5 washes. TMB Peroxidase Substrate (Vector Laboratories) was incubated in each well (50 µL) for 20 min, and the reaction was stopped by addition of 0.25 M sulfuric acid. OD values were measured using a plate reader at 450 nm with background readings at 655 nm subtracted. Boiled enzyme reaction buffer controls contain reaction mixtures incubated under the same conditions, except GAUT1:GAUT7 enzyme was inactivated by boiling prior to addition to the reaction mixture.

Endopolygalacturonase digestion. Following incubation of the HG:GalAT reaction, the mixture was adjusted to pH 4.2 by addition of 1 M sodium acetate buffer, pH 4.2 (3 μ L) and 2 M acetic acid (15 μ L). The mixture was incubated overnight at 30°C with 20 mU of endopolygalacturonase-I (Aspergillus niger, EC 3.2.1.15) (Benen et al., 1999); 1 U = 1 μ mol of reducing sugar produced per min as determined by a p-Hydroxybenzoic Acid Hydrazide reducing sugars assay (Sigma). The EPG reaction was terminated by addition of 1 M NaOH (30 μ L). The final reaction mixture was assayed using the filter assay, as described above. Control samples labeled "Boiled EPG" were incubated with EPG that was deactivated by boiling for 1 h prior to use.

Modeling of Michaelis-Menten kinetics. Standard Michaelis-Menten kinetics and substrate inhibition kinetics were modeled using formulas for non-linear regression analysis using Graphpad Prism 7 for Windows, GraphPad Software, La Jolla California USA (www.graphpad.com). Kinetic parameters ($V_{\rm max}$, $K_{\rm M}$, and $K_{\rm i}$) were calculated for each independent experiment, measured using 8-12 different concentrations of the variable substrate spanning a range of 0.1- to-10-times $K_{\rm M}$. Replicate experiments were calculated as separate data sets.

Standard Michaelis-Menten equation:

$$V_0 = \frac{V_{\text{max}}[S]}{K_{\text{M}} + [S]}$$

Substrate inhibition equation:

$$V_0 = \frac{V_{\text{max}}[S]}{K_{\text{M}} + [S](1 + \frac{[S]}{K_{\text{i}}})}$$

Table 2.1. Results of Michaelis-Menten Kinetics assay experiments of the Arabidopsis heterologously-expressed

GAUT1:GAUT7 complex. Kinetic parameters and associated standard deviations (±) were derived from nonlinear regression of assays containing at least 8 measurements. Representative Michaelis-Menten kinetics data are displayed in Fig. 2, D and E, as well as Fig. 4, B and C. Data displayed in the listed figures and in independent replicate experiments are reported in this table.

Variable substrate	Donor [UDP-GalA]	Acceptor [HG]	k_{cat}	K_{M}	$k_{\rm cat}$ / $K_{ m M}$	$K_{\rm i}$
	(μ M)	(µM)	(s^{-1})	(μ M)	$(\mu M^{-1} s^{-1})$	(μ M)
UDP-GalA	5-1000	10	1.48 ± 0.10	219 ± 37.4	0.0068	-
UDP-GalA	5-1000	10	1.36 ± 0.06	231 ± 24.5	0.0058	-
UDP-GalA	5-2000	100	$\boldsymbol{0.92 \pm 0.02}$	151 ± 10.6	0.0061	-
UDP-GalA	5-2000	100	0.95 ± 0.03	136 ± 16.7	0.0070	-
HG DP7-23	1000	0.01-50	1.99 ± 0.06	$\boldsymbol{0.8 \pm 0.01}$	2.5	40.9 ± 3.6
HG DP7-23	1000	0.01-50	1.63 ± 0.19	1.0 ± 0.30	1.6	32.7 ± 10.6
HG DP11	1000	0.01-100	3.92 ± 0.30	1.4 ± 0.2	2.8	14.6 ± 2.1
HG DP11	1000	0.01-100	4.60 ± 0.80	1.8 ± 0.5	2.6	10.3 ± 3.1
HG DP7	1000	0.01-100	$\boldsymbol{0.61 \pm 0.02}$	10 ± 1.4	0.061	-
HG DP7	1000	0.01-100	$0.44 {\pm}~0.02$	8.6 ± 2.0	0.051	-

CONCLUSIONS

In this study, we demonstrated the initiation and synthesis of high molecular weight HG polysaccharide from the GAUT1:GAUT7 complex. Given available UDP-GalA substrate, GAUT1:GAUT7 synthesized HG chains of indefinite length. Initiation of HG synthesis *de novo* was a previously undiscovered activity and was demonstrated using multiple techniques, including radiolabeled GalA incorporation, ELISA with anti-HG monoclonal antibodies, and alcian blue stained polyacrylamide gels.

An unexpected consequence of the ability of GAUT1:GAUT7 to initiate HG synthesis from UDP-GalA and also to elongate acceptors of all sizes is the major differences observed depending on the size of the acceptor used in the assay. With DP11 acceptors as a representative of longer chains and DP7 acceptors as a representative of shorter chains, the longer acceptors were elongated at faster rates and with a 10-fold lower $K_{\rm M}$, ultimately representing large increases in catalytic efficiency as the reaction transitions from synthesis of short-chain to long-chain HG products. Short-chain acceptors were elongated with a non-linear initial rate of the reaction progress due to observed rate increases with each monosaccharide addition to the acceptor. Because standard models of GT mechanism could not account for the changes in activity observed with increasing acceptor chain length, we proposed a "two-phase distributive mechanism" as a model to describe HG synthesis.

As a result of these experiments, GAUT1:GAUT7 may be considered to be the most thoroughly characterized plant cell wall GT from the standpoint of biochemical mechanism.

Many cell wall GT activities that have been discovered are lacking reaction kinetics and polysaccharide chain length analysis data. Verifying the monosaccharide linkage formed by a GT is the first step in understanding the biosynthetic activity, but using GAUT1:GAUT7 as a guide, the mechanism of polysaccharide synthesis requires evaluating the reaction progress under many reaction conditions, with acceptors of varied chain lengths, and with a careful analysis of the linearity of the reaction.

Biosynthesis of homogalacturonan

Use of the recombinant GAUT1:GAUT7 enzyme has resolved several outstanding questions resulting from previous studies of HG biosynthesis. The ability of HG:GalAT to synthesize high MW polymeric HG (> 100 kDa) and the lack of evidence for the presumed enzyme processivity were sources of conflicting results in earlier studies. Microsomes isolated from *N. tabacum* containing HG:GalAT activity were able to incorporate [14C]GalA into high MW polymeric products, potentially due to incorporation into large endogenous acceptors (Doong et al., 1995a). Solubilized enzyme from tobacco membranes (using 40 mM CHAPS detergent) was found to have a distributive activity because DP15 acceptors were elongated by a single GalA unit to DP16, whereas partially solubilized membranes (using 5 mM CHAPS detergent) resulted in a bimodal distribution of products containing DP16 and high MW products (Doong and Mohnen, 1998).

Because the synthesis of a polymeric product was interpreted as evidence that HG:GalAT should be a processive activity, three explanations were proposed (Doong and Mohnen, 1998):

1. Detergent solubilization disrupts a larger complex and/or cofactor, reducing processivity.

- 2. The HG oligosaccharide acceptor lacks structural information required to convert the enzyme to a processive mode of action.
- 3. The large size of the endogenous acceptor accounts for the bulk of the 105 kDa mass, and that "neither solubilized PGA-GalAT nor membrane-bound PGA-GalAT is very processive in vitro."

In light of the new model for HG synthesis, we can revisit these proposed explanations. The underlying assumption is that synthesis of HG, which is a polymer, should occur through a processive mechanism. From our work with the recombinant GAUT1:GAUT7 complex and our review of other polymerizing GTs, it is now clear that processive and distributive mechanisms are simply two different methods of polysaccharide elongation, but that there is no necessary connection between the size of a polymer and the mechanism of elongation. Therefore, the existence of long polymers should never be used to assume processivity. In response to the above three proposed explanations:

- 1. The GAUT1:GAUT7 complex synthesizes high MW polymers using a distributive mechanism. Regardless of whether other complex members do associate with GAUT1:GAUT7 *in vivo*, only reduction of disulfide bonding between GAUT1 and GAUT7 should result in any changes to the elongation activity.
 - 2. High MW product elongation is independent of the size of the acceptor.
- 3. The polysaccharide composition of the microsomal membrane preparation is unknown, but it is likely that acceptable endogenous HG acceptors were present and [14C]GalA was incorporated into them. Therefore, the pre-existence of high MW endogenous acceptors in tobacco microsomal membranes is probably true. However, GAUT1:GAUT7 is also capable of initiating new chains of GalA *de novo*, so this 105 kDa product could have been synthesized in

membranes even if no acceptable endogenous acceptor was present. The quote selected from this proposed explanation also implies that the *in vivo* activity is processive but that the *in vitro* activity is less processive. Unless a protein complex binding partner that serves as a translocation pore is found to be a necessary component of *in vivo* HG synthesis, it is not necessary to propose processivity in discussions of HG elongation.

Even with the inclusion of these updated explanations, it is still unclear whether or not the HG:GalAT activity measured in tobacco membranes did initiate high MW synthesis. It is also unclear why the exogenous DP15 acceptor was elongated by only a single monosaccharide, as the distributive mechanism should also imply continued elongation given an excess of UDP-GalA donor. The addition of the single GalA onto the supplied exogenous acceptor may have been due to limiting donor substrate because the concentrations of UDP-GalA used in these studies were typically lower than the concentration of HG acceptors (Doong and Mohnen, 1998). The tobacco microsomes are likely to contain many enzymes responsible for HG:GalAT activity, and the activity in these studies could have been dominated by an enzyme that functions differently than GAUT1:GAUT7, which would need to be studied independently. The correlation between enzyme concentration and chain length has not yet been studied, but it is also possible that minimal elongation of exogenous acceptors resulted from the low enzyme concentration in solubilized microsomal membranes.

From the experiments with tobacco microsomes, only exogenous acceptors of $DP \ge 10$ raised activity to above-background levels (Doong and Mohnen, 1998). Although the precise change to catalytic efficiency within the intermediate range of DP7 - DP11 has not been measured, this size range is consistent with the acceptor size that resulted in large increases in elongation rate and the loss of the bimodal product distribution. This acceptor size,

approximately DP11, is what we labeled as the "critical DP." Because the microsomal experiments were conducted on short time scales to account for the basal activity, it was thought that acceptors DP < 10 were not able to function as acceptors. It is more likely that these were inefficient acceptors that required longer time scales to measure the incorporation.

In the initial study of GAUT1 activity, HA-tagged proteins were immunoabsorbed with anti-HA antibodies directly from the cell culture media and assayed. Only cells transfected with GAUT1 Δ 41, but not with GAUT7 Δ 43, increased activity over vector controls (Sterling et al., 2006). The protein expression levels from this study are not known because GAUT proteins were not purified and quantified. At the time of this study, neither the association of GAUT1:GAUT7 as a disulfide-linked complex or the in vivo N-terminal truncation of GAUT1 at residue 167 was known (Atmodjo et al., 2011). Our results showed that GAUT1Δ41 expressed relatively poorly compared to GAUT1Δ167, which itself expressed poorly unless co-transfected with GAUT7Δ43. We did not attempt to purify GAUT7 due to low media fluorescence that indicated minimal secretion as a single enzyme. GAUT7 was detected in the culture media by western blotting in the Sterling et al. (2006) experiments, and so the original conclusion that GAUT7 does not have HG:GalAT activity as a single enzyme is likely correct. However, the large enhancement to expression, secretion, and activity after co-expression of GAUT1 with GAUT7 caution against making definitive conclusions using the single-expressed enzymes, which both express poorly compared to the complex.

In another assay of HG:GalAT activity, GAUT1 antiserum was used to deplete GAUT1 from activity-enriched Arabidopsis membranes (Sterling et al., 2006). The activity attributed to GAUT1 in these assays must have actually been derived from the native GAUT1:GAUT7 complex, although the existence of the complex was not known at the time. In alcian blue-

stained polyacrylamide gels similar to many of the experiments carried out here using the recombinant GAUT1:GAUT7 complex, acceptors of DP13 were elongated to a final size of ~DP26. The laddering is consistent with the distributive synthesis that we have observed using recombinant GAUT1:GAUT7, although the product sizes are smaller than we may expect (~20:1 UDP-GalA:DP13 acceptor ratio was used in these experiments). These results represent another experiment where the enzyme concentration assayed was unknown, but the limited chain length of products may have resulted from low total enzyme in the assay.

Open questions in pectin biosynthesis

The biological significance of the two-phase distributive synthesis mechanism is an important question that has not been investigated in this work. We have identified that enhanced activity with longer acceptors has been noted in studies of other plant cell wall GTs, and that it is likely to be a more common mechanism than previously recognized. The slow initiation of new chains combined with the control of UDP-GalA concentration within the Golgi could be a mechanism by which plant cells balance the activities of HG initiation with high MW polymer synthesis. The UDP-GalA concentration within the Golgi and the size of HG exported to the cell wall are not known and may be impossible to measure given current technologies. Rather than having evolved to achieve a sophisticated regulatory function, the two-phase mechanism of biosynthesis could be a simple consequence of enzyme active site structure that more favorably supports high MW polymerization over chain initiation. Experiments to be published from Kristen Engle's doctoral thesis indicate that several of the GAUT enzymes, including GAUT10, 11, and 14, are able to initiate HG synthesis de novo. The low efficiency of de novo synthesis

would direct GAUT1:GAUT7 toward long-chain polymerization and leave initiation activities to other enzymes.

The significance of the critical DP, approximately DP11, is also an area for future study. Although we tend to depict HG and other polysaccharides as linear chains in enzymatic models, longer-chain oligosaccharides have the potential to form three-dimensional structures. HG synthesized in vitro is non-esterified and has the potential for ionic crosslinking and adopting helical conformations. Pectin gels are usually discussed in relation to interaction with Ca²⁺ ions, which are not present in our assays, but HG also forms gels upon interaction with Mn²⁺, which is a cofactor for UDP-GalA binding to GAUT1:GAUT7. The precipitation of HG may explain why high concentrations of MnCl₂ decrease activity above the optimum range of 0.1-1 mM. HG chains require ~10 monosaccharide units to form stable gels (Vincken, 2003). The potential for gel formation and the loss of solubility above a DP of 10 may be expected to decrease the efficiency of these oligosaccharides as acceptors, but perhaps the active site of GAUT1:GAUT7 is structured to accommodate HG chains with this helical three-dimensional structure. HG may not form ionic crosslinks with Mn²⁺ at the relatively low concentrations used in vitro. As proposed in the discussion in Chapter 2, the possibility also exists that the exposed carboxylic acid groups of HG interact with an extended, positively charged binding groove predicted to exist outside of the active site.

One of the previously-proposed goals of developing a heterologous expression system was to compare the activity of GAUT1 to the GAUT1:GAUT7 complex. Without the ability to express GAUT7 as a single enzyme, the question of the potential catalytic contribution of GAUT7 remains unanswered. Our data do expand on the original model, in which GAUT7 was proposed to be a non-catalytic membrane anchor for GAUT1, by presenting preliminary

evidence that GAUT1 has a limited ability to elongate HG and does not synthesize high MW products without GAUT7. If this finding is not simply due to a lower overall activity of GAUT1, then GAUT7 does contribute to a tertiary structure that is necessary for high MW polymer synthesis, even if it does not have a standard glycosyltransfer activity. As described in the material presented in the appendices, the poor expression of GAUT1 as a single enzyme resulted in much lower purification of this enzyme than expected. Using large-scale cultures and more advanced purification methods, it will be possible in future studies to account for the low yield of GAUT1 and to purify enough enzyme to study the activity of GAUT1 relative to GAUT1:GAUT7.

The differences observed in comparing GAUT1 to GAUT1:GAUT7 activity and in comparing the recombinant enzyme to earlier studies using the Arabidopsis membrane protein emphasize the importance of developing assays to correlate activity level to product chain length. Given available enzyme and substrates, this could be accomplished using the methods developed within this thesis. By finding reaction conditions that yield an equal amount of total GalA transferred by GAUT1 or GAUT1:GAUT7, it could be shown whether or not the presence of GAUT7 in the complex contributes to high MW polymer elongation. Other GAUT enzymes are also likely to show differences in the chain lengths of products synthesized. By comparing the chain length of products synthesized by each enzyme on an equal-activity basis, these studies would help determine polysaccharide length control within a given GT family. Expression of individual recombinant enzymes would also be relevant to the other plant cell wall polysaccharides that are synthesized by multi-gene families, for which almost no data are available to explain why so many apparently redundant GTs exist in plant genomes.

For de novo synthesis of HG and elongation of short-chain acceptors, we have described the reaction progress as having a "non-linear" lag phase. There may be a linear initial rate for the elongation of acceptors of each individual size, but the pool of acceptors is continuously changing as the starting acceptors are elongated. Our data suggest that for each acceptor size up until DP11, the elongation rate will increase with each monosaccharide added to the acceptor. The linear initial rate measured with DP ≥ 11 acceptors may be the maximum rate of HG synthesis. The reaction progress curves for de novo synthesis and for the elongation of individual DP acceptors have not been fully detailed with extensive assays. We can predict that all acceptors should reach a linear reaction phase, and that the lag phase is extended as acceptor size decreases. By mapping the entire reaction progress for *de novo* synthesis, the true rate difference between initiation and elongation phases could be determined. Our data have estimated the difference in catalytic efficiency between elongation of a DP11 and a DP7 acceptor as ~45-fold, but the true difference could be as high as >1000-fold when accounting for the true initial rate of de novo synthesis. Because this difference may be common for the initiation of polysaccharide synthesis with a number of different GTs, this knowledge would serve to guide future experimental designs and to explain why polysaccharide initiation has not been measured from low abundance membrane enzyme preparations in most cases.

Activities of plant cell wall biosynthetic glycosyltransferases

Verification of the activities of plant cell wall GTs by heterologous expression has been a challenge for the international community over the past 20 years. We carried out the first experiments showing the co-expression of the GAUT1:GAUT7 complex and the potential for high-yield purification of recombinant enzyme in 2012. Transient expression of GAUT1 in

HEK293 cells had already been published previously (Sterling et al., 2006), but the utility of this system for high-yield purification had not been established. New vectors and expression conditions were in the process of development for the expression of recombinant mammalian GTs (Barb et al., 2012). The successful co-expression of GAUT1:GAUT7 was immediately influential for the adoption of HEK293 cells for the expression of plant cell wall GTs and for GT complexes. Several publications describing the biochemical characterization of cell wall GTs (Urbanowicz et al., 2014; Jensen et al., 2018), and even the first crystal structures (Urbanowicz et al., 2017; Culbertson et al., 2018), using the same system have been completed. Other GAUT genes, including GAUT10, 11, and 14, have been expressed and progress is being made in comparing the biochemical activities and differences in HG products synthesized by different members of the GAUT family. HEK293 cells are likely to be the dominant expression system for cell wall GTs, potentially hundreds of which remain to be characterized.

We have shown for the first time that GAUT1:GAUT7 synthesizes long-chain HG polysaccharides, which prompted investigations into the nature of glycosyltransferase processivity. Building off of ideas previously presented for processive enzymes in general (Breyer and Matthews, 2001), we have presented a more direct hypothesis than has previously been proposed: processivity is limited to GTs with a structural domain that prevents dissociation of the elongating polysaccharide chain, most likely an N-terminal multi-transmembrane helical domain. For the synthesis of plant cell wall polysaccharides, this description includes the GT2-family enzymes of the Cellulose Synthase-Like (CSL) superfamily. Therefore, we hypothesize that none of the type II transmembrane proteins, which contain a single transmembrane domain and make up the majority of putative GTs, are processive enzymes. The connection between the multi-transmembrane domain structure of GT2-family enzymes and processivity has been

previously proposed for bacterial enzymes (Bi et al., 2015). This hypothesis limits the matrix polysaccharides synthesized by a processive mechanism to the backbones of xyloglucan, heteromannans, and mixed-linkage glucans. Biosynthesis of these polymers has been associated with various CSL-family enzymes, but none of these enzymes have been expressed with a high enough yield for crystallographic studies. In the meantime, the closest model for polysaccharide translocation is from the bacterial BcsA:BcsB cellulose synthase complex (Morgan et al., 2013). The expression and purification of these enzymes presents a new challenge because the compatibility of the HEK293 system with CSL expression is uncertain. The bacterial cellulose synthase, a two-gene heterocomplex, was expressed in *E. coli* cells using periplasmic-directed expression and purified by nickel-affinity from solubilized membranes using standard methods (Morgan et al., 2013). Current HEK293 expression methods have been designed for secretion of transmembrane-truncated proteins, but adaptation of vectors for membrane expression could result in high-yield purification that has not been achievable from other expression systems.

Although processive enzymes may have an intrinsic chain length limit, distributive enzymes should have no theoretical limit to the product length synthesized *in vitro*, which could be adjusted by control of the donor:acceptor ratio. This was demonstrated for GAUT1:GAUT7, but only short-chain products have been detected for two other cell wall GTs, xylan synthesis by Xys1 (Urbanowicz et al., 2014) and galactan synthesis by GALS1 (Laursen et al., 2018a). In these cases, the limited product size may more reflect the limits of the enzymatic conditions and detection methods used rather than a property of the biosynthetic enzymes.

Polysaccharide elongation mechanisms

Discussions of GT mechanism have been constrained by the processive vs. distributive dichotomy, even though previous authors have noted that glycan product distributions frequently do not match results predicted from purely processive or distributive synthesis models (Keys et al., 2014). The data presented from GAUT1:GAUT7 provides clarity to this discussion by demonstrating that large differences in catalytic efficiency from acceptors of different sizes may explain why *in vitro* reactions often result in irregular product distributions. The two-phase distributive mechanism was adapted from earlier works, specifically from studies of polysialic acid synthesis where the transferase uses a non-processive mechanism but does not show a typical distributive elongation pattern (Vionnet and Vann, 2007), but to our knowledge, GAUT1:GAUT7 is the first explicit proposal of the two phase model as presented (Figure 2.15).

Further confusion exists in the literature due to older, less precise definitions of processivity. Instead of referring to an enzyme mechanism in which a GT retains a polysaccharide chain through many rounds of elongation without release, a frequently-cited early review referred to processive GTs as "those that add a number of sugar residues" (Saxena et al., 1995). This definition encompasses all polymerizing GTs of all mechanisms, and is only useful to distinguish polymerizing transferases from single-addition or side-chain transferases. Based on this definition, CSL-family proteins were previously proposed to be processive, but not for the reason outlined here (the multi-transmembrane translocation pore) (Richmond and Somerville, 2000). Just as we have attempted to demonstrate that results such as bimodal product distributions and progress curve lag phases, which are not direct tests of processivity, are not sufficient evidence to propose a processive mechanism, even the definition of processivity used in older literature needs to be carefully scrutinized. The most widely cited review of pectin

biosynthesis likewise uses the terms "processivity" and "processive" to refer to the addition of many GalA residues (Ridley et al., 2001), rather than the more precise mechanistic definition that is now in use.

In Chapter 1, several examples of plant cell wall GTs were presented with low activity toward short-chain acceptors, raising the possibility that a two-phase mechanism is a common feature of GTs. The features that distinguish this proposed mechanism from standard definitions of processive and distributive glycosyltransfer invites many polysaccharide synthases to be revisited with the knowledge of this alternative proposed mechanism. Numerous examples exist for which standard models of processivity may have been an unnecessary restraint on the interpretation of the data, including polysialic acid (Keys et al., 2014), *Neisseria meningitidis* Serogroup X (Fiebig et al., 2018), and levan (Raga-Carbajal et al., 2016). Processivity is even a point of contention for the well-studied enzyme glycogen synthase (Roach et al., 2012). The polysaccharide elongation model presented here may continue to be revised in the future as more sophisticated techniques for measuring reaction kinetics and elongation patterns become available. Acknowledging that numerous alternative hypotheses are possible, the future of glycobiology presents an opportunity to resolve longstanding questions related to the mechanisms of polysaccharide synthesis unconstrained by conventional models.

REFERENCES

- Akita, K., Ishimizu, T., Tsukamoto, T., Ando, T., and Hase, S. (2002). Successive glycosyltransfer activity and enzymatic characterization of pectic polygalacturonate 4-alpha-galacturonosyltransferase solubilized from pollen tubes of Petunia axillaris using pyridylaminated oligogalacturonates as substrates. *Plant Physiol* 130, 374-379.
- Albersheim, P., Darvill, A., Roberts, K., Sederoff, R., and Staehelin, A. (2010). *Plant cell walls*. Garland Science.
- Amos, R.A., Pattathil, S., Yang, J.Y., Atmodjo, M.A., Urbanowicz, B.R., Moremen, K.W., and Mohnen, D. (2018). A two-phase model for the non-processive biosynthesis of homogalacturonan polysaccharides by the GAUT1:GAUT7 complex. *J Biol Chem*.
- Anders, N., Wilkinson, M.D., Lovegrove, A., Freeman, J., Tryfona, T., Pellny, T.K., Weimar, T., Mortimer, J.C., Stott, K., Baker, J.M., Defoin-Platel, M., Shewry, P.R., Dupree, P., and Mitchell, R.A. (2012). Glycosyl transferases in family 61 mediate arabinofuranosyl transfer onto xylan in grasses. *Proc Natl Acad Sci U S A* 109, 989-993.
- Arabidopsis Genome Initiative (2000). Analysis of the genome sequence of the flowering plant Arabidopsis thaliana. *Nature* 408, 796-815.
- Atmodjo, M.A., Hao, Z., and Mohnen, D. (2013). Evolving views of pectin biosynthesis. *Annu Rev Plant Biol* 64, 747-779.
- Atmodjo, M.A., Sakuragi, Y., Zhu, X., Burrell, A.J., Mohanty, S.S., Atwood, J.A., 3rd, Orlando, R., Scheller, H.V., and Mohnen, D. (2011). Galacturonosyltransferase (GAUT)1 and GAUT7 are the core of a plant cell wall pectin biosynthetic homogalacturonan:galacturonosyltransferase complex. *Proc Natl Acad Sci U S A* 108, 20225-20230.
- Bambara, R.A., Fay, P.J., and Mallaber, L.M. (1995). Methods of analyzing processivity. *Methods Enzymol* 262, 270-280.
- Bar-Even, A., Noor, E., Savir, Y., Liebermeister, W., Davidi, D., Tawfik, D.S., and Milo, R. (2011). The moderately efficient enzyme: evolutionary and physicochemical trends shaping enzyme parameters. *Biochemistry* 50, 4402-4410.
- Barb, A.W., Meng, L., Gao, Z., Johnson, R.W., Moremen, K.W., and Prestegard, J.H. (2012). NMR characterization of immunoglobulin G Fc glycan motion on enzymatic sialylation. *Biochemistry* 51, 4618-4626.

- Bartetzko, M.P., and Pfrengle, F. (2018). Automated Glycan Assembly of Plant Oligosaccharides and Their Application in Cell-Wall Biology. *Chembiochem*.
- Basu, D., Liang, Y., Liu, X., Himmeldirk, K., Faik, A., Kieliszewski, M., Held, M., and Showalter, A.M. (2013). Functional identification of a hydroxyproline-ogalactosyltransferase specific for arabinogalactan protein biosynthesis in Arabidopsis. *J Biol Chem* 288, 10132-10143.
- Basu, D., Tian, L., Wang, W., Bobbs, S., Herock, H., Travers, A., and Showalter, A.M. (2015a). A small multigene hydroxyproline-O-galactosyltransferase family functions in arabinogalactan-protein glycosylation, growth and development in Arabidopsis. *BMC Plant Biol* 15, 295.
- Basu, D., Wang, W., Ma, S., Debrosse, T., Poirier, E., Emch, K., Soukup, E., Tian, L., and Showalter, A.M. (2015b). Two Hydroxyproline Galactosyltransferases, GALT5 and GALT2, Function in Arabinogalactan-Protein Glycosylation, Growth and Development in Arabidopsis. *PLoS One* 10, e0125624.
- Beckham, G.T., Stahlberg, J., Knott, B.C., Himmel, M.E., Crowley, M.F., Sandgren, M., Sorlie, M., and Payne, C.M. (2014). Towards a molecular-level theory of carbohydrate processivity in glycoside hydrolases. *Curr Opin Biotechnol* 27, 96-106.
- Benen, J.A., Kester, H.C., and Visser, J. (1999). Kinetic characterization of Aspergillus niger N400 endopolygalacturonases I, II and C. *Eur J Biochem* 259, 577-585.
- Berardini, T.Z., Reiser, L., Li, D., Mezheritsky, Y., Muller, R., Strait, E., and Huala, E. (2015). The Arabidopsis information resource: Making and mining the "gold standard" annotated reference plant genome. *Genesis* 53, 474-485.
- Berg, J.M., Tymoczko, J.L., and Stryer, L. (2002). *Biochemistry*. New York: W H Freeman.
- Bi, Y., Hubbard, C., Purushotham, P., and Zimmer, J. (2015). Insights into the structure and function of membrane-integrated processive glycosyltransferases. *Curr Opin Struct Biol* 34, 78-86.
- Biswal, A.K., Atmodjo, M.A., Li, M., Baxter, H.L., Yoo, C.G., Pu, Y., Lee, Y.C., Mazarei, M., Black, I.M., Zhang, J.Y., Ramanna, H., Bray, A.L., King, Z.R., Lafayette, P.R., Pattathil, S., Donohoe, B.S., Mohanty, S.S., Ryno, D., Yee, K., Thompson, O.A., Rodriguez, M., Jr., Dumitrache, A., Natzke, J., Winkeler, K., Collins, C., Yang, X., Tan, L., Sykes, R.W., Gjersing, E.L., Ziebell, A., Turner, G.B., Decker, S.R., Hahn, M.G., Davison, B.H., Udvardi, M.K., Mielenz, J.R., Davis, M.F., Nelson, R.S., Parrott, W.A., Ragauskas, A.J., Neal Stewart, C., Jr., and Mohnen, D. (2018a). Sugar release and growth of biofuel crops are improved by downregulation of pectin biosynthesis. *Nat Biotechnol* 36, 249-257.
- Biswal, A.K., Atmodjo, M.A., Pattathil, S., Amos, R.A., Yang, X., Winkeler, K., Collins, C., Mohanty, S.S., Ryno, D., Tan, L., Gelineo-Albersheim, I., Hunt, K., Sykes, R.W., Turner, G.B., Ziebell, A., Davis, M.F., Decker, S.R., Hahn, M.G., and Mohnen, D. (2018b). Working towards recalcitrance mechanisms: increased xylan and homogalacturonan

- production by overexpression of GAlactUronosylTransferase12 (GAUT12) causes increased recalcitrance and decreased growth in Populus. *Biotechnol Biofuels* 11, 9.
- Biswal, A.K., Hao, Z., Pattathil, S., Yang, X., Winkeler, K., Collins, C., Mohanty, S.S., Richardson, E.A., Gelineo-Albersheim, I., Hunt, K., Ryno, D., Sykes, R.W., Turner, G.B., Ziebell, A., Gjersing, E., Lukowitz, W., Davis, M.F., Decker, S.R., Hahn, M.G., and Mohnen, D. (2015). Downregulation of GAUT12 in Populus deltoides by RNA silencing results in reduced recalcitrance, increased growth and reduced xylan and pectin in a woody biofuel feedstock. *Biotechnol Biofuels* 8, 41.
- Bloom, L.B., and Goodman, M.F. (2001). "Polymerase Processivity: Measurement and Mechanisms", in: *eLS*. (Chichester, UK: Wiley).
- Boevink, P., Oparka, K., Santa Cruz, S., Martin, B., Betteridge, A., and Hawes, C. (1998). Stacks on tracks: the plant Golgi apparatus traffics on an actin/ER network. *Plant J* 15, 441-447.
- Breyer, W.A., and Matthews, B.W. (2001). A structural basis for processivity. *Protein Sci* 10, 1699-1711.
- Brown, D.M., Zeef, L.A., Ellis, J., Goodacre, R., and Turner, S.R. (2005). Identification of novel genes in Arabidopsis involved in secondary cell wall formation using expression profiling and reverse genetics. *Plant Cell* 17, 2281-2295.
- Broxterman, S.E., and Schols, H.A. (2018). Interactions between pectin and cellulose in primary plant cell walls. *Carbohydr Polym* 192, 263-272.
- Burton, R.A., Wilson, S.M., Hrmova, M., Harvey, A.J., Shirley, N.J., Medhurst, A., Stone, B.A., Newbigin, E.J., Bacic, A., and Fincher, G.B. (2006). Cellulose synthase-like CslF genes mediate the synthesis of cell wall (1,3;1,4)-beta-D-glucans. *Science* 311, 1940-1942.
- Busse-Wicher, M., Gomes, T.C., Tryfona, T., Nikolovski, N., Stott, K., Grantham, N.J., Bolam, D.N., Skaf, M.S., and Dupree, P. (2014). The pattern of xylan acetylation suggests xylan may interact with cellulose microfibrils as a twofold helical screw in the secondary plant cell wall of Arabidopsis thaliana. *Plant J* 79, 492-506.
- Busse-Wicher, M., Li, A., Silveira, R.L., Pereira, C.S., Tryfona, T., Gomes, T.C., Skaf, M.S., and Dupree, P. (2016). Evolution of Xylan Substitution Patterns in Gymnosperms and Angiosperms: Implications for Xylan Interaction with Cellulose. *Plant Physiol* 171, 2418-2431.
- Cabrera, J.C., Boland, A., Messiaen, J., Cambier, P., and Van Cutsem, P. (2008). Egg box conformation of oligogalacturonides: the time-dependent stabilization of the elicitoractive conformation increases its biological activity. *Glycobiology* 18, 473-482.
- Carpita, N.C., and Gibeaut, D.M. (1993). Structural models of primary cell walls in flowering plants: consistency of molecular structure with the physical properties of the walls during growth. *Plant J* 3, 1-30.

- Carpita, N.C., and Mccann, M.C. (2010). The maize mixed-linkage (1->3),(1->4)-beta-D-glucan polysaccharide is synthesized at the golgi membrane. *Plant Physiol* 153, 1362-1371.
- Cavalier, D.M., and Keegstra, K. (2006). Two xyloglucan xylosyltransferases catalyze the addition of multiple xylosyl residues to cellohexaose. *J Biol Chem* 281, 34197-34207.
- Chaikuad, A., Froese, D.S., Berridge, G., Von Delft, F., Oppermann, U., and Yue, W.W. (2011). Conformational plasticity of glycogenin and its maltosaccharide substrate during glycogen biogenesis. *Proc Natl Acad Sci U S A* 108, 21028-21033.
- Chavaroche, A.A., Springer, J., Kooy, F., Boeriu, C., and Eggink, G. (2010). In vitro synthesis of heparosan using recombinant Pasteurella multocida heparosan synthase PmHS2. *Appl Microbiol Biotechnol* 85, 1881-1891.
- Chen, Y., Seepersaud, R., Bensing, B.A., Sullam, P.M., and Rapoport, T.A. (2016). Mechanism of a cytosolic O-glycosyltransferase essential for the synthesis of a bacterial adhesion protein. *Proc Natl Acad Sci U S A* 113, E1190-1199.
- Chiniquy, D., Sharma, V., Schultink, A., Baidoo, E.E., Rautengarten, C., Cheng, K., Carroll, A., Ulvskov, P., Harholt, J., Keasling, J.D., Pauly, M., Scheller, H.V., and Ronald, P.C. (2012). XAX1 from glycosyltransferase family 61 mediates xylosyltransfer to rice xylan. *Proc Natl Acad Sci U S A* 109, 17117-17122.
- Chou, Y.H., Pogorelko, G., Young, Z.T., and Zabotina, O.A. (2015). Protein-protein interactions among xyloglucan-synthesizing enzymes and formation of Golgi-localized multiprotein complexes. *Plant Cell Physiol* 56, 255-267.
- Chou, Y.H., Pogorelko, G., and Zabotina, O.A. (2012). Xyloglucan xylosyltransferases XXT1, XXT2, and XXT5 and the glucan synthase CSLC4 form Golgi-localized multiprotein complexes. *Plant Physiol* 159, 1355-1366.
- Chung, D., Pattathil, S., Biswal, A.K., Hahn, M.G., Mohnen, D., and Westpheling, J. (2014). Deletion of a gene cluster encoding pectin degrading enzymes in Caldicellulosiruptor bescii reveals an important role for pectin in plant biomass recalcitrance. *Biotechnol Biofuels* 7, 147.
- Ciceron, F., Rocha, J., Kousar, S., Hansen, S.F., Chazalet, V., Gillon, E., Breton, C., and Lerouxel, O. (2016). Expression, purification and biochemical characterization of AtFUT1, a xyloglucan-specific fucosyltransferase from Arabidopsis thaliana. *Biochimie* 128-129, 183-192.
- Cocuron, J.C., Lerouxel, O., Drakakaki, G., Alonso, A.P., Liepman, A.H., Keegstra, K., Raikhel, N., and Wilkerson, C.G. (2007). A gene from the cellulose synthase-like C family encodes a beta-1,4 glucan synthase. *Proc Natl Acad Sci U S A* 104, 8550-8555.
- Copeland, R. (2002). Enzymes A Practical Introduction To Structure, Mechanism And Data Analysis. Wiley-VCH, Inc.

- Cornish-Bowden, A. (2012). Fundamentals of Enzyme Kinetics. Weinheim, Germany: Weinheim: Wiley-VCH.
- Cosgrove, D.J. (2014). Re-constructing our models of cellulose and primary cell wall assembly. *Curr Opin Plant Biol* 22, 122-131.
- Cosgrove, D.J. (2016a). Catalysts of plant cell wall loosening. F1000Res 5.
- Cosgrove, D.J. (2016b). Plant cell wall extensibility: connecting plant cell growth with cell wall structure, mechanics, and the action of wall-modifying enzymes. *J Exp Bot* 67, 463-476.
- Cosgrove, D.J. (2018). Diffuse Growth of Plant Cell Walls. Plant Physiol 176, 16-27.
- Culbertson, A.T., Chou, Y.H., Smith, A.L., Young, Z.T., Tietze, A.A., Cottaz, S., Faure, R., and Zabotina, O.A. (2016). Enzymatic Activity of Xyloglucan Xylosyltransferase 5. *Plant Physiol* 171, 1893-1904.
- Culbertson, A.T., Ehrlich, J.J., Choe, J.Y., Honzatko, R.B., and Zabotina, O.A. (2018). Structure of xyloglucan xylosyltransferase 1 reveals simple steric rules that define biological patterns of xyloglucan polymers. *Proc Natl Acad Sci U S A* 115, 6064-6069.
- Culbertson, A.T.Z., O. A. (2015). The Glycosyltransferases involved in Synthesis of Plant Cell Wall Polysaccharides: Present and Future. *JSM Enzymol Protein Sci* 1, 1004.
- Daher, F.B., and Braybrook, S.A. (2015). How to let go: pectin and plant cell adhesion. *Front Plant Sci* 6, 523.
- Davis, J., Brandizzi, F., Liepman, A.H., and Keegstra, K. (2010). Arabidopsis mannan synthase CSLA9 and glucan synthase CSLC4 have opposite orientations in the Golgi membrane. *Plant J* 64, 1028-1037.
- De Oliveira, D.M., Finger-Teixeira, A., Mota, T.R., Salvador, V.H., Moreira-Vilar, F.C., Molinari, H.B., Mitchell, R.A., Marchiosi, R., Ferrarese-Filho, O., and Dos Santos, W.D. (2015). Ferulic acid: a key component in grass lignocellulose recalcitrance to hydrolysis. *Plant Biotechnol J* 13, 1224-1232.
- Deangelis, P.L., and White, C.L. (2002). Identification and molecular cloning of a heparosan synthase from Pasteurella multocida type D. *J Biol Chem* 277, 7209-7213.
- Dheilly, E., Gall, S.L., Guillou, M.C., Renou, J.P., Bonnin, E., Orsel, M., and Lahaye, M. (2016). Cell wall dynamics during apple development and storage involves hemicellulose modifications and related expressed genes. *BMC Plant Biol* 16, 201.
- Dhugga, K.S., Barreiro, R., Whitten, B., Stecca, K., Hazebroek, J., Randhawa, G.S., Dolan, M., Kinney, A.J., Tomes, D., Nichols, S., and Anderson, P. (2004). Guar seed beta-mannan synthase is a member of the cellulose synthase super gene family. *Science* 303, 363-366.

- Dick-Perez, M., Zhang, Y., Hayes, J., Salazar, A., Zabotina, O.A., and Hong, M. (2011). Structure and interactions of plant cell-wall polysaccharides by two- and three-dimensional magic-angle-spinning solid-state NMR. *Biochemistry* 50, 989-1000.
- Dilokpimol, A., and Geshi, N. (2014). Arabidopsis thaliana glucuronosyltransferase in family GT14. *Plant Signal Behav* 9, e28891.
- Dilokpimol, A., Poulsen, C.P., Vereb, G., Kaneko, S., Schulz, A., and Geshi, N. (2014). Galactosyltransferases from Arabidopsis thaliana in the biosynthesis of type II arabinogalactan: molecular interaction enhances enzyme activity. *BMC Plant Biol* 14, 90.
- Dimitroff, G., Little, A., Lahnstein, J., Schwerdt, J.G., Srivastava, V., Bulone, V., Burton, R.A., and Fincher, G.B. (2016). (1,3;1,4)-beta-Glucan Biosynthesis by the CSLF6 Enzyme: Position and Flexibility of Catalytic Residues Influence Product Fine Structure. *Biochemistry* 55, 2054-2061.
- Doblin, M.S., Pettolino, F.A., Wilson, S.M., Campbell, R., Burton, R.A., Fincher, G.B., Newbigin, E., and Bacic, A. (2009). A barley cellulose synthase-like CSLH gene mediates (1,3;1,4)-beta-D-glucan synthesis in transgenic Arabidopsis. *Proc Natl Acad Sci U S A* 106, 5996-6001.
- Doong, R.L., Liljebjelke, K., Fralish, G., Kumar, A., and Mohnen, D. (1995a). Cell-Free Synthesis of Pectin (Identification and Partial Characterization of Polygalacturonate 4-[alpha]-Galacturonosyltransferase and Its Products from Membrane Preparations of Tobacco Cell-Suspension Cultures). *Plant Physiol* 109, 141-152.
- Doong, R.L., Liljebjelke, K., Fralish, G., Kumar, A., and Mohnen, D. (1995b). Cell-Free Synthesis of Pectin (Identification and Partial Characterization of Polygalacturonate 4-α-Galacturonosyltransferase and Its Products from Membrane Preparations of Tobacco Cell-Suspension Cultures). *Plant Physiol* 109, 141-152.
- Doong, R.L., and Mohnen, D. (1998). Solubilization and characterization of a galacturonosyltransferase that synthesizes the pectic polysaccharide homogalacturonan. *Plant Journal* 13, 363-374.
- Drakakaki, G. (2015). Polysaccharide deposition during cytokinesis: Challenges and future perspectives. *Plant Sci* 236, 177-184.
- Du, J., Vepachedu, V., Cho, S.H., Kumar, M., and Nixon, B.T. (2016). Structure of the Cellulose Synthase Complex of Gluconacetobacter hansenii at 23.4 A Resolution. *PLoS One* 11, e0155886.
- Ebert, B., Birdseye, D., Liwanag, A.J.M., Laursen, T., Rennie, E.A., Guo, X., Catena, M., Rautengarten, C., Stonebloom, S.H., Gluza, P., Pidatala, V.R., Andersen, M.C.F., Cheetamun, R., Mortimer, J.C., Heazlewood, J.L., Bacic, A., Clausen, M.H., Willats, W.G.T., and Scheller, H.V. (2018). The Three Members of the Arabidopsis Glycosyltransferase Family 92 are Functional beta-1,4-Galactan Synthases. *Plant Cell Physiol* 59, 2624-2636.

- Ebringerová, A., Hromádková, Z., and Heinze, T. (2005). "Hemicellulose," in *Polysaccharides I.*), 1-67.
- Edwards, M.E., Dickson, C.A., Chengappa, S., Sidebottom, C., Gidley, M.J., and Reid, J.S. (1999). Molecular characterisation of a membrane-bound galactosyltransferase of plant cell wall matrix polysaccharide biosynthesis. *Plant J* 19, 691-697.
- Egelund, J., Damager, I., Faber, K., Olsen, C.E., Ulvskov, P., and Petersen, B.L. (2008). Functional characterisation of a putative rhamnogalacturonan II specific xylosyltransferase. *FEBS Lett* 582, 3217-3222.
- Egelund, J., Petersen, B.L., Motawia, M.S., Damager, I., Faik, A., Olsen, C.E., Ishii, T., Clausen, H., Ulvskov, P., and Geshi, N. (2006). Arabidopsis thaliana RGXT1 and RGXT2 encode Golgi-localized (1,3)-alpha-D-xylosyltransferases involved in the synthesis of pectic rhamnogalacturonan-II. *Plant Cell* 18, 2593-2607.
- Egelund, J., Skjot, M., Geshi, N., Ulvskov, P., and Petersen, B.L. (2004). A complementary bioinformatics approach to identify potential plant cell wall glycosyltransferase-encoding genes. *Plant Physiol* 136, 2609-2620.
- Ellis, M., Egelund, J., Schultz, C.J., and Bacic, A. (2010). Arabinogalactan-proteins: key regulators at the cell surface? *Plant Physiol* 153, 403-419.
- Faik, A., Bar-Peled, M., Derocher, A.E., Zeng, W., Perrin, R.M., Wilkerson, C., Raikhel, N.V., and Keegstra, K. (2000). Biochemical characterization and molecular cloning of an alpha-1,2-fucosyltransferase that catalyzes the last step of cell wall xyloglucan biosynthesis in pea. *J Biol Chem* 275, 15082-15089.
- Faik, A., Price, N.J., Raikhel, N.V., and Keegstra, K. (2002). An Arabidopsis gene encoding an alpha-xylosyltransferase involved in xyloglucan biosynthesis. *Proc Natl Acad Sci U S A* 99, 7797-7802.
- Fiebig, T., Berti, F., Freiberger, F., Pinto, V., Claus, H., Romano, M.R., Proietti, D., Brogioni, B., Stummeyer, K., Berger, M., Vogel, U., Costantino, P., and Gerardy-Schahn, R. (2014a). Functional expression of the capsule polymerase of Neisseria meningitidis serogroup X: a new perspective for vaccine development. *Glycobiology* 24, 150-158.
- Fiebig, T., Freiberger, F., Pinto, V., Romano, M.R., Black, A., Litschko, C., Bethe, A., Yashunsky, D., Adamo, R., Nikolaev, A., Berti, F., and Gerardy-Schahn, R. (2014b). Molecular cloning and functional characterization of components of the capsule biosynthesis complex of Neisseria meningitidis serogroup A: toward in vitro vaccine production. *J Biol Chem* 289, 19395-19407.
- Fiebig, T., Litschko, C., Freiberger, F., Bethe, A., Berger, M., and Gerardy-Schahn, R. (2018). Efficient solid-phase synthesis of meningococcal capsular oligosaccharides enables simple and fast chemoenzymatic vaccine production. *J Biol Chem* 293, 953-962.

- Fisher, A.C., Haitjema, C.H., Guarino, C., Celik, E., Endicott, C.E., Reading, C.A., Merritt, J.H., Ptak, A.C., Zhang, S., and Delisa, M.P. (2011). Production of secretory and extracellular N-linked glycoproteins in Escherichia coli. *Appl Environ Microbiol* 77, 871-881.
- Forsee, W.T., Cartee, R.T., and Yother, J. (2006). Role of the carbohydrate binding site of the Streptococcus pneumoniae capsular polysaccharide type 3 synthase in the transition from oligosaccharide to polysaccharide synthesis. *J Biol Chem* 281, 6283-6289.
- Fujiki, Y., Hubbard, A.L., Fowler, S., and Lazarow, P.B. (1982). Isolation of intracellular membranes by means of sodium carbonate treatment: application to endoplasmic reticulum. *J Cell Biol* 93, 97-102.
- Fukuda, M., Bierhuizen, M.F., and Nakayama, J. (1996). Expression cloning of glycosyltransferases. *Glycobiology* 6, 683-689.
- Geshi, N. (2014). Arabinogalactan Glycosyltransferases: Enzyme Assay, Protein-Protein Interaction, Subcellular Localization, and Perspectives for Application. *Advances in Botany* 2014, 1-7.
- Geshi, N., Johansen, J.N., Dilokpimol, A., Rolland, A., Belcram, K., Verger, S., Kotake, T., Tsumuraya, Y., Kaneko, S., Tryfona, T., Dupree, P., Scheller, H.V., Hofte, H., and Mouille, G. (2013). A galactosyltransferase acting on arabinogalactan protein glycans is essential for embryo development in Arabidopsis. *Plant J* 76, 128-137.
- Gibbons, B.J., Roach, P.J., and Hurley, T.D. (2002a). Crystal structure of the autocatalytic initiator of glycogen biosynthesis, glycogenin. *J Mol Biol* 319, 463-477.
- Gibbons, B.J., Roach, P.J., and Hurley, T.D. (2002b). Crystal Structure of the Autocatalytic Initiator of Glycogen Biosynthesis, Glycogenin. *Journal of Molecular Biology* 319, 463-477.
- Goubet, F., Barton, C.J., Mortimer, J.C., Yu, X., Zhang, Z., Miles, G.P., Richens, J., Liepman, A.H., Seffen, K., and Dupree, P. (2009). Cell wall glucomannan in Arabidopsis is synthesised by CSLA glycosyltransferases, and influences the progression of embryogenesis. *Plant J* 60, 527-538.
- Grant, G.T., Morris, E.R., Rees, D.A., Smith, P.J.C., and Thom, D. (1973). Biological Interactions between Polysaccharides and Divalent Cations Egg-Box Model. *Febs Letters* 32, 195-198.
- Grantham, N.J., Wurman-Rodrich, J., Terrett, O.M., Lyczakowski, J.J., Stott, K., Iuga, D., Simmons, T.J., Durand-Tardif, M., Brown, S.P., Dupree, R., Busse-Wicher, M., and Dupree, P. (2017). An even pattern of xylan substitution is critical for interaction with cellulose in plant cell walls. *Nat Plants* 3, 859-865.
- Groff, D., Armstrong, S., Rivers, P.J., Zhang, J., Yang, J., Green, E., Rozzelle, J., Liang, S., Kittle, J.D., Jr., Steiner, A.R., Baliga, R., Thanos, C.D., Hallam, T.J., Sato, A.K., and

- Yam, A.Y. (2014). Engineering toward a bacterial "endoplasmic reticulum" for the rapid expression of immunoglobulin proteins. *MAbs* 6, 671-678.
- Halmo, S.M., Singh, D., Patel, S., Wang, S., Edlin, M., Boons, G.J., Moremen, K.W., Live, D., and Wells, L. (2017). Protein O-Linked Mannose β-1,4-N-Acetylglucosaminyl-transferase 2 (POMGNT2) Is a Gatekeeper Enzyme for Functional Glycosylation of alpha-Dystroglycan. *J Biol Chem* 292, 2101-2109.
- Harding, S.E.V., K.; Stoke B.; Smidsrod, O. (1991). Molecular weight determination of polysaccharides. *Advances in Carbohydrate Analysis* 1, 63-144.
- Hatahet, F., Boyd, D., and Beckwith, J. (2014). Disulfide bond formation in prokaryotes: history, diversity and design. *Biochim Biophys Acta* 1844, 1402-1414.
- Hoch, G. (2007). Cell wall hemicelluloses as mobile carbon stores in non-reproductive plant tissues. *Functional Ecology* 21, 823-834.
- Hocq, L., Pelloux, J., and Lefebvre, V. (2017). Connecting Homogalacturonan-Type Pectin Remodeling to Acid Growth. *Trends Plant Sci* 22, 20-29.
- Horn, S.J., Sikorski, P., Cederkvist, J.B., Vaaje-Kolstad, G., Sorlie, M., Synstad, B., Vriend, G., Varum, K.M., and Eijsink, V.G. (2006). Costs and benefits of processivity in enzymatic degradation of recalcitrant polysaccharides. *Proc Natl Acad Sci U S A* 103, 18089-18094.
- Inamori, K., Yoshida-Moriguchi, T., Hara, Y., Anderson, M.E., Yu, L., and Campbell, K.P. (2012). Dystroglycan function requires xylosyl- and glucuronyltransferase activities of LARGE. *Science* 335, 93-96.
- Ishii, T. (2002). A sensitive and rapid bioassay of homogalacturonan synthase using 2-aminobenzamide-labeled oligogalacturonides. *Plant Cell Physiol* 43, 1386-1389.
- Ishii, T., Ohnishi-Kameyama, M., and Ono, H. (2004). Identification of elongating beta-1,4-galactosyltransferase activity in mung bean (Vigna radiata) hypocotyls using 2-aminobenzaminated 1,4-linked beta- D-galactooligosaccharides as acceptor substrates. *Planta* 219, 310-318.
- Jacobs, A., and Dahlman, O. (2001). Enhancement of the quality of MALDI mass spectra of highly acidic oligosaccharides by using a nafion-coated probe. *Anal Chem* 73, 405-410.
- Jensen, J.K., Busse-Wicher, M., Poulsen, C.P., Fangel, J.U., Smith, P.J., Yang, J.Y., Pena, M.J., Dinesen, M.H., Martens, H.J., Melkonian, M., Wong, G.K., Moremen, K.W., Wilkerson, C.G., Scheller, H.V., Dupree, P., Ulvskov, P., Urbanowicz, B.R., and Harholt, J. (2018). Identification of an algal xylan synthase indicates that there is functional orthology between algal and plant cell wall biosynthesis. *New Phytol* 218, 1049-1060.
- Jensen, J.K., Johnson, N.R., and Wilkerson, C.G. (2014). Arabidopsis thaliana IRX10 and two related proteins from psyllium and Physcomitrella patens are xylan xylosyltransferases. *Plant J* 80, 207-215.

- Jensen, J.K., Sorensen, S.O., Harholt, J., Geshi, N., Sakuragi, Y., Moller, I., Zandleven, J., Bernal, A.J., Jensen, N.B., Sorensen, C., Pauly, M., Beldman, G., Willats, W.G., and Scheller, H.V. (2008). Identification of a xylogalacturonan xylosyltransferase involved in pectin biosynthesis in Arabidopsis. *Plant Cell* 20, 1289-1302.
- Jiang, N., Wiemels, R.E., Soya, A., Whitley, R., Held, M., and Faik, A. (2016). Composition, Assembly, and Trafficking of a Wheat Xylan Synthase Complex. *Plant Physiol* 170, 1999-2023.
- Kaur, J., Kumar, A., and Kaur, J. (2018). Strategies for optimization of heterologous protein expression in E. coli: Roadblocks and reinforcements. *Int J Biol Macromol* 106, 803-822.
- Keegstra, K., Talmadge, K.W., Bauer, W.D., and Albersheim, P. (1973). The Structure of Plant Cell Walls: III. A Model of the Walls of Suspension-cultured Sycamore Cells Based on the Interconnections of the Macromolecular Components. *Plant Physiol* 51, 188-197.
- Kellokumpu, S., Hassinen, A., and Glumoff, T. (2016). Glycosyltransferase complexes in eukaryotes: long-known, prevalent but still unrecognized. *Cell Mol Life Sci* 73, 305-325.
- Keys, T.G., Fuchs, H.L., Ehrit, J., Alves, J., Freiberger, F., and Gerardy-Schahn, R. (2014). Engineering the product profile of a polysialyltransferase. *Nat Chem Biol* 10, 437-442.
- Kim, S.J., and Brandizzi, F. (2014). The plant secretory pathway: an essential factory for building the plant cell wall. *Plant Cell Physiol* 55, 687-693.
- Kim, S.J., Zemelis, S., Keegstra, K., and Brandizzi, F. (2015). The cytoplasmic localization of the catalytic site of CSLF6 supports a channeling model for the biosynthesis of mixed-linkage glucan. *Plant J* 81, 537-547.
- Knoch, E., Dilokpimol, A., Tryfona, T., Poulsen, C.P., Xiong, G., Harholt, J., Petersen, B.L., Ulvskov, P., Hadi, M.Z., Kotake, T., Tsumuraya, Y., Pauly, M., Dupree, P., and Geshi, N. (2013a). A beta-glucuronosyltransferase from Arabidopsis thaliana involved in biosynthesis of type II arabinogalactan has a role in cell elongation during seedling growth. *Plant J* 76, 1016-1029.
- Knoch, E., Dilokpimol, A., Tryfona, T., Poulsen, C.P., Xiong, G., Harholt, J., Petersen, B.L., Ulvskov, P., Hadi, M.Z., Kotake, T., Tsumuraya, Y., Pauly, M., Dupree, P., and Geshi, N. (2013b). A β-glucuronosyltransferase from Arabidopsis thaliana involved in biosynthesis of type II arabinogalactan has a role in cell elongation during seedling growth. *Plant J* 76, 1016-1029.
- Kumar, R., Khurana, A., and Sharma, A.K. (2014). Role of plant hormones and their interplay in development and ripening of fleshy fruits. *J Exp Bot* 65, 4561-4575.
- Kuznetsova, I.M., Turoverov, K.K., and Uversky, V.N. (2014). What macromolecular crowding can do to a protein. *Int J Mol Sci* 15, 23090-23140.

- Laemmli, U.K. (1970). Cleavage of structural proteins during the assembly of the head of bacteriophage T4. *Nature* 227, 680-685.
- Lairson, L.L., Henrissat, B., Davies, G.J., and Withers, S.G. (2008). Glycosyltransferases: structures, functions, and mechanisms. *Annu Rev Biochem* 77, 521-555.
- Lao, J., Oikawa, A., Bromley, J.R., Mcinerney, P., Suttangkakul, A., Smith-Moritz, A.M.,
 Plahar, H., Chiu, T.Y., Gonzalez Fernandez-Nino, S.M., Ebert, B., Yang, F.,
 Christiansen, K.M., Hansen, S.F., Stonebloom, S., Adams, P.D., Ronald, P.C., Hillson,
 N.J., Hadi, M.Z., Vega-Sanchez, M.E., Loque, D., Scheller, H.V., and Heazlewood, J.L.
 (2014). The plant glycosyltransferase clone collection for functional genomics. *Plant J*79, 517-529.
- Laursen, T., Stonebloom, S.H., Pidatala, V.R., Birdseye, D.S., Clausen, M.H., Mortimer, J.C., and Scheller, H.V. (2018a). Bifunctional glycosyltransferases catalyze both extension and termination of pectic galactan oligosaccharides. *Plant J* 94, 340-351.
- Laursen, T., Stonebloom, S.H., Pidatala, V.R., Birdseye, D.S., Clausen, M.H., Mortimer, J.C., and Scheller, H.V. (2018b). Bifunctional glycosyltransferases catalyze both extension and termination of pectic galactan oligosaccharides. *Plant J*, 340-351.
- Lee, C., Teng, Q., Zhong, R., and Ye, Z.H. (2012a). Arabidopsis GUX proteins are glucuronyltransferases responsible for the addition of glucuronic acid side chains onto xylan. *Plant Cell Physiol* 53, 1204-1216.
- Lee, C., Zhong, R., and Ye, Z.H. (2012b). Arabidopsis family GT43 members are xylan xylosyltransferases required for the elongation of the xylan backbone. *Plant Cell Physiol* 53, 135-143.
- Levengood, M.R., Splain, R.A., and Kiessling, L.L. (2011). Monitoring processivity and length control of a carbohydrate polymerase. *J Am Chem Soc* 133, 12758-12766.
- Liepman, A.H., Wilkerson, C.G., and Keegstra, K. (2005). Expression of cellulose synthase-like (Csl) genes in insect cells reveals that CslA family members encode mannan synthases. *Proc Natl Acad Sci U S A* 102, 2221-2226.
- Liljebjelke, K., Adolphson, R., Baker, K., Doong, R.L., and Mohnen, D. (1995). Enzymatic synthesis and purification of uridine diphosphate [14C]galacturonic acid: a substrate for pectin biosynthesis. *Anal Biochem* 225, 296-304.
- Lionetti, V., Francocci, F., Ferrari, S., Volpi, C., Bellincampi, D., Galletti, R., D'ovidio, R., De Lorenzo, G., and Cervone, F. (2010). Engineering the cell wall by reducing de-methylesterified homogalacturonan improves saccharification of plant tissues for bioconversion. *Proc Natl Acad Sci U S A* 107, 616-621.
- Litschko, C., Romano, M.R., Pinto, V., Claus, H., Vogel, U., Berti, F., Gerardy-Schahn, R., and Fiebig, T. (2015). The capsule polymerase CslB of Neisseria meningitidis serogroup L

- catalyzes the synthesis of a complex trimeric repeating unit comprising glycosidic and phosphodiester linkages. *J Biol Chem* 290, 24355-24366.
- Little, A., Schwerdt, J.G., Shirley, N.J., Khor, S.F., Neumann, K., O'donovan, L.A., Lahnstein, J., Collins, H.M., Henderson, M., Fincher, G.B., and Burton, R.A. (2018). Revised Phylogeny of the Cellulose Synthase Gene Superfamily: Insights into Cell Wall Evolution. *Plant Physiol* 177, 1124-1141.
- Liu, X.L., Liu, L., Niu, Q.K., Xia, C., Yang, K.Z., Li, R., Chen, L.Q., Zhang, X.Q., Zhou, Y., and Ye, D. (2011). Male gametophyte defective 4 encodes a rhamnogalacturonan II xylosyltransferase and is important for growth of pollen tubes and roots in Arabidopsis. *Plant J* 65, 647-660.
- Liwanag, A.J., Ebert, B., Verhertbruggen, Y., Rennie, E.A., Rautengarten, C., Oikawa, A., Andersen, M.C., Clausen, M.H., and Scheller, H.V. (2012a). Pectin biosynthesis: GALS1 in Arabidopsis thaliana is a beta-1,4-galactan beta-1,4-galactosyltransferase. *Plant Cell* 24, 5024-5036.
- Liwanag, A.J., Ebert, B., Verhertbruggen, Y., Rennie, E.A., Rautengarten, C., Oikawa, A., Andersen, M.C., Clausen, M.H., and Scheller, H.V. (2012b). Pectin biosynthesis: GALS1 in Arabidopsis thaliana is a β -1,4-galactan β -1,4-galactosyltransferase. *Plant Cell* 24, 5024-5036.
- Lombard, V., Golaconda Ramulu, H., Drula, E., Coutinho, P.M., and Henrissat, B. (2014). The carbohydrate-active enzymes database (CAZy) in 2013. *Nucleic Acids Res* 42, D490-495.
- Lundqvist, J., Teleman, A., Junel, L., Zacchi, G., Dahlman, O., Tjerneld, F., and Stalbrand, H. (2002). Isolation and characterization of galactoglucomannan from spruce (Picea abies). *Carbohydrate Polymers* 48, 29-39.
- Ly, H.D., Lougheed, B., Wakarchuk, W.W., and Withers, S.G. (2002). Mechanistic studies of a retaining α-galactosyltransferase from Neisseria meningitidis. *Biochemistry* 41, 5075-5085.
- Madson, M., Dunand, C., Li, X., Verma, R., Vanzin, G.F., Caplan, J., Shoue, D.A., Carpita, N.C., and Reiter, W.D. (2003). The MUR3 gene of Arabidopsis encodes a xyloglucan galactosyltransferase that is evolutionarily related to animal exostosins. *Plant Cell* 15, 1662-1670.
- Makabe, T., Komiya, S., Prawitwong, P., Takahashi, R., Takigami, M., Nagasawa, N., Tamada, M., and Takigami, S. (2009). Characterization of γ-irradiated Konjac Glucomannan by Light Scattering and Scanning Probe Microscope. *Transactions of the Materials Research Society of Japan* 34, 469-472.
- Mccann, M.C., Wells, B., and Roberts, K. (1990). Direct Visualization of Cross-Links in the Primary Plant-Cell Wall. *Journal of Cell Science* 96, 323-334.

- Mcneil, M., Darvill, A.G., and Albersheim, P. (1980). Structure of Plant Cell Walls: X. Rhamnogalacturonan I, A Structurally Complex Pectic Polysaccharide in the Walls of Suspension-Cultured Syacamore Cells. *Plant Physiol* 66, 1128-1134.
- Meng, L., Forouhar, F., Thieker, D., Gao, Z., Ramiah, A., Moniz, H., Xiang, Y., Seetharaman, J., Milaninia, S., Su, M., Bridger, R., Veillon, L., Azadi, P., Kornhaber, G., Wells, L., Montelione, G.T., Woods, R.J., Tong, L., and Moremen, K.W. (2013). Enzymatic basis for N-glycan sialylation: structure of rat α2,6-sialyltransferase (ST6GAL1) reveals conserved and unique features for glycan sialylation. *J Biol Chem* 288, 34680-34698.
- Moremen, K.W., Ramiah, A., Stuart, M., Steel, J., Meng, L., Forouhar, F., Moniz, H.A., Gahlay, G., Gao, Z., Chapla, D., Wang, S., Yang, J.Y., Prabhakar, P.K., Johnson, R., Rosa, M.D., Geisler, C., Nairn, A.V., Seetharaman, J., Wu, S.C., Tong, L., Gilbert, H.J., Labaer, J., and Jarvis, D.L. (2018). Expression system for structural and functional studies of human glycosylation enzymes. *Nat Chem Biol* 14, 156-162.
- Morgan, J.L., Strumillo, J., and Zimmer, J. (2013). Crystallographic snapshot of cellulose synthesis and membrane translocation. *Nature* 493, 181-186.
- Morris, E.R., Powell, D.A., Gidley, M.J., and Rees, D.A. (1982). Conformations and Interactions of Pectins .1. Polymorphism between Gel and Solid States of Calcium Polygalacturonate. *Journal of Molecular Biology* 155, 507-516.
- Mort, A.J., Moerschbacher, B.M., Pierce, M.L., and Maness, N.O. (1991). Problems Encountered during the Extraction, Purification, and Chromatography of Pectic Fragments, and Some Solutions to Them. *Carbohydrate Research* 215, 219-227.
- Mort, A.J.M., B. M.; Pierce, M. L.; Maness, N. O. (1991). Problems encountered during the extraction, purification, and chromatography of pectic fragments, and some solutions to them. *Carbohydr Res* 215, 219-227.
- Mortimer, J.C., Miles, G.P., Brown, D.M., Zhang, Z., Segura, M.P., Weimar, T., Yu, X., Seffen, K.A., Stephens, E., Turner, S.R., and Dupree, P. (2010). Absence of branches from xylan in Arabidopsis gux mutants reveals potential for simplification of lignocellulosic biomass. *Proc Natl Acad Sci U S A* 107, 17409-17414.
- Mravec, J., Kracun, S.K., Rydahl, M.G., Westereng, B., Pontiggia, D., De Lorenzo, G., Domozych, D.S., and Willats, W.G.T. (2017). An oligogalacturonide-derived molecular probe demonstrates the dynamics of calcium-mediated pectin complexation in cell walls of tip-growing structures. *Plant J* 91, 534-546.
- Nakamura, A., Furuta, H., Maeda, H., Takao, T., and Nagamatsu, Y. (2002). Structural studies by stepwise enzymatic degradation of the main backbone of soybean soluble polysaccharides consisting of galacturonan and rhamnogalacturonan. *Biosci Biotechnol Biochem* 66, 1301-1313.

- Nardone, G., George, J., and Chirikjian, J.G. (1986). Differences in the kinetic properties of BamHI endonuclease and methylase with linear DNA substrates. *J Biol Chem* 261, 12128-12133.
- Ndeh, D., Rogowski, A., Cartmell, A., Luis, A.S., Basle, A., Gray, J., Venditto, I., Briggs, J., Zhang, X., Labourel, A., Terrapon, N., Buffetto, F., Nepogodiev, S., Xiao, Y., Field, R.A., Zhu, Y., O'neil, M.A., Urbanowicz, B.R., York, W.S., Davies, G.J., Abbott, D.W., Ralet, M.C., Martens, E.C., Henrissat, B., and Gilbert, H.J. (2017). Complex pectin metabolism by gut bacteria reveals novel catalytic functions. *Nature* 544, 65-70.
- Ng, J.K., Schroder, R., Sutherland, P.W., Hallett, I.C., Hall, M.I., Prakash, R., Smith, B.G., Melton, L.D., and Johnston, J.W. (2013). Cell wall structures leading to cultivar differences in softening rates develop early during apple (Malus x domestica) fruit growth. *BMC Plant Biol* 13, 183.
- Nothaft, H., and Szymanski, C.M. (2013). Bacterial protein N-glycosylation: new perspectives and applications. *J Biol Chem* 288, 6912-6920.
- Ogawa-Ohnishi, M., and Matsubayashi, Y. (2015). Identification of three potent hydroxyproline O-galactosyltransferases in Arabidopsis. *Plant J* 81, 736-746.
- Oikawa, A., Lund, C.H., Sakuragi, Y., and Scheller, H.V. (2013). Golgi-localized enzyme complexes for plant cell wall biosynthesis. *Trends Plant Sci* 18, 49-58.
- Palin, R., and Geitmann, A. (2012). The role of pectin in plant morphogenesis. *Biosystems* 109, 397-402.
- Paniagua, C., Pose, S., Morris, V.J., Kirby, A.R., Quesada, M.A., and Mercado, J.A. (2014). Fruit softening and pectin disassembly: an overview of nanostructural pectin modifications assessed by atomic force microscopy. *Ann Bot* 114, 1375-1383.
- Park, Y.B., and Cosgrove, D.J. (2015). Xyloglucan and its interactions with other components of the growing cell wall. *Plant Cell Physiol* 56, 180-194.
- Pattathil, S., Avci, U., Baldwin, D., Swennes, A.G., Mcgill, J.A., Popper, Z., Bootten, T., Albert, A., Davis, R.H., Chennareddy, C., Dong, R., O'shea, B., Rossi, R., Leoff, C., Freshour, G., Narra, R., O'neil, M., York, W.S., and Hahn, M.G. (2010). A comprehensive toolkit of plant cell wall glycan-directed monoclonal antibodies. *Plant Physiol* 153, 514-525.
- Pattathil, S., Avci, U., Miller, J.S., and Hahn, M.G. (2012). Immunological approaches to plant cell wall and biomass characterization: Glycome Profiling. *Methods Mol Biol* 908, 61-72.
- Pauly, M., and Keegstra, K. (2016). Biosynthesis of the Plant Cell Wall Matrix Polysaccharide Xyloglucan. *Annu Rev Plant Biol* 67, 235-259.
- Peaucelle, A., Braybrook, S., and Hofte, H. (2012). Cell wall mechanics and growth control in plants: the role of pectins revisited. *Front Plant Sci* 3, 121.

- Pena, M.J., Zhong, R., Zhou, G.K., Richardson, E.A., O'neill, M.A., Darvill, A.G., York, W.S., and Ye, Z.H. (2007). Arabidopsis irregular xylem8 and irregular xylem9: implications for the complexity of glucuronoxylan biosynthesis. *Plant Cell* 19, 549-563.
- Pereira, C.S., Silveira, R.L., Dupree, P., and Skaf, M.S. (2017). Effects of Xylan Side-Chain Substitutions on Xylan-Cellulose Interactions and Implications for Thermal Pretreatment of Cellulosic Biomass. *Biomacromolecules* 18, 1311-1321.
- Perrin, R.M., Derocher, A.E., Bar-Peled, M., Zeng, W., Norambuena, L., Orellana, A., Raikhel, N.V., and Keegstra, K. (1999). Xyloglucan fucosyltransferase, an enzyme involved in plant cell wall biosynthesis. *Science* 284, 1976-1979.
- Persson, K., Ly, H.D., Dieckelmann, M., Wakarchuk, W.W., Withers, S.G., and Strynadka, N.C. (2001). Crystal structure of the retaining galactosyltransferase LgtC from Neisseria meningitidis in complex with donor and acceptor sugar analogs. *Nat Struct Biol* 8, 166-175.
- Petersen, B.L., Egelund, J., Damager, I., Faber, K., Jensen, J.K., Yang, Z., Bennett, E.P., Scheller, H.V., and Ulvskov, P. (2009). Assay and heterologous expression in Pichia pastoris of plant cell wall type-II membrane anchored glycosyltransferases. *Glycoconj J* 26, 1235-1246.
- Piszkiewicz, D. (1977). *Kinetics of chemical and enzyme-catalyzed reactions*. New York: Oxford University Press.
- Praissman, J.L., Live, D.H., Wang, S., Ramiah, A., Chinoy, Z.S., Boons, G.J., Moremen, K.W., and Wells, L. (2014). B4GAT1 is the priming enzyme for the LARGE-dependent functional glycosylation of alpha-dystroglycan. *eLife* 3.
- Praissman, J.L., Willer, T., Sheikh, M.O., Toi, A., Chitayat, D., Lin, Y.Y., Lee, H., Stalnaker, S.H., Wang, S., Prabhakar, P.K., Nelson, S.F., Stemple, D.L., Moore, S.A., Moremen, K.W., Campbell, K.P., and Wells, L. (2016). The functional O-mannose glycan on alphadystroglycan contains a phospho-ribitol primed for matriglycan addition. *eLife* 5.
- Purushotham, P., Cho, S.H., Diaz-Moreno, S.M., Kumar, M., Nixon, B.T., Bulone, V., and Zimmer, J. (2016). A single heterologously expressed plant cellulose synthase isoform is sufficient for cellulose microfibril formation in vitro. *Proc Natl Acad Sci U S A* 113, 11360-11365.
- Qu, Y., Egelund, J., Gilson, P.R., Houghton, F., Gleeson, P.A., Schultz, C.J., and Bacic, A. (2008). Identification of a novel group of putative Arabidopsis thaliana beta-(1,3)-galactosyltransferases. *Plant Mol Biol* 68, 43-59.
- Quesada, M.A., Blanco-Portales, R., Pose, S., Garcia-Gago, J.A., Jimenez-Bermudez, S., Munoz-Serrano, A., Caballero, J.L., Pliego-Alfaro, F., Mercado, J.A., and Munoz-Blanco, J. (2009). Antisense down-regulation of the FaPG1 gene reveals an unexpected central role for polygalacturonase in strawberry fruit softening. *Plant Physiol* 150, 1022-1032.

- Raga-Carbajal, E., Carrillo-Nava, E., Costas, M., Porras-Dominguez, J., Lopez-Munguia, A., and Olvera, C. (2016). Size product modulation by enzyme concentration reveals two distinct levan elongation mechanisms in Bacillus subtilis levansucrase. *Glycobiology* 26, 377-385.
- Ray, P.M., Shininger, T.L., and Ray, M.M. (1969). Isolation of beta-glucan synthetase particles from plant cells and identification with Golgi membranes. *Proc Natl Acad Sci U S A* 64, 605-612.
- Reiter, W.D., Chapple, C., and Somerville, C.R. (1997). Mutants of Arabidopsis thaliana with altered cell wall polysaccharide composition. *Plant J* 12, 335-345.
- Rennie, E.A., Hansen, S.F., Baidoo, E.E., Hadi, M.Z., Keasling, J.D., and Scheller, H.V. (2012). Three members of the Arabidopsis glycosyltransferase family 8 are xylan glucuronosyltransferases. *Plant Physiol* 159, 1408-1417.
- Richmond, T.A., and Somerville, C.R. (2000). The cellulose synthase superfamily. *Plant Physiol* 124, 495-498.
- Ridley, B.L., O'neill, M.A., and Mohnen, D. (2001). Pectins: structure, biosynthesis, and oligogalacturonide-related signaling. *Phytochemistry* 57, 929-967.
- Roach, P.J., Depaoli-Roach, A.A., Hurley, T.D., and Tagliabracci, V.S. (2012). Glycogen and its metabolism: some new developments and old themes. *Biochem J* 441, 763-787.
- Rocha, J., Ciceron, F., De Sanctis, D., Lelimousin, M., Chazalet, V., Lerouxel, O., and Breton, C. (2016). Structure of Arabidopsis thaliana FUT1 Reveals a Variant of the GT-B Class Fold and Provides Insight into Xyloglucan Fucosylation. *Plant Cell* 28, 2352-2364.
- Round, A.N., Rigby, N.M., Macdougall, A.J., and Morris, V.J. (2010). A new view of pectin structure revealed by acid hydrolysis and atomic force microscopy. *Carbohydr Res* 345, 487-497.
- Ruprecht, C., Dallabernardina, P., Smith, P.J., Urbanowicz, B.R., and Pfrengle, F. (2018). Analyzing Xyloglucan Endotransglycosylases by Incorporating Synthetic Oligosaccharides into Plant Cell Walls. *Chembiochem* 19, 793-798.
- Sandhu, A.P., Randhawa, G.S., and Dhugga, K.S. (2009). Plant cell wall matrix polysaccharide biosynthesis. *Mol Plant* 2, 840-850.
- Sarria, R., Wagner, T.A., O'neill, M.A., Faik, A., Wilkerson, C.G., Keegstra, K., and Raikhel, N.V. (2001). Characterization of a family of Arabidopsis genes related to xyloglucan fucosyltransferase1. *Plant Physiol* 127, 1595-1606.
- Saxena, I.M., Brown, R.M., Jr., Fevre, M., Geremia, R.A., and Henrissat, B. (1995). Multidomain architecture of beta-glycosyl transferases: implications for mechanism of action. *J Bacteriol* 177, 1419-1424.

- Scheller, H.V., Doong, R.L., Ridley, B.L., and Mohnen, D. (1999). Pectin biosynthesis: a solubilized alpha 1,4-galacturonosyltransferase from tobacco catalyzes the transfer of galacturonic acid from UDP-galacturonic acid onto the non-reducing end of homogalacturonan. *Planta* 207, 512-517.
- Scheller, H.V., and Ulvskov, P. (2010). Hemicelluloses. Annu Rev Plant Biol 61, 263-289.
- Sechet, J., Htwe, S., Urbanowicz, B., Agyeman, A., Feng, W., Ishikawa, T., Colomes, M., Kumar, K.S., Kawai-Yamada, M., Dinneny, J.R., O'neill, M.A., and Mortimer, J.C. (2018). Suppression of Arabidopsis GGLT1 affects growth by reducing the L-galactose content and borate cross-linking of rhamnogalacturonan-II. *Plant J* 96, 1036-1050.
- Seymour, G., Tucker, G.A., Poole, M., and Giovannoni, J. (2013). *The Molecular Biology and Biochemistry of Fruit Ripening*. Somerset, United States: John Wiley & Sons, Incorporated.
- Sheikh, M.O., Halmo, S.M., Patel, S., Middleton, D., Takeuchi, H., Schafer, C.M., West, C.M., Haltiwanger, R.S., Avci, F.Y., Moremen, K.W., and Wells, L. (2017). Rapid screening of sugar-nucleotide donor specificities of putative glycosyltransferases. *Glycobiology* 27, 206-212.
- Shi, H., Yu, L., Shi, Y., Lu, J., Teng, H., Zhou, Y., and Sun, L. (2017). Structural Characterization of a Rhamnogalacturonan I Domain from Ginseng and Its Inhibitory Effect on Galectin-3. *Molecules* 22.
- Showalter, A.M., and Basu, D. (2016). Extensin and Arabinogalactan-Protein Biosynthesis: Glycosyltransferases, Research Challenges, and Biosensors. *Front Plant Sci* 7, 814.
- Smith, P.J., Wang, H.T., York, W.S., Pena, M.J., and Urbanowicz, B.R. (2017). Designer biomass for next-generation biorefineries: leveraging recent insights into xylan structure and biosynthesis. *Biotechnol Biofuels* 10, 286.
- Sterling, J.D., Atmodjo, M.A., Inwood, S.E., Kumar Kolli, V.S., Quigley, H.F., Hahn, M.G., and Mohnen, D. (2006). Functional identification of an Arabidopsis pectin biosynthetic homogalacturonan galacturonosyltransferase. *Proc Natl Acad Sci U S A* 103, 5236-5241.
- Sterling, J.D., Lemons, J.A., Forkner, I.F., and Mohnen, D. (2005). Development of a filter assay for measuring homogalacturonan: α-(1,4)-Galacturonosyltransferase activity. *Anal Biochem* 343, 231-236.
- Sterling, J.D., Quigley, H.F., Orellana, A., and Mohnen, D. (2001). The catalytic site of the pectin biosynthetic enzyme alpha-1,4-galacturonosyltransferase is located in the lumen of the Golgi. *Plant Physiol* 127, 360-371.
- Subedi, G.P., Johnson, R.W., Moniz, H.A., Moremen, K.W., and Barb, A. (2015). High Yield Expression of Recombinant Human Proteins with the Transfection of HEK293 Cells in Suspension. *J Vis Exp*, e53568.

- Takenaka, Y., Kato, K., Ogawa-Ohnishi, M., Tsuruhama, K., Kajiura, H., Yagyu, K., Takeda, A., Takeda, Y., Kunieda, T., Hara-Nishimura, I., Kuroha, T., Nishitani, K., Matsubayashi, Y., and Ishimizu, T. (2018). Pectin RG-I rhamnosyltransferases represent a novel plant-specific glycosyltransferase family. *Nat Plants* 4, 669-676.
- Tal, M., Silberstein, A., and Nusser, E. (1985). Why does Coomassie Brilliant Blue R interact differently with different proteins? A partial answer. *J Biol Chem* 260, 9976-9980.
- Tan, L., Eberhard, S., Pattathil, S., Warder, C., Glushka, J., Yuan, C., Hao, Z., Zhu, X., Avci, U., Miller, J.S., Baldwin, D., Pham, C., Orlando, R., Darvill, A., Hahn, M.G., Kieliszewski, M.J., and Mohnen, D. (2013). An Arabidopsis cell wall proteoglycan consists of pectin and arabinoxylan covalently linked to an arabinogalactan protein. *Plant Cell* 25, 270-287.
- Titz, A., Butschi, A., Henrissat, B., Fan, Y.Y., Hennet, T., Razzazi-Fazeli, E., Hengartner, M.O., Wilson, I.B., Kunzler, M., and Aebi, M. (2009). Molecular basis for galactosylation of core fucose residues in invertebrates: identification of caenorhabditis elegans N-glycan core alpha1,6-fucoside beta1,4-galactosyltransferase GALT-1 as a member of a novel glycosyltransferase family. *J Biol Chem* 284, 36223-36233.
- Toivonen, P.M.A., and Brummell, D.A. (2008). Biochemical bases of appearance and texture changes in fresh-cut fruit and vegetables. *Postharvest Biology and Technology* 48, 1-14.
- Tryfona, T., Theys, T.E., Wagner, T., Stott, K., Keegstra, K., and Dupree, P. (2014). Characterisation of FUT4 and FUT6 alpha-(1 --> 2)-fucosyltransferases reveals that absence of root arabinogalactan fucosylation increases Arabidopsis root growth salt sensitivity. *PLoS One* 9, e93291.
- Turner, S.R., and Somerville, C.R. (1997). Collapsed xylem phenotype of Arabidopsis identifies mutants deficient in cellulose deposition in the secondary cell wall. *Plant Cell* 9, 689-701.
- Uehara, Y., Tamura, S., Maki, Y., Yagyu, K., Mizoguchi, T., Tamiaki, H., Imai, T., Ishii, T., Ohashi, T., Fujiyama, K., and Ishimizu, T. (2017). Biochemical characterization of rhamnosyltransferase involved in biosynthesis of pectic rhamnogalacturonan I in plant cell wall. *Biochem Biophys Res Commun* 486, 130-136.
- Uluisik, S., Chapman, N.H., Smith, R., Poole, M., Adams, G., Gillis, R.B., Besong, T.M., Sheldon, J., Stiegelmeyer, S., Perez, L., Samsulrizal, N., Wang, D., Fisk, I.D., Yang, N., Baxter, C., Rickett, D., Fray, R., Blanco-Ulate, B., Powell, A.L., Harding, S.E., Craigon, J., Rose, J.K., Fich, E.A., Sun, L., Domozych, D.S., Fraser, P.D., Tucker, G.A., Grierson, D., and Seymour, G.B. (2016). Genetic improvement of tomato by targeted control of fruit softening. *Nat Biotechnol* 34, 950-952.
- Urbanowicz, B.R., Bharadwaj, V.S., Alahuhta, M., Pena, M.J., Lunin, V.V., Bomble, Y.J., Wang, S., Yang, J.Y., Tuomivaara, S.T., Himmel, M.E., Moremen, K.W., York, W.S., and Crowley, M.F. (2017). Structural, mutagenic and in silico studies of xyloglucan fucosylation in Arabidopsis thaliana suggest a water-mediated mechanism. *Plant J* 91, 931-949.

- Urbanowicz, B.R., Pena, M.J., Moniz, H.A., Moremen, K.W., and York, W.S. (2014). Two Arabidopsis proteins synthesize acetylated xylan in vitro. *Plant J* 80, 197-206.
- Vaaje-Kolstad, G., Horn, S.J., Sorlie, M., and Eijsink, V.G. (2013). The chitinolytic machinery of Serratia marcescens--a model system for enzymatic degradation of recalcitrant polysaccharides. *FEBS J* 280, 3028-3049.
- Valderrama-Rincon, J.D., Fisher, A.C., Merritt, J.H., Fan, Y.Y., Reading, C.A., Chhiba, K., Heiss, C., Azadi, P., Aebi, M., and Delisa, M.P. (2012). An engineered eukaryotic protein glycosylation pathway in Escherichia coli. *Nat Chem Biol* 8, 434-436.
- Van De Meene, A.M., Doblin, M.S., and Bacic, A. (2017). The plant secretory pathway seen through the lens of the cell wall. *Protoplasma* 254, 75-94.
- Vanzin, G.F., Madson, M., Carpita, N.C., Raikhel, N.V., Keegstra, K., and Reiter, W.D. (2002). The mur2 mutant of Arabidopsis thaliana lacks fucosylated xyloglucan because of a lesion in fucosyltransferase AtFUT1. *Proc Natl Acad Sci U S A* 99, 3340-3345.
- Verhertbruggen, Y., Yin, L., Oikawa, A., and Scheller, H.V. (2011). Mannan synthase activity in the CSLD family. *Plant Signal Behav* 6, 1620-1623.
- Villemez, C.L., Lin, T.Y., and Hassid, W.Z. (1965). Biosynthesis of the polygalacturonic acid chain of pectin by a particulate enzyme preparation from Phaseolus aureus seedlings. *Proc Natl Acad Sci US A* 54, 1626-1632.
- Vincken, J.P. (2003). If Homogalacturonan Were a Side Chain of Rhamnogalacturonan I. Implications for Cell Wall Architecture. *Plant Physiology* 132, 1781-1789.
- Vionnet, J., and Vann, W.F. (2007). Successive glycosyltransfer of sialic acid by Escherichia coli K92 polysialyltransferase in elongation of oligosialic acceptors. *Glycobiology* 17, 735-743.
- Voiniciuc, C., Dama, M., Gawenda, N., Stritt, F., and Pauly, M. (2019). Mechanistic insights from plant heteromannan synthesis in yeast. *Proc Natl Acad Sci U S A* 116, 522-527.
- Voiniciuc, C., Engle, K.A., Gunl, M., Dieluweit, S., Schmidt, M.H., Yang, J.Y., Moremen, K.W., Mohnen, D., and Usadel, B. (2018a). Identification of Key Enzymes for Pectin Synthesis in Seed Mucilage. *Plant Physiol* 178, 1045-1064.
- Voiniciuc, C., Pauly, M., and Usadel, B. (2018b). Monitoring Polysaccharide Dynamics in the Plant Cell Wall. *Plant Physiol* 176, 2590-2600.
- Voiniciuc, C., Schmidt, M.H., Berger, A., Yang, B., Ebert, B., Scheller, H.V., North, H.M., Usadel, B., and Gunl, M. (2015). MUCILAGE-RELATED10 Produces Galactoglucomannan That Maintains Pectin and Cellulose Architecture in Arabidopsis Seed Mucilage. *Plant Physiol* 169, 403-420.

- Voxeur, A., and Hofte, H. (2016). Cell wall integrity signaling in plants: "To grow or not to grow that's the question". *Glycobiology* 26, 950-960.
- Vuttipongchaikij, S., Brocklehurst, D., Steele-King, C., Ashford, D.A., Gomez, L.D., and Mcqueen-Mason, S.J. (2012a). Arabidopsis GT34 family contains five xyloglucan alpha-1,6-xylosyltransferases. *New Phytol* 195, 585-595.
- Vuttipongchaikij, S., Brocklehurst, D., Steele-King, C., Ashford, D.A., Gomez, L.D., and Mcqueen-Mason, S.J. (2012b). Arabidopsis GT34 family contains five xyloglucan α-1,6-xylosyltransferases. *New Phytol* 195, 585-595.
- Wang, D., Yeats, T.H., Uluisik, S., Rose, J.K.C., and Seymour, G.B. (2018). Fruit Softening: Revisiting the Role of Pectin. *Trends Plant Sci* 23, 302-310.
- Wang, T., and Hong, M. (2016). Solid-state NMR investigations of cellulose structure and interactions with matrix polysaccharides in plant primary cell walls. *J Exp Bot* 67, 503-514.
- Wang, T., Zabotina, O., and Hong, M. (2012). Pectin-cellulose interactions in the Arabidopsis primary cell wall from two-dimensional magic-angle-spinning solid-state nuclear magnetic resonance. *Biochemistry* 51, 9846-9856.
- Weigel, P.H., Baggenstoss, B.A., and Washburn, J.L. (2017). Hyaluronan synthase assembles hyaluronan on a [GlcNAc(β 1,4)]n-GlcNAc(α 1 \rightarrow)UDP primer and hyaluronan retains this residual chitin oligomer as a cap at the nonreducing end. *Glycobiology* 27, 536-554.
- Weigel, P.H., West, C.M., Zhao, P., Wells, L., Baggenstoss, B.A., and Washburn, J.L. (2015). Hyaluronan synthase assembles chitin oligomers with -GlcNAc($\alpha 1 \rightarrow$)UDP at the reducing end. *Glycobiology* 25, 632-643.
- Welner, D.H., Shin, D., Tomaleri, G.P., Degiovanni, A.M., Tsai, A.Y., Tran, H.M., Hansen, S.F., Green, D.T., Scheller, H.V., and Adams, P.D. (2017). Plant cell wall glycosyltransferases: High-throughput recombinant expression screening and general requirements for these challenging enzymes. *PLoS One* 12, e0177591.
- Wu, Y., Williams, M., Bernard, S., Driouich, A., Showalter, A.M., and Faik, A. (2010a). Functional identification of two nonredundant Arabidopsis alpha(1,2)fucosyltransferases specific to arabinogalactan proteins. *J Biol Chem* 285, 13638-13645.
- Wu, Y., Williams, M., Bernard, S., Driouich, A., Showalter, A.M., and Faik, A. (2010b). Functional identification of two nonredundant Arabidopsis α(1,2)fucosyltransferases specific to arabinogalactan proteins. *J Biol Chem* 285, 13638-13645.
- Xu, C., and Ng, D.T. (2015). Glycosylation-directed quality control of protein folding. *Nat Rev Mol Cell Biol* 16, 742-752.

- Xu, J., Shpak, E., Gu, T., Moo-Young, M., and Kieliszewski, M. (2005). Production of recombinant plant gum with tobacco cell culture in bioreactor and gum characterization. *Biotechnol Bioeng* 90, 578-588.
- Xu, M., Li, D.S., Li, B., Wang, C., Zhu, Y.P., Lv, W.P., and Xie, B.J. (2013). Comparative Study on Molecular Weight of Konjac Glucomannan by Gel Permeation Chromatography-Laser Light Scattering-Refractive Index and Laser Light-Scattering Methods. *Journal of Spectroscopy*.
- Yapo, B.M. (2011). Rhamnogalacturonan-I: A Structurally Puzzling and Functionally Versatile Polysaccharide from Plant Cell Walls and Mucilages. *Polymer Reviews* 51, 391-413.
- Yapo, B.M., Lerouge, P., Thibault, J.-F., and Ralet, M.-C. (2007). Pectins from citrus peel cell walls contain homogalacturonans homogenous with respect to molar mass, rhamnogalacturonan I and rhamnogalacturonan II. *Carbohydrate Polymers* 69, 426-435.
- Yasui, K.J., J.; Ohashi, T.; Ishimizu, T. (2009). "In vitro synthesis of polygalacturonic acid," in *Pectin and pectinases*, ed. H.A. Schols, Visser, R.G.F, Voragen, A.G.J. (Wagenigen, The Netherlands: Wagenigen Academic Publishers), 167-175.
- Yin, L., Verhertbruggen, Y., Oikawa, A., Manisseri, C., Knierim, B., Prak, L., Jensen, J.K., Knox, J.P., Auer, M., Willats, W.G., and Scheller, H.V. (2011). The cooperative activities of CSLD2, CSLD3, and CSLD5 are required for normal Arabidopsis development. *Mol Plant* 4, 1024-1037.
- Yin, Y., Chen, H., Hahn, M.G., Mohnen, D., and Xu, Y. (2010). Evolution and function of the plant cell wall synthesis-related glycosyltransferase family 8. *Plant Physiol* 153, 1729-1746.
- Yoko-O, T., Wiggins, C.A., Stolz, J., Peak-Chew, S.Y., and Munro, S. (2003). An Nacetylglucosaminyltransferase of the Golgi apparatus of the yeast Saccharomyces cerevisiae that can modify N-linked glycans. *Glycobiology* 13, 581-589.
- Yu, H., Takeuchi, M., Lebarron, J., Kantharia, J., London, E., Bakker, H., Haltiwanger, R.S., Li, H., and Takeuchi, H. (2015). Notch-modifying xylosyltransferase structures support an SNi-like retaining mechanism. *Nat Chem Biol* 11, 847-854.
- Yuguchi, Y., Hirotsu, T., and Hosokawa, J. (2005). Structural Characteristics of Xyloglucan Congo Red Aggregates as Observed by Small Angle X-ray Scattering. *Cellulose* 12, 469-477.
- Zeng, W., Jiang, N., Nadella, R., Killen, T.L., Nadella, V., and Faik, A. (2010). A glucurono(arabino)xylan synthase complex from wheat contains members of the GT43, GT47, and GT75 families and functions cooperatively. *Plant Physiol* 154, 78-97.
- Zeng, W., Lampugnani, E.R., Picard, K.L., Song, L., Wu, A.M., Farion, I.M., Zhao, J., Ford, K., Doblin, M.S., and Bacic, A. (2016). Asparagus IRX9, IRX10, and IRX14A Are

Components of an Active Xylan Backbone Synthase Complex that Forms in the Golgi Apparatus. *Plant Physiol* 171, 93-109.

Zhang, G.F., and Staehelin, L.A. (1992). Functional compartmentation of the Golgi apparatus of plant cells: immunocytochemical analysis of high-pressure frozen- and freeze-substituted sycamore maple suspension culture cells. *Plant Physiol* 99, 1070-1083.

APPENDICES

ADDITIONAL STUDIES AND FUTURE DIRECTIONS FOR THE EXPRESSION AND ACTIVITY OF RECOMBINANT GAUT PROTEINS EXPRESSED IN HEK293 CELLS

APPENDIX A

EXPRESSION AND ACTIVITY VARIATION OF GAUT1:GAUT7 PRODUCED IN HEK293 CELL CULTURES

Purpose:

A major goal of this project was to establish a heterologous expression system from which soluble forms of the GAUT1:GAUT7 complex could be purified and which could be adapted to the expression of other plant cell wall-related enzymes. Because the project spanned several years, we co-expressed GAUT1 and GAUT7 from multiple cultures and assayed the activity under different conditions. We have observed variation in expression and activity levels of GAUT1:GAUT7 produced in these cultures. Documenting these results may help to guide future enzyme expression and activity studies.

Background:

The biochemical characterization of HG:GalAT activity of the GAUT1:GAUT7 complex (Ch. 2, Fig. 2.2) was performed using replicate assays with an enzyme preparation purified from a single heterologous expression HEK293 cell culture. This enzyme preparation was #6 of 11 large-scale co-expression cultures and was used as a positive control in future experiments, labeled "Batch #6". A "standard condition" for assaying the specific activity of GAUT1:GAUT7 was established based on reaction conditions that would allow for measurement of HG:GalAT

activity within a linear time range using the standard HG acceptor mix, DP7-23 (also referred to as the OGA acceptor mix, DP7-23 in Mohnen lab papers and protocols). The "standard condition" assay conditions were: 100 nM enzyme, 5 minute reaction time, 5 μM UDP-[14C]GalA, 1 mM total UDP-GalA (1:200 hot:cold donor substrate mix), and 10 μM HG acceptor in a reaction buffer containing 50 mM HEPES, pH 7.2, 0.25 mM MnCl₂, and 0.05% BSA. The enzyme concentration is based on a MW of 285 kDa for a GAUT1:GAUT1:GAUT7 trimer with N-terminal tags from the pGEn2 expression vector. To achieve this enzyme concentration, 30 μL assays contained 0.86 μg purified enzyme.

Kinetics assays to measure the $K_{\rm M}$ of UDP-GalA were also performed with HG acceptor concentrations from 50-100 μ M to establish saturating conditions. Compared to preliminary assays using lower, non-saturating concentrations of HG acceptor (1-10 μ M), these higher substrate concentrations yielded more consistent results in replicate experiments and data that fit the hyperbolic Michaelis-Menten curve. Substrate inhibition was observed at higher concentrations of HG acceptor, so $K_{\rm cat}$ values obtained from kinetics assays were lower when using concentrations above 10 μ M HG acceptor. Therefore, lower HG acceptor concentrations are likely to yield higher activity values within the linear time range for specific activity measurements, but higher concentrations are necessary to obtain saturating conditions for measuring reaction kinetics.

Assaying under the standard condition, the results presented in Ch. 2 yield net cpm values between 2000-3000. At a concentration of 5 μM, the UDP-[14C]GalA used in these assays equals a total of ~66,000 cpm, indicating that <5% of total UDP-GalA substrate was consumed at the 5 minute point of measurement. Specific activity measurements, designed to compare the activities of different preparations of the same enzyme, different enzymes (such as GAUT1:GAUT7

relative to mutants or other GAUT family members), or one enzyme under different conditions (such as acceptors of different DP), should be measured within the linear range of the progress curve. As a general guideline, the linear range is measured from 0-10% of total substrate depletion (Copeland, 2002).

Ideally, multiple purifications of GAUT1:GAUT7 should have consistent specific activity values. During the experiments performed over the course of this dissertation, HEK293 cell expression cultures ranging from 1-1000 mL were used to express GAUT1:GAUT7. As an unexpected consequence, expression levels (determined by media GFP fluorescence), protein purification amounts (determined by UV-Vis spectroscopy and/or GFP fluorescence), and activity values varied widely between expression cultures. The precise reasons for these differences are not clear, but numerous factors may contribute: the purity and age of expression plasmids, the age and viability of HEK293 cells used for cell culture, difficulty in measuring enzyme concentrations in stocks purified from small culture volumes, distortion of enzyme concentration measurements due to the presence of aggregate protein, purification of inactive protein, and/or different nickel-affinity columns and resin used for purification. Activity measured *in vitro* in dilute aqueous solution may suffer due to the lack of the intracellular crowded environment (Kuznetsova et al., 2014).

These complications were not realized until multiple replications of the GAUT1:GAUT7 co-expression experiment had been performed and "standard condition" assays had been developed. Because the standard condition uses a high dilution of UDP-[14C]GalA with non-radiolabeled UDP-GalA (1:200 dilution) and short assay times, low-activity cultures may yield no activity when assayed under "standard conditions." The data presented here serves to document variations in expression and activity values, to caution future heterologous expression

experiments about the possibility for variable activities, and to emphasize the importance of establishing multiple standard conditions for cross-culture specific activity comparisons.

Early experiments used long reaction times (3 hours) based on previously-published protocols for HG:GalAT activity. For this reason, the enzymes labeled Batch #0-4 do not have specific activity values. Wherever available, activity measurements are presented as range of net cpm values determined from assays performed under the conditions listed in Table 4.2.

Methods:

All cultures and activity assay methods are outlined in Chapter 2. HEK293F suspension culture cells were co-transfected with pGEn2 plasmids containing *GAUT1*Δ167 (2 μg/mL) and *GAUT7*Δ43 (2 μg/mL). Cultures were incubated in a humidified shaking 37°C incubator at 150 rpm for six days. Media GFP fluorescence was measured by centrifugation of 1 mL of the total expression culture at 12,000 rpm and measurement of 100 μL media in a 96-well plate using a SpectraMAX Gemini XS reader at 450 nm excitation and 515 nm emission wavelengths. Enzyme was purified from media using HisTrap HP nickel-affinity columns attached to an AKTA FPLC or using TALON metal-affinity resin. Activity was measured using radiolabeled filter assays at "standard conditions", defined above (p.1), or under conditions listed in Table 4.2.

Technical Notes:

For the HG acceptor mix, molarity was calculated using the MW of a DP15 acceptor (2658.6 mg/mmol). Therefore, a reaction labeled "10 μ M HG acceptor" with a total volume of 30 μ L contained 0.8 μ g of the acceptor mix.

$$\frac{2658.6 \ \mu g}{\mu mol} * \frac{10 \ \mu mol}{L} * \frac{L}{10^6 \mu L} * 30 \ \mu L = 0.8 \ \mu g$$

For GAUT1:GAUT7, molarity was calculated using the MW of a GFP-tagged heterotrimer containing two subunits of GAUT1 and one subunit of GAUT7. Therefore, a reaction under standard conditions (100 nM enzyme) with a total volume of 30 μ L contains 0.86 μ g of Ni-affinity purified enzyme.

$$\frac{285370.3 \text{ } \mu\text{g}}{\text{umol}} * \frac{0.1 \text{ } \mu\text{mol}}{\text{L}} * \frac{\text{L}}{10^6 \text{uL}} * 30 \text{ } \mu\text{L} = 0.86 \text{ } \mu\text{g}$$

The molar extinction coefficient at 280 nm for GFP-tagged GAUT1:GAUT7 protein was 354125 M⁻¹ cm⁻¹. For converting to mg/mL (molar extinction coefficient / molecular mass), the mass extinction coefficient is 1.24 L g⁻¹ cm⁻¹. The mass extinction coefficient is the protein absorbance value for a 1 mg/mL solution, and is reported by proteins analyzed using the ExPASy ProtParam tool as Abs 0.1%. For UV-Vis measurement on a Nanodrop, the equivalent setting is $\epsilon 1\% = 12.4$.

For measuring protein concentrations based on UV-Vis absorbance at 280 nm, the formula (A280 / Abs 0.1%) = protein concentration. For GAUT1:GAUT7 batch #6, (9.79 / 1.24 = 7.9 mg/mL). If using different enzymes, non-GFP tagged constructs, or complexes of different stoichiometry, different extinction coefficients will need to be calculated.

Results:

The summary of expression and activity measurements from 12 total independent co-expression cultures of GAUT1:GAUT7 are displayed in Fig. A.1.

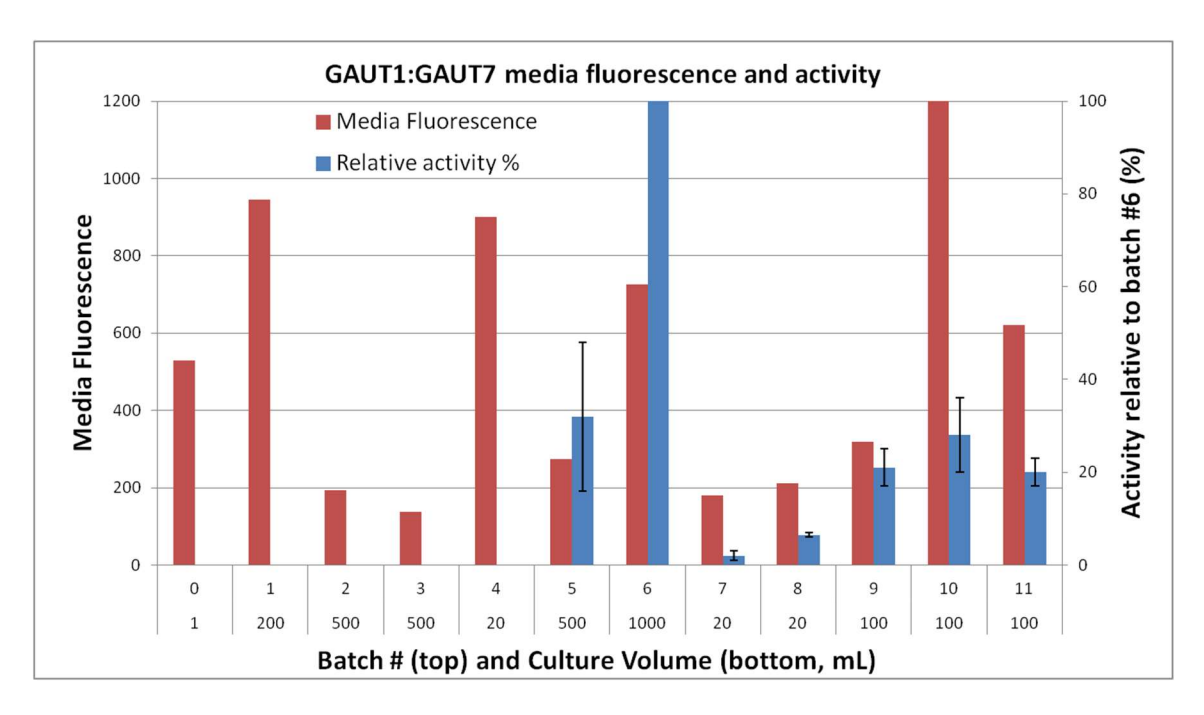


Figure A.1. Expression and activity comparison for 12 GAUT1:GAUT7 co-expression cultures. Media fluorescence (red bars) and relative activity percentage (blue bars) from twelve different GAUT1:GAUT7 cultures, numbered #0 - #11 are shown. Because the enzyme purified from Batch #6 was used in the assays published in Chapter 2 and was the highest activity culture, activity from that culture was normalized to 100%. On the x-axis, culture batches numbered 0-11 are labeled on the top row and culture volume in mL is listed on the bottom row. Activity relative to batch #6 was calculated as a range of values from "standard condition" assays where available. For assays deviating from standard conditions, relative activity accounts for dilution of radiolabeled UDP-GalA or increased assay time is detailed in Table 4.2. The culture labeled #0 was incubated in a microtiter plate rather than in cell culture flasks and was not purified. Relative specific activity assays were not conducted for cultures #0-4. The activity recovered from GAUT1:GAUT7 produced in those assays was measured only using non-linear, three hour reactions. Error bars represent high/low values for estimated relative activity from all conditions reported

Table A.1. Protein expression levels from 12 total co-expressions of GAUT1:GAUT7 in HEK293 cultures. Co-expression cultures of GAUT1:GAUT7 are organized by date. The first co-expression experiment, labeled batch #0, was performed in a 1 mL shaking culture plate and was not purified. All other stocks were cultured in flasks at larger volumes and purified by nickel-affinity. All enzyme amount measurements are based on UV-Vis A280 readings. The mg/mL purified column lists final concentration of enzyme stocks following concentration using an Amicon centrifugal concentration unit.

Batch	Date	Culture	Media	mg	mg/mL after	Notes
#		volume	Fluorescence	purified	concentration	
		(mL)				
0	8/22/2012	1	529	N/A	N/A	
1	11/7/2012	200	946	13.4	2.6	
2	2/5/2014	500	193	2.5	2	Low expression likely due to old plasmid.
3	4/9/2014	500	137	2	0.7	Low expression likely due to old plasmid.
4	5/29/2014	20	900	0.6	1.6	First use of UV-Vis for concentration measurements.
5	6/8/2014	500	275	4	2.6	1000 Fluorescence in 20 mL culture, unexplained drop-off in large cultures.
6	3/3/2016	1000	725	52	7.9	Main purification used in published experiments.
7	6/27/2016	20	180	0.1	0.6	Purified for DxD mutant experiments.
8	7/28/2016	20	212	0.1	0.5	Purified for DxD mutant experiments.
9	8/24/2016	100	319	1	0.4	Purified for GAUT1:GAUT7 vs. GAUT1 stability experiments. Low expression likely due to old plasmid.
10	9/15/2016	100	1200	3	1.5	Purified for GAUT1:GAUT7 vs. GAUT1 stability experiments. New plasmid.
11	3/27/2017	100	621	5.4	10.8	Purified for GAUT1 and double mutant experiments.

Table A.2. HG:GalAT activity measurements of GAUT1:GAUT7 purified from 12 different co-expression trials in HEK293 cells. All assays used 5 μM UDP-[14C]GalA. Donor concentrations are listed as a total including non-radiolabeled UDP-GalA. Deviations from Standard Conditions, including assay time and the concentrations of enzyme, donor, and acceptor in assays are listed under "Reaction Conditions." All conditions are equal to the standard condition if not listed. Where net cpm is reported as a single value, it represents the T0subtracted average of duplicate measurements from a single experiment. A range of values are reported from net cpm readings from independent experiments using the same enzyme stock. For clarity, net cpm values are rounded to the nearest ten. All activities are estimated relative to Batch #6, which was the highest amount of protein purified, the largest cell culture volume, the highest specific activity, and the main stock of enzyme used for biochemical characterization (Ch. 2, Fig. 2.2). Estimated activity was calculated from standard condition assays, reported reaction conditions from column #3, or Michaelis-Menten kinetics k_{cat} values where available. These estimates are reported to represent the variability in activity that has been measured across multiple GAUT1:GAUT7 cultures. Because different conditions were used, these values should be interpreted as estimates rather than precise calculations.

Batch #	Activity (net cpm)	Reaction conditions	Estimated activity relative to batch #6	Notes
0	2000	3 hours, 5 μM UDP-GalA, pH 7.8, 80 μg (100 μM) HG acceptor, 10 μL unpurified media	N/A	Activity in unpurified media
1	3300- 3700	3 hours, 5 μM UDP-GalA, pH 7.8, 80 μg (100 μM) HG acceptor, 20 ug enzyme	N/A	
2	1500	3 hours, 5 μM UDP-GalA, pH 7.8, 80 μg (100 μM) HG acceptor, 20 ug enzyme	N/A	
3	850	3 hours, 5 μM UDP-GalA, pH 7.8, 80 μg (100 μM) HG acceptor, 7 ug enzyme	N/A	
4	12000	3 hours, 5 μM UDP-GalA, 1 μg enzyme	N/A	
5	440-720 4280	100 μM HG acceptor, 1 μg enzyme 100 μM UDP-GalA, 1 μg enzyme	17-48%	First purification with kinetics experiments $k_{\text{cat}} = 0.25 \cdot 0.33 \text{ s}^{-1}$
6	2000- 3000 8800- 10000	Standard 100 µM UDP-GalA (1:20 UDP- [14C]GalA dilution)	100%	Activity replicated in at least 10 assays under standard conditions, displayed in Fig.2 of manuscript. $k_{\text{cat}} = 0.92 \cdot 1.99 \text{ s}^{-1}$
7	50-100 2000- 2500	Standard 60 minutes, 100 uM UDP-GalA	1-3%	Longer reaction times and lower hot:cold dilutions of UDP-[14C]GalA were used due to low cpm readings under standard conditions.
8	6300- 7750	60 minutes, 100 uM UDP-GalA	6-7%	Batch#7 adjusted conditions were replicated.
9	500 1900	Standard 100 µM UDP-GalA	17-25%	
10	600	Standard 100 µM UDP-GalA	20-37%	
11	1500 650-1000	100 μM UDP-GalA 200 μM UDP-GalA	17-24%	

Activity from batch #6 under standard conditions consistently ranged from 2000-3000 from at least 10 independent experiments during biochemical characterization, Michaelis-Menten kinetics, and as a positive control in subsequent assays. Activity measured with 100 nM enzyme, measured at 5 minutes with 10 μM HG acceptor and 1 mM UDP-GalA (1:200 dilution of UDP-[¹⁴C]GalA) yielding net cpm values ranging from 2000-3000 corresponds to 180-270 pmol GalA transferred/min.

Activity with a lower UDP-GalA dilution, 100 µM total (1:20 dilution) yielded net cpm values ranging from 8800-10000, corresponding to a total activity yield of 80-90 pmol GalA transferred/min.

As an example calculation to convert cpm to pmol transferred:

1000 cpm *
$$\left(\frac{\text{dpm}}{0.8 \text{ cpm}}\right)$$
 * $\left(\frac{1 \mu \text{Ci}}{2.22 * 10^6 \text{ dpm}}\right)$ * $\left(\frac{\mu \text{mol}}{249 \mu \text{Ci}}\right)$ * $\left(\frac{10^6 \text{ pmol}}{1 \mu \text{mol}}\right)$
= 2.26 pmol * dilution factor (200) = 452 pmol total

The conversion factor (0.8 cpm/dpm) is standard for ¹⁴C.

249 $\mu Ci/\mu mol$ is the specific activity of the UDP-[\$^{14}C\$]GalA used in these experiments, confirmed by the manufacturer.

Conclusion and future directions:

Batch #6 yielded the highest enzyme purified and specific activity measurements, which was a 1L culture with 725 media fluorescence. A total of 47.5 mg was purified by nickel-affinity. Because the *N*-terminal tags account for ~35% of the MW of the protein and high MW aggregates account for ~10% of the protein, a final yield of ~25 mg active GAUT1:GAUT7 complex may be expected for a culture of this size and expression level.

Although the available data do not allow us to conclude precise reasons for activity variation, low activity cultures appear to be correlated with smaller culture volumes and lower fluorescence yields. The lowest activities measured were associated with 20 mL cultures, which ranged from 1-7% activity relative to batch #6. Because we used 20 mL cultures when attempting to assay DxD mutants, the recovered enzyme was too low in both yield and activity to compare to the Batch #6 enzyme under standard conditions. These smaller culture sizes were used to simplify purification of WT and multiple mutant cultures incubated simultaneously.

For future GT expression projects, the WT enzyme should first be purified in multiple cell culture experiments performed on different days and assayed to establish a standard condition that can be reproduced across biological replicates. The relationship between culture size and activity may need to be tested to determine if high activity is able to be recovered from small-scale cultures. If not, independent large-scale cultures will need to be used for the testing of variables such as mutant constructs. For experiments where multiple variables are to be compared, such as multiple enzymes or mutants, it may not be realistic to purify large numbers of side-by-side cultures, so data may need to be obtained from WT and mutant cultures that were purified on different days.

For some comparative assays, such as low-activity enzymes including GAUT1 expressed alone, other GAUT enzymes, and low-activity mutants, a separate "low-activity standard condition" should be established. The high activity cultures of GAUT1:GAUT7 may yield activity values that are at least 10-fold higher than other GAUT enzymes that have been tested in this system and other plant cell wall glycosyltransferases that have been published. Standard assay conditions that use 5 minute reactions and 200-fold dilutions of UDP-[14C]GalA may result in false-negative data for other enzymes assayed under the same condition.

Recommended modifications to the standard assay condition are summarized in the table below.

Table A.3. Recommended modifications to standard assay conditions for comparison of specific activity of different GTs.

Modification	Precaution	Recommendation
Increase enzyme amount	Requires high enzyme stock	For low activity mutants, use
	concentration, may need large-	higher enzyme amounts. Two
	scale cultures.	plant cell wall GT publications
		comparing kinetics using variable
		enzyme amounts: (Chou et al.,
		2012; Urbanowicz et al., 2017).
Longer reaction time	Verification of linear range of	A linear range progress curve
	reaction requires many	should also be independently
	measurements.	established for all enzymes and
		mutants.
Lower dilution of radiolabeled	May not reach saturating	UDP-Glo (Promega) is a
UDP-GalA	conditions ($K_{\rm M}$ of	promising non-radiolabeled
	GAUT1:GAUT7 for UDP-GalA	quantitative system that would
	is ~150 mM.)	eliminate issues of radiolabel
		dilution.

APPENDIX B

ACTIVITY OF GAUT1: GAUT7 ACTIVE-SITE DXD MUTANTS

Purpose:

Because GAUT7 is insoluble when expressed in the absence of GAUT1, it cannot be assayed alone. To determine if GAUT7 has HG:GalAT activity or if GAUT1 or GAUT7 have additional GT domains outside of the predicted GT8 domains, the GAUT1:GAUT7 complex were expressed with mutations in each Asp-X-Asp (DXD) motif.

Background:

Despite the diversity in glycosyltransferase sequences, activities, and mechanisms, many GTs share similar structural features. For nucleotide sugar-dependent GTs, there are two major structural folds (Lairson et al., 2008). GAUT1 and GAUT7 are GT-A fold glycosyltransferases, most of which contain a conserved active site domain with the residues Asp-X-Asp, where X represents any amino acid, also called the DXD motif. The DXD motif has a functional role in coordinating a divalent cation (e.g. Mn²⁺) which stabilizes departure of the nucleotide leaving group during the GT reaction (Lairson et al., 2008). Mutation of this motif leads to abolished or significantly reduced activity, as has been shown for the GT8 enzyme LgtC (Persson et al., 2001).

As a heterocomplex, GAUT1:GAUT7 has a total of 6 DXD motifs. The location of putative DXD motifs are displayed in Fig. B.1 and Table B.1.

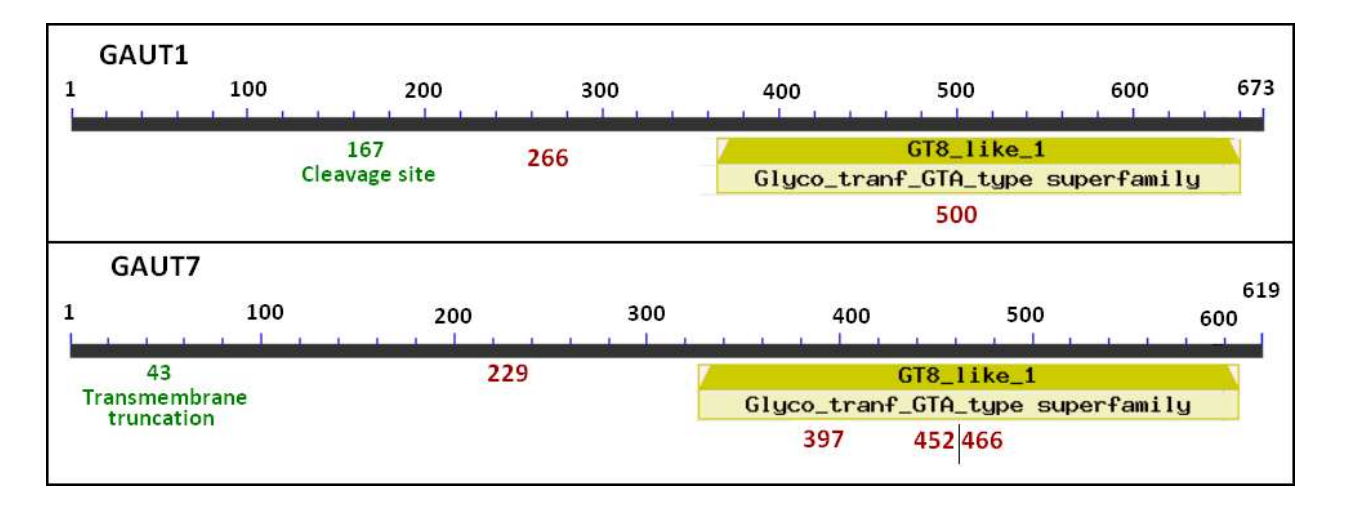


Figure B.1. Location of putative DXD motifs in GAUT1 and GAUT7 full-length sequences.

The full sequences of GAUT1 (673 residues) and GAUT7 (619 residues) are shown with the location of the predicted GT8 domains (pfam database). The locations of each putative DXD motif are shown in red and the GAUT1 Δ 167 cleavage site and the GAUT7 Δ 43 transmembrane truncation site are shown in green.

Table B.1. Putative DXD motif locations in GAUT1 and GAUT7. Amino acid residues mutated in this study are listed based on the full amino acid sequences of GAUT1 and GAUT7. Both enzymes were expressed as truncated constructs, GAUT1 Δ 167 and GAUT7 Δ 43. After subtraction of the truncated *N*-terminal domains, the truncated amino acid and nucleotide numbers are identified. The original and mutant nucleotide sequences are identified.

Mutant	Motif	Full	Truncated	Truncated	Original	Mutant
name		length	amino	Nucleotide #	Sequence	Sequence
		amino	acid#			
		acid#				
				GAUT1		
1-266	DAD	264/266	97/99	289-297	GATGCTGAT	AATGCTAAT
1-500	DDD	498/500	331/333	991-999	GACGATGAC	AACGATAAC
GAUT7						
7-229	DAD	227/229	184/186	550-558	GATGCTGAC	AATGCTAAC
7-397	DSD	395/397	352/354	1054-1062	GATTCTGAT	AATTCTAAT
7-452	DDD	450/452	407/409	1219-1227	GATGATGAC	AATGATAAC
7-466	DLD	464/466	421/423	1261-1269	GACCTTGAT	AACCTTAAT

Because GAUT1 is the putative catalytic GT, the most relevant DXD motif lies within the GT8 domain of GAUT1, here named mutant 1-500. GAUT7 has three putative DXD motifs within the GT8 domain. GAUT1 and GAUT7 both have a single DXD motif outside of the GT8 domain. In individual co-expression constructs, all six motifs were tested for activity compared to WT GAUT1:GAUT7.

Due to inability to express and assay GAUT7 as a single protein, this method of DXD motif mutation is the simplest method to attempt to determine the contribution of GAUT7 to activity or to investigate the possibility that GAUT1:GAUT7 has active domains outside of the predicted GT8 domain. In this experiment, all seven constructs (WT complex plus six mutants) were purified side-by-side from small scale (20 mL) cultures. As summarized in the previous section, the WT enzyme and all mutants yielded low enzyme amounts and low activities relative

to the standard GAUT1:GAUT7 assay from batch #6 protein. Some of the mutations also caused high amounts of protein aggregation compared to WT enzyme. The results summarized in this section suggest the relevance of the 1-500 mutant and some of the other putative mutants, but these experiments will need to be repeated with larger-scale cultures and with further purification steps taken to remove aggregate protein.

Methods:

DXD motifs were identified by searching the protein sequences of GAUT1 and GAUT7 for three-residue sequences containing two Asp residues separated by a single amino acid. Site-directed mutagenesis was performed by designing primers to insert mutations into both Asp residues of the DXD motif, creating Asp->Asn mutants. Each Asp residue was mutated individually, using two rounds of PCR followed by cloning and re-introduction of the mutated plasmid into *E. coli* cells (strain JM109) to create the final constructs containing mutations in both Asp residues. All primer sequences used are listed in Table 3.5.

Table B.2. Primer sequences used to create DXD mutations Each mutant contained two Asp->Asn mutations that were introduced by separate primers. The adjacent nucleotide sequence contained 25-30 nucleotides total to overlap with the WT plasmid by at least 10 nucleotides on each side of the introduced mutation. In each original sequence, the G nucleotide to be mutated is highlighted in green for the first Asp residue of the DXD pair and in purple for the second Asp residue. In the forward and reverse primer sequences, the A/T nucleotides corresponding to the mutant Asn residue are also highlighted.

Mutant name	Mutation location	Adjacent nucleotide #	Identifier	Nucleotide sequence
1-266	D264	276-303	Original Sequence	GGGAAGCAACATCT <mark>G</mark> ATGCTGATCTTCCTC
			Forward Primer	GGGAAGCAACATCT <mark>A</mark> ATGCTGATCTTCCTC
			Reverse Primer	GAGGAAGATCAGCAT <mark>T</mark> AGATGTTGCTTCCC
	D266	280-309	Original Sequence	GCAACATCT <mark>A</mark> ATGCT <mark>G</mark> ATCTTCCTCGGAGT
			Forward Primer	GCAACATCT <mark>A</mark> ATGCT <mark>A</mark> ATCTTCCTCGGAGT
			Reverse Primer	ACTCCGAGGAAGAT <mark>T</mark> AGCAT <mark>T</mark> AGATGTTGC
1-500	D498	977-1006	Original Sequence	AAATCCTCTTCCTG <mark>G</mark> ACGATGACATCATTG
			Forward Primer	AAATCCTCTTCCTG <mark>A</mark> ACGATGACATCATTG
			Reverse Primer	CAATGATGTCATCGTTCAGGAAGAGGATTT
	D500	982-1011	Original Sequence	CTCTTCCTG <mark>A</mark> ACGAT <mark>G</mark> ACATCATTGTTCAG
			Forward Primer	CTCTTCCTG <mark>A</mark> ACGAT <mark>A</mark> ACATCATTGTTCAG
			Reverse Primer	CTGAACAATGATGT <mark>T</mark> ATCGT <mark>T</mark> CAGGAAGAG
7-229	D227	536-565	Original Sequence	GTGAAAGTTCTCAA <mark>G</mark> ATGCTGACCTTCCAC
			Forward Primer	GTGAAAGTTCTCAA <mark>A</mark> ATGCTGACCTTCCAC
			Reverse Primer	GTGGAAGGTCAGCATTTTGAGAACTTTCAC
	D229	541-570	Original Sequence	AGTTCTCAA <mark>A</mark> ATGCT <mark>G</mark> ACCTTCCACCACAG
			Forward Primer	AGTTCTCAA <mark>A</mark> ATGCT <mark>A</mark> ACCTTCCACCACAG
			Reverse Primer	CTGTGGTGGAAGGT <mark>T</mark> AGCAT T TTGAGAACT

Mutant name	Mutation location	Adjacent nucleotide #	Identifier	Nucleotide sequence
7-397	7-395	1040-1069	Original Sequence	AACTCGAGCTGGAC <mark>G</mark> ATTCTGATATGAAAC
			Forward Primer	AACTCGAGCTGGAC <mark>A</mark> ATTCTGATATGAAAC
			Reverse	GTTTCATATCAGAAT <mark>T</mark> GTCCAGCTCGAGTT
			Primer	_
	7-397	1045-1074	Original Sequence	GAGCTGGAC <mark>A</mark> ATTCT <mark>G</mark> ATATGAAACTGTCT
			Forward Primer	GAGCTGGAC <mark>A</mark> ATTCT <mark>A</mark> ATATGAAACTGTCT
			Reverse Primer	AGACAGTTTCATAT <mark>T</mark> AGAAT <mark>T</mark> GTCCAGCTC
7-452	7-450	1205-1234	Original	AGGTTGTGATTCTG <mark>G</mark> ATGATGACGTTGTAG
7 132	7 150	1203 123 1	Sequence	need to to the test to the est to the
			Forward	AGGTTGTGATTCTG <mark>A</mark> ATGATGACGTTGTAG
			Primer	_
			Reverse	CTACAACGTCATCAT <mark>T</mark> CAGAATCACAACCT
			Primer	
	7-452	1210-1239	Original	GTGATTCTG <mark>A</mark> ATGAT <mark>G</mark> ACGTTGTAGTCCAG
			Sequence	
			Forward Primer	GTGATTCTG <mark>A</mark> ATGAT <mark>A</mark> ACGTTGTAGTCCAG
			Reverse Primer	CTGGACTACAACGT <mark>T</mark> ATCAT <mark>T</mark> CAGAATCAC
7-466	7-464	1250-1279	Original Sequence	CTCCCCTTTGG <mark>G</mark> ACCTTGATATGGAAGGGA
			Forward Primer	CTCCCCTTTGG <mark>A</mark> ACCTTGATATGGAAGGGA
			Reverse	TCCCTTCCATATCAAGGTTCCAAAGGGGAG
			Primer	Tees Tee Time Internet Tee In Model No
	7-466	1250-1279	Original	CTCCCCTTTGG <mark>A</mark> ACCTT <mark>G</mark> ATATGGAAGGGA
			Sequence	
			Forward	CTCCCCTTTGG <mark>A</mark> ACCTT <mark>A</mark> ATATGGAAGGGA
			Primer	
			Reverse	TCCCTTCCATAT <mark>T</mark> AAGGT <mark>T</mark> CCAAAGGGGAG
			Primer	

Entry vectors (pDONR221) containing WT *GAUT1* and *GAUT7* genes were isolated from *E. coli* cells. Template plasmids were mixed with the Forward/Reverse primer pair and were elongated using Invitrogen Phusion HF Polymerase for 20 cycles of 98°C for 30 seconds followed by 72°C for 5 minutes. The template DNA, containing methylation due to expression in the *E. coli* cloning strain, was digested with the restriction enzyme Dpn1. Newly synthesized PCR product vectors did not contain methylation and were not sensitive to digestion by Dpn1. Following degradation of template DNA, the polymerized PCR products were re-introduced into competent *E. coli* cells, colonies were isolated, and the plasmid was isolated by alkaline lysis (Qiagen miniprep kit).

The PCR process was repeated using the second pair of Forward/Reverse primers to introduce the second Asp->Asn mutation. The final pDONR221 plasmids containing mutants were verified by sequencing and comparison to the WT gene sequence. Mutant gene sequences were transformed into pGEn2 destination vectors for expression using LR Clonase (Invitrogen).

Each mutant GAUT1:GAUT7 complex was expressed by co-transfection of the indicated mutant with the WT partner enzyme. As an example, the mutant 1-500 contained the GAUT1-500 mutant co-expressed with WT GAUT7. Each construct was purified from 20 mL cultures as previously described for the WT complex.

Purified enzyme concentrations were determined by UV-Vis (Nanodrop) and by GFP fluorescence in a microtiter plate. To determine enzyme concentration by fluorescence, a standard curve was generated by serial dilution of the 7.9 mg/mL Batch #6 WT enzyme.

Results:

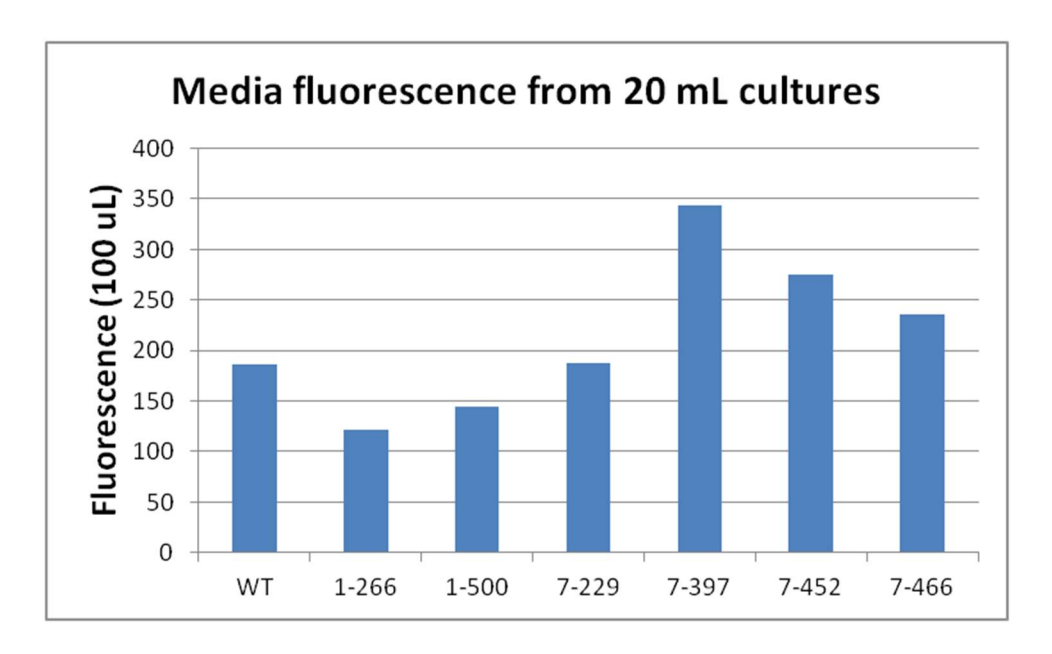


Figure B.2. Fluorescence in culture medium of each mutant expressed in 20 mL cell cultures. Fluorescence was measured from 100 μ L of medium following centrifugation as described in the previous section.

Table B.3. Concentrations of purified constructs measured by UV-Vis and fluorescence.

Concentration was measured by UV-Vis (nanodrop) and by GFP fluorescence in a plate reader. Duplicate fluorescence measurements of 5 μ L of each mutant construct were diluted in 95 μ L of 50 mM HEPES, pH 7.2 buffer. Average fluorescence values were compared to a standard curve of dilutions made from the previously-purified batch #6 enzyme and converted to mg/mL. The comparison column is a ratio of the mg/mL value measured by fluorescence relative to the UV-Vis measurement.

	UV-Vis mg/mL	Fluorescence mg/mL	Comparison (Fluorescence UV
WT	0.58	0.47	0.81
1-266	0.38	0.23	0.61
1-500	0.07	0.11	1.6
7-229	0.64	0.22	0.34
7-397	1.16	0.46	0.40
7-452	1.04	0.29	0.28
7-466	0.22	0.24	1.1

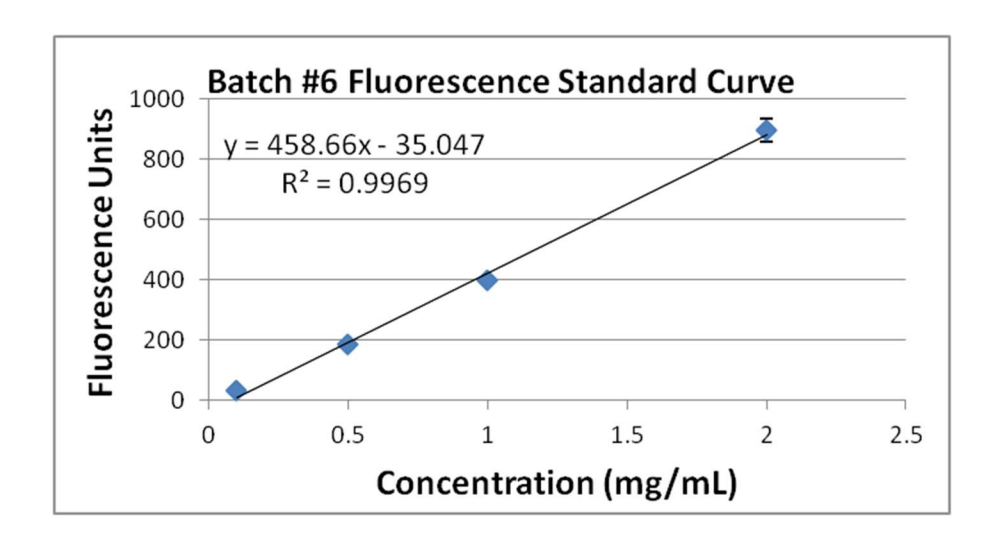


Figure B.3. Standard curve for WT used to determine fluorescence mg/mL. WT Batch #6 enzyme was measured at 7.9 mg/mL by UV-Vis spectroscopy. This enzyme stock was used as a standard and diluted to the indicated concentrations. Duplicate samples were prepared by mixing 12.5 μL of each diluted enzyme stock in 237.5 μL HEPES buffer, vortexing to mix, and pipetting 100 μL into separate wells in a microtiter plate. Error bars represent standard deviation from duplicate measurements. The concentration of each WT and mutant sample was determined by comparison to the standard curve.

When each mutant construct concentration was measured by two different methods, much lower values were obtained by fluorescence for some constructs (1-226, 7-229, 7-397, and 7-452). Quality of protein purification and equal loading measurements were verified by SDS-PAGE.

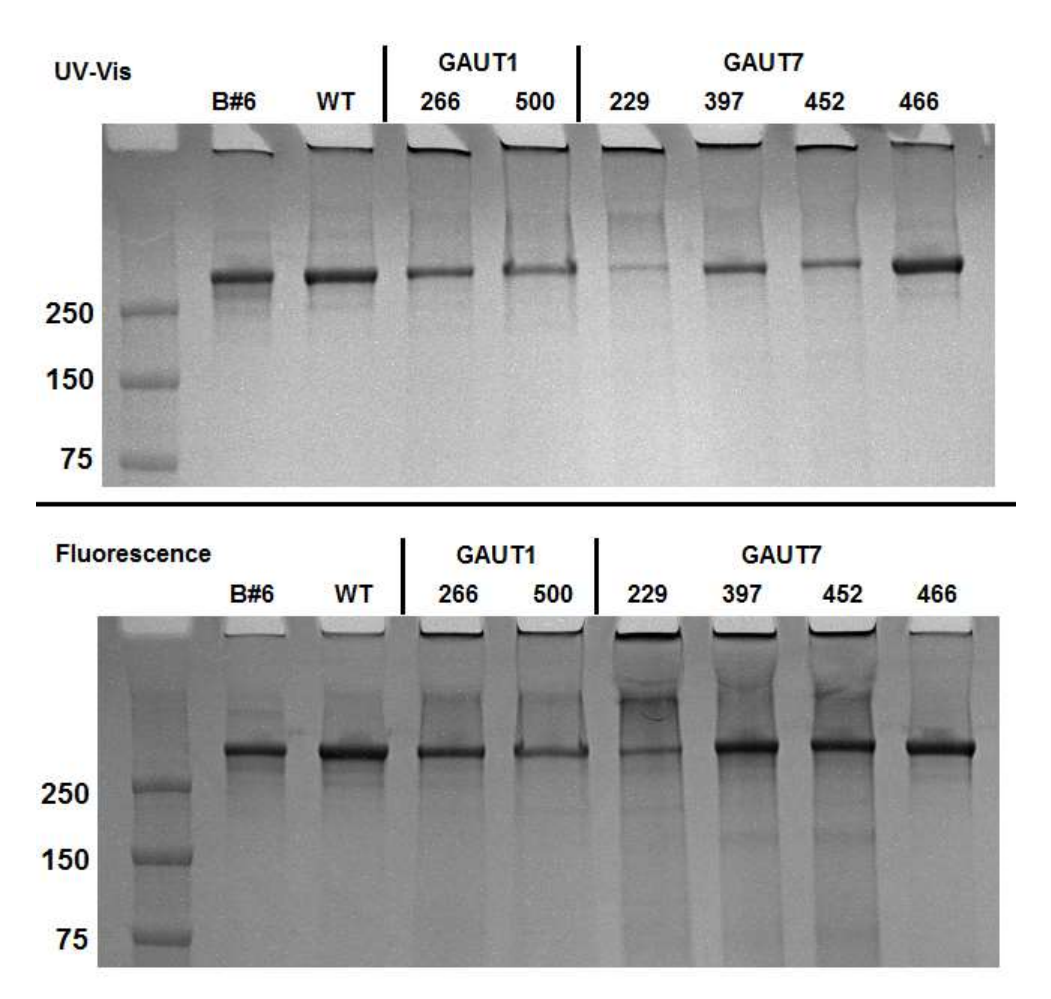


Figure B.4. SDS-PAGE of equal loading of enzymes based on UV-Vis and fluorescence measurements. Previously-purified Batch #6 standard GAUT1:GAUT7 enzyme (labeled B#6), WT, and the six mutant complexes were loaded. All lanes contained 4 μg total protein as determined by UV-Vis (top panel) and GFP fluorescence (bottom panel) and were resolved by non-reducing SDS-PAGE on a 12% acrylamide gel.

The difference in UV-Vis versus fluorescence measurements appears to be due to high concentrations of aggregates, particularly in the constructs 1-226, 7-229, 7-397, and 7-452. Improperly folded aggregates containing inactive protein contribute to UV-Vis signal but are less likely to contribute to GFP fluorescence signal. Therefore, protein concentration measured by fluorescence appeared to be more accurate and was used for calculating equal protein loading in activity assays.

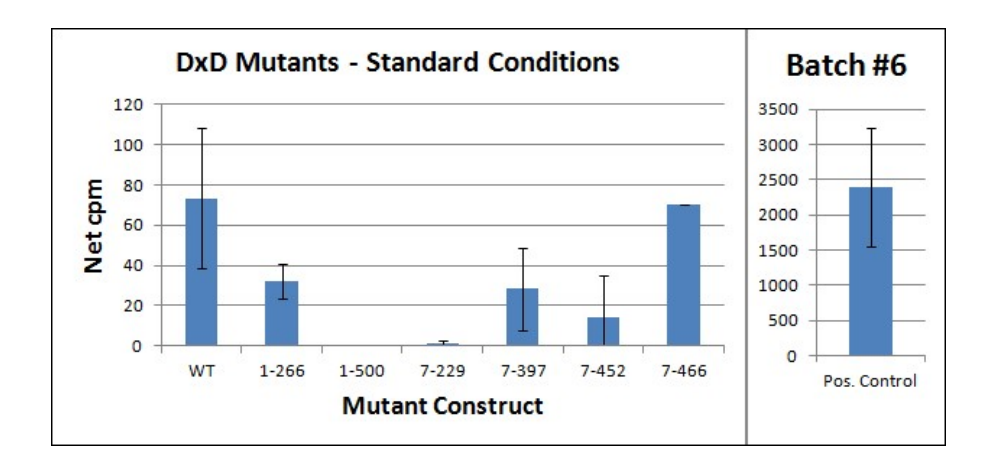


Figure B.5. Initial assay of purified DXD mutant enzymes under standard conditions. WT and mutant constructs were assayed under standard conditions (100 nM enzyme, 5-minute assay, 1 mM total UDP-GalA). Error bars represent standard deviation from duplicate measurements. All constructs, including WT, had very low activity (<3% relative to Batch #6 control).

Due to the low activity measurements under standard conditions, the linearity of the WT enzyme was measured from 0-90 minutes using a lower dilution of UDP-GalA (5 μ M UDP[14 C]GalA, 100 μ M total UDP-GalA, 1:20 hot:cold ratio).

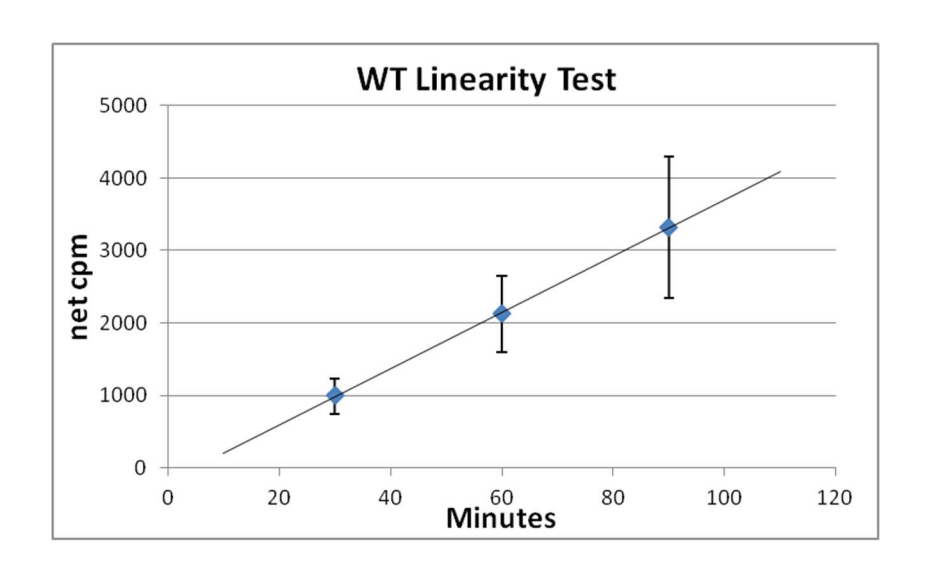


Figure B.6. Linearity assay for low activity WT conditions (Culture #1). GAUT1:GAUT7 WT enzyme was measured at 30, 60, and 90 minutes with 100 μ M total UDP-GalA. Error bars represent standard deviation from duplicate measurements.

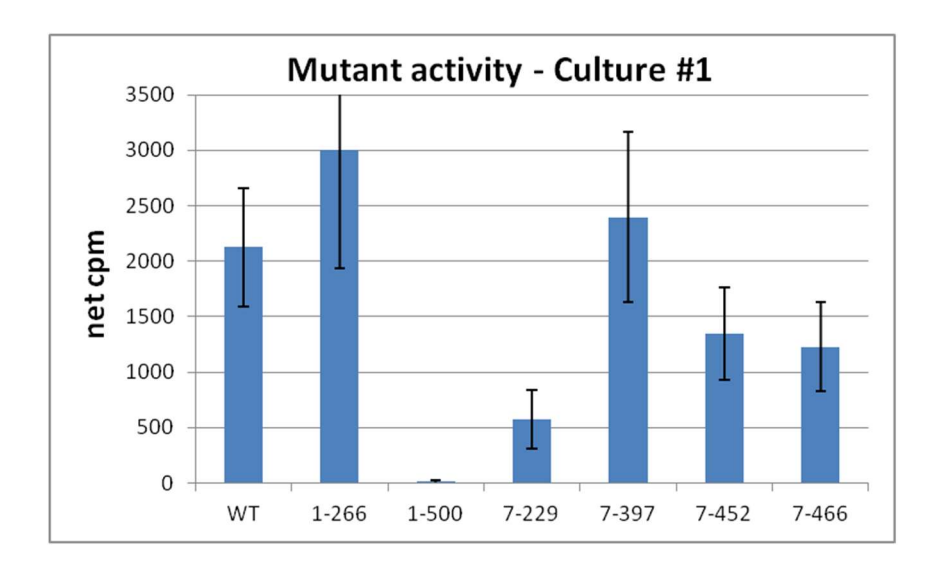


Figure B.7. Assay of WT and DXD mutant enzymes under low activity conditions (Culture #1). All samples were measured at 60 minutes with 100 μ M total UDP-GalA. Error bars represent standard deviation from duplicate measurements.

WT and mutant constructs were purified from replicate 20 mL cultures. Protein concentration was determined by fluorescence compared using batch #6 assay enzyme as a standard. The linearity test and specific activity assays were repeated under low activity conditions described in Fig. B.6 and B.7.

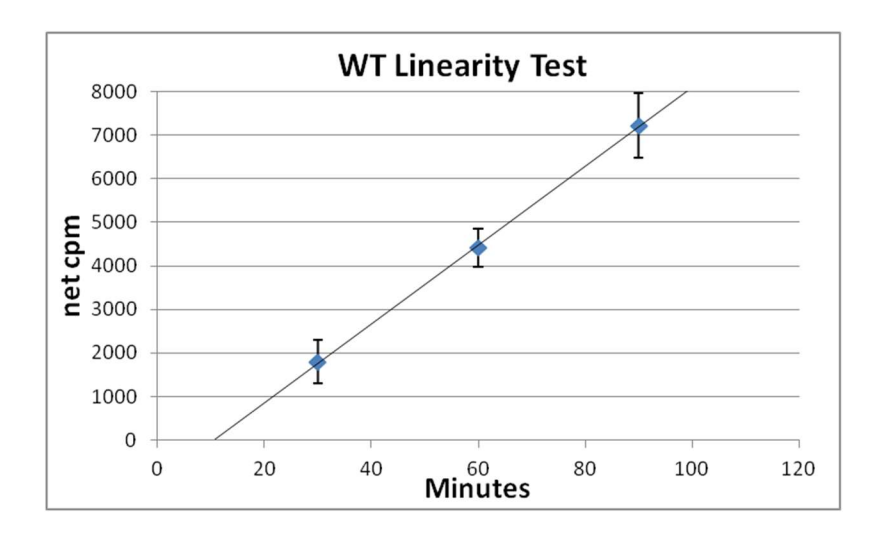


Figure B.8. Linearity assay for WT construct and mutant activity assay (Culture #2). WT GAUT1:GAUT7 enzyme was measured at 30, 60, and 90 minutes with 100 μM total UDP-GalA. Error bars represent standard deviation from duplicate measurements.

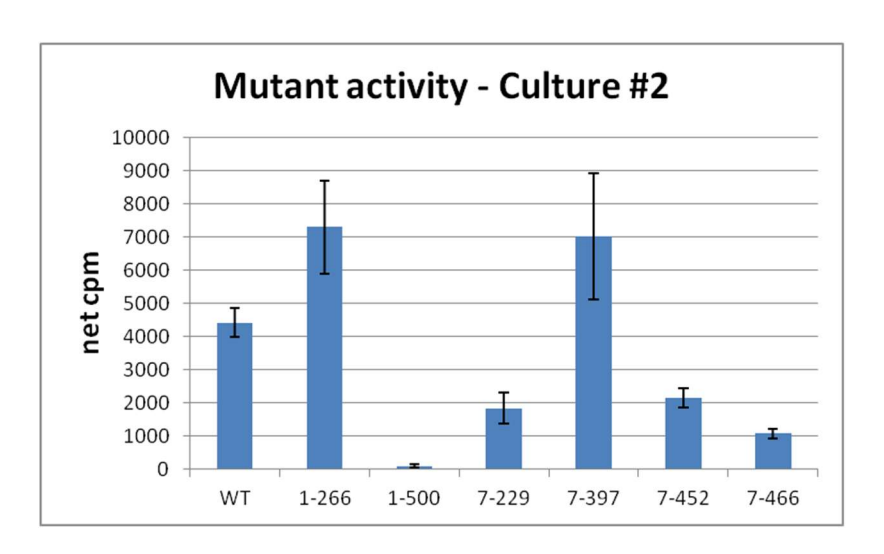


Figure B.9. Assay of WT and DXD mutant enzymes under low activity conditions (Culture #2). All samples were measured at 60 minutes with 100 μM total UDP-GalA. Error bars represent standard deviation from duplicate measurements.

There was an ~2-fold difference in specific activity of the WT samples between the two independent cultures, but the activity trends relative to WT for all mutants were consistent in both cultures. The activity of each mutant relative to WT was calculated for the two cultures and relative measurements were averaged.

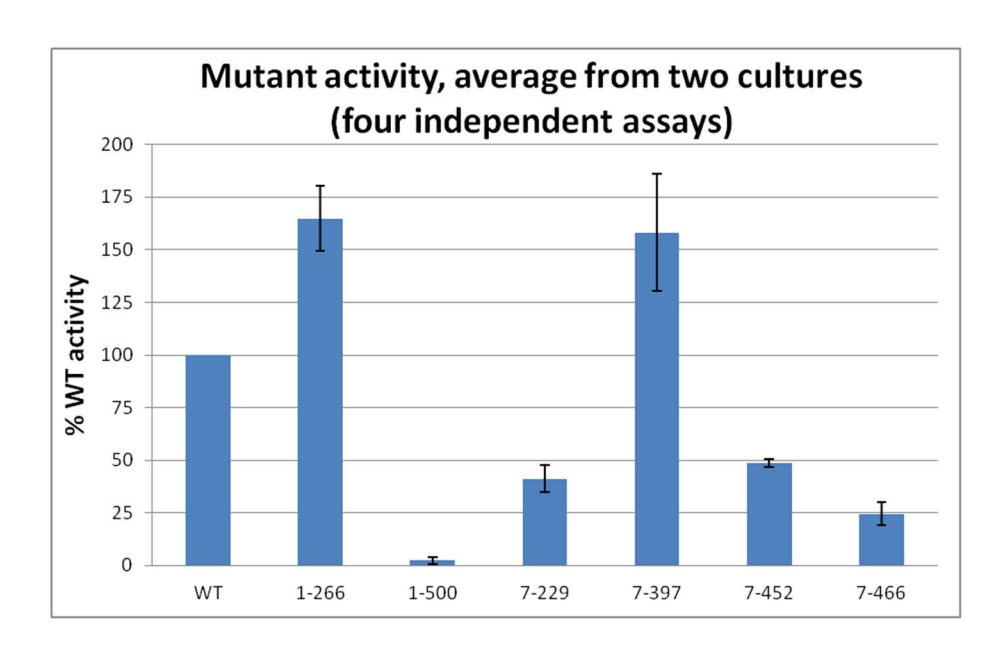


Figure B.10. Summary of mutant activities relative to WT. Setting WT activity to 100%, the activity of each mutant construct from two independent cultures, assayed twice (four independent activity measurements), was displayed relative to WT activity.

As expected, mutating the predicted GT DXD active site motif in GAUT1 mutant 1-500 nearly abolished activity (<2% compared to WT). Several other mutants had reduced activity relative to WT, such as GAUT7 7-229 mutant. However, as discussed above, the reduced activity of mutant 7-229 is likely due to an increase in protein aggregation induced by the mutation. Thus, those results were not conclusive, and the role of the DXD motifs in GAUT7 in binding UDP-GalA or affecting HG:GalAT activity require futher investigation.

GAUT7 has two DxD motifs in the GT8 domain within 14 residues of each other, 7-452 and 7-466. The 7-452 mutant is aligned with the catalytic DXD motif from GAUT1 and the bacterial GT8 enzyme LgtC. From the above single-mutant assays, both mutants appeared to have reduced in activity, ranging from 25-50% of WT activity. This result suggested that these DXD motifs in GAUT7 may represent active sites and be involved in binding UDP-GalA, and

thus, that GAUT7 may have HG:GalAT activity. To test this, we reasoned that he reduction in HG:GalAT activity contributed by both sites may be additive if both of these sites were mutated. Thus, a GAUT7 double mutant with both 7-452 and 7-466 sites mutated was created. The GAUT7-452 pDONR221 plasmid was used as a template with the two PCR primer pairs for the 7-466 mutant. A double mutant plasmid (containing four total Asp->Asn mutations) was synthesized using the methods described above and the sequence containing all mutations was verified.

As described in the following section (3-C), the GAUT7 double mutant had an increased amount of high MW aggregates relative to the WT enzyme. The active complexes for WT constructs and GAUT7-452/466 double mutant (also named double mutant or dmut in results figures) were purified by size exclusion chromatography to ensure equal protein loading. Verification of equal protein loading after SEC is shown in Appendix C, Fig. C.4.

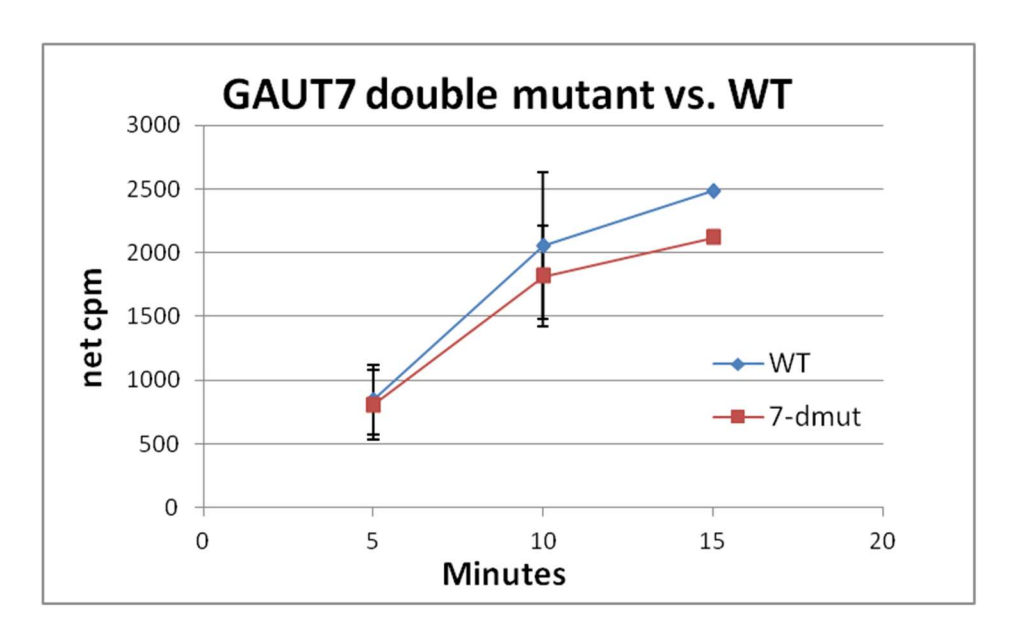


Figure B.11. Activity of GAUT7 double mutant compared to WT. WT and GAUT7-double mutant (7-dmut) constructs were purified from 100 mL cultures (batch #11). Enzyme (100 nM) was assayed using 200 μM total UDP-GalA (1:40 hot:cold dilution). Error bars represent the standard deviation of duplicate assays. The point at 15 minutes represents results from a single assay.

The WT enzyme (Batch #11), purified from 100 mL cultures, yielded 4.6-9.6-fold greater activity than the activity in enzyme stocks purified from two respective 20 mL cultures (batch #7-8). Therefore, the HG:GalAT activity for Batch #11 could be measured at 5 minutes, which was expected from the original assays of the Batch #6 protein (Ch. 2, Fig. 2.2). Under these conditions, the GAUT7 double mutant has 95% of the WT HG:GalA activity.

Because in this experiment the concentration of these proteins was more accurately quantified due to the removal of protein aggregates by size exclusion, these results suggest that the DxD motifs in GAUT7 are unlikely to represent motifs with an HG:GalAT active site. Based on the combined results, we conclude that any effects on HG:GalAT activity or product size

contributed by the presence of GAUT7 in the GAUT1:GAUT7 complex may be due to structural domains outside of the typical enzyme active sites predicted by GT motif analysis.

Using nickel-affinity purified protein (high MW aggregates were not removed by size exclusion chromatography), four additional replicate assays suggest that GAUT1:GAUT7 WT and double mutant activity are identical if the difference in the amount of active protein due to increased aggregation in the double mutant is accounted for (data not shown).

Conclusions and future directions:

The GAUT1-500 mutant retained less than 2% WT HG:GalAT activity. The Asp-Asp-Asp (DDD) motif, residues 489-500 of GAUT1, is most likely the Mn²⁺ / UDP-GalA binding domain predicted from sequence alignment analysis.

Two of the mutations, 1-226 and 7-397, yielded activity values greater than the WT enzyme. These results are unexpected if the mutation of interest does not affect substrate binding. However, similar results have been observed during the mutation of non-active site Asp residues in other GT8-family enzymes measured at a single time point (Yu et al., 2015).

Introduction of active site mutants causes different amounts of protein aggregation. Enzyme concentration using UV-Vis and fluorescence methods is not sufficient to demonstrate equal loading of different nickel-affinity purified enzyme constructs. In future mutant analyses, all proteins will need to be purified by size exclusion chromatography to remove high MW aggregates.

Although four activity assays from two independent small-scale cultures showed lower activity in two GAUT7 GT8-domain mutants, assays of a double mutant showed activity

approximately equal to WT. The current results do not suggest that GAUT7 is an HG:GalAT that incorporates UDP-GalA in the predicted active site.

GAUT1 has lower activity (Appendix E, E.2 and E.3) and synthesizes shorter-chain HG products (Ch. 2, Fig. 2.14C) compared to GAUT1:GAUT7. Based on mutant analyses, the contribution of GAUT7 to activity is most likely to be due to a structural domain formed by the disulfide-linked heterocomplex than to HG:GalAT activity by GAUT7.

Rather than single-point time point mutant analyses, individual progress curves will need to be measured for all mutants. All of the single mutants were assayed at 60 minutes based on a WT progress curve, but the lower relative activity may be due to changes in the linear range of the progress curve in these low-activity cultures. Cultures large enough to yield >1 mg protein and assays with non-aggregate concentrations >1 mg/mL should be used, and reproducibility of the WT enzyme activity should be established from multiple biological replicates.

APPENDIX C

PURIFICATION OF ACTIVE ENZYMES BY SIZE EXCLUSION CHROMATOGRAPHY TO REMOVE PROTEIN AGGREGATES

Purpose:

Following expression and secretion of GAUT1 or GAUT1:GAUT7, the active enzymes co-purify with inactive protein aggregates and truncation products. To perform quantitative enzyme assays, for example, to compare GAUT1 activity to GAUT1:GAUT7 or to compare GAUT1:GAUT7 WT to mutants, these aggregates need to be removed to ensure equal loading of enzymatically active protein prior to measurement of enzyme activity.

Background:

The presence of high amounts of aggregates and truncation products were observed upon the expression of GAUT1 in the absence of GAUT7 (Ch. 2, Fig. 1B). Different amounts of aggregates were also detected resulting upon generation of mutations via introduced DXD motifs in the GAUT1:GAUT7 subunits (Fig. B.4). These aggregates affect protein concentration measurements using UV-Vis or fluorescence and lead to an overestimation of active protein amounts in the GAUT stock cultures.

Methods:

GAUT1, GAUT1:GAUT7, and the GAUT1:GAUT7-double mutant were expressed in 100 mL HEK293 cell cultures as previously described (Batch #11). Following nickel-affinity purification of enzymes, 100 μg aliquots of the three enzymes were analyzed by size exclusion chromatography using a Superose 12 column attached to an ÄKTA FPLC with UV-Vis A280 detection. Separation was performed using a 0.5 mL/min flow rate in 50 mM sodium phosphate buffer containing 150 mM NaCl. Three peaks were detected, an early peak labeled high MW aggregates, a main peak containing the enzymatically active disulfide-linked protein complex, and a late peak containing truncation products.

To verify that the HG:GalAT activity was associated with the main peak, GAUT1:GAUT7 from the standard stock (Batch #6) was separated by size exclusion chromatography. Aggregate and main peaks were eluted, desalted using a PD-10 column (GE Healthcare) into a 50 mM HEPES, pH 7.2 storage buffer, and protein was concentrated. Protein concentrations were determined by UV-Vis. HG:GalAT activity was assayed using 1 μg protein (Batch #6 standard, main peak, and aggregate), 100 μM UDP-GalA (1:20 hot:cold dilution), and 10 μM HG acceptor mix for 5 minutes.

GAUT1:GAUT7 WT, double mutant, and GAUT1 proteins were separated by the same procedure, but only the main peak was collected. Equal amounts of protein were determined by fluorescence. To visualize the proteins purified by these methods, the proteins were incubated for 10 minutes in SDS-PAGE loading buffer at 30°C (non-denaturing conditions), separated by SDS-PAGE, and the separated proteins in the resulting SDS-PAGE gel visualized using Biorad Gel Doc Image Lab software with fluorescence detection and an Alexa 488 filter to detect GFP signal.

Results:

Representative SEC profiles from nickel-affinity purified protein are shown in Figure C.1.

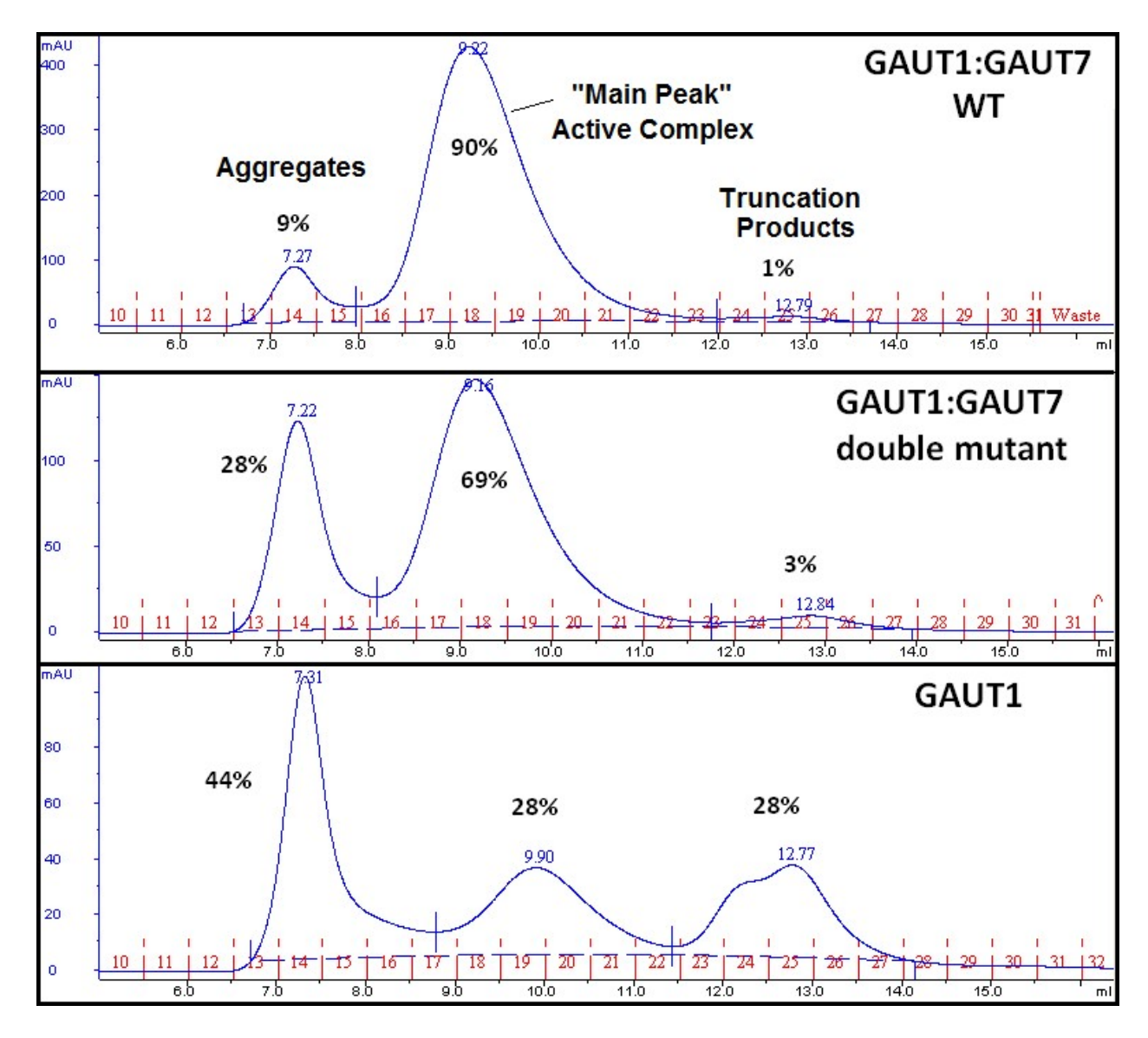


Figure C.1. Size exclusion chromatography of GAUT1 and GAUT1:GAUT7 protein constructs. Nickel-affinity purified GAUT protein was separated by Superose 12 size exclusion column chromatography. The protein resolved as three individual peaks corresponding to high molecular weight aggregates, the main protein complex peak, and low MW truncation products.

The percentage of total mass was calculated from integrated peak area. The GAUT1:GAUT7 double mutant has a 3.1-fold increase in the amount of high MW aggregates relative to the WT construct.

Similar size exclusion chromatography experiments with GAUT1:GAUT7 WT purified from at least 4 independent cultures showed that the percentage of aggregates was consistent across independent HEK293 cell cultures, ranging from 9-14% of total UV signal (data not shown).

Unless main peaks are purified following nickel-affinity purification, an assay containing 100 nM protein as measured by UV-Vis, will contain only approximately 90 nM of enzymatically active GAUT1:GAUT7 WT, 69 nM native GAUT1:GAUT7 double mutant or 28 nM native GAUT1. Thus, experiments done to compare the activity of these proteins, but which do not use proteins purified by SEC, will not contain equal amounts of enzymatically active protein.

To verify that the main peak corresponds to the majority of the HG:GalAT activity, GAUT1:GAUT7 from Batch #6 was further purified by SEC, as shown above. Both the "Main Peak" and aggregate fractions were collected. Activity was assayed using 1 µg of total protein from the nickel-affinity control protein (labeled Ni-1 purified control), as well as from the main peak and aggregate peak purified by SEC.

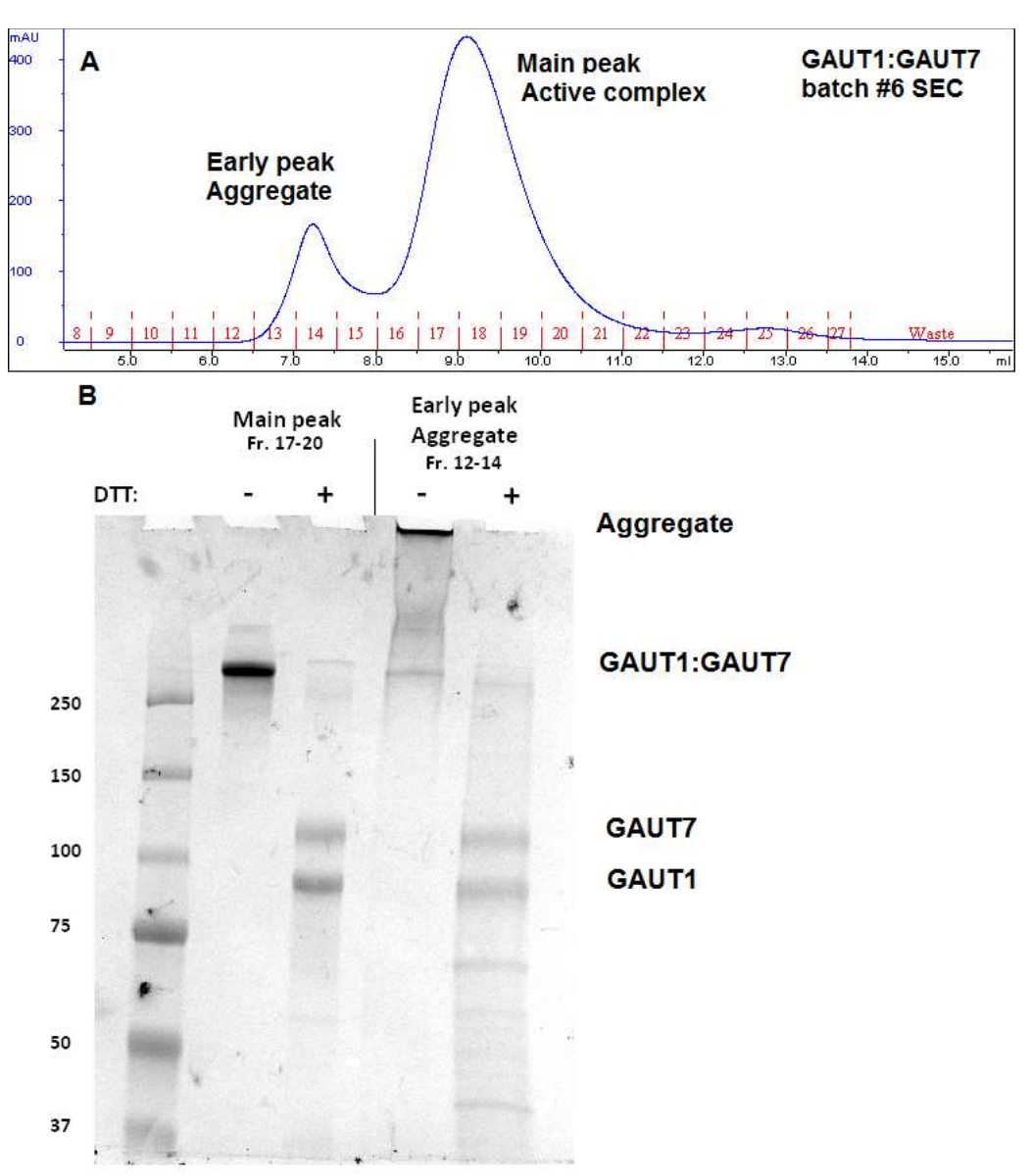


Figure C.2. Purification of GAUT1:GAUT7 main and aggregate peaks. A, Size exclusion chromatography of GAUT1:GAUT7 from Batch #6. The aggregate (Fractions 12-14) and main peaks (Fractions 17-20) were collected separately and desalted into HEPES storage buffer. B, SDS-PAGE under reducing (+DTT) and non-reducing (-DTT) conditions. High molecular weight aggregate staining is eliminated from the main peak fraction. GAUT1 and GAUT7 monomers electrophorese at the predicted MW while additional bands representing the aggregate fraction electrophoresis at smaller molecular weights under reducing conditions, suggesting that

the aggregate does contain full-length protein, but potentially misfolded GAUT1 and GAUT7 protein.

For activity assays, equal protein loading was established on the basis of equal UV-Vis A280 signal.

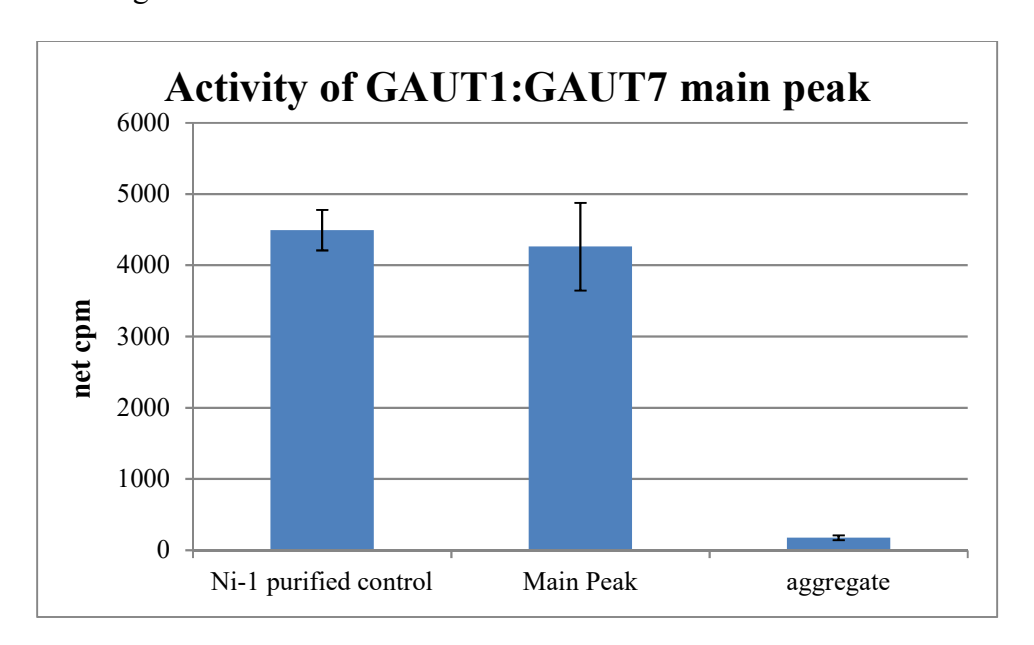


Figure C.3. HG:GalAT activity assay of main and aggregate GAUT1:GAUT7 protein peaks following SEC. From 1 μg total protein, the main peak has 94.9% activity relative to the Ni-affinity purified control and the aggregate peak has 3.9% of the activity. Error bars represent standard deviation from three independent experiments.

Because the main peak represents the active HG:GalAT complex, equal loading of the active protein was verified by SDS-PAGE of SEC-purified GAUT1:GAUT7, double mutant, and GAUT1 proteins (Fig. C.4) on the basis of equal GFP fluorescence. SDS-PAGE was performed under non-reducing, non-denaturing conditions (proteins were mixed with SDS loading buffer and heated at 30°C for 10 min prior to gel loading).

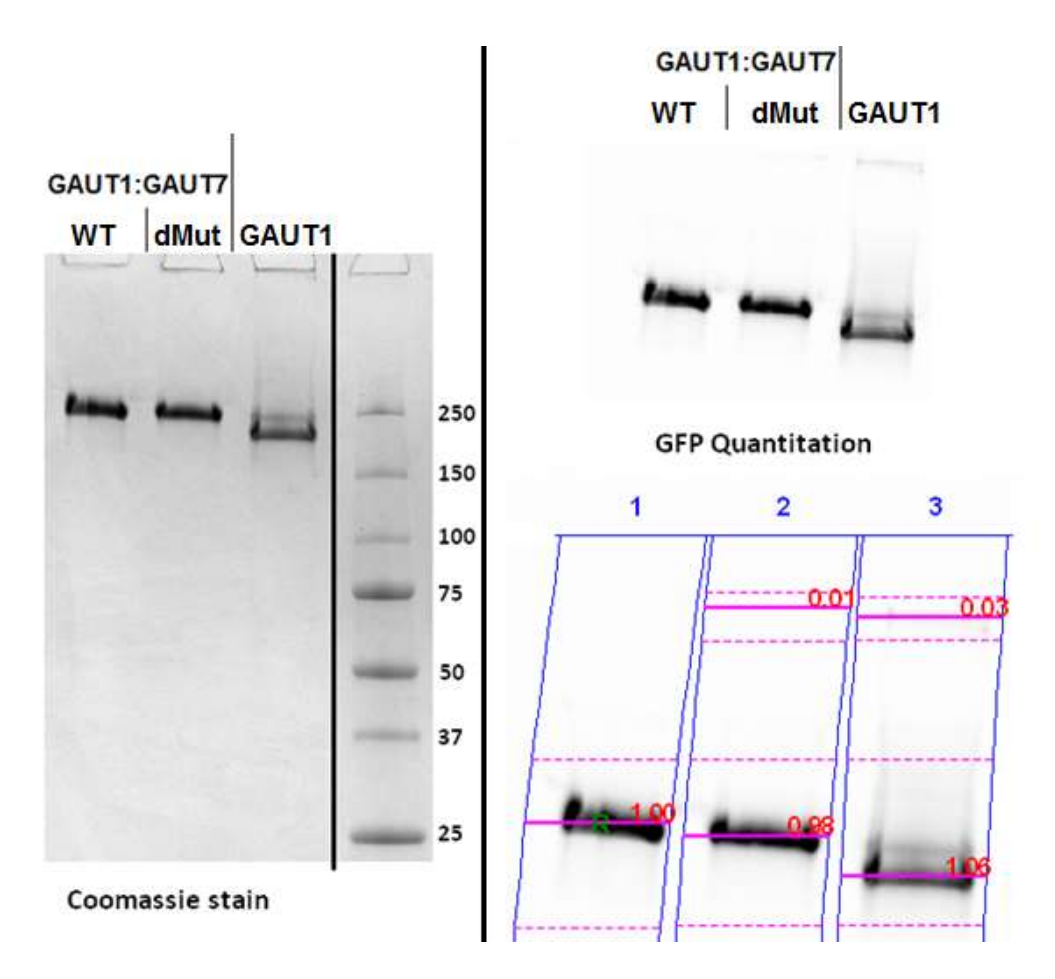


Figure C.4. SDS-PAGE of main protein peaks following SEC purification of GAUT1:GAUT7. Left panel: Coomassie-stained gel. No aggregates are visible in SEC-purified main peak proteins and samples appear to have staining of equal intensity. Right panel: in-gel GFP fluorescence. The three lanes are the same as in the left panel (WT, double mutant, GAUT1). Relative quantitation of protein was performed using Image Lab software. GAUT1:GAUT7 WT (Lane 1) was normalized to 1.00. GFP signal associated with the double mutant is 98% of WT and the indicated region around the GAUT1 protein is 106% of WT GAUT1:GAUT7.

Conclusions and future directions:

During nickel-affinity purification, all constructs are co-purified with some proportion of high MW aggregates and truncation products. Co-expression of GAUT1 with GAUT7 strongly reduces these impurities to ~10% of the sample, compared to ~72% of the sample for GAUT1. When protein are reduced using DTT, the aggregates do appear to contain full-length GAUT1 and GAUT7 protein, but retain minimal activity on the basis of equal protein loading. The reason that some percentage of expressed protein forms aggregates is not known, but could be due to improper disulfide bonding or hydrophobic interaction. For future expression studies, the presence of large amounts of aggregates or truncation products may be an indication that a protein requires co-expression with a binding partner for proper folding and secretion.

Introducing mutations into the GAUT1:GAUT7 construct also caused increased amounts of aggregates to appear. The relative activities measured using Ni-affinity purified proteins were inaccurate due to the presence of these aggregates. Purification of GAUT1:GAUT7 WT, double mutant, and GAUT1 by size exclusion chromatography eliminated the aggregates and allowed more accurate protein quantitation to be completed. Preliminary activity comparisons have been performed using these SEC-purified proteins to compare GAUT1:GAUT7 WT to double mutant activity (Appendix B, Fig. B.11) and GAUT1:GAUT7 to GAUT1 (Appendix E, Fig. E.3)

All GAUT proteins and individual mutant constructs may be expected to have some amount of non-active aggregates upon expression in HEK293 cells. Future assays of mutants and other specific activity experiments should be carried out using protein purified by SEC in order to ensure equal protein loadings during assays.

APPENDIX D

STABILITY OF GAUT1:GAUT7 AND GAUT1 ENZYMES FOLLOWING NICKEL-AFFINITY PURIFICATION

Purpose:

Preliminary data suggested that stocks of GAUT1:GAUT7 retain activity for at least one week when stored at 4°C and for many months stored at -80°C, but that GAUT1 may rapidly lose activity after purification. To determine if GAUT1:GAUT7 complex formation enhances the stability of GAUT1 activity, the loss of activity during storage at -4°C for up to 24 hours after harvesting the culture media was tested.

Background:

One of the goals of this project was to compare the relative activity of GAUT1 to the GAUT1:GAUT7 complex. From the original 1 mL expression culture of GAUT1, HG:GalAT activity (net cpm = 240-300) was detected from the medium when assayed immediately after harvesting the culture, but this activity was unable to be reproduced after storage of medium at 4°C for one week or storage at -80°C for one month. In contrast, high activity values (net cpm = 2000) were recovered from GAUT1:GAUT7 co-transfection medium stored at 4°C for one week.

This result led us to propose that GAUT1 rapidly loses activity after harvesting from medium, whereas co-expression with GAUT7 enhanced enzyme stability.

Comparisons of GAUT1 with GAUT1:GAUT7 activity require protein purification and verification of equal protein loading, a process that can delay the initial activity assay by several hours to days, depending on the size of the cell culture used and the number of independent samples being processed. Rapid loss of activity by GAUT enzymes could account for differences in specific activity measurements if enzymes cannot maintain stability during the period of time required to replicate assay results.

Methods:

Medium from 100 mL GAUT1 and GAUT1:GAUT7 cultures was harvested and enzymes were purified by Ni-affinity chromatography, desalted, and concentrated. A timer was started (0 hours) and activity was assayed immediately, as well as after storage at 4°C for 6, 12, and 24 hours. Due to the relatively low activity of GAUT1, 100 μM UDP-GalA (1:20 hot:cold dilution) was used in all assays. All assays included four independent measurements for T0 and activity at 5, 30, and 60 minutes.

Results:

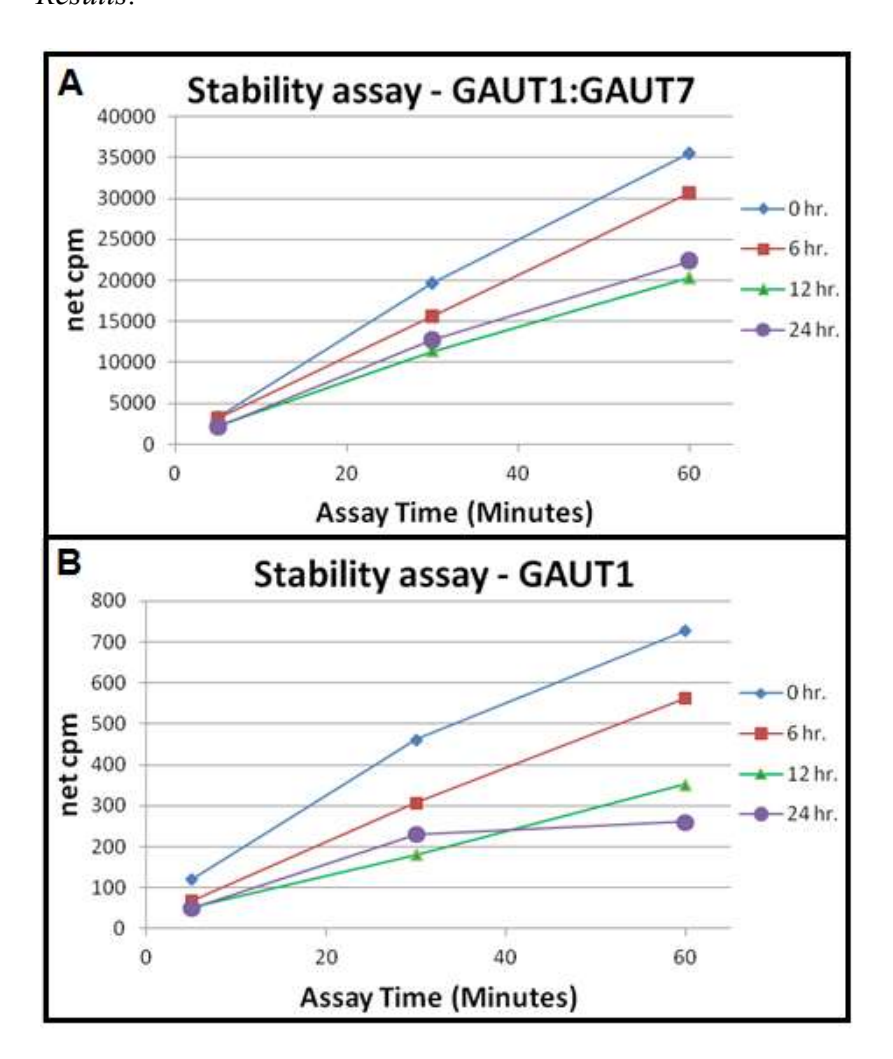


Figure D.1. GAU1:GAUT7 versus GAUT1 stability assays. GAUT1:GAUT7 **(A)** and GAUT1 **(B)** were assayed immediately after purification (0 hr) and after storage at 4°C for 6, 12, and 24 hr. Each time point is a single measurement. Three separate time measurements were made for each storage period.

The three activity measurements at each time point, corresponding to remaining activity after storage, were compared to the original activity measured at 0 hr. The results are summarized in Fig. D.2 and Table D.1.

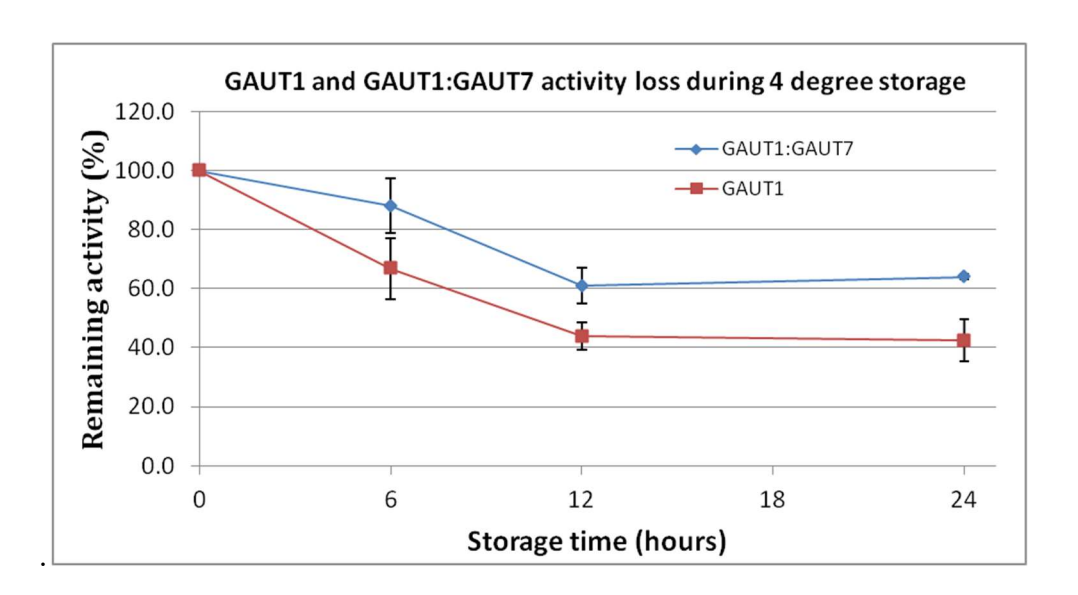


Figure D.2. Percentage of HG:GalAT activity recovered during GAUT1:GAUT7 and GAUT1 stability assays. From the results presented in Fig. D.1, the average HG:GalAT activity remaining at each time point (0, 6, 12, and 24 hr. storage time) is shown. Error bars represent the standard deviation from three assays (5, 30, and 60 minutes). The individual results from each assay are displayed in Table 4.7.

Table D.1. Percentage of HG:GalAT activity recovered during GAUT1:GAUT7 and GAUT1 stability assays at 4°C. At each assay point (5, 30, and 60 minutes), the activity measured after 0 hr storage is normalized to 100%. The net cpm at each time point following storage (6, 12, and 24 hr.) is compared to the net cpm of the value measured at each time point during the 0 hr assay. The results listed under the row "Average" are the average percentage activity remaining plotted in Fig. 4.18.

Hours after purification:		0	6	12	24
	Assay time	Percentage activity remaining			
GAUT1:GAUT7	5 min.	100	98.1	68.1	64.3
	30 min.	100	79.7	57.9	64.8
	60 min.	100	86.2	57.1	62.9
	Average	100	88.0	61.0	64.0
GAUT1	5 min.	100	56.7	44.2	41.7
	30 min.	100	66.7	39.0	50.0
	60 min.	100	77.3	48.4	35.9
	Average	100	66.9	43.8	42.5

Using the initial 0 hr measurements, GAUT1 activity was estimated relative to GAUT1:GAUT7 (Table D.2).

Table D.2. Relative activity of GAUT1 compared to GAUT1:GAUT7 following storage at 4°C. On an equal protein basis using Ni-affinity purified protein, GAUT1 has 4% activity relative to GAUT1:GAUT7. However, rhese samples were not purified by size exclusion to remove aggregates. Accounting for the difference in the amount of aggregates, in which GAUT1:GAUT7 is made up of 90% active protein, but active protein accounts for only 28% of GAUT1, the estimated activity of GAUT1 is 12% of the GAUT1:GAUT7 complex.

	Assay time	Net cpm	Relative activity	Main peak factor	Adjusted net cpm	Relative adjusted activity
GAUT1:GAUT7	5	3282		0.9	3647	1
•	30	19628		0.9	21809	1
	60	35533		0.9	39481	1
GAUT1	5	120	0.04	0.28	429	0.12
	30	462	0.02	0.28	1650	0.08
	60	727	0.02	0.28	2596	0.07

Conclusions and future directions:

Both GAUT1 and GAUT1:GAUT7 lost 40-60% of the initial activity after purification and storage at 4°C. However, the loss of activity of GAUT1 is not substantially faster than GAUT1:GAUT7. The large relative difference in activity is more likely due to the low specific activity of GAUT1 when it is expressed in the absence of GAUT7.

Based on the preliminary data and hypotheses, we expected to observe a much more rapid decline in GAUT1 activity. Although both GAUT1 and GAUT1:GAUT7 activities experienced a decline from the initial assay immediately after purification to 12 hours when stored at 4°C, HG:GalAT activity did not continue to decrease between 12-24 hours of storage at 4°C. The full series of experiments was not repeated with protein purified from new cell cultures. The initial drop-off of activity that occurred during the first 12 hours of storage at 4°C may not be as severe in all purifications. GAUT1:GAUT7 is known to retain activity for at least 1 week

during the multiple purification, deglycosylation, and tag cleavage steps that are required for X-ray crystallography screening (data not shown), but the specific activity loss during these purification steps has not been monitored.

Enzyme preparations should be stored at -80°C as soon as possible after purification, but it is also recommended that an additional size exclusion purification step is included to isolate the active complex. If using enzymes that retain *N*-terminal tags, these purification steps can be accomplished within 24 hours of harvesting media, which is an appropriate time scale for GAUT1 to retain activity prior to storage.

Although the presence of aggregates complicates the use of these results for accurate GAUT1 specific activity measurements, GAUT1 has an estimated 12% specific activity relative to GAUT1:GAUT7.

APPENDIX E

EFFORTS TO DETERMINE THE SPECIFIC ACTIVITY OF GAUT1 RELATIVE TO GAUT1:GAUT7

Purpose:

GAUT1 has HG:GalAT activity and appears to be the main catalytic subunit of the GAUT1:GAUT7 complex. Preliminary attempts to measure activity suggest that GAUT1 activity is low when expressed in the absence of GAUT7, but the specific activity has not been directly compared to GAUT1:GAUT7. Here we establish conditions to measure the specific activity of GAUT1 relative to GAUT1:GAUT7.

Background:

GAUT1:GAUT7 expressed in HEK293 cells and purified by nickel-affinity chromatography has a high level of purity and was used for biochemical characterization (Ch. 2, Fig. 2.1 and 2.2). As a result of the success of these experiments, it was proposed that GAUT1 expressed without GAUT7 could be purified and assayed using the same methods.

The use of SDS-PAGE (Chapter 2, Fig. 2.1B) and size exclusion chromatography (Appendix C, Fig. C.1) to verify the purity of GAUT1 showed that Ni-affinity purified protein cannot be used to compare the specific activity of GAUT1 to GAUT1:GAUT7 due to the

presence of aggregates and truncation products that account for >70% of the protein in the expressed GAUT1 samples.

As described in Ch. 2, Fig. 14C, GAUT1 elongates both DP7 and DP11 acceptors without the formation of high MW polysaccharide products, even after long incubation times. It is not yet known if the limited length of HG products elongated by GAUT1 is due to the low relative activity or due to the loss of an elongation domain that requires GAUT7.

From a 100 mL culture with 427 media fluorescence, <100 µg GAUT1 protein was recovered following size exclusion chromatography carried out to isolate the peak containing the active enzyme. The majority of this enzyme was used to reproduce the polyacrylamide gel product length analysis experiments (Ch. 2, Fig. 2.14C). Therefore, specific activity measurements of GAUT1 will require large-scale purification and replication from independent cell cultures.

Methods:

GAUT1 and GAUT1 co-transfected with GAUT7 were expressed in HEK293 cell cultures as described in previous sections. Enzyme activity was assayed under modified standard conditions (5 μ M UDP-[14 C]GalA, 100 μ M UDP-GalA total [1:20 hot:cold dilution]) unless otherwise noted.

Results:

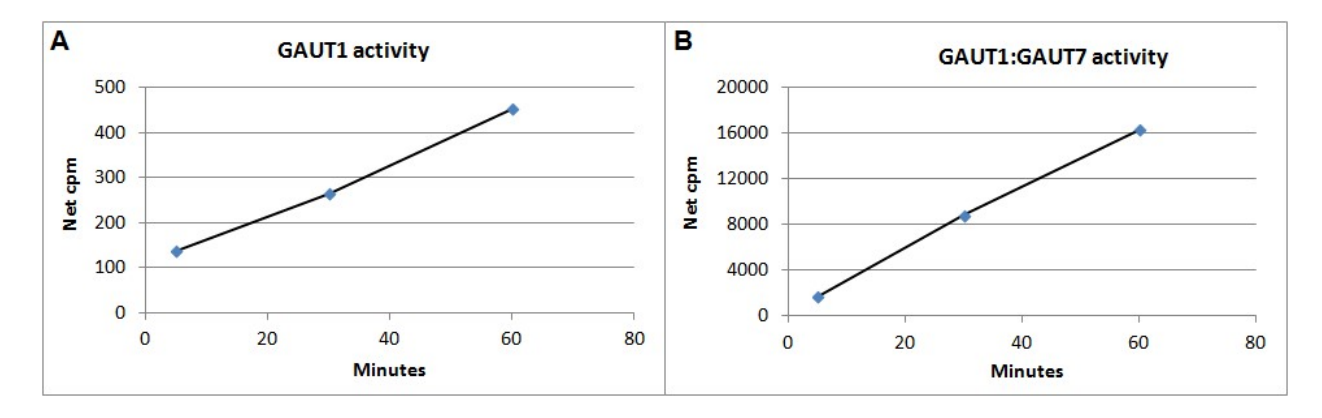


Figure E.1. Preliminary assay of GAUT1 and GAUT1:GAUT7 activity purified from 100 mL cultures. In an initial assay to verify a single time point to be used for specific activity comparisons, GAUT1 and GAUT1:GAUT7 (100 nM Ni-affinity purified enzyme) were assayed at 5, 30, and 60 minutes with 100 μ M UDP-GalA and 10 μ M HG acceptor mix. Results are from a single experiment.

Because 5 minutes of incubation was sufficient to measure an above-background activity signal at the given reaction conditions, the specific activity assay was replicated at this time point.

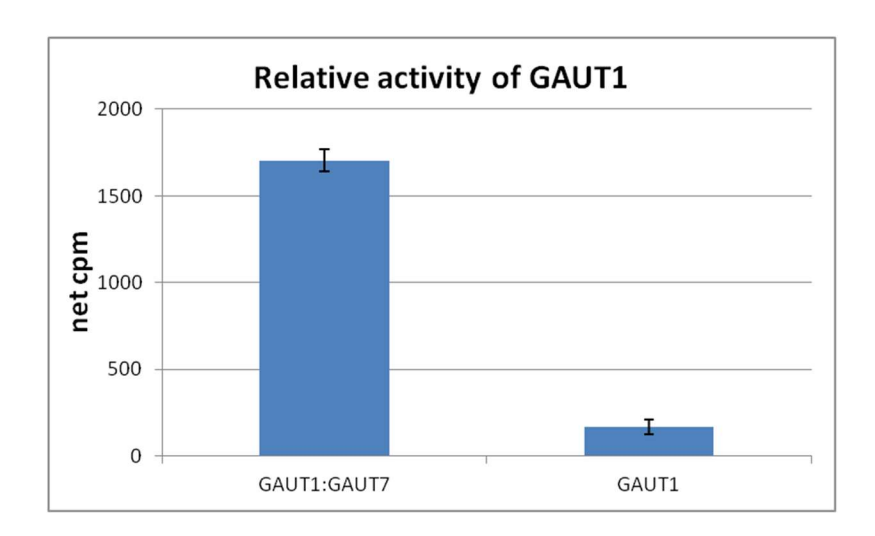


Figure E.2. Relative initial rate activity of GAUT1. HG:GalAT activity was assayed at 5 minutes, 100 μM UDP-GalA (1:20 hot:cold dilution). Error bars represent the standard deviation from two independent assays.

GAUT1 activity measured at 5 minutes is 9.9% of GAUT1:GAUT7 activity. Accounting for the lower active enzyme concentration due to aggregates, GAUT1 activity is estimated to be as high as 31.8% of GAUT1:GAUT7 activity.

Both GAUT1 and GAUT1:GAUT7 were purified by size exclusion chromatography to remove aggregates (Fig. C.1). Equal protein quantitation was verified by in-gel fluorescence (Fig. C.4).

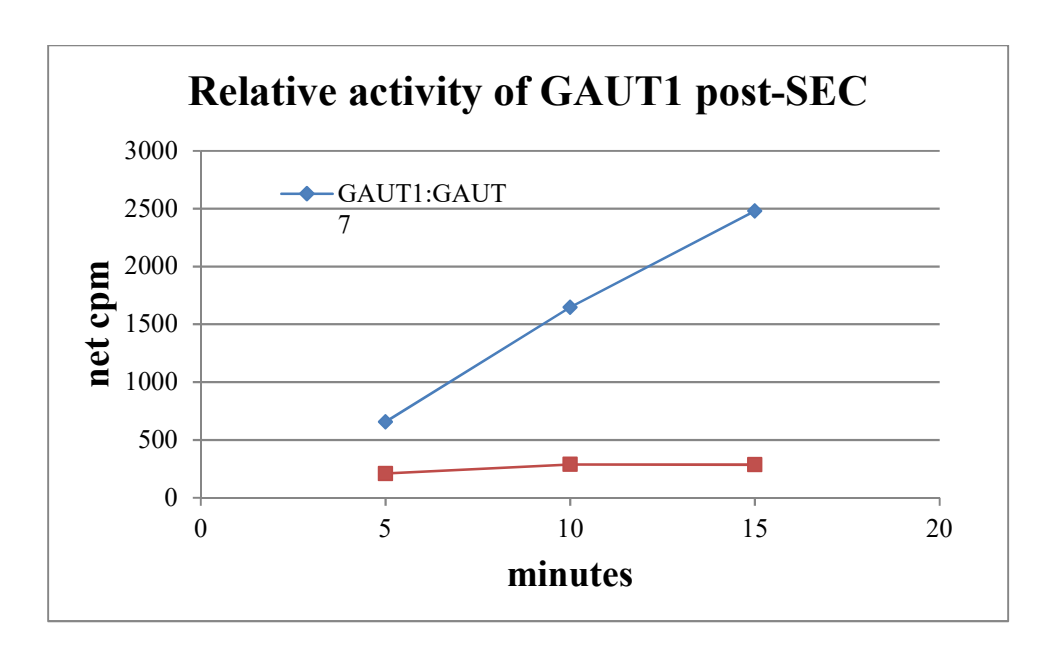


Figure E.3. Relative activity of GAUT1 after main peak purification. GAUT1 and GAUT1:GAUT7 were assayed following purification of the main peak containing active enzyme (200 μM UDP-GalA total, 1:40 hot:cold dilution) at 5, 10, and 15 minutes. Results are from a single experiment.

Based on net cpm measured at 5 minutes, the initial rate of GAUT1 is 31.9% relative to GAUT1:GAUT7. However, there was only a minor increase in GAUT1 activity measured at 10 and 15 minutes, and the increase in activity does not follow a linear trend during the 15 minute reaction period.

Conclusions and future directions:

From two independent cultures (GAUT1:GAUT7 batch #10 and #11), GAUT1 activity is measured at 4-10% relative to GAUT1:GAUT7 using Ni-affinity purified protein. However, GAUT1 activity is underestimated in these assays due to a >3-fold difference in the amount of active enzyme. GAUT1 activity may be as high as ~32% relative to GAUT1:GAUT7. These

studies will need to be repeated with enzyme purified from large-scale cultures to account for the low amount of GAUT1 protein recoverable after size exclusion purification of the active enzyme. Amounts as low as 1 mg protein/L cell culture may be an expected yield for GAUT1, compared to >40 mg/L cell culture for GAUT1:GAUT7.

The range of relative activity is also due to differences in GAUT1:GAUT7 specific activity between cultures. Future experiments should establish the reproducibility of GAUT1:GAUT7 specific activity purified from multiple independent cell cultures to determine the range of specific activity variations expected from independent cell cultures.

Preliminary data suggest that GAUT1 activity may follow a nonstandard progress curve (Fig. E.1 and E.3). Activity could be detected at 5 minutes, but the progress curve appears to be nonlinear at early time points. Rather than attempting to use a single time point analysis for comparison to GAUT1:GAUT7, the full progress curves should be made to determine the most appropriate linear time range for estimating specific activity.

From the data presented in Ch. 2, Fig. 2.14C, GAUT1 can elongate DP7 acceptors by at least 5 GalA units and DP11 acceptors by at least 20 GalA units in overnight reactions. The correlation between activity measured by incorporation of radiolabeled GalA and chain length remains unknown.

APPENDIX F

STOICHIOMETRY OF THE GAUT1:GAUT7 COMPLEX

Purpose:

The original model of GAUT1:GAUT7 presented in Atmodjo et al. 2011 describes GAUT1:GAUT1:GAUT7 as a heterotrimeric complex. This model has not been verified, and the complex may be a heterodimer. In-gel fluorescence and size exclusion chromatography with multiangle light scattering (SEC-MALS) were used to find evidence for or against the heterotrimeric model of GAUT1:GAUT7.

Background:

The MS experiments from immunoprecipitated GAUT1:GAUT7 complex in Atmodjo et al. (2011) showed a range of estimated normalized spectral abundance factor (NSAF) values. When only considering GAUT1 and GAUT7, the ratio of NSAF values, representing the number of GAUT1 molecules per GAUT7, were 1.08, 1.66, 1.66, and 1.40, depending on immunoprecipitation with anti-GAUT1, anti-GAUT7, and two different methods of analysis (False discovery rate and Probability) (Atmodjo et al., 2011). The possibility of a molar excess of GAUT1, as well as the large size of the complex observed in non-reducing SDS-PAGE (running at a MW higher than the 150 kDa marker), led to the GAUT1:GAUT7 complex be proposed as a heterotrimer consisting of two GAUT1 subunits and one GAUT7 subunit (Atmodjo et al., 2011).

The co-expressed GAUT1:GAUT7 complex purified from HEK293 cells was shown to be N-glycosylated in both the GAUT1 and GAUT7 subunits and electrophoreses close to the 150 kDa MW marker in SDS-PAGE following deglycosylation (Ch. 2, Fig. 2.1A). Because this value is intermediate between a dimer and a trimer, the stoichiometry of the complex remains unclear. Two methods were used to investigate the stoichiometry of the GAUT1:GAUT7 complex: in-gel GFP fluorescence and SEC-MALS.

Table F.1: Molecular weight of GAUT1 and GAUT7 monomers and complexes. Any additional size of each enzyme due to *N*-glycosylation is not included in these calculations.

Construct	MW (kDa)
GAUT1Δ167	58.7
GAUT7Δ43	65.6
N-terminal tags	34.1
GAUT1 + tags	92.8
GAUT7 + tags	99.8
GAUT1:GAUT1:GAUT7 trimer	183.0
GAUT1:GAUT1:GAUT7 trimer + tags	285.4
GAUT1:GAUT7 dimer	124.3
GAUT1:GAUT7 dimer + tags	192.6

Methods:

For in-gel GFP fluorescence quantitation, proteins were incubated for 10 minutes in SDS-PAGE loading buffer at 30°C (non-denaturing conditions). The SDS-PAGE gel was analyzed in a Biorad Gel Doc using Image Lab software with fluorescence detection using an Alexa 488 filter to detect GFP signal. Rectangular sections encompassing the GFP signal corresponding to GAUT1, GAUT7, or the GAUT1:GAUT7 complex were designated within respective SDS-PAGE gel lanes. Relative quantitation was performed by normalizing the GAUT1 monomer or the GAUT1:GAUT7 complex to 1.00 relative intensity.

For measurement of GAUT1:GAUT7 by SEC-MALS, a 1 mg/mL protein solution (10 μL) was applied to a Superdex 200 10/300 GL column connected to a Shimadzu UFLC system that was coupled with a multiangle light-scattering instrument (MiniDAWN TREOS, Wyatt Technology). The light scattering data were recorded and analyzed by using Astra V software (Wyatt Technology). His-tagged TEV Protease and peptide N-glycosidase F (PNGase F) were expressed in *E. coli* and purified by nickel-affinity chromatography. To remove *N*-terminal tags and *N*-glycosylation, GAUT1:GAUT7 was incubated with a 10:1 molar ratio with TEV Protease and PNGase F overnight at room temperature. The product was injected into a nickel-affinity column and the flow-through containing processed GAUT1:GAUT7 was collected and concentrated to 1 mg/mL in 50 mM HEPES buffer.

Results:

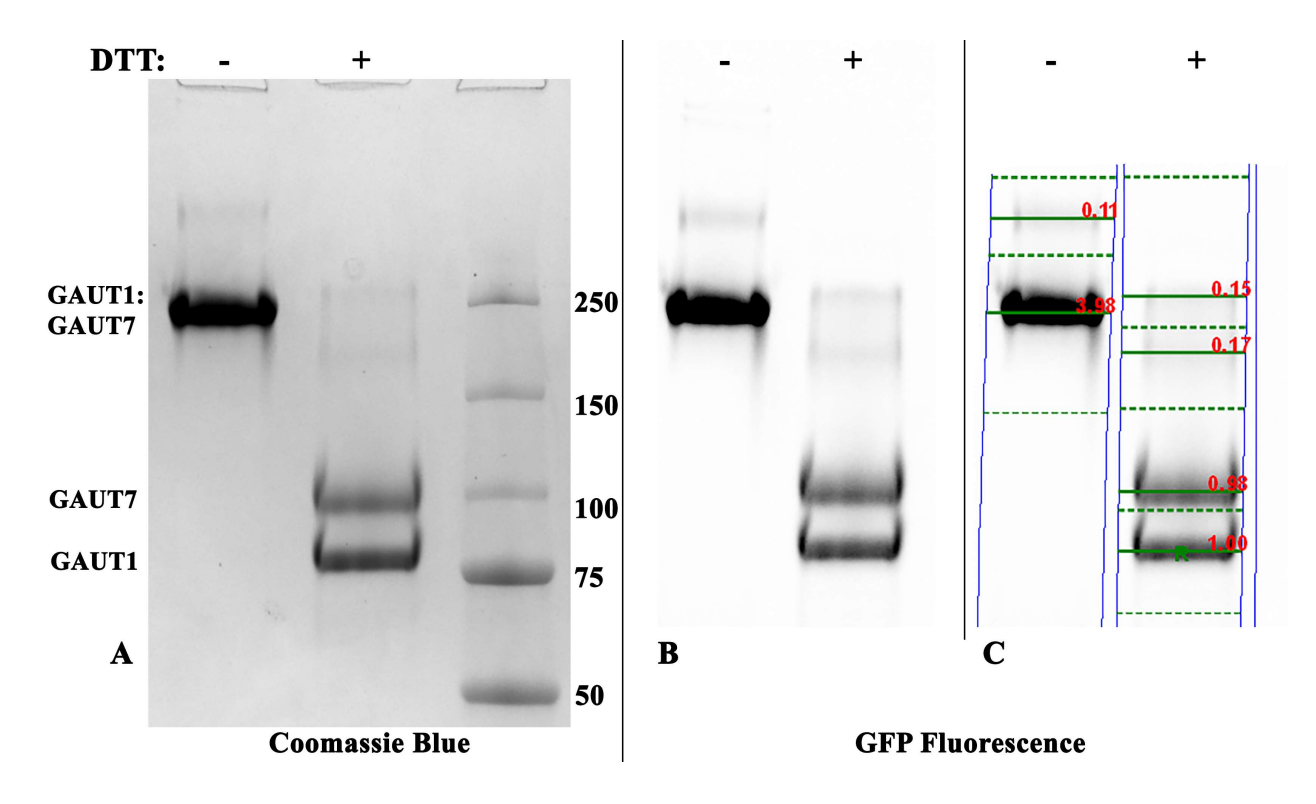


Figure F.1. In-gel GFP fluorescence quantitation of GAUT1 and GAUT7 monomers vs. non-reduced complex. GAUT1:GAUT7 (4 μg) was mixed with SDS loading buffer and incubated under non-denaturing conditions, 30°C for 10 minutes under non-reducing (-DTT) or reducing (+DTT) conditions. A, Coomassie Blue staining. B and C, prior to Coomassie Blue staining, an Alexa 488 filter was used to detect GFP fluorescence in the unstained gel. GFP fluorescence with selected bands is reproduced in C. Blue lines indicate SDS-PAGE lane boundaries and green dotted lines indicate boundaries of selected bands. Band intensity was quantified relative to GAUT1 monomer (1.00, indicated by green R). Relative GFP signal for each gel section is shown in red numbers as calculated by ImageLab.

In Coomassie-stained gels (Fig F.1A and Fig. 2.1A), the GAUT1 monomer is darker and more intensely stained than the GAUT7 monomer after disulfide bonding is reduced with DTT. This result is consistent with the original trimeric GAUT1:GAUT7 model with a 2:1 stoichiometry. However, quantitation of GFP staining, in which an equal number of molecules yields equal signal, measures GAUT1 and GAUT7 intensity as equal, supportive of a complex with 1:1 stoichiometry. An unexpected result from this experiment is that the GAUT1:GAUT7 complex band gives a signal that is four times the monomer signal, which is not consistent with either a dimer or a trimer and equals 2X the total relative signal for the same amount of protein under non-reducing conditions.

The linearity of in-gel GFP quantitation was tested under five different dilutions of GAUT1:GAUT7.

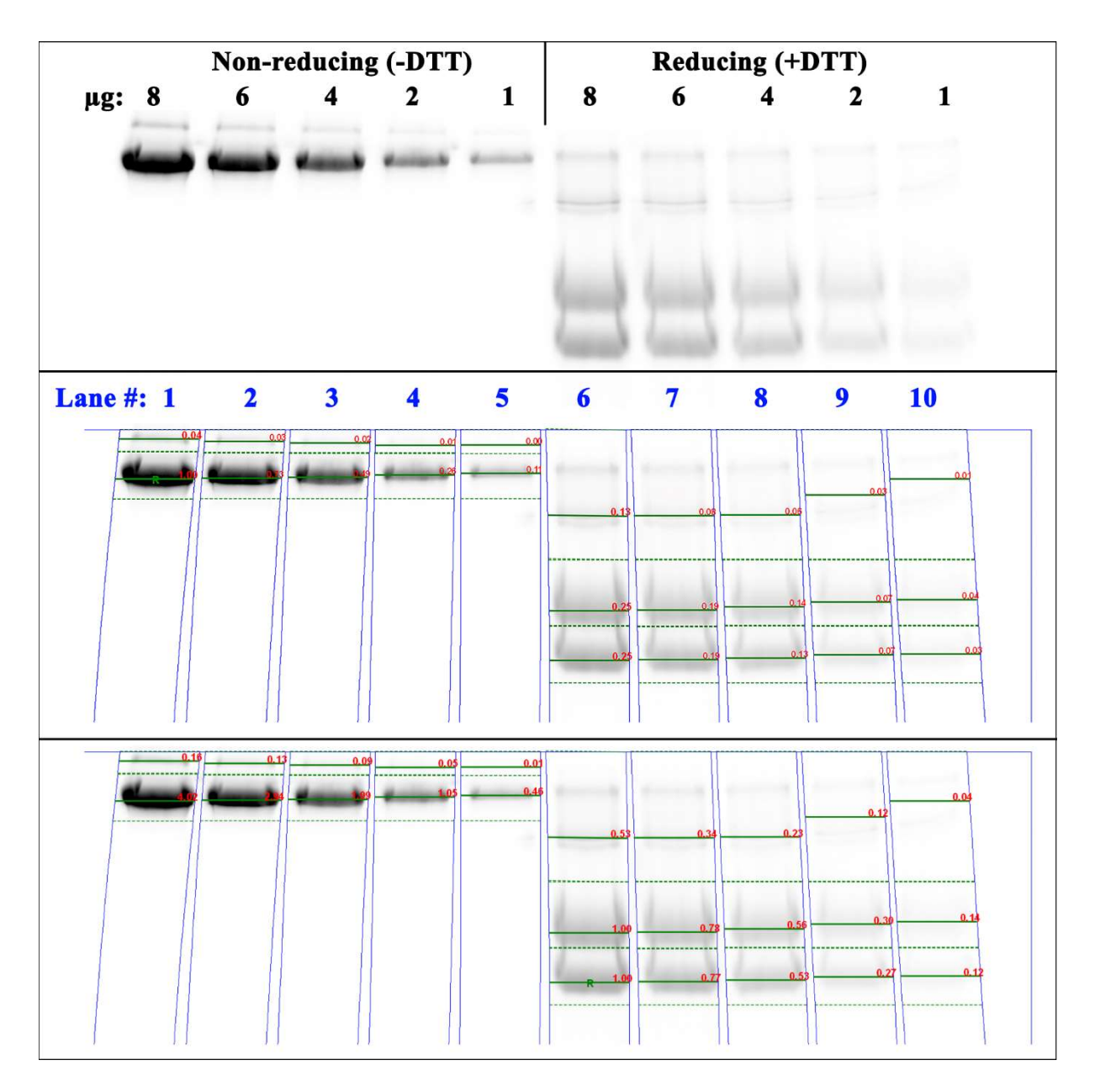


Figure F.2. Linear dilution of in-gel GFP fluorescence signal. GAUT1:GAUT7 protein was loaded at 8, 6, 4, 2, and 1 μg under non-reducing (Lanes 1-5) and reducing (Lanes 6-10) conditions to verify the linearity of GFP quantitative measurements. The gel is shown with no quantitation (top panel), quantitation relative to the GAUT1:GAUT7 complex (middle panel), or quantitation relative to a GAUT1 monomer (lower panel). Relative GFP signal for each gel section is shown in red numbers as calculated by ImageLab.

Quantitation is linear for both the complex and monomer signals. Under all dilutions, GAUT1 and GAUT7 are calculated at a 1:1 ratio and the complex intensity is 4X the intensity of the GAUT1 monomer. This method does not support a trimeric complex with a 2:1 ratio of GAUT1:GAUT7.

The molecular weight of the nickel-affinity purified GAUT1:GAUT7 complex with *N*-terminal tags and N-glycosylation as well as a TEV/PNGase F-treated form of the complex was measured by SEC-MALS.

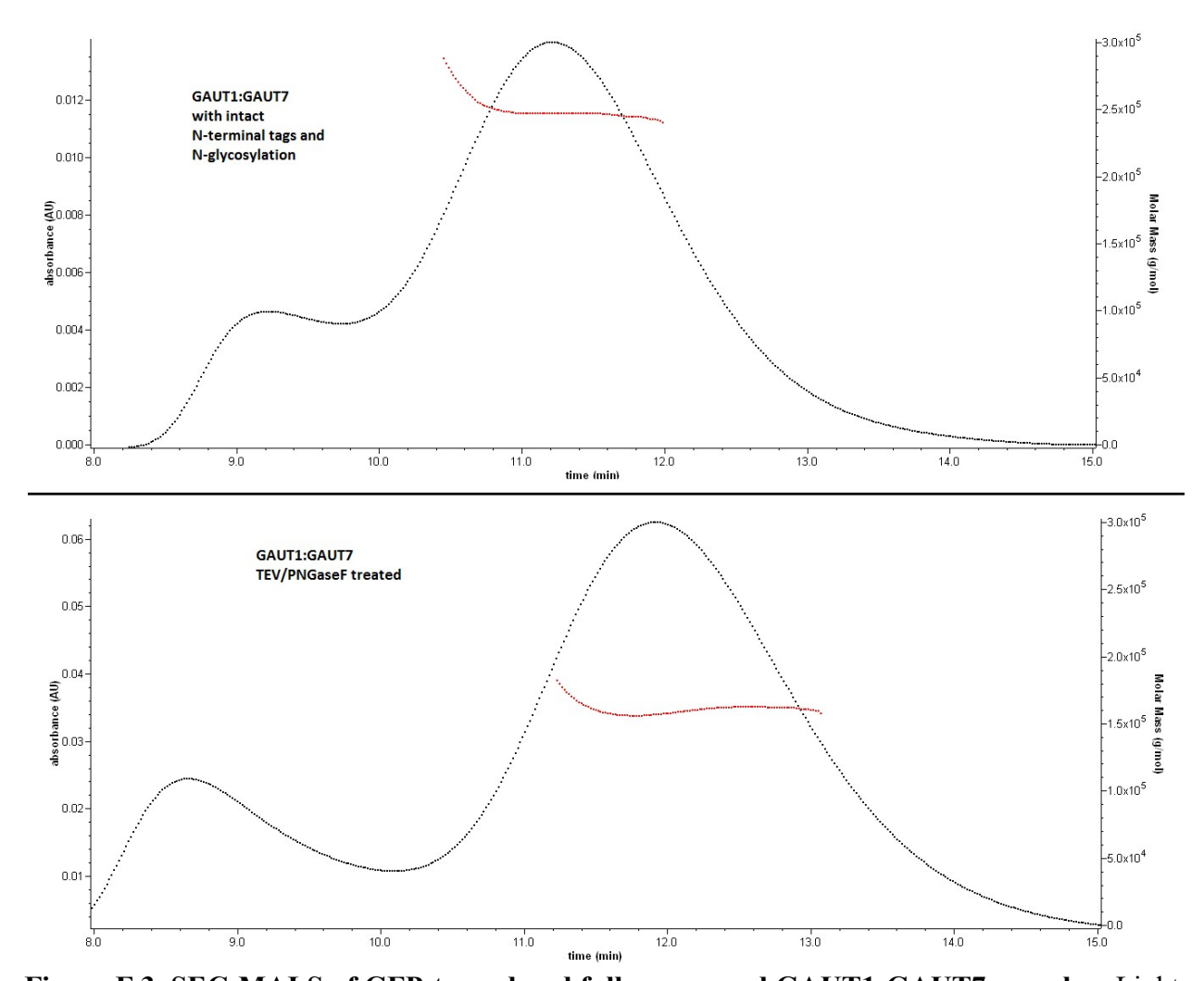


Figure F.3. SEC-MALS of GFP-tagged and fully processed GAUT1:GAUT7 complex. Light scattering absorbance data and measured molar mass of GAUT1:GAUT7 containing *N*-terminal

tags and *N*-glycosylation (top panel) or GAUT1:GAUT7 treated with TEV protease and PNGase F (bottom panel). Molecular mass data is summarized in Table 4.10.

Table F.1. Molecular weight of GAUT1:GAUT7 measurements by SEC-MALS. Molecular weight measurements (g/mol) reported from SEC-MALS measurements are summarized along with calculations resulting from TEV Protease and PNGase F treatment.

	MW (kDa)
GFP-tagged GAUT1:GAUT7	250
TEV/PNGaseF-treated	160
GAUT1:GAUT7	
Difference	90
MW due to N-terminal tags (if	68
complex is a dimer)	
MW due to N-glycoslyation	22

There is a 90 kDa difference in the measured MW of the N-terminally tagged and N-glycosylated GAUT1:GAUT7 complex from the fully processed complex. If each N-terminal tag is 34 kDa, in a dimeric complex, 22 kDa would remain. Based on SDS-PAGE gel shifts, this 22 kDa could be accounted for by the MW change due to removal of N-glycans. Although the reported MW from MALS experiments is intermediate between the predicted MW for a dimeric or trimeric complex (Table 4.9), the MW shift more likely suggests a dimer, which is consistent with the 1:1 stoichiometry suggested by in-gel GFP fluorescence.

Conclusions and future directions:

Although some uncertainty remains as to the precise MW measurement of the GAUT1:GAUT7 complex, both of these methods are more consistent with the conclusion that GAUT1:GAUT7 is a dimer, at least when heterologously expressed in HEK293 cells.

The in-gel GFP fluorescence suggests that the reduced complex contains a 1:1 stoichiometry of GAUT1:GAUT7. The GAUT7 monomer appears lighter after Coomassie staining, but Coomassie blue binding is not directly quantitative between different proteins because factors such as differences in electrostatic interactions with basic residues can change the number of molecules of stain that bind to a given protein (Tal et al., 1985). These results remain suggestive because the 4:1 ratio of monomer to complex GFP fluorescence is unexplained, whereas a 2:1 ratio should be expected of a dimer.

Preliminary attempts to measure the precise molecular weight by light scattering have yielded MW estimates intermediate between the expected MW of a dimer or a trimer. However, the MW shift measured by MALS following removal of N-terminal tags and N-glycosylation is also consistent with a GAUT1:GAUT7 dimer.

The GAUT7 monomer also resolves at higher molecular weights than expected in SDS-PAGE gels, suggesting the possibility for other post-translational modifications that have not been investigated.

For future experiments, full TEV-cleavage/deglycosylation followed by size exclusion chromatography of a larger-scale preparation of GAUT1 and GAUT1:GAUT7 should be done before analysis by light scattering. The light scattering experiment requires injection of an enzyme sample with a concentration of 1 mg/mL. Due to losses during processing and purification, starting with at least 5 mg enzyme would be preferable. Rather than attempting to use smaller aliquots of protein, as we have done here, this process is more likely to be successful starting from a large culture that is completely processed and purified before storage.

APPENDIX G

ELISA-BASED HG:GALAT ACTIVITY ASSAY

Purpose:

To develop a sensitive, non-radioactive assay for HG:GalAT activity, to determine the binding properties of HG acceptors to ELISA plates, and to obtain evidence for *de novo* synthesis of HG by GAUT1 in the absence of GAUT7.

Background:

As outlined in Ch. 2, Fig. 2.7, when GAUT1:GAUT7 is incubated with UDP-GalA, a *de novo* synthesis product can be detected by anti-HG antibodies. These experiments also demonstrated that anti-HG antibodies, including CCRC-M38, CCRC-M131, and JIM5, do not have reactivity toward GAUT1:GAUT7 or UDP-GalA, so they can be used to detect polymerized products. Although antibodies such as CCRC-M38 can bind to HG containing >4 GalA glyosyl residue units, the ability of short-chain HG acceptors to bind to ELISA plates and the linear quantitation of HG binding was unknown.

Here, the A450 signal obtained from ELISAs and the relative binding strength of HG acceptors of different degrees of polymerization were determined. The ELISA assay for HG:GalAT activity was shown to be useful for the detection of acceptor-dependent activity. Finally, preliminary evidence for *de novo* synthesis activity by GAUT1 was obtained using the ELISA assay.

Methods:

ELISAs were performed as described in Ch. 2 ("ELISA of HG:GalAT activity using anti-HG monoclonal antibodies"). All samples, either reaction mixes or HG control samples were diluted to a final volume of 50 μL and evaporated to dryness overnight in a 96-well plate (Costar 5398). All ELISAs were performed using the anti-HG monoclonal antibody CCRC-M38. Unless otherwise noted, M38 from the hybridoma supernatant was diluted 1/10 in Tris-buffered saline prior to antibody incubation.

All HG:GalAT reactions were incubated under standard conditions for 12 hours.

Technical Notes:

HG:GalAT assays have been performed with acceptor concentrations up to 100 μM.

$$\frac{1954.4 \, \mu g}{\mu \text{mol}} * \frac{100 \, \mu \text{mol}}{L} * \frac{L}{10^6 \mu L} = \frac{0.195 \, \mu g}{\mu L}$$

From a 30 μL reaction with 100 μM acceptor, if 1 μL is loaded into the ELISA plate per replicate sample, the starting acceptor is 195 ng for DP11 or 125 ng for DP7.

Because the reaction contains 1 mM UDP-GalA, up to 1 mM of the the 176 Da GalA moiety is transferred assuming 100% donor substrate usage during the reaction. Therefore, each μ L of reaction loaded onto the ELISA plate contains up to 176 ng GalA in addition to the mass of the acceptor loaded.

$$\frac{176 \, \mu g}{\mu \text{mol}} * \frac{1000 \, \mu \text{mol}}{L} * \frac{L}{10^6 \mu L} = \frac{0.176 \, \mu g}{\mu L}$$

Accounting for the original HG acceptor and the GalA transferred during the reaction, overnight reaction samples contain 371 ng/ μ L loaded onto the ELISA plate for a DP11 acceptor or 301 ng/ μ L for a DP7 acceptor.

Results:

The sensitivity of ELISAs and the ability of polysaccharides to bind to the plates are likely to be microtiter plate-dependent. All assays were performed using 96-well Costar 3598 microtiter plates. The monoclonal antibody CCRC-M38 is reported to bind to HG of DP>4 (www.wallmabdb.net). The sensitivity was tested toward the HG acceptor mix (DP 7-23).

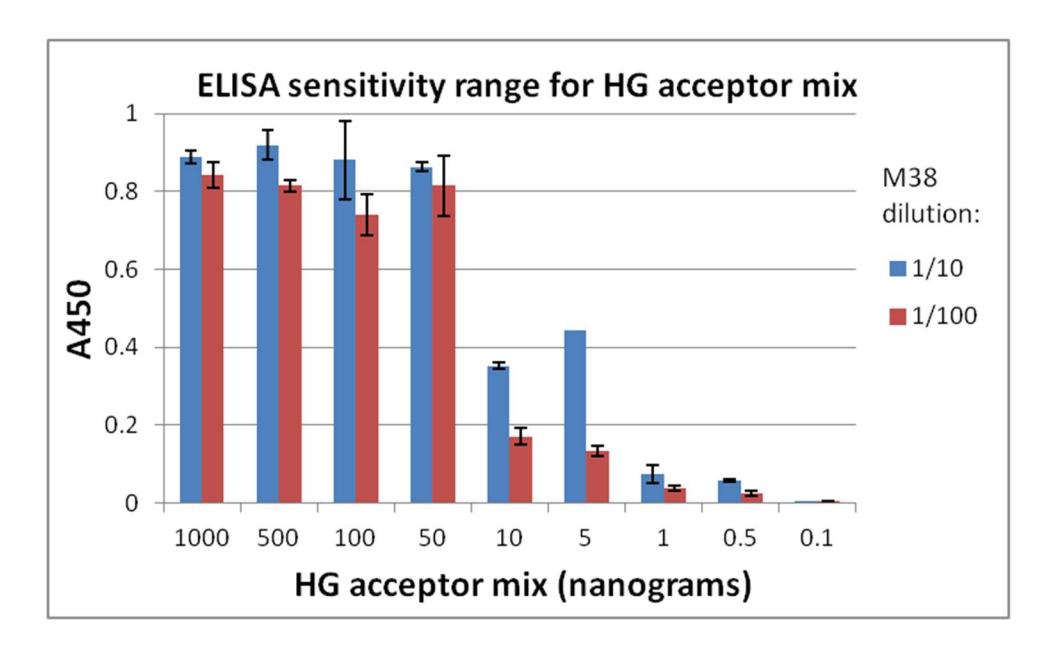


Figure G.1. CCRC-M38 reactivity toward HG acceptor mix. CCRC-M38 shows reactivity toward at least 5 ng of HG acceptor mix (DP 7-23), with maximum signal observed above 50 ng. M38 was diluted 1/10 from the hybridoma supernatant (blue bars) or 1/100 (red bars). Error bars represent standard deviation from triplicate samples. Data are representative of at least 3 independent experiments.

In all following assays, a 1/10 dilution of M38 antibody was used.

The HG acceptor mix, sometimes labeled "OGA DP7-23 mix," contains longer-chain acceptors up to approximately DP40 as visualized in PAGE assays (Ch. 2, Fig. 2.4E). M38 is

reported to bind to HG DP>4, but ELISA signal may be low if individual HG acceptors of lower DP are not able to bind to ELISA plates.

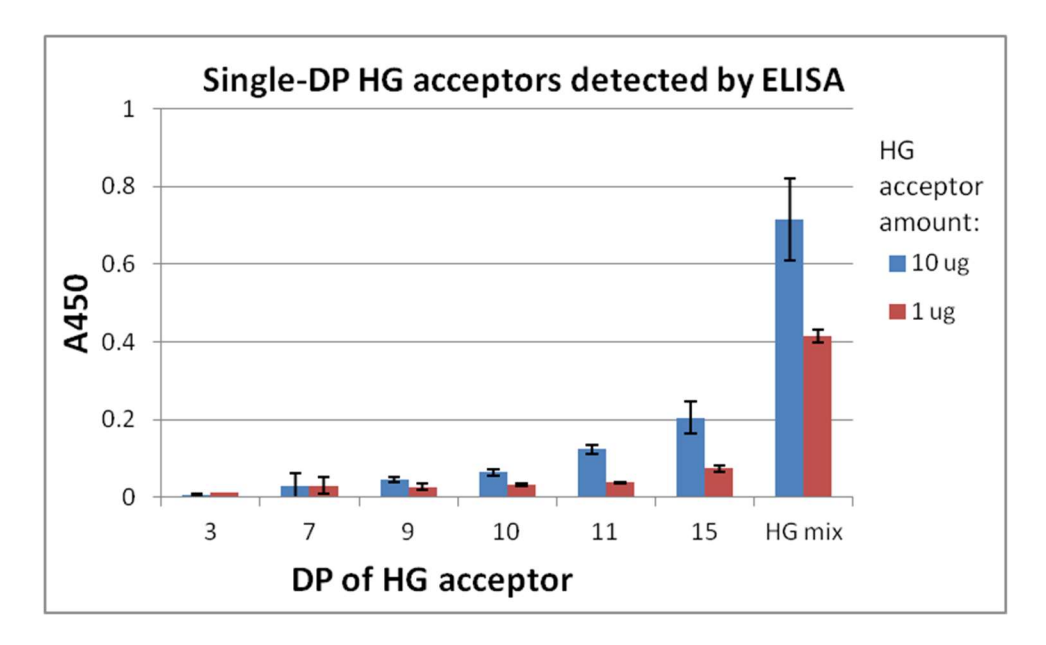


Figure G.2. Sensitivity of CCRC-M38 antibody to HG acceptors enriched for homogenous degrees of polymerization. M38 shows minimal reactivity toward HG acceptors DP11 and smaller, and quantities up to 10 μg (blue bars) are required to enhance signal. Error bars represent standard deviation from triplicate samples. Results are from a single experiment.

The ability of ELISA to detect *de novo* synthesis was shown in Ch. 2, Fig. 2.7C. Because HG acceptors DP≤11 have minimal binding to ELISA plates, this method may also be adapted as a non-radioactive method of screening acceptor-dependent HG:GalAT activity. A preliminary test of detection of elongation of DP7 and DP11 acceptors by both GAUT1 and GAUT1:GAUT7 was attempted.

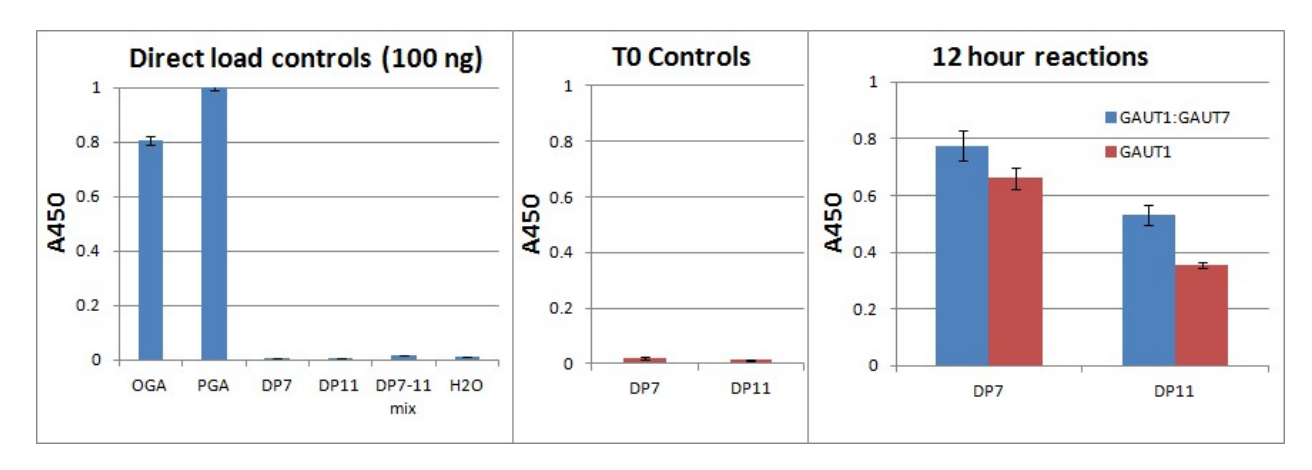


Figure G.3. Acceptor-dependent activity detected by ELISA. The elongation of DP7 and DP11 acceptors by GAUT1:GAUT7 can be distinguished from the T0 controls, which are not of sufficient length to bind to the ELISA plate. All reactions were incubated in 30 μL total volume. Each measurement is from 1 μL representing 1/30 of the total reaction. In the left panel, OGA corresponding to the HG DP7-23 mix and PGA (polygalacturonic acid, Sigma) react to M38 when loaded at 100 ng, but DP7-11 acceptors do not. The T0 controls are reaction mixtures containing DP7 and DP11 acceptors with pre-boiled GAUT1:GAUT7 enzyme. In the right panel, reactions were incubated with 100 nM GAUT1:GAUT7 (blue bars) or GAUT1 (red bars) of size exclusion-purified enzyme (main peak).

Prior to size exclusion purification, GAUT1, the GAUT1:GAUT7 co-expressed complex containing a double mutant in GAUT7 (previously described in Fig. B.11), and GAUT1:GAUT7 were assayed for their ability to initiate HG synthesis *de novo* by ELISA. In these assays, the amount of enzyme is described as "Factor-adjusted concentration" to account for the percentage of active enzyme in the nickel-affinity-purified stock. The concentration factors are: GAUT1:GAUT7 (0.9), double mutant (0.69), GAUT1 (0.28). The following formula was used to adjust enzyme concentrations:

$$\frac{Effective\ concentration}{Concentration\ Factor} = Concentration\ loaded\ in\ assay$$

Therefore, a reaction containing 100 nM effective concentration of GAUT1 contains 357 nM or 3 µg enzyme measured by UV-Vis in a 30 µL reaction.

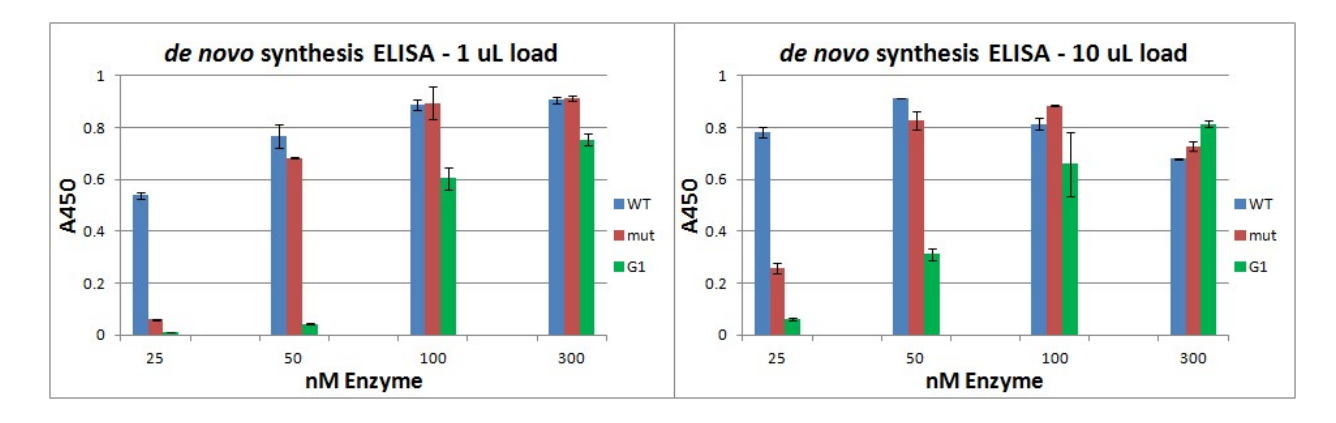


Figure G.4. GAUT1 *de novo* synthesis activity detected by ELISA. GAUT1:GAUT7 (blue bars), the double mutant GAUT7-452/GAUT7-466 co-expressed with GAUT1 (red bars), and GAUT1 (green bars) all synthesize HG *de novo*. GAUT1, and to a lesser extent the double mutant, require higher enzyme concentrations to detect activity. HG products are detected following overnight incubation with 1 mM UDP-GalA. Enzyme concentrations are calculated from Ni-affinity purified protein using UV-Vis based on factor-adjusted concentrations. All reactions were 30 μL. In the left panel, each measurement is from 1 μL representing 1/30 of the total reaction. In the right panel, each measurement is from 10 uL representing 1/3 of the total reaction. Error bars are standard deviation of triplicate samples. Similar results have been replicated in at least three independent experiments. Enzyme controls (no UDP-GalA added) do not yield above-background signal (data not shown).

These results suggest that GAUT1 by itself is sufficient to initiate the *de novo* synthesis product. The chain length or reaction progress curves of *de novo* synthesis by GAUT1 have not been further analyzed.

Conclusions and future directions:

ELISA with anti-HG antibodies can be used as an effective and reproducible assay for both acceptor-dependent and *de novo* HG:GalAT activity. HG acceptors of roughly DP15 are necessary to detect signal in ELISA. Small amounts of signal can be detected with DP11 at high concentrations. Concentrations typically used in assays (containing <200 ng HG acceptor/μL reaction) are not sufficient to detect signal from DP11 or smaller acceptors, allowing ELISA to be used as a non-radioactive assay for acceptor-primed HG:GalAT synthesis, as long as DP≤11 acceptors are used.

The HG acceptor mix, which contains longer-chain acceptors (up to ~DP40), can be detected at very low concentrations by ELISA, with signal being obtained with acceptor amounts as low as 5 ng. The HG acceptor mix is a strong positive control for anti-HG antibody binding, but cannot be used in ELISA-based acceptor-dependent reactions since the starting acceptor itself is detected by ELISA.

GAUT1 is able to initiate HG *de novo*. Because GAUT1 is unexpected to be able to synthesize high MW products from reactions primed with DP7 or DP11 acceptors (Ch. 2, Fig. 2.14C), the *de novo* synthesis product synthesized by GAUT1 may be limited to relatively short-chain oligosaccharides/polysaccharides. Using GAUT1 to synthesize short-chain products may be a method for detecting whether the reducing end of *de novo* synthesis products contains a UDP, which was not able to be analyzed using products synthesized by GAUT1:GAUT7 due to

their large size (Ch. 2, Fig. 2.7E). Although *de novo* synthesis activity can be detected with low concentrations of GAUT1:GAUT7 (25 nM), there appears to be a minimum threshold for activity detection by GAUT1.

APPENDIX H

COMPARISON OF METHODS FOR ASSAYING HG:GALAT ACTIVITY

Table H.1. Methods for assaying HG:GalAT activity. HG:GalAT activity has been detected by nine different methods with varying advantages and limitations. The utility of each method for quantitative measurements or chain length analysis are compared.

	Advantages	Disadvantages
¹⁴ C Filter Assay	Quantitative, comparative rate/kinetic data. 20-30 samples can be simultaneously assayed without additional difficulty.	Expensive and time- consuming creation of UDP- [14C]GalA. No product size elongation distribution data. Unknown product size required to bind filters. Uncertain binding of non-HG acceptors.
¹⁴ C Precipitation Assay	Expanded use of acceptors (RG-I/RG-II) that may, or may not bind filters. Empirical determination of binding to filters is required.	Expensive and time- consuming creation of UDP- [14C]GalA. No product size elongation data. More difficult processing of samples than the filter assay.
¹⁴ C SEC	High sensitivity detection of high MW products. No signal interference from enzyme or other buffer components.	Special rad-use HPLC equipment required. Time-consuming to run multiple samples. High use of scintillation vials when collecting fractions. Potential loss of ¹⁴ C sensitivity due to small HPLC injection volumes.

Refractive Index SEC	Estimation of product sizes, detection of HMW products.	Signal is proportional to longer chain length products: difficult to detect lower concentrations of smaller-DP products. BSA in reaction buffer interferes with signal and is not eliminated by boiling. Uncertain MW of products due to anomalous running
		patterns of HG glycans compared to dextran standards.
Fluorescence SEC	Signal is proportional to number of molecules. Highly sensitive – sensitivity of fluorescence detector can be adjusted for low-activity reactions. Quantitative comparison of high MW vs. oligosaccharide products.	Requires use of pre-labeled fluorescent acceptors. Unknown effect of 2AB or other fluorescent molecules on enzyme activity. Highsensitivity measurements can overload detector. May require running many samples to determine appropriate sensitivity.
Alcian Blue PAGE	Individual bands up to ~DP30 can be counted. Easy to distinguish between low, high, and intermediate length products. Highly sensitive (strong staining from fraction of reaction containing 200 ng oligosaccharide). Multiple replicate measurements can be made from same reaction.	Time consuming creation and running of gels. Precise size of larger products not determined – need to use complementary methods (SEC).
ELISA	Highly sensitive. Multiple replicate measurements can be made from same reaction. 96-well plates allow many samples to be assayed simultaneously.	Non-quantitative. No product length information.

MALDI	Product length information	Non-quantitative.
	from oligosaccharide	Products above ~DP20 do not
	products.	ionize well. Loss of
	Use of pre-labeled fluorescent	information from higher DP
	acceptor substrates allows	products.
	fast screening of multiple	
	enzymes.	
	Data is complementary with	
	PAGE.	
UDP-Glo	Potential for measuring	No elongation data.
	reaction kinetics. Large	Linearity and sensitivity has
	number of simultaneous	not yet been established for
	samples can be assayed.	HG:GalAT. Complementary
	Cheaper, non-radiolabeled	methods required to
	UDP-GalA substrate.	distinguish non-productive
		nucleotide sugar hydrolysis
		from <i>de novo</i> synthesis.